Function and Regulation of RhoBTB1

Brandao Haga, Raquel

Awarding institution:
King's College London

Function and Regulation of RhoBTB1

A thesis submitted to King's College London for the degree of Doctor of Philosophy, June 2016

by

Raquel Brandão Haga

Randall Division of Cell and Molecular Biophysics
King's College London
2nd floor New Hunt's House
London SE1 1UL

Abstract

Rho GTPases are a family of proteins known to be involved in cytoskeletal regulation and are important for several processes including cell migration, cell polarity, vesicle trafficking and cytokinesis. RhoBTB1 is an atypical member of the Rho GTPase family. It consists of a non-functional GTP-binding domain followed by a proline-rich region and two tandem BTB domains. The only known interacting partner for RhoBTB1 is cullin3, a scaffold protein in ubiquitin ligase complexes. So far RhoBTB1 has not been shown to affect the cytoskeleton and it has no known cellular function. Most Rho GTPases are regulated by GEFs, GAPs, RhoGDIs and post-translational lipid modifications at the C-terminus. However, RhoBTB1 is not regulated by any of these mechanisms. RhoBTB1 has additional domains that could be involved in protein-protein interaction, leading to an alternative mechanism for RhoBTB1 regulation. This project has shown that RhoBTB1 can interact with RhoA and ROCK1 as well as cullin3. The interaction between RhoA and RhoBTB1 was explored since RhoBTB1 has the potential to recruit substrates for ubiquitination by cullin3 complexes. The region of interaction between RhoA and RhoBTB1 was mapped and RhoBTB1 influenced the protein level of RhoA, suggesting that it inhibits RhoA degradation by the proteasome. RhoBTB1 was found to localise diffusely in the cytoplasm or to punctate structures. Knockdown of RhoBTB1 led to a change in cell morphology in a 3D Matrigel matrix, indicating that it influences cell shape in 3D, although it did not alter cell shape on 2D substrata. RhoBTB1 can be phosphorylated by ROCK1 *in vitro* and the region of interaction between RhoBTB1 and ROCK1 was mapped using ROCK1 deletion mutants. I hypothesize that RhoBTB1 interacts with RhoA to affect its ubiquitination and degradation and hence affects cell morphology in a 3D matrix, and that RhoBTB1 activity is regulated by ROCK1-mediated phosphorylation.

Acknowledgements

Firstly, I would like to thank my supervisor Professor Anne Ridley for giving me the opportunity of conducting my PhD in her laboratory and for her guidance. This experience has given me the opportunity to improve my skills as an independent researcher. I would like also to thank my second supervisor, Dr Claire Wells, for all the suggestions throughout my PhD.

Of course a big thank you goes to the members of Ridley's lab. Thank you to Silvia, Naren, Christina and Elvira who welcomed me into the lab and helped me in my first months. A very special thank you goes to Barbara who came back to the lab and shared with me all the challenges of working on a new protein ("Go BTB team!"). Thank you for all your support and most of all for your friendship. A big thank you to Magali who was my bench and office buddy. Thank you to the current members Sofia, Camilla, Vicky, Campbell and Ritu for all the discussions and friendly environment. A big special thank you goes to Richard who helped me to go through the endless cloning and IP assays; and who has been a good friend. Thank you for teaching me about British culture, for correcting my eds and for not taking all my "British" points after all my complaints about the weather and British beef. It was a pleasure to meet and work with all of you.

Furthermore, thank you to all the nice people I have met throughout these four years. Thank you for the pubs after work, comedy nights and great pizza nights. I would like to thank specially Rimple for always making me laugh and being a good friend.

Finally, I would like to thank my family and friends in Brazil. I am really greatful for all your support and friendship. Mãe, Pai, Be e Elo, obrigada pelo amor e suporte de vocês. Eu tenho muita sorte de poder contar com uma familia que sempre me apoia em tudo que eu faço.

Table of Contents

List of Figures

List of Tables

List of supplementary movies

Movie 3.1	MDA-MB-231 cell intercalation
Movie 3.2	Cal51 cell intercalation
Movie 3.3	HCC1954 cell intercalation
Movie 3.4	MCF-7 cell intercalation

Abbreviations

ABP	actin-binding protein
ADF	actin-depolymerizing factor
ADP	adenosine diphosphate
Akt	Akt serine/threonine kinase/Protein kinase B
AP-1	activating protein-1
Arp2/3	actin-related protein 2/3
ATP	adenosine triphosphate
BCR	BTB-cullin3-Rbx1
BSA	bovine serum albumin
BTB	broad complex, tramtrack, bric à brac
CAND1	cullin-associated and neddylation-associated 1
CFSE	carboxyfluorescein succinimidyl ester
CRL	CULLIN-RING ubiquitin ligase
CRL3	cullin3-RING ubiquitin ligase
DAPI	4’,6-diamidino-2-phenylindole
DH	Dbl-homology
DHR	Dock Homology Region
DMEM	Dulbeco’s modified eagle medium
DMSO	dimethyl sulphoxide
DNA	deoxyribonucleic acid
DSS	disuccinimidyl suberate
DTT	dithiothreitol
EBM-2	endothelial cell basal medium-2
ECL	enhanced chemiluminescence
ECM	extracellular matrix
EGF(R)	epidermal growth factor (receptor)
EGTA	ethylene-glycol-tetra-acetic acid
EMT	epithelial-mesenchymal transition
Ena/VASP	Enabled/vasodilator-stimulated phosphoprotein
ER	oestrogen receptor
ERK	extracellular signal-regulated protein kinase
F-actin	actin filaments
FCS	fetal calf serum
FH	formin homology
G-actin	globular actin

GAP	GTPase-activating protein
GDI	guanine nucleotide dissociation inhibitor
GDP	guanosine diphosphate
GEF	guanine nucleotide exchange factor
GFP	green fluorescent protein
GPCR	G protein-coupled receptor
GST	glutathione S-transferase
GTP	guanosine triphosphate
HEPES	4-(2-hydroxyethyl)-1-piperazine-ethanesulfonic acid
HER2	human epidermal growth factor receptor
IPTG	Isopropyl β-D-1-thiogalactopyranoside
JNK	c-Jun N-terminal kinase
LB	L-Broth
LIMK	LIM kinase
MBS	myosin-binding subunit
mDia	mammalian homolog of Drosophila diaphanous
MLC	myosin light chain
MMP	matrix metalloprotease
MRCK	actin-myosin regulatory kinase
MTOC	microtubule-organizing centre
NADPH oxidase	nicotinamide adenine dinucleotide phosphate-oxidase
NAE	NEDD8-activating enzyme
NFκB	nuclear factor kappa B
NLS	nuclear localization sequence
NPF	nucleation promoting factor
N-WASP	neuronal WASP
PAE	primary aortic endothelial
PAK	p21-activating kinase
PBS	phosphate –buffered saline
PCR	polymerase chain reaction
PECAM-1	platelet endothelial cell adhesion molecule
PEI	polyethylenimine
PFA	paraformaldehyde
PH	pleckstrin homology
PI3K	phosphatidylinositide 3-kinase

$PI(3,4,5)P_3$	phosphatidylinositol (3,4,5)-triphosphate
PIP2	phosphatidylinositol (4,5)-bisphosphate
PIP5K	phosphatidylinositol-4-phosphate 5-kinase
PKA	protein kinase A
PKC	protein kinase C
PKN	protein kinase N
PMSF	phenylmethylsulphonyl fluoride
POZ	Pox virus and Zinc finger
PR	progesterone receptor
PRM	proline-rich motif
RBD	Rho GTPase-binding domain
REM	Ras exchange motif
RING	really interesting new gene
RNA	ribonucleic acid
ROCK	Rho-associated kinase
ROS	reactive oxygen species
RPMI	Roswell Park Memorial Institute
RT	room temperature
SAPK	stress-activated protein kinase
SCAR	suppressor of cyclic AMP repressor
SCF complex	Skp, Cullin, F-box containing complex
SDS	sodium dodecyl sulphate
SH3	Src homology 3
SRE	serum response element
SRF	serum response factor
TAE	Tris-acetate-EDTA
TBS	Tris-buffered saline
TEM	transendothelial migration
VCA	verprolin-homology, central and acidic
VSVG	vesicular stomatitis virus glycoprotein
WASP	Wiskott-Aldrich Syndrome protein
WAVE	WASP-family verprolin-homologous protein
WH2	WASP-homology-2
WRC	WAVE regulatory complex
WT	wild-type

1 Introduction

1.1 Rho GTPases

The Rho family of GTPases is a subfamily of the Ras superfamily. Rho GTPases are highly conserved and found in nearly all eukaryotes. The human Rho GTPase family consists of 20 proteins that are divided into 8 subfamilies: Rac1, Rac2, Rac3 and RhoG subfamily, Cdc42, RhoQ and RhoJ subfamily, RhoA, RhoB and RhoC subfamily, RhoV and RhoU subfamily, RhoH subfamily, RhoBTB1 and RhoBTB2 subfamily, Rnd1, Rnd2 and Rnd3 subfamily, and RhoF and RhoD subfamily (Heasman and Ridley, 2008). These subfamilies can be classified as typical or atypical depending on their mode of regulation (Figure 1.1). Rac, Rho, Cdc42 and RhoF/RhoD subfamilies are considered typical because they act as molecular switches, cycling between an active GTP-bound form and an inactive GDP-bound form. The ratio of GTP-bound form/GDP-bound form is regulated by guanine nucleotide exchange factors (GEFs), GTPase-activating proteins (GAPs) and guanine nucleotide dissociation inhibitors (GDIs). The atypical Rho GTPases are mostly constitutively GTP-bound, therefore they are likely to be regulated by different mechanisms; and their function might involve their additional domains that are not found in classical Rho proteins (Aspenstrom et al., 2007). For example, RhoBTB proteins have broad complex, tramtrack, bric à brac (BTB) domains that are able to interact with cullin3, a scaffold protein of ubiquitin ligase complexes involved in protein ubiquitination (Berthold et al., 2008a). This interaction points to a potential role of RhoBTB proteins in protein degradation.

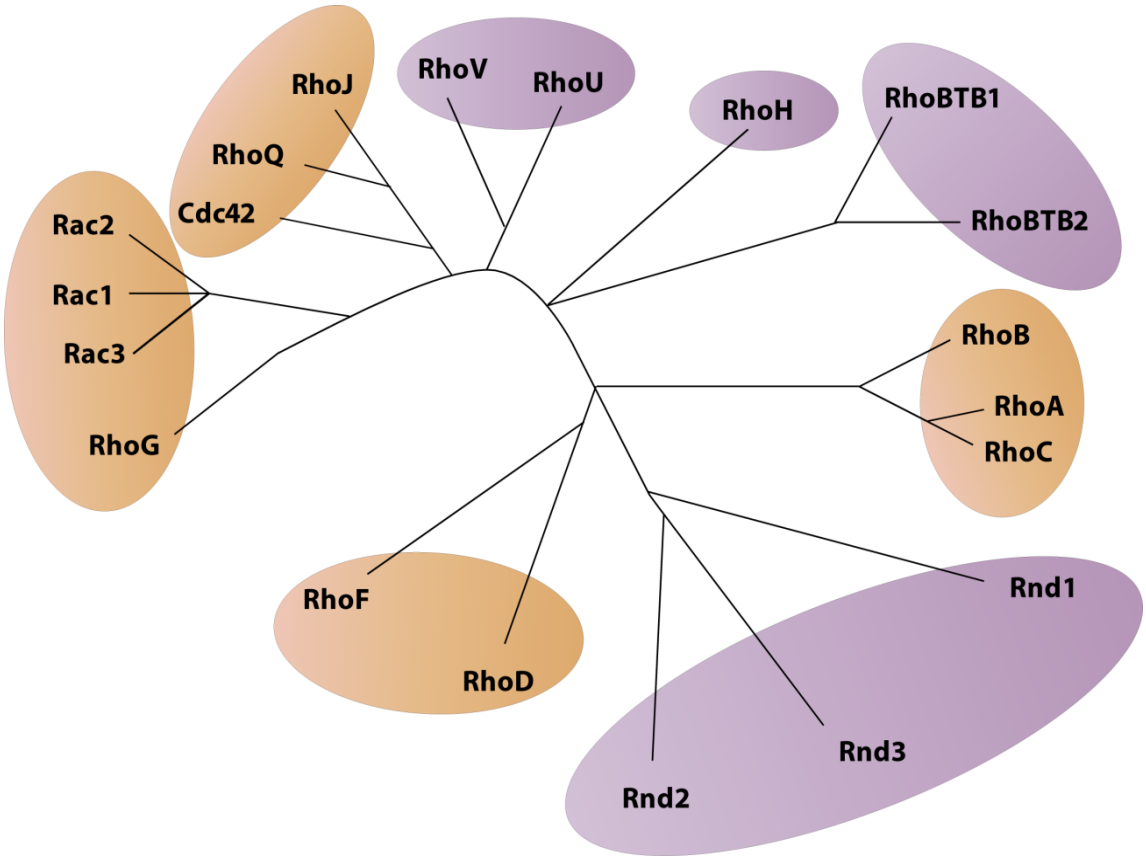

Figure 1.1 - Rho GTPase family

The Rho GTPase family consists of 20 proteins that are subdivided into 8 subfamilies. These proteins can be classified as typical (orange circle) or atypical (purple circle) depending on their mode of regulation (modified from Heasman and Ridley (2008)).

Most Rho GTPases undergo post-translational modifications at their C-terminal CAAX motif (where C represents cysteine, A is an aliphatic amino acid, and X is a terminal amino acid). This motif is post-translationally prenylated, either by a farnesyl or geranylgeranyl isoprenoid lipid. These modifications are important for the translocation of Rho GTPases to the plasma membrane and/or endomembranes and are required for their biological activity (Roberts et al., 2008). Another modification that occurs near the C-terminus of several Rho GTPases is palmitoylation. For example, RhoU and RhoV do not have a functional CAAX motif, but a C-terminal CFV motif that can be palmitoylated and target these proteins to membranes. The only subfamily that does not undergo lipid modifications near the C-terminus is the RhoBTB subfamily. These

Rho GTPases lack a CAAX motif and they are localized mainly in the cytoplasm (Aspenstrom et al., 2007). There is no evidence that RhoBTB proteins could be palmitoylated.

Rho GTPases have been implicated in several cellular processes including organisation of the actin and microtubule cytoskeletons, regulation of gene expression, vesicle trafficking, cell cycle progression, cell morphogenesis, cell polarity and cell migration (Etienne-Manneville and Hall, 2002). Furthermore, Rho GTPases also play an important role in some pathological processes including cancer progression, inflammation and wound repair (Vega and Ridley, 2008).

After cells are stimulated by extracellular factors such as soluble molecules, adhesive interactions or mechanical stresses, Rho GTPases can be activated and initiate signalling cascades through a wide range of effectors or targets including kinases and scaffold/adaptor-like proteins. The activation of Rho GTPases (GTP-bound form for the typical proteins) leads to changes in the conformation of these molecules, increasing their ability to bind to effectors (Hall, 2012; Schwartz, 2004). The most well-known effectors are those that interact with the best characterized Rho GTPases: RhoA, Rac1 and Cdc42 (Figure 1.2).

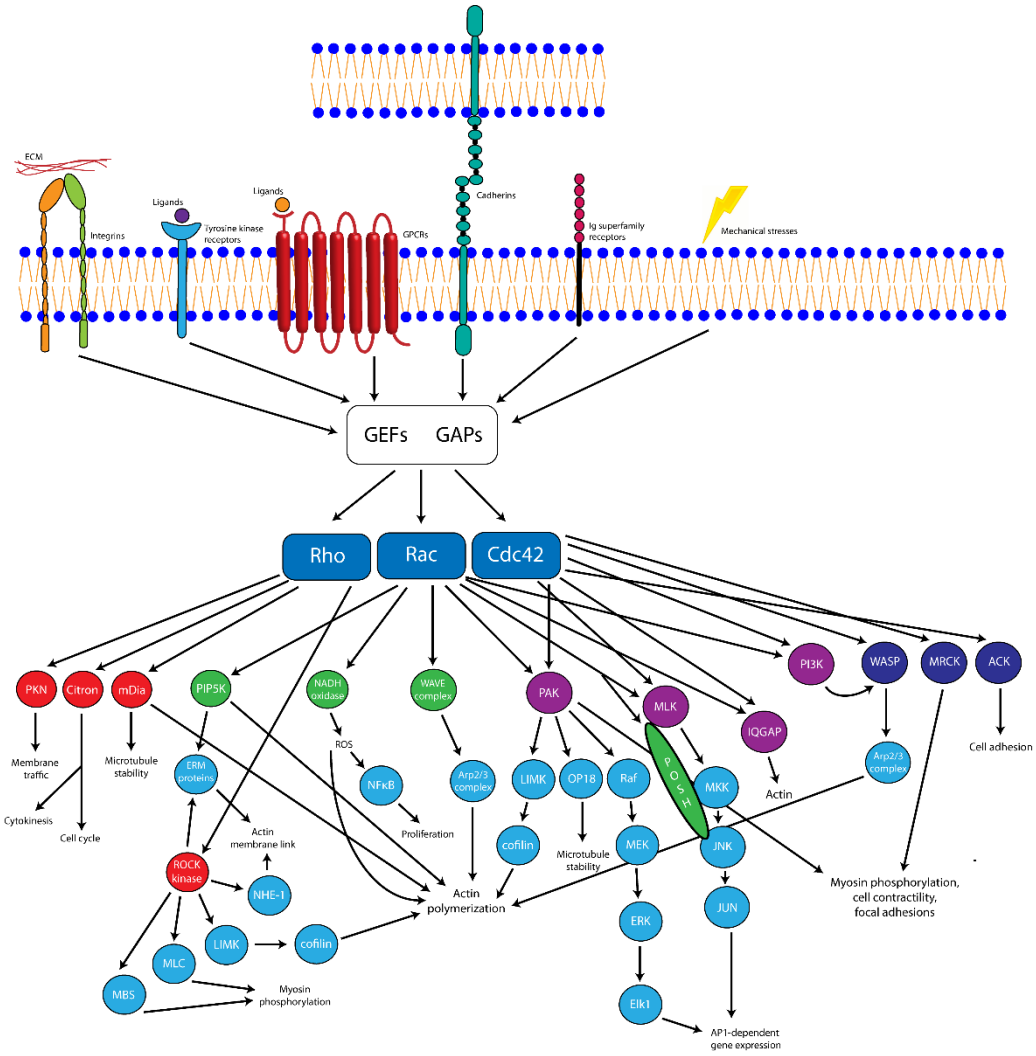

Figure 1.2 - Rho GTPase effectors

Regulation of Rho, Rac and Cdc42 by GEFs and GAPs after extracellular stimuli leads to the activation of several signalling pathways involved in actin polymerization, membrane trafficking, cytokinesis, cell cycle, microtubule stability, myosin phosphorylation, AP1-dependent gene expression, cell contractility, focal adhesion, cell adhesion, and proliferation (adapted from Schwartz (2004)).

1.1.1 Regulation of Rho GTPases

Classically, Rho GTPases are known to be regulated by GEFs, GAPs and GDIs. These proteins control the cycling between the active GTP-bound form and the inactive GDP-bound form. However, new ways of regulating Rho GTPases are emerging, which is important, especially to understand how the atypical Rho GTPases are regulated (Figure 1.3).

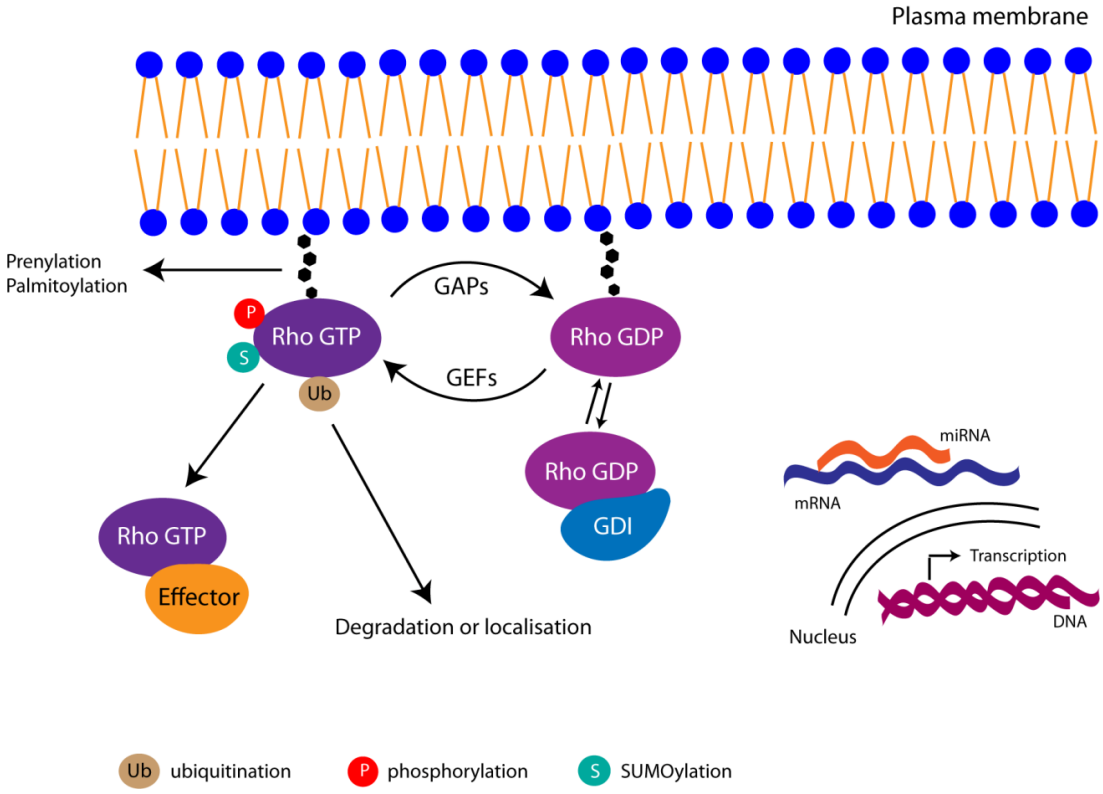

Figure 1.3 - Regulation of Rho GTPases

Rho GTPases can be regulated by classic regulators such as GEFs, GAPs and GDIs. These proteins control the cycling between the active GTP-bound form and the inactive GDP-bound form. RhoGDIs can also regulate the localisation and degradation of Rho GTPases. Other modes of regulating Rho GTPases include post-translational modification (lipid modification, phosphorylation, ubiquitination and SUMOylation); and transcriptional and post-transcriptional (miRNA) regulation.

1.1.1.1 GEFs

Guanine nucleotide exchange factors (GEFs) are proteins that accelerate release of bound GDP that is replaced with GTP, activating the GTPase. The nucleotide-binding site is found between two loops called switch 1 and switch 2. The switch regions together with the P-loop (phosphate-binding loop) interact with the phosphates and the Mg^{2+}-binding pocket to determine the conformation and the affinity of the binding between GDP/GTP and the GTPase (Figure 1.4) (Bos et al., 2007; Rossman et al., 2005).

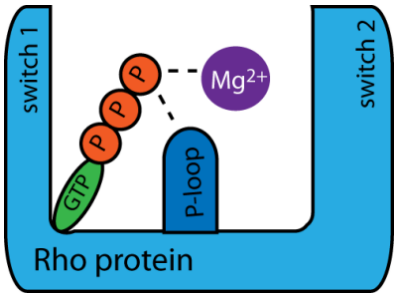

Figure 1.4 – Nucleotide-binding site of Rho proteins
The switch regions (switch 1 and switch 2) together with the P-loop (phosphate-binding loop) interact with the phosphates and the Mg^{2+}-binding pocket to determine the conformation and the affinity of the binding between GDP/GTP and the GTPase.

In mammals, GEFs that regulate Rho GTPases are divided into two unrelated families: Dbl-homology (DH) domain family (at least 70 members) and Dock Homology Region (DHR) domain family (11 members). Most GEFs are part of the DH family and they consist of a catalytic Dbl-homology (DH) domain followed by a pleckstrin homology (PH) domain. The DH domain catalyzes the exchange of GDP for GTP and the PH domain is believed to play a role in localising Dbl proteins to plasma membranes, and/or to affect the catalytic activity of the DH domain (Bos et al., 2007; Cook et al., 2014; Schmidt and Hall, 2002). GEFs of the DHR family have two conserved domains called DHR-1 and DHR-2. The DHR-2 domain interacts with the nucleotide-free form of

Rho GTPases and forms an intermediate in the catalytic reaction for exchange of GDP to GTP (Gadea and Blangy, 2014; Laurin and Cote, 2014).

GEFs act by remodelling the switch regions of the Rho GTPases and insert residues close to or into the P-loop and Mg^{2+}-binding pocket that inhibit the binding of phosphates and Mg^{2+}. This promotes GTPase intermediates that lack nucleotide and Mg^{2+}. GTP is then preferentially loaded into Rho GTPases, because GTP is found in higher concentrations than GDP inside cells (Bos et al., 2007; Cherfils and Zeghouf, 2013). Several GEFs insert an acidic residue in the P-loop, creating repulsive electrostatic interactions that expel GDP from the binding site. Other GEFs bring a hydrophobic residue close to the Mg^{2+}-binding pocket, which lowers its affinity and consequently the affinity for GDP. Some GEFs modify the conformation of switch 2 in the binding site, bringing the methyl group of a conserved alanine close to the Mg^{2+}-binding pocket, having a similar effect on GDP affinity (Cherfils and Zeghouf, 2013) (Figure 1.5).

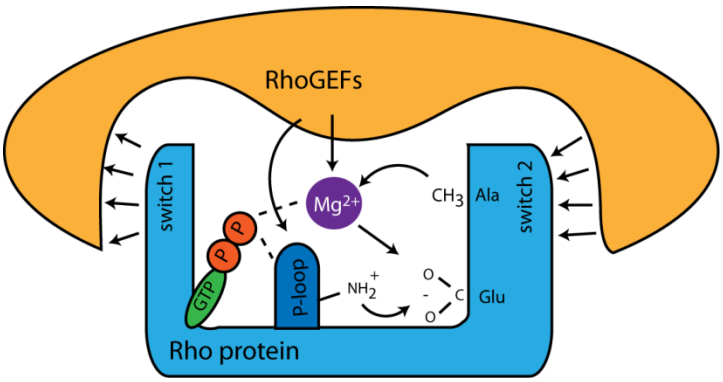

Figure 1.5 - Interaction between Rho proteins and RhoGEFs

GEFs can remodel the switch regions and insert residues close to or into the nucleotide-binding site that alter binding of phosphates and Mg^{2+}. Several GEFs insert an acidic residue in the P-loop, creating repulsive electrostatic interactions that expel GDP from the binding site. Other GEFs bring a hydrophobic residue close to the Mg^{2+}-binding pocket, which lowers its affinity and consequently the affinity for GDP. Some GEFs modify the conformation of switch 2 in the binding site, bringing the methyl group of a conserved alanine close to the Mg^{2+}-binding pocket, having a similar effect on GDP affinity.

1.1.1.2 GAPs

GTPase-activating factors (GAPs) are proteins that promote the hydrolysis of GTP by providing an essential catalytic group that accelerates the intrinsic GTPase activity of the GTPases. The human genome encodes around 80 GAPs. However, less than half of them have been studied so far. RhoGAPs have a GAP domain of about 150 amino acids with a highly conserved arginine in a loop structure (arginine "finger"). This domain alone can bind to GTP-bound Rho proteins and catalyze their GTPase activity (Jacobs and Hall, 2005; Moon and Zheng, 2003).

The arginine "finger" in the GAP domain is inserted into the phosphate-binding site to stabilize negative charges at the γ-phosphate during the transition state of GTP hydrolysis. The arginine also interacts with a glutamine from the switch 2 of the GTPase that places a water molecule for the nucleophilic attack of the γ-phosphate of GTP (Figure 1.6) (Bos et al., 2007; Cherfils and Zeghouf, 2013; Jacobs and Hall, 2005; Moon and Zheng, 2003).

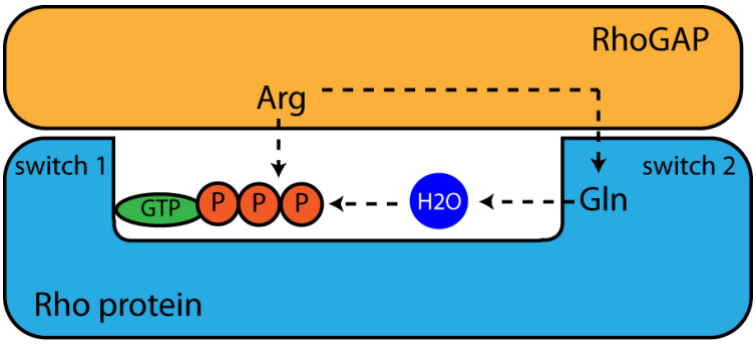

Figure 1.6 - Interaction between Rho proteins and RhoGAPs

The arginine "finger" in the GAP domain is inserted into the phosphate-binding site to stabilize negative charges at the γ-phosphate during the transition state of GTP hydrolysis. The arginine also interacts with a glutamine from the switch 2 of the GTPase that places a water molecule for the nucleophilic attack of the γ-phosphate of GTP.

1.1.1.3 GDIs

Guanine nucleotide dissociation inhibitors (GDIs) are proteins known to control the cycling of the Rho GTPases between cytosol and membranes; and to regulate the activation/inactivation of Rho GTPases.

There are three RhoGDIs in humans: RhoGDI1-3. RhoGDIs consist of a N-terminal domain that interacts with the switch 1 and switch 2 domains of Rho GTPases, restricting the flexibility that is important for the GDP/GTP cycling; and a C-terminal domain that includes the geranylgeranyl-binding pocket that is important to extract Rho GTPases from the membrane (Cherfils and Zeghouf, 2013; Garcia-Mata et al., 2011).

RhoGDIs have been shown to play three distinctive roles in regulating Rho GTPases. They inhibit the release of GDP and hence prevent Rho GTPase activation by GEFs; they interact with the GTP-bound form of Rho GTPases and inhibit GTP hydrolysis, both intrinsic and GAP-catalysed; and they control the cycling of Rho GTPases between cytosol and membrane by forming high-affinity complexes with prenylated Rho GTPases in the cytosol (DerMardirossian and Bokoch, 2005; Garcia-Mata et al., 2011). RhoGDIs have also been shown to protect some Rho GTPases from proteasomal degradation (Boulter and Garcia-Mata, 2010).

1.1.1.4 Transcriptional and post-transcriptional regulation

Expression of the classical Rho GTPases, RhoA, Rac1 and Cdc42, are relatively similar in most tissues. However, some Rho GTPases are restricted to particular tissues and in some cases, they need specific stimuli to be expressed (Wennerberg and Der, 2004). For example, the *RhoB* gene is an immediate early gene and it can be induced after stimulation with EGF (Jähner and Hunter, 1991) and genotoxic stress (Fritz et al., 1995). Atypical Rho GTPases have also been shown to be regulated at a

transcriptional level. For example, expression of Rnd3 is induced after Raf activation (Hansen et al., 2000) and expression of RhoU is increased by Wnt-1 (Tao et al., 2001).

Rac1 and Cdc42 have been shown to have splice variants. A Rac1 splice variant Rac1b has enhanced intrinsic guanine nucleotide exchange (self-activation), impaired GTPase reaction and fails to interact with RhoGDIs, leading to accumulation of the GTP-bound conformation of Rac1b in cells (Fiegen et al., 2004; Singh et al., 2004). A Cdc42 splice variant is a brain-specific isoform that can be palmitoylated (Cdc42-palm) instead of or in addition to being prenylated (Cdc42-prenyl). This change in lipid modification has an effect on protein localisation and function (Kang et al., 2008; Wirth et al., 2013).

Rho GTPases undergo post-transcriptional regulation. microRNAs (miRNAs) are non-coding RNA molecules that can control the expression of mRNAs. These short sequences silence target genes by either inhibiting translation or degrading mRNA. Several Rho GTPases can be regulated by miRNAs. Most of the work on miRNAs has been done in cancer models, showing how the regulation of Rho GTPase expression by miRNAs can affect cancer progression (Liu et al., 2012). For example, it has been shown that RhoA is target of miRNA-155 (Bijkerk et al., 2012; Kong et al., 2008) and miRNA-125a-3p (Huang et al., 2013); RhoB is a target of miRNA-21 (Liu et al., 2011b); RhoBTB1 is a target of miRNA-31 (Xu et al., 2013); and Cdc42 is a target of miRNA-29 (Park et al., 2009) and miRNA-137 (Chen et al., 2011). Sometimes the same miRNA can target two different Rho GTPases. miRNA-185 has been reported to decrease the levels of RhoA and Cdc42, leading to inhibition of proliferation in human colorectal cancer cells (Liu et al., 2011a).

1.1.1.5 Covalent modifications

Rho GTPases undergo several covalent modifications in addition to lipids that can regulate the proteins in a positive (activation) or negative (inactivation/degradation) way. These include ubiquitination and phosphorylation.

Ubiquitination is the covalent attachment of an ubiquitin to lysine resides in the target protein. This modification often leads to protein degradation. However, it can also change the localisation of proteins or their activity (Xu and Jaffrey, 2011). Ubiquitination of Rho GTPases can be triggered by bacterial toxins and growth factors (Visvikis et al., 2010), but other factors could be involved as well. Several Rho GTPases have been reported to undergo ubiquitination, including RhoA, Rac1, Rac1b, Cdc42, RhoB and RhoBTB2 (de la Vega et al., 2011; Nethe and Hordijk, 2010). Ubiquitination has been proposed to be a mechanism to control the local activity of Rho GTPases (de la Vega et al., 2011; Mettouchi and Lemichez, 2012; Sahai et al., 2007; Tian et al., 2011) and it can affect either the GTP-bound form (active) or GDP-bound form (inactive). For example, Rac1 is ubiquitinated only when in the active form and bound to the plasma membrane (Kovacic et al., 2001; Lynch et al., 2006; Nethe et al., 2010; Visvikis et al., 2008). However, RhoA can be ubiquitinated in different conformations by different mechanisms. Nucleotide free RhoA and GDP-RhoA are substrates of Smurf1 ubiquitin ligase (Wang et al., 2003) while only GDP-RhoA is a substrate of the BACURD-cullin3 complex (Chen et al., 2009). Recently, it has been proposed that GDP-RhoA and GTP-RhoA are substrates of SCF^{FBXL19} E3 ubiquitin ligase, facilitated by Erk2-mediated phosphorylation of RhoA (Wei et al., 2013). In all cases, the ubiquitination of RhoA leads to degradation by the proteasome.

Phosphorylation is another covalent modification that can regulate Rho GTPases. Some protein kinases such as PKA, ROCK1, Src and Akt have been shown to phosphorylate RhoA, Rnd3 (RhoE), Cdc42 and Rac1, respectively (Kwon et al., 2000;

Lang et al., 1996; Riento et al., 2005; Tu et al., 2003). In most cases, phosphorylation seems to have a negative effect on the activity of Rho GTPases. RhoA can be phosphorylated on serine 188 (Ser188) by PKA and this allows RhoGDIs to bind with high-affinity to RhoA, translocating RhoA from membranes to the cytosol. Although binding to RhoGDIs inhibits RhoA activity, the interaction can protect RhoA from ubiquitin-mediated degradation (Ellerbroek et al., 2003; Lang et al., 1996; Rolli-Derkinderen et al., 2005). Phosphorylation of Rnd3 by ROCK1 and PKC on 7 serines increases protein stability and translocates Rnd3 to the cytosol which reduces its activity in inducing stress fibre disruption (Riento et al., 2005; Riou et al., 2013). Rac1 is phosphorylated on serine 71 (Ser71) by Akt and threonine 108 (Thr108) by ERK. Phosphorylation of Ser71 appears to decrease GTP-binding without affecting GTPase activity of Rac1 while phosphorylation of Thr108 inhibits interaction of Rac1 with PLCγ1 and induces translocation of Rac1 to the nucleus (Kwon et al., 2000; Tong et al., 2013).

1.1.2 Regulation of the actin cytoskeleton

A highly conserved function of Rho GTPases is the control of the actin cytoskeleton. Several cellular processes including cell migration, cell division, endocytosis and chemotaxis depend on the actin cytoskeleton (Jaffe and Hall, 2005).

Initial studies using fibroblasts have shown that RhoA induces the assembly of focal adhesions and formation of stress fibres while Rac1 stimulates the formation of lamellipodia (Ridley and Hall, 1992; Ridley et al., 1992), giving the first clues about the role of Rho GTPases in actin cytoskeleton regulation. Later, Cdc42 was shown to regulate the formation of filopodia (Nobes and Hall, 1995).

The actin cytoskeleton consists of actin filaments (F-actin) that are formed by the self-assembly of monomeric globular actin (G-actin). The filaments are double helical and each asymmetric filament has a dynamic barbed end and a less active pointed end. The dynamics of assembly and disassembly is dependent on ATP hydrolysis. ATP-actin associates at the barbed end and ADP-actin dissociates from the pointed end. Moreover, this process is under the control of over a hundred actin-binding proteins (ABPs). ABPs interact directly with F-actin or G-actin; and control the structure and dynamics of the actin cytoskeleton (Goley and Welch, 2006; Pollard and Borisy, 2003). ABPs can regulate different steps including filament nucleation, elongation, severing, capping, and depolymerization (Lee and Dominguez, 2010). Rho GTPases are known to interact with or alter the activity of ABPs and therefore regulate the assembly/disassembly of the actin cytoskeleton. Extracellular signals, such as cytokines, growth factors and hormones, are sensed by cell surface receptors and transmitted to Rho GTPases. Active Rho GTPases then interact with their effector proteins, activating signal cascades that will lead to stress fibres, lamellipodia and filopodia (Jaffe and Hall, 2005) (Figure 1.2).

The first step of actin polymerization is known as nucleation, which involves the formation of a stable multimer of actin monomers that will function as a template to the elongation of the new filament. This is controlled by actin-nucleating proteins, including the actin-related protein 2/3 (Arp2/3) complex and formins. Each actin-nucleating protein acts in a distinctive mechanism. For example, Arp2/3 complex initiates a new actin filament that branches off an existing filament while formins promote nucleation of unbranched filaments at the barbed end (Firat-Karalar and Welch, 2011; Goley and Welch, 2006).

The Arp2/3 complex is not an efficient nucleator and it requires the activity of nucleation promoting factor (NPF) proteins, including Wiskott-Aldrich Syndrome protein (WASP), neuronal WASP (N-WASP) and WASP-family verprolin-homologous protein (WAVE; also known as suppressor of cyclic AMP repressor (SCAR)) (Campellone and Welch, 2010; Firat-Karalar and Welch, 2011). These proteins have in common a WCA domain, which consist of a WASP-homology-2 (WH2 or W); and a central (also called cofilin-homology or connector) and acidic (CA) region. These regions are important to bring G-actin to the complex and to change the conformation of the Arp2/3 complex that leads to the initiation of actin polymerization. NPFs are regulated by other proteins, including Rho GTPases (Dominguez, 2009; Goley and Welch, 2006; Ladwein and Rottner, 2008; Suetsugu, 2013).

Formins are large multidomain proteins defined by the presence of a catalytic formin homology 2 (FH2) domain. There are eight formin subfamilies identified in humans including Dia, FMNL and FHOD. Formins act both as nucleation and elongation factors. These proteins processively associate with barbed ends, allowing the addition of G-actin while inhibiting capping proteins from ending elongation (Breitsprecher and Goode, 2013; Chesarone et al., 2010; Dominguez, 2009; Schonichen and Geyer, 2010).

Another family of proteins that control elongation is Enabled/vasodilator-stimulated phosphoprotein (Ena/VASP) proteins. All members of the family have an amino-terminal Ena/VASP homology 1 (EVH1) domain followed by a proline-rich central region and a carboxy-terminal Ena/VASP homology 2 (EVH2) domain. Ena/VASP proteins elongate filaments that have been initiated by W-based filament nucleators such as an Arp2/3/NPF complex. These proteins are able to bind to both G-actin and F-actin. They act by binding at barbed ends of actin filaments and inhibiting filament capping by capping protein. Moreover, Ena/VASP proteins can control actin filament branching by reducing the density of Arp2/3-dependent actin filament branches (Chen et al., 2014b; Dominguez, 2009; Krause et al., 2003).

Filaments grow until they are capped. Capping is important to control the length of the growing branches and localise where the filaments generate propulsive forces. The two main proteins involved in this process are capping protein (also known as CapZ in muscle) and gelsolin (Pollard and Borisy, 2003). Another process that controls the dynamics of the actin cytoskeleton is depolymerization. The actin-depolymerizing factor (ADF)/cofilin family are involved in this step. These proteins are known to sever filaments and elevate the levels of monomeric actin. Both ADF and cofilin bind to ADP-bound subunits of the F-actin, promoting their disassembly. Cofilin can also bind to released ADP-actin monomers, controlling the recycling of disassociated actin subunits. The extent of depolymerization of the actin filaments relies on several factors including the relative concentration of other actin-binding proteins (Bamburg and Bernstein, 2010; Dos Remedios et al., 2003). The protrusive motility depends on the treadmilling of the actin filaments that consists in the addition of subunits at the barbed end and loss of subunits at the pointed end (Pollard and Borisy, 2003).

1.1.2.1 Cell migration

To illustrate the importance of Rho GTPases in the regulation of the actin cytoskeleton, the steps of cell migration of single cells will be briefly explained. Cell migration is a multistep process in which cells need to extend membrane protrusions in the cell front (lamellipodia, filopodia or membrane blebs), form new adhesions, contract the cell body and detach the cell rear from the surrounding environment (Figure 1.7). Rho GTPases are critical molecules in this process, sending signals from the membrane receptors to the cytoskeleton and cell adhesions (Ridley, 2001; Ridley et al., 2003). Single cells are able to migrate in two interchangeable modes of migration: amoeboid and mesenchymal (Pankova et al., 2010). RhoA has been implicated in both amoeboid and mesenchymal migration in 3D environments (Vega and Ridley, 2008). The amoeboid mode of migration is characterized by actomyosin-based cortical contractility mediated by Rho/ROCK signalling. The consistent tension results in blebbing, which contributes to cell motility (Pankova et al., 2010; Vega and Ridley, 2008). The mesenchymal mode of migration has an elongated fibroblast-like morphology that depends on cell adhesion dynamics and traction forces between both poles of the cell. Formation of focal adhesions and actomyosin-mediated contractility is controlled by Rho/ROCK signalling (Friedl and Wolf, 2003; Pankova et al., 2010).

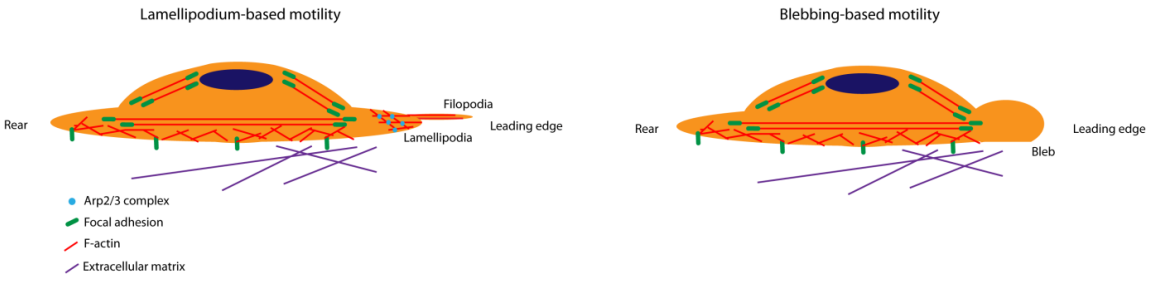

Figure 1.7 - Single cell migration

Single cell migration is a multistep process in which cells need to extend membrane protrusions at the cell front (lamellipodia, filopodia or membrane blebs), form new adhesions, contract the cell body and detach the cell rear from the surrounding environment. Lamellipodium and filopodium formation involves the rearrangement of the actin cytoskeleton with the help of nucleators such as the Arp2/3 complex. Blebs are protrusions of the cell membrane due to actomyosin contractions of the cell cortex.

Lamellipodia are transient structures and their formation is driven by actin polymerization. The Arp2/3 complex is associated with actin filaments throughout the cell front, and together with WAVE proteins, it stimulates the formation of a “dendritic” actin network that is important for lamellipodium extension (Ridley, 2011). Activation of Rac is necessary for lamellipodium formation. GTP-Rac binds directly to Sra1 protein, activating the WAVE regulatory complex (WRC) (hetero-pentameric complex formed by Sra1/Cyfit1, Nap1/Hem2/Kette, Abi2, HSPC300/Brick1 and WAVE1/SCAR) (Chen et al., 2014a; Krause and Gautreau, 2014). WRC activity is controlled by inhibition of the verprolin-homology, central and acidic (VCA) region. It is believed that the interaction of GTP-Rac with Sra1, and perhaps with the meander region of WAVE1 (a meandering path across a concave surface of Sra1 that is formed by five helices (α2-α6 and a series of intervening loops)), could lead to changes in the conformation of the complex and release of the VCA region, which is important for the activation of the Arp2/3 complex (Chen et al., 2014a; Chen et al., 2010).

The presence of $PI(3,4,5)P_3$ increases GTP-bound Rac in several cell types. It is thought that $PI(3,4,5)P_3$ promotes GTP loading on Rac through direct interaction with Rac GEFs. Several Rac GEFs, including Tiam-1, β-PIX and DOCK180, are known to activate Rac to induce lamellipodia. Rac activation also stimulates PI3K (Fritsch et al., 2013), which leads to the production of $PI(3,4,5)P_3$. This creates a positive feedback loop, accumulating active Rac at the cell front (Raftopoulou and Hall, 2004; Ridley, 2011, 2015). Another example of a mechanism to control actin polymerization in the cell front is through the PAK family of serine/threonine kinases. Activation of Rac and Cdc42 activates PAKs, which then phosphorylate and activate LIM kinase (LIMK). Activation of LIMK leads to phosphorylation and inactivation of cofilin. Cofilin is an important protein to promote filament treadmilling at the leading edge (Bamburg and Bernstein, 2010; Raftopoulou and Hall, 2004).

Formins are also involved in lamellipodium extension. It was found that mDia1, a RhoA effector, localises at the leading edge of some cells, including T-cells, and it can cooperate with the Arp2/3 complex to initiate lamellipodium formation (Heasman et al., 2010; Isogai et al., 2015). RhoA is mainly active at the cell rear, but it has been shown to be active at the cell front as well. During membrane protrusion, RhoA is active at the leading edge, but it is inactivated during membrane retraction (Pertz, 2010). Activation of mDia1 by RhoA in the cell front could stimulate actin polymerization (Heasman et al., 2010).

In the rest of the cell, active RhoA is associated with focal adhesion formation (sites of contact of the cell with the extracellular matrix) and cell contractility during cell migration. One important Rho effector that is involved in actin-myosin filament assembly is serine/threonine kinase ROCK. Activation of ROCK leads to phosphorylation and activation of LIMK, which then phosphorylates and inactivates cofilin. ROCK also phosphorylates myosin light chain (MLC) phosphatase, inactivating it. This leads to an increase in the levels of phosphorylated myosin light chain (pMLC), which then stimulates the cross-linking of actin filaments by myosin II and generates contractile forces. Contraction promotes movements of the cell body and contribute to detachment of the cell rear (Ananthakrishnan and Ehrlicher, 2007; Raftopoulou and Hall, 2004). Another important effector of RhoA at the cell rear is mDia. This effector cooperates with ROCK for the assembly of actomyosin bundles such as stress fibres. mDia is found at the front and back of the cell, and its function is dependent on the cell type and conditions during cell migration (Narumiya et al., 2009; Raftopoulou and Hall, 2004).

Cell polarity is important for directional migration. Formation of protrusions and retraction of the cell rear are not enough to direct the cells to a specific place. The nucleus, Golgi apparatus and microtubule-organizing centre (MTOC) also need to be repositioned towards the leading edge (Vicente-Manzanares et al., 2005). Cdc42 has

been shown to regulate MTOC positioning through recruitment of Par6 and aPKC to the leading edge (Etienne-Manneville and Hall, 2001). Nuclear movement can also be regulated by Cdc42, probably through actin flow controlled by actin-myosin regulatory kinase (MRCK) (Gomes et al., 2005; Luxton and Gundersen, 2011; Sit and Manser, 2011).

1.1.3 Other activities of Rho GTPases

Rho GTPases have been reported to take part in signalling pathways that do not involve regulation of the actin cytoskeleton. For example, RhoA, Rac1 and Cdc42 are involved in signalling pathways that lead to the activation of a variety of transcription factors including activating protein-1 (AP-1) transcription factor (Benitah et al., 2004; Rajakyla and Vartiainen, 2014). AP-1 proteins are dimeric transcription factors formed by Jun, Fos or ATF subunits. AP-1 binds to the AP-1-binding sites on DNA and regulates the transcription of genes that are important for cell proliferation, death, survival and differentiation (Shaulian and Karin, 2002). It is well-known that Rac/Cdc42 activates JNK/SAPK and p38 signalling cascades, leading to Jun phosphorylation. Phosphorylated Jun homodimers have high AP-1 activity and are responsible for the transcription of several genes (Coso et al., 1995; Minden et al., 1995). RhoA also has a role in Jun regulation, but at a transcriptional level. It has been shown that RhoA activates *jun* transcription through the activation of two different kinases, PKN and ROCK (Marinissen et al., 2001; Marinissen et al., 2004). Activation of AP-1 by RhoA, Rac1 and Cdc42 can also be achieved through serum response factor (SRF), a transcription factor that activates the *fos* promoter serum response element (SRE) (Hill et al., 1995).

Another known pathway regulated by Rho GTPases is the activation of NFκB. NFκB proteins (RelA/p65, RelB, c-Rel, p50 (NF-κB1) and p52 (NF-kB2)) are transcription factors that are found as dimers. In the cytoplasm, they are associated with IκB proteins in an inactive state. After stimulation, NFκB dissociates from IκB and moves to the nucleus where it can control the transcription of genes that are important for the maintenance of the immune system, skeletal system and epithelium (Hayden and Ghosh, 2012). RhoA, Rac1 and Cdc42 are able to induce phosphorylation of IκBa which leads to the translocation of p50/p50 and p50/p65 dimers to the nucleus where they are active transcription factors (Perona et al., 1997).

Atypical Rho GTPases may also regulate gene expression. Depletion of RhoBTB1 and RhoBTB2 in normal primary human keratinocytes leads to a decrease of CXCL14 mRNA levels. CXCL14 is a homeostatic chemokine that has reduced expression in a wide range of epithelial tumours. Further analysis using head and neck squamous cell carcinoma (HNSCC) cell lines have shown that the levels of RhoBTB2 and CXCL14 in these cell lines were lower than the levels found in primary keratinocytes. Restoration of RhoBTB2 expression was able to increase the levels of CXCL14 in all HNSCC cell lines. The mechanism for this regulation is still unknown, but it does not involve cullin3, a known RhoBTB-binding protein (McKinnon et al., 2008).

Rac also plays a role in the activation of NADPH oxidase enzyme complex. NADPH oxidase, the main component of the complex, generates superoxide radicals that are important to kill microorganisms that are phagocytosed by cells. Reactive oxygen species (ROS) are also known to be involved in the regulation of the cytoskeleton. One of the mechanisms appears to be through inhibition of RhoA which allows Rac1-mediated cytoskeletal reorganization. Activation of NADPH relies on a protein multicomplex that consists of two integral membrane proteins, pg91^{phox} and p21^{phox}, and two cytosolic proteins, p67^{phox} and p47^{phox}. Rac1 has been shown to interact with p67^{phox} and be the fifth component in the complex that leads to NADPH complex activation (Abo et al., 1991; Diekmann et al., 1994; Elnakish et al., 2013; Hall, 2012; Petry et al., 2009; Stanley et al., 2014).

1.1.4 Crosstalk between Rho GTPases

The signalling networks that are controlled by Rho GTPases are really dynamic and they need to be regulated in time and space. Members of the Rho GTPase family are known to overlap in many signalling pathways, acting sometimes in a cooperative manner and sometimes in an antagonistic manner. Because they act so close to each other, it is not surprising that there is a crosstalk regulation between the Rho GTPases. This interaction can occur in three different levels: regulation of activity; regulation of protein expression and stability; and regulation of downstream signalling pathways (Guilluy et al., 2011).

The classic example of crosstalk that regulates GTPase activity is between RhoA and Rac1. For example, the Tiam1-mediated activation of Rac in NIH3T3 fibroblasts results in the downregulation of Rho activity at the GTP-level and leads to an epithelial-like morphology. Re-expression of RhoA reverses the phenotype to a migratory fibroblast-like morphology without affecting Rac activity (Sander et al., 1999). However, it was observed that RhoA can also inhibit the activity of Rac through ROCK-mediated inhibition of FilGAP (Ohta et al., 2006). Although RhoA and Rac act in antagonistic ways most of the time, they can also positively regulate each other (Guilluy et al., 2011) (Figure 1.8). Other Rho GTPases can also crosstalk with RhoA and Rac, including RhoG and Rnd3. All these crosstalks are mainly mediated by the activation or inhibition of GEFs and GAPs (Guilluy et al., 2011).

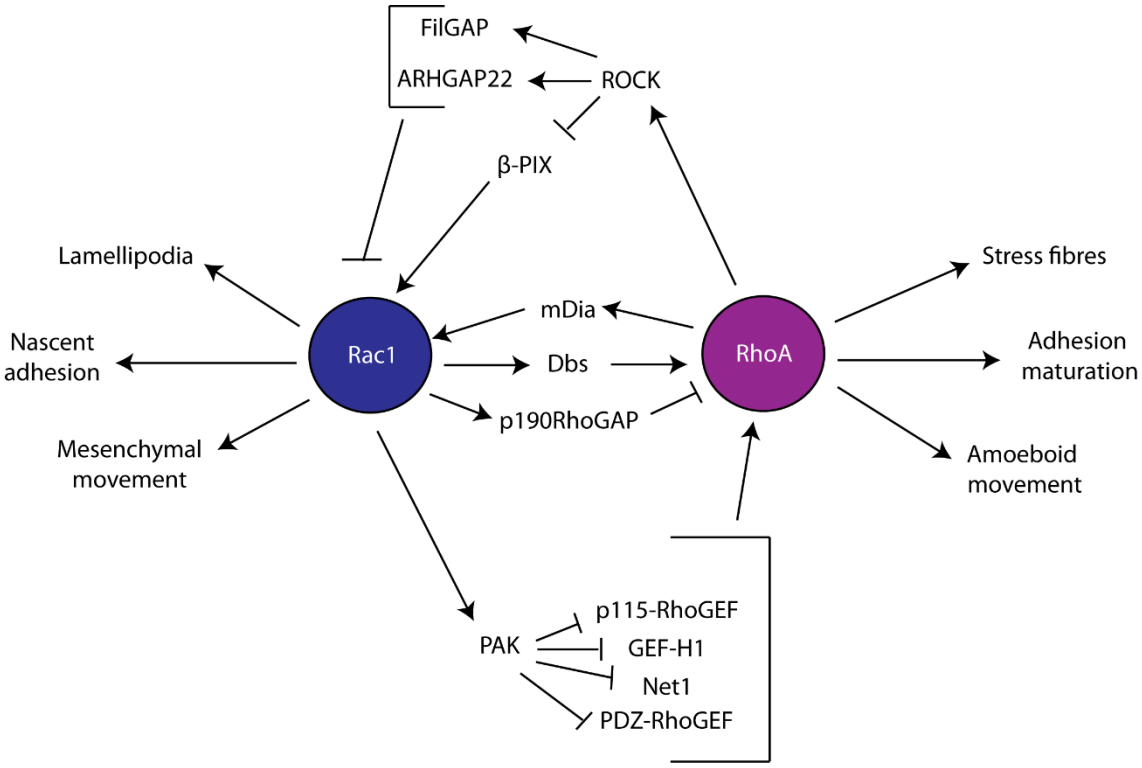

Figure 1.8 – Rac1 and RhoA crosstalk

Crosstalk between Rac1 and RhoA involves a complex network that includes effectors, RhoGAPs and RhoGEFs. RhoA activates Rac1 through activation of mDia while activation of ROCK leads to inhibition of Rac1 through activation of FilGAP and ArhGAP22 and/or inhibition of Rac1 GEF β-PIX. Rac1 activates RhoA through activation of RhoA GEF Dbs. However, Rac1 inhibits RhoA through activation of p190RhoGAP. In addition, RhoA is also inhibited when Rac1 activates PAK proteins which leads to inhibition of Rho GEFs such as p115-RhoGEF, GEF-H1, RhoA GEF Net1 and PDZ-RhoGEF (re-drawn from Guilluy et al. (2011)).

As mentioned above, levels of Rho GTPases can be regulated by ubiquitin-mediated degradation. One mechanism that Rho GTPases use to avoid degradation is binding to RhoGDIs. The limited amount of RhoGDIs can cause a competition among the Rho GTPases to avoid degradation. However, in some cases, the displacement of a Rho GTPase from the RhoGDI complex has a positive effect. The released Rho GTPase is activated and able to interact with other proteins (Garcia-Mata et al., 2011). Overexpression of only one Rho GTPase leads to competition with endogenous Rho proteins to bind RhoGDIs in a dose-dependent manner, showing that changes in the

levels of a single protein can affect the equilibrium of the whole Rho GTPase network (Boulter et al., 2010; Garcia-Mata et al., 2011).

The crosstalk of Rho GTPases can also be mediated by their effectors (Figure 1.8). Rho, Rac and Cdc42 share some common effectors and signalling pathways, leading to a dynamic downstream crosstalk. Depending on the cell type, the Rho GTPases can act in a synergistic or antagonistic way (Boulter et al., 2010).

1.1.5 Rho GTPases in tumorigenesis

Rho GTPases are important signal transducers in signalling pathways that regulate cell migration, proliferation, survival and death. All these cellular processes are crucial for maintenance of normal tissues. However, any misbalance in the control of these pathways could lead to the development of many diseases including cancer, cardiovascular disease, hepatic disease, developmental disorders and neurodegenerative disorders (Boettner and Van Aelst, 2002; DeGeer and Lamarche-Vane, 2013; Sahai and Marshall, 2002; Toksoz and Merdek, 2002).

The role of Rho GTPases in tumorigenesis will be discussed in more detail since these proteins are involved in all steps of tumour progression. The development of human tumours is a multistep process that consists in dysregulation of cell proliferation, resistance to growth suppressors, inhibition of cell death, uncontrolled replication leading to immortalization and activation of angiogenesis, invasion and metastasis (Hanahan and Weinberg, 2011).

Accumulation of mutations in genes that affect proliferation and survival is one of the key steps for primary tumour formation. Until recently, it was believed that Rho GTPases were rarely mutated in human tumours. However, it was found that proline 29 in Rac1 is mutated in a subset of melanomas, breast tumours and head and neck tumours (Alan and Lundquist, 2013). RhoA is also mutated in some tumours including diffuse gastric cancer and angioimmunoblastic T cell lymphoma (Kakiuchi et al., 2014;

Sakata-Yanagimoto et al., 2014; Wang et al., 2014; Yoo et al., 2014; Zhou et al., 2014). Although these mutations seem to be important for tumour development, in most cases, Rho GTPases are found to be upregulated or to have their activity increased by misregulation of GAPs, GEFs and/or GDIs (Boettner and Van Aelst, 2002; Vega and Ridley, 2008). Several Rho GTPases are upregulated in human tumours including RhoA, RhoC, Rac1, Rac2, Rac3, Cdc42, RhoV and RhoF (Pajic et al., 2015; Vega and Ridley, 2008).

The classical Rho GTPases, RhoA, Rac1 and Cdc42, are known to be essential for Ras-induced transformation in NIH 3T3 cells (Qiu et al., 1995a; Qiu et al., 1997; Qiu et al., 1995b). Moreover, they have been shown to be important for the progression and metastasis of different human tumours including breast cancer, liver cancer, melanoma, testicular cancer and ovarian cancer (Gomez del Pulgar et al., 2005; Kamai et al., 2004; Wang et al., 2007).

RhoA appers to be involved in almost all stages of tumour progression. For example, in gastric cancer cell lines, RhoA is found to be hyperactive and its suppression leads to partially inhibition of the proliferation phenotype. This effect involves regulation of cell cycle through G1-S progression. Downregulation of the RhoA target mDia1 in gastric cancer cell lines leads to increase in the expression of cell cycle inhibitors $p21^{Waf1/Cip1}$ and $p27^{Kip1}$ while downregulation of ROCK increases the levels of another family of cell cycle inhibitors called INK4 (Zhang et al., 2009). Several studies *in vitro* and *in vivo* suggest that RhoA has a role during tumour angiogenesis. One example is the knockout of $G\alpha_{13}$ receptors in endothelial cells in mice, which causes a decrease in tumour growth and normalization of tumour vasculature. $G\alpha_{13}$ induces expression of VEGF2 mediated by activation of RhoA which leads to transcription of NFκB (Sivaraj et al., 2013). Local invasion is an early step in the metastatic process by which cells need to detach from the primary tumour and migrate through the surrounding tissue. Although RhoA seems to play an active role in cancer progression, recent findings in

diffuse gastric cancer and angioimmunoblastic T cell lymphoma have shown that mutations in RhoA that lead to loss of GTPase activity are important to drive cancer progression (Kakiuchi et al., 2014; Sakata-Yanagimoto et al., 2014; Wang et al., 2014; Yoo et al., 2014; Zhou et al., 2014).

RhoC has also been found to promote tumour progression while RhoB seems to act as a tumour suppressor (Ridley, 2013). RhoC promotes tumour progression in some tumours including melanoma, ovarian cancer and head and neck cancer (Horiuchi et al., 2003; Islam et al., 2009; Ruth et al., 2006). RhoC is able to control invadopodium formation in tumour cells by locally regulating cofilin activity. Invadopodia are cell protrusions capable of penetrating and degrading the extracellular matrix, increasing the metastatic potential of tumour cells. RhoC activity is spatially regulated by activation of p190RhoGEF outside the invadopodia and activation of p190RhoGAP inside the invadopodium core. This leads to restriction of cofilin activity only inside the invadopodium core (Bravo-Cordero et al., 2011). RhoB, on the other hand, is often downregulated in human tumours (Huang and Prendergast, 2006; Vega and Ridley, 2008). For example, the expression of RhoB in human lung tissues decreases going from normal tissue to invasive carcinoma. In addition, overexpression of RhoB in the lung cancer cell line A549 leads to inhibition of cell growth *in vitro* and *in vivo* (Mazieres et al., 2004). Also, overexpression of RhoB in gastric cancer cell lines inhibits proliferation, migration and invasion; and increases chemosensitivity while overexpression of RhoA and RhoC leads to opposite effects (Zhou et al., 2011).

Rac1 is another Rho GTPase that is found altered in several stages of tumour progression. Deregulation of Rac signalling can be caused by changes in the upstream signalling including tyrosine kinase receptors, PI3Ks, GEFs and GAPs. One example is the activation of Rac1 by Rac GEF P-Rex1 after stimulation of tyrosine kinase receptors and GPCRs in breast cancer cells (Wertheimer et al., 2012). In colorectal tumours, the expression of a Rac1 splice variant, Rac1b, is increased in different

stages of tumour progression (Jordan et al., 1999). Expression of Rac1b has also been found in breast cancer and lung cancer (Schnelzer et al., 2000; Zhou et al., 2013). Rac1b has been shown to be involved in MMP-3-mediated malignant transformation of mammary epithelial cells. MMP-3 induces the expression of Rac1b which increases the levels of cellular ROS, leading to expression of the transcription factor Snail, which induces epithelial-mesenchymal transition (EMT) as well as oxidative damage to DNA and genomic instability (Radisky et al., 2005).

The role of Cdc42 in tumour progression may be tissue-specific. Cdc42 is found to be upregulated in many tumours including non-small cell lung cancer, colorectal adenocarcinoma, melanoma, breast cancer and testicular cancer. However, loss of Cdc42 in liver cancer leads to an increase in tumour development (Stengel and Zheng, 2011; Vega and Ridley, 2008). Some other Rho GTPases also appear to have a dual role in tumorigenesis. Rnd3 is downregulated in some tumours and acts as a tumour suppressor (Grise et al., 2012; Karlsson et al., 2009; Muller et al., 2011; Villalonga et al., 2004). However, in some cases, Rnd3 has been shown to be upregulated and mediate drug resistance in cancer cells (Li et al., 2009; Zhang et al., 2007). RhoBTBs also do not have a well-defined role in tumorigenesis (see section 1.1.7).

These examples illustrate how complex the role of Rho GTPases in tumour progression is. Their contribution is dependent on cell type, extracellular stimulus and signalling pathway involved in the cell transformation.

1.1.6 Atypical Rho GTPases

The atypical Rho GTPase subgroup consists of four subfamilies: RhoV and RhoU subfamily, RhoH subfamily, Rnd1, Rnd2 and Rnd3 subfamily; and RhoBTB1 and RhoBTB2 subfamily. Each subfamily will be briefly described in this section.

RhoV (also known as Chp or Wrch2) and RhoU (also known as Wrch1) proteins are members of the RhoV and RhoU subfamily. These proteins have significant sequence identity to Cdc42 (~ 52-55%), but they contain extra N- and C- terminal extensions that are critical for their activity (Aronheim et al., 1998; Shutes et al., 2004). RhoV and RhoU have an extremely rapid intrinsic guanine nucleotide exchange activity, and are therefore found mainly in the GTP-bound form in cells (Shutes et al., 2004). So far, RhoV and RhoU GAPs and GEFs have not been identified. In addition, these proteins are palmitoylated instead of prenylated in their C-terminal domain as mentioned in section 1.1. This lipid modification is important to regulate their membrane localisation and activity. However, membrane localisation is not regulated by RhoGDIs like for the classic Rho GTPases (Berzat et al., 2005; Chenette et al., 2005; Chenette et al., 2006). Expression of RhoV and RhoU is regulated at the transcriptional level by Wnt-1; and RhoU has also been shown to be regulated by STAT3 (Faure and Fort, 2015; Schiavone et al., 2009; Tao et al., 2001). Like Cdc42, RhoV and RhoU affect the actin cytoskeleton (lamellipodium formation and filopodium formation, respectively), cell migration and formation of focal adhesions (Aronheim et al., 1998; Chuang et al., 2007; Saras et al., 2004; Tao et al., 2001). Although RhoV and RhoU are very similar, only RhoU binds to Grb2 through its N-terminal domain and is phosphorylated on tyrosine 254 by Src in its C-terminal domain (Alan et al., 2010; Shutes et al., 2004). Other known binding partners are PAK1, PAK2, PAK4 and NCKβ (Aronheim et al., 1998; Dart et al., 2015; Saras et al., 2004; Tao et al., 2001). Another interesting feature in this subfamily is that the N-terminal domain is able to regulate RhoV and RhoU function in

a negative way, a characteristic found for the first time in the Rho GTPase family (Chenette et al., 2005; Shutes et al., 2004).

RhoH, also known as TTF (translocation three four), is normally expressed only in hematopoietic tissues, similar to Rac2 (Dallery-Prudhomme et al., 1997). RhoH is GTPase deficient, and is therefore constantly in a GTP-bound form (Li et al., 2002). The C-terminal region of RhoH has a CKIF motif (a typical CAAX motif) that can be prenylated *in vitro* (Fueller and Kubatzky, 2008; Roberts et al., 2008). Due to the lack of GTPase activity, RhoH is not regulated by GAPs and GEFs. However, RhoH is able to interact with RhoGDIs; and it has been shown to be regulated at the transcriptional level and by phosphorylation (Delestre et al., 2011; Gu et al., 2006; Li et al., 2002). RhoH is important in the regulation of proliferation, survival, migration and engraftment of murine hematopoietic progenitor cells (Gu et al., 2005); and it has been implicated in T-cell differentiation (Dorn et al., 2006). RhoH does not seem to have any direct effect on actin reorganization (Aspenstrom et al., 2004). However, RhoH can antagonize the activity of other Rho GTPases. For example, Rac1 and RhoA-mediated activation of NFκB is inhibited by RhoH through inhibition of IκB degradation (Li et al., 2002). Loss of RhoH in murine hematopoietic progenitor cells leads to an increase in Rac1-mediated migration and cortical F-actin assembly (Chae et al., 2008).

Rnd1, Rnd2 and Rnd3 (also known as RhoE) proteins are members of the Rnd subfamily. Although these proteins are highly similar to the classic Rho GTPases, Rnd proteins are GTPase deficient, and are therefore constitutively in the GTP-bound form; and they are modified by the farnesyl group instead of geranylgeranyl group in their C-terminal domain (Foster et al., 1996; Riou et al., 2010). Rnd1 and Rnd3 are mainly associated with membranes and RhoGDIs do affect their localisation. Rnd2 seems to be localised predominantly in the cytoplasm (Chardin, 2006; Riou et al., 2010; Roberts et al., 2008). Since Rnd proteins have not been shown to interact with any GAPs or GEFs, these proteins should be regulated by other mechanisms such as

phosphorylation, expression and localisation. In fact, it has been shown that Rnd proteins can be phosphorylated and phosphorylation (in combination with farnesylation) allows these proteins to interact with 14-3-3 proteins. This interaction leads to translocation of Rnd proteins from the plasma membrane to the cytosol, inactivating these proteins (Riou et al., 2013). Rnd3 is known to be phosphorylated on 5 serines and 1 threonine by ROCK1 and on serine 210 by PKC (Madigan et al., 2009; Riento et al., 2005). Moreover, expression of Rnd3 is induced by activation of Raf, leading to changes in the actin cytoskeleton (Hansen et al., 2000). One important function of Rnd1 and Rnd3 is that they can antagonize RhoA interaction with p190RhoGAP. This interaction leads to loss of stress fibres and cell rounding (Guasch et al., 1998; Nobes et al., 1998; Oinuma et al., 2012; Wennerberg et al., 2003). Other proteins also interact with Rnd proteins, which could also contribute to Rnd-induced responses.

1.1.7 RhoBTB proteins

In mammals, RhoBTB1 and RhoBTB2 form the RhoBTB subfamily. Members of the RhoBTB subfamily were identified during a study using a *Dictyostelium discoideum* model to identify Rho-related proteins. Orthologues of RhoBTB1 and RhoBTB2 are present in vertebrates and insects, but not in plants and fungi (Boureux et al., 2007; Rivero et al., 2001). Although RhoBTB3 shares some similarities with RhoBTB1 and RhoBTB2, this protein is not considered a Rho GTPase due to its low similarity to other Rho proteins (Boureux et al., 2007; Wennerberg and Der, 2004).

RhoBTB1 gene is located in chromosome 10 while *RhoBTB2* gene in chromosome 8. The coding sequence of these two proteins is split into 9 exons. Additional exons are placed upstream of the start codon, two in *RhoBTB1* and one in *RhoBTB2*. The exon-intron organization of RhoBTB1 and RhoBTB2 is very similar except for exon 4. This exon encodes the complete first BTB domain and it is 45 bp longer in *RhoBTB2* (Ramos et al., 2002). *RhoBTB1* is ubiquitously expressed in human tissue, showing

high levels in skeletal muscle, placenta, stomach, kidney, testis, adrenal gland and uterus. *RhoBTB2* is overall weakly expressed with relatively high levels in neural and cardiac tissues (Berthold et al., 2008b; Ramos et al., 2002).

RhoBTB1 and RhoBTB2 are atypical Rho GTPases as they do not cycle between a GTP-bound form and a GDP-bound form. The GTP-binding domain of RhoBTBs is Rho-related but is around 18 residues longer and rich in charged residues. Due to a deletion in a glutamine equivalent to Q61 in Ras and a substitution of a glycine equivalent to G12 in Ras by asparagine, the GTP-binding domain of RhoBTBs could be expected not to hydrolyse GTP (Berthold et al., 2008b). It has been reported that the GTP-binding domain of RhoBTB2 does not bind to GTP *in vitro* (Chang et al., 2006), but nothing has been published for RhoBTB1. RhoBTB1 (79 kDa) and RhoBTB2 (82 kDa) are also bigger than classical GTPases (~ 20 kDa) due to the presence of extradomains in addition to the GTP (Rho) domain. The non-functional GTPase domain (Rho domain) is followed by a proline-rich motif (PRM), a tandem of 2 broad-complex, tramtrack, bric à brac (BTB) domains, and a conserved C-terminal region (Figure 1.9).

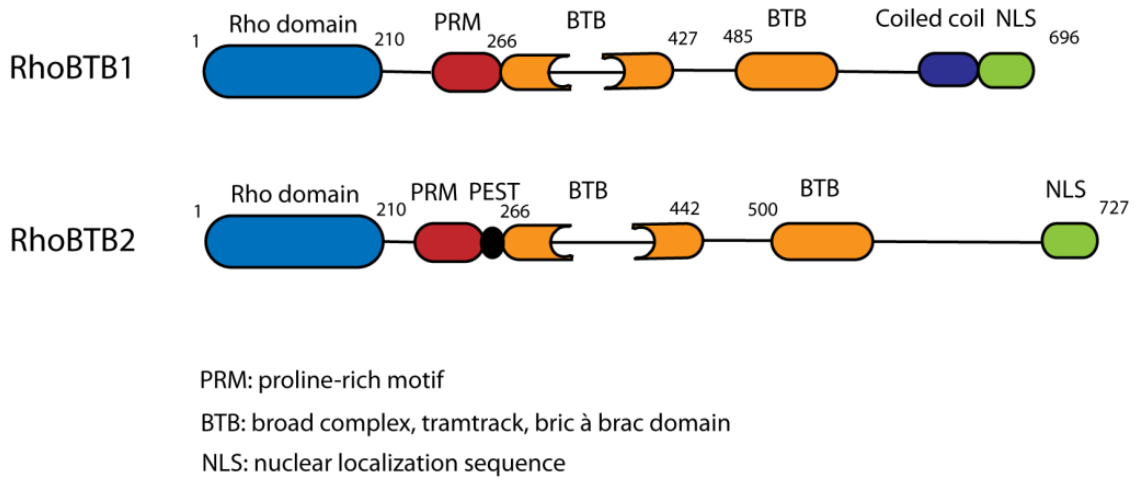

Figure 1.9 – Members of the RhoBTB subfamily
Domain structure of the RhoBTB proteins.

Proline-rich motifs are known to be important for protein-protein interaction. Proline-rich regions can bind to SH3 (Src homology 3), WW and EVH1 domains (Kay et al., 2000). All these domains are present in proteins that are important for regulating the actin cytoskeleton. The proline sequence found in RhoBTB1 is the PxxP motif (where x denotes any amino acid) and is classified as a class II motif. The PxxP motif is the core binding motif of the SH3 domain and this could indicate a potential interaction of RhoBTB1 with proteins with SH3 domains (Berthold et al., 2008b).

The BTB domain, also known as Pox virus and Zinc finger (POZ) domain, is a conserved protein-protein motif present in proteins involved in transcription repression, cytoskeleton regulation and protein ubiquitination/degradation. Some proteins contain only the BTB domain, but it is more usual for BTB to be combined with other domains. The most frequent ones are MATH, Kelch, NPH3, Ion transport and Zinc finger (ZF) domains (Perez-Torrado et al., 2006). However, RhoBTB1 and RhoBTB2 have an unusual organization with a tandem of 2 BTB domains. The first BTB is divided in two by an extension of unknown function that has a different length and composition among RhoBTB proteins. It has been shown so far that the BTB domains in RhoBTB proteins are important for the formation of homodimers and heterodimers (Berthold et al., 2008a) and for the interaction with cullin3, a scaffold protein in ubiquitin-ligase complexes (Berthold et al., 2008a).

The C-terminal region is conserved in all members of the RhoBTB subfamily and it is not found in any other protein (Rivero et al., 2001). Although RhoBTBs have a potential nuclear localization signal (NLS) near the C-terminus, these proteins have not been reported to be found in the nucleus. Unlike the classical GTPases, RhoBTBs do not have a CAAX motif, a sequence important for post-translational modification that signals proteins to the membrane.

The functions of RhoBTB1 and RhoBTB2 have not been well determined yet. Although RhoBTB1 and RhoBTB2 have domains that could interact with proteins involved in actin cytoskeleton regulation, these proteins do not interact with the CRIB domain of WASP and PAK or the Rho-binding domain of Rhotekin; and ectopic expression of RhoBTBs in primary aortic endothelial (PAE) cells does not seem to affect the organization of the actin filament system. Moreover, it was observed that RhoBTB1 and RhoBTB2 are localised in vesicles, suggesting that RhoBTBs might be involved in vesicle trafficking (Aspenstrom et al., 2004). It has been shown that RhoBTB2 is involved in transporting vesicular stomatitis virus glycoprotein (VSVG) in a microtubule-dependent manner (Chang et al., 2006). RhoBTB2 has been studied more than RhoBTB1. It has been reported that RhoBTB2 has an active role in cell cycle progression and apoptosis through the transcription factor E2F1 (Freeman et al., 2008). Moreover, RNA profiling using Hela cells has shown that RhoBTB2 affects cell cycle, apoptosis, cytoskeleton and membrane trafficking pathways (Siripurapu et al., 2005). Because RhoBTB1 and RhoBTB2 share 79% homology, some of RhoBTB2 functions could also be performed by RhoBTB1.

One protein interaction that is common to the RhoBTBs is the interaction with cullin3. Both RhoBTB1 and RhoBTB2 bind to the N-terminus of cullin3 (Berthold et al., 2008a; Wilkins et al., 2004). The same has been reported for other BTB containing proteins and cullin3; and this interaction has been shown to be important for targeting proteins for ubiquitination and hence degradation (Geyer et al., 2003). Indeed, RhoBTB2 has been shown to be a substrate for the cullin3 ubiquitin ligase complex (Wilkins et al., 2004).

RhoBTB1 and RhoBTB2 have been described as tumour suppressors. RhoBTB2 is also known as ‘deleted in breast cancer 2’ (DBC2) and its levels are reduced in some breast cancers (Hamaguchi et al., 2002). RhoBTB1 is downregulated in some cancers like head and neck cancer (Beder et al., 2006), breast cancer and kidney cancer

(Berthold et al., 2008b); but it has also been reported to be upregulated in some cancer cell lines (Ramos et al., 2002; Vega and Ridley, 2008). The *RhoBTB2* gene has been shown to be a target of E2F1, a transcription factor involved in cell cycle and apoptosis (Freeman et al., 2008) and *RhoBTB1* is a target of microRNA-31 (miR-31) in human colon cancer (Xu et al., 2013). PPARγ, a regulator of adipogenesis, can also regulate RhoBTB1. Overexpression of PPARγ increases mRNA levels of RhoBTB1 (Pelham et al., 2012). As mentioned above, RhoBTB2 is a substrate of the cullin3 ubiquitin ligase complex and it is degraded via the proteasome (Wilkins et al., 2004). Not much is known about RhoBTB regulation. Since they do not behave as typical GTPases, RhoBTBs are not regulated by GAPs, GEFs and GDIs. Unconventional mechanisms such as phosphorylation, SUMOylation, post-transcriptional regulation by microRNAs and ubiquitination could be involved in RhoBTB regulation, leading to inhibition/activation or degradation of the proteins.

1.2 Ubiquitination and cullin3

1.2.1 Ubiquitination process

Ubiquitination is a three-step process in which ubiquitin, a highly conserved protein of 8.5 kDa, becomes covalently attached to lysine residues of target proteins. This mechanism controls the stability and/or localisation of cellular substrates involved in the regulation of many cellular processes. Firstly, ubiquitin is activated in an ATP-dependent reaction and it is bound to an E1 activating enzyme. Second, ubiquitin-loaded E1 transfers the ubiquitin to an E2 ubiquitin conjugating enzyme. Ubiquitin is attached to the E2 catalytic cysteine residue through a trans(thio)esterification reaction. In the last step, E3 ubiquitin ligases facilitate the formation of an isopeptide bound between ubiquitin and substrate. In humans, there are 2 E1 enzymes, 37 E2 enzymes and more than 600 E3 ligases (Haglund and Dikic, 2005; Komander, 2009; Sarikas et al., 2011). E3 ubiquitin ligases are important to mediate substrate specificity. They are

divided in several classes, the major ones are HECT (homologous to E6-associated protein C-terminus), RING (really interesting new gene) finger and U-box (a modified RING motif without the full complement of Zn^{2+}-binding ligands) (Ardley and Robinson, 2005).

Ubiquitin modification can occur in three general ways: mono-ubiquitination (a single ubiquitin is attached), multi-mono-ubiquitination (several lysine residues are tagged with a single ubiquitin) and polyubiquitination (a chain of ubiquitins is attached to one or more lysines). Polyubiquitination is possible because there are seven lysines (Lys6, Lys11, Lys27, Lys29, Lys33, Lys48 and Lys63) in the ubiquitin molecule that can be involved in chain formation. Polyubiquitination on lysine 48 signals for proteasomal degradation of the substrate. However, other types of ubiquitin modification are involved in the regulation of different processes such as endocytosis and DNA repair (Figure 1.10) (Haglund and Dikic, 2005; Komander, 2009).

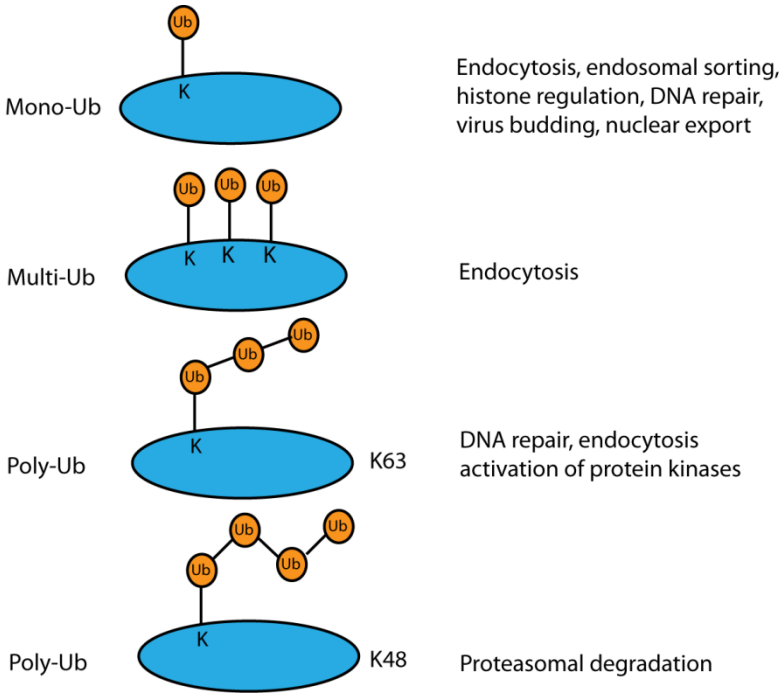

Figure 1.10 – Rotes of ubiquitin modifications in regulating proteins

Ubiquitination of proteins can lead to different outcomes depending on the ubiquitin modification and lysine involved. There are three general types of ubiquitination: mono-ubiquitination (a single ubiquitin is attached), multi-mono-ubiquitination (several lysine residues are tagged with a single ubiquitin) and polyubiquitination (a chain of ubiquitins is attached to one or more lysines). Mono and multi-mono-ubiquitination are involved in endocytosis, endosomal sorting, histone regulation, DNA repair, virus budding and nuclear export. Polyubiquitination on lysine 63 (K63) leads to DNA repair, endocytosis and activation of protein kinases while polyubiquitination on lysine 48 (K48) leads to proteasomal degradation.

1.2.2 Cullin3

Cullin3 is part of the cullin family. The cullin family is evolutionarily conserved throughout bacteria and eukaryotes. In mammals, there are seven cullins (Cul1, Cul2, Cul3, Cul4a, Cul4b, Cul5, Cul7) and the closely related p-53-associated parkin-like cytoplasmic protein (PARC). All members have a signature cullin homology domain (CH) of about 200 amino acids. Cullin1 to cullin5 are considered classic cullins and they consist of an amino-terminal domain (NTD) with three cullin repeats (CR1 to CR3) and a globular carboxy-terminal domain (CTD) with the CH domain (Sarikas et al., 2011). Cul7 and Parc are atypical cullins. Apart from the conserved CH domain, they have extra-domains such as DOC (destruction of cyclin B) domain and IBR (in-between-ring) domain (Chen et al., 2015) (Figure 1.11).

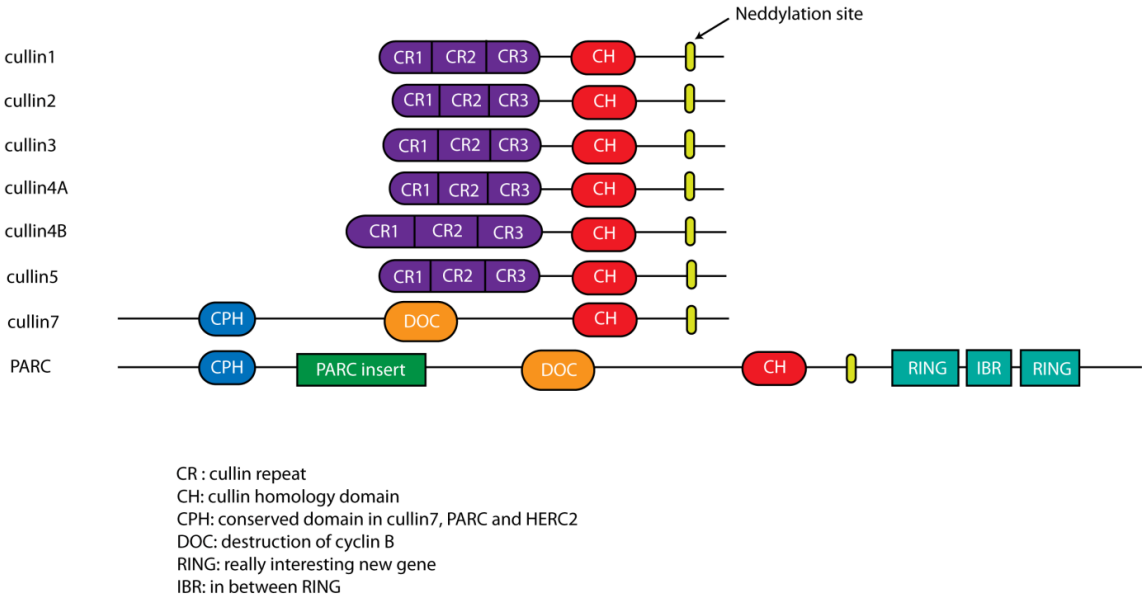

Figure 1.11 - Cullin proteins

Domain organization of cullin proteins in humans.

Cullins are molecular scaffolds of CULLIN-RING ubiquitin ligases (CRLs), the most prevalent class of E3 ubiquitin ligases. CRLs are composed by a cullin that serves as a link between the catalytic module, formed by a RING finger domain protein that is responsible for recruiting an ubiquitin loaded E2 ubiquitin-conjugating enzyme; and a specific substrate recognition module, formed by a substrate recognition protein and an adaptor protein (Genschik et al., 2013; Petroski and Deshaies, 2005). In the case of cullin3-RING ubiquitin ligases (CRL3s), BTB/POZ proteins are the adaptor proteins that bind to cullin3 and bring the substrate to the complex; and Roc1-Rbx1-Hrt1 is the RING component (Genschik et al., 2013). CRL3s can be regulated by mechanisms such as inhibition/activation of cullins, dimerisation of cullin3 with BTB proteins; and post-translational modification of substrates and adaptors (Genschik et al., 2013; Petroski and Deshaies, 2005).

Cullins can be covalently modified at a conserved lysine residue in their C-terminus by the attachment of an ubiquitin-like protein called NEDD8 (Figure 1.11). A sequential action of a NEDD8-activating enzyme (NAE), the APPBP1-UBA3 heterodimer, and a NEDD8-conjugating enzyme, UBC12, is required for the neddylation. Roc1, the RING finger domain protein of this complex, it is also required for the neddylation. NEDD8 is removed from cullins by the isopeptidase activity of the zinc-dependent metalloenzyme called CSN5, a component of the COP9 signalosome (CSN) complex (Duda et al., 2011; Genschik et al., 2013; Lyapina et al., 2001). Neddylation leads to changes in cullins leading to an “open” conformation. This increases recruitment of ubiquitin-charged E2 enzymes and facilitates the positioning of the E2 active site for ubiquitin transfer onto substrates (Boh et al., 2011; Duda et al., 2008; Duda et al., 2011; Genschik et al., 2013). Another mechanism to regulate CRLs is through the binding of cullin-associated and neddylation-dissociated protein 1 (CAND1) to deneddylated cullins. CAND1 inhibits CRL assembly and NEDD8 activation. It has been shown that the C-terminus of CAND1 binds to cullin1 in the site that recruits the adaptor complex

for substrate recognition; and the N-terminus of CAND1 binds at the junction between the RING component and cullin that is found only when cullin is deneddylated. CAND1 also binds directly to the lysine in cullin1 where NEDD8 is supposed to bind (Duda et al., 2011). Probably the same occurs with cullin3 since it has been shown that CAND1 can affect neddylation of cullin3 in *Drosophila* (Kim et al., 2010). It is believed that the neddylation/deneddylation cycle is important for the functionality of the cullin complex.

Several CRL3s can dimerise through the BTB domains of their BTB adaptor proteins. One example is the ubiquitination of Nrf2 by the Keap1-cullin3 complex. The dimerisation of Keap1 is crucial for the binding of the substrate to the complex (McMahon et al., 2006). Moreover, it has been reported that cullin3 (Wimuttisuk and Singer, 2007) and other cullins (Chew et al., 2007) can also dimerise (Figure 1.12). In the case of cullin3, a substrate recognition unit is necessary for the dimerisation to occur. Cullin3 constructs that were unable to bind to BTB adaptor proteins could not form dimers (Chew et al., 2007). The dimerisation is believed not only to be important for substrate recruitment, but also to increase the avidity for substrate and to increase the concentration of associated E2, leading to an increase in the catalytic rate of ubiquitination (Genschik et al., 2013).

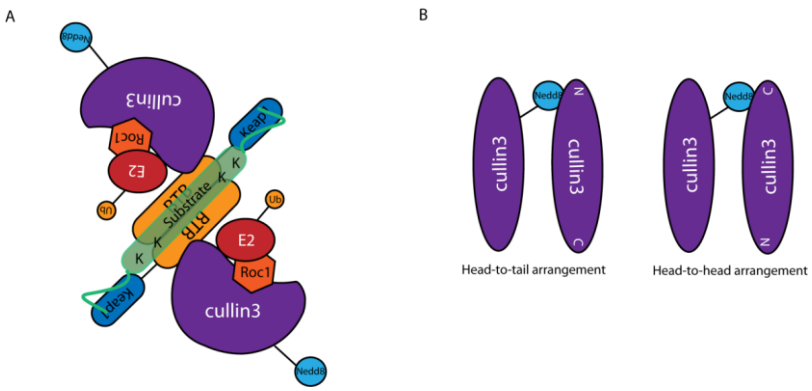

Figure 1.12 - Dimerization of BTB-protein and dimerisation of cullin3

A) CRL3 can dimerise through the BTB domains of their BTB adaptor proteins. One example is the ubiquitination of Nrf2 by the Keap1-cullin3 complex. The dimerisation of Keap1 is crucial for the binding of the substrate to the complex. B) Cullin3 can directly dimerise. A proposed model is that two cullins interact through the NEDD8 molecule attached to one of them.

Post-translational modification of substrates and adaptor proteins is also an important mechanism to regulate CRLs. Substrates can be phosphorylated, glycosylated, and/or prolyl hydroxylated. These modifications can promote or inhibit affinity of the substrate for the adaptor protein (Duda et al., 2011). Adaptor proteins can also undergo modifications that affect their activity. One example is the modification of thiol groups in Keap1 cysteine residues after oxidative stress, leading to a decrease in E3 activity (Genschik et al., 2013).

Cullin3 forms a BTB-cullin3-Rbx1 (BCR) ubiquitin ligase complex. This complex is best known to control the degradation of many proteins that are important in several cellular processes such as cell cycle, actin cytoskeleton regulation, apoptosis and oxidative stress (Bade et al., 2014; Furukawa and Xiong, 2005; Jin et al., 2009; Sumara et al., 2007). It has been reported that RhoA, RhoBTB2 and Tiam1 are substrates of BCR complexes (Berthold et al., 2008b; Chen et al., 2009; Genau et al., 2015; Wilkins et al., 2004). Recently cullin3 has been shown to be a regulator of the endolysosomal pathway. Knockdown of cullin3 leads to defects in trafficking of influenza A virus (IAV) and epidermal growth factor receptor (EGFR). However, the mechanisms through which cullin3 regulates endosome maturation are still unclear (Huotari et al., 2012).

Knockdown of RhoBTB1 in MDA-MB-231 cells led to a decrease in cancer cell interaction with endothelial cells *in vitro*, leading to decrease in cell adhesion and transendothelial migration (Chapter 3) (Borda D'Agua, 2012). A decrease in RhoA protein levels and activity was also observed, without affecting its mRNA levels (Borda D'Agua, 2012). The mechanistic basis for the effect of RhoBTB1 depletion on cancer cells remains to be determined. Because cullin3 is involved in RhoA degradation (Chen et al., 2009) and RhoBTB1 is known to interact with cullin3, the hypothesis is that RhoBTB1 protects RhoA from degradation and this affects cancer cell/endothelial cell interaction. In addition, RhoBTB1 will be characterized based on what is published for RhoBTB2 and other potential binding partners will be explored.

1.3 Aims of the project

RhoBTB1 depletion in MDA-MB-231 and PC3 cancer cells reduces their adhesion to endothelial cells and transendothelial migration. RhoBTB1 depletion was also reported to reduce RhoA protein expression levels in MDA-MB-231 cells (Borda D'Agua, 2012). Based on these results, the initial aims of this project were to test the role of RhoBTB1 in regulating the transendothelial migration of other breast cancer cell lines, to determine how RhoBTB1 regulates RhoA and how this relates to its function in transendothelial migration; and to investigate which targets of RhoBTB1 are critical for its effects on cancer-endothelial cell interaction and transendothelial migration.

The first step of the project was to optimise different breast cancer cell lines in the 2D and 3D models used in the laboratory to study cancer cell-endothelial cell interaction and transendothelial migration. After finding the best conditions for each cell line, RhoBTB1 would be depleted in these cell lines and the results would be compared with the ones obtained for MDA-MB-231 cells (Borda D'Agua, 2012). However, as shown in Chapter 3, two out of the three breast cancer cell lines selected did not seem suitable to be used to study endothelial interaction with the laboratory protocols. In addition, depletion of RhoBTB1 in Cal51 cells did not reproduce the results obtained with MDA-MB-231 cells: it did not decrease cancer cell adhesion to or intercalation between endothelial cells; or decrease RhoA expression.

For these reasons, this project focused subsequently on the characterization of RhoBTB1 signalling to RhoA and in the interaction of RhoBTB1 with RhoA and ROCK1.

2 Materials and Methods

2.1 Materials

2.1.1 Reagents and Kits

Table 2-1 Reagents and Kits

Reagents/Kits	Supplier
4-12% SDS-polyacrylamide gel (1.5 mm; 10 wells/15 wells)	Invitrogen
^{32}P-ATP	PerkinElmer Health Sciences B.V.
Agarose	Sigma
Ampicillin sodium salt	Sigma
Anti-c-Myc Agarose Affinity Gel antibody produced in rabbit	Sigma
Anti-FLAG® M2 Affinity Gel	Sigma
ATP, lithium salt 100 mM, pH 7	Roche
Bovine Collagen I	INAMED/BioMatrix
Brilliant III Ultra-Fast SYBR® Green QRT-PCR Master Mix	STRATAGENE, Agilent Technologies Division
Cell Dissociation Solution Non-enzymatic	Sigma
Carboxyfluorescein succinimidyl ester (CFSE)	Molecular Probes, Invitrogen
Complete, mini EDTA-free protease inhibitor cocktail	Roche Applied Science
Coverslips (13, 25 mm)	VWR
Cycloheximide	Calbiochem
Dako Pen, S2002	Dako Cytomation www.dako.com
DH5α	Invitrogen
Disuccinimidyl suberate (DSS) crosslinker	Thermo Scientific Pierce
DNA sample buffer (6x)	Promega
DNA-free™ DNAse Treatment Kit	Ambicon
dNTP Mix	Promega
Dried, skimmed milk	Marvel
Dulbeco's modified eagle medium (DMEM) (4500 mg/L glucose + 580 mg/L L-glutamine + 25 mM HEPES)	Gibco www.invitrogen.com
Enhanced chemiluminescence (ECL) reagent	GE Healthcare
EndoFree Maxiprep Kit	Qiagen
Endothelial cell basal medium-2 (EBM-2), supplemented with ascorbic acid, R3-IGF-1, heparin, rhFGF-B, hydrocortisone, GA-1000, rhEGF, VEGF, 2% fetal bovine serum. Supplements are provided as part of a bullet kit, purchased with the basal medium	Clonetics®, Lonza
Ethidium bromide	Sigma

Fetal calf serum (FCS)	Biosera www.biosera.com
Fibronectin	Sigma
Fluorescent mounting medium	Dako Cytomation www.dako.com
GFP-Trap®	chromotek www.chromotek.com
Glutatione Sepharose™	GE Healthcare
GST-ROCK1 17-535	SignalChem www.signalchem.com
Immobilion low fluorescence PVDF	Millipore
Isopropyl β-D-1-thiogalactopyranoside (IPTG)	Sigma
Kanamycin sulphate	Gibco
L-Broth	Sigma
LDS Sample Buffer 4x	Invitrogen
Lipofectamine™2000	Invitrogen
MG132 proteasomal inhibitor	Cambridge Biosciences
MLN4924 (NEDD8 E1 Activating Enzyme Inhibitor)	BostonBiochem, R&D Systems Company
Monoclonal Anti-HA Agarose Conjugate Clone HA-7	Sigma
Nitrocellulose membrane	Amersham
Oligofectamine™	Invitrogen
Opti-MEM + GlutaMax™-I	Gibco
Phosphate buffered saline (PBS) (-) $CaCl_2/MgCl_2$ ($PBS^{-/-}$) (+)$CaCl_2/MgCl_2$ ($PBS^{+/+}$)	Gibco
Penicillin (10.000 units/ml)/Streptomycin (10.000 µg/ml)	Gibco
Pfu DNA Polymerase	Promega
Phosphatase cocktail inhibitors (II and IV)	Calbiochem
Polyethylenimine (PEI)	Polisciences
Precision Plusprotein™ standards	Bio-Rad
ProQ® Diamond Phosphoprotein Blot Stain Kit	Invitrogen
Protein G Sepharose™ 4 Fast Flow	GE Healthcare
PureCol®	Advanced BioMatrix
Pyruvate 100 mM	Thermo Scientific
QIAEX II® Gel Extraction Kit	Qiagen
Quantum Prep® Plasmid Miniprep Kit	Bio-Rad
QuikChange II XL Site-Directed Mutagenesis Kit	Agilent Technologies, Inc
Rho Kinase Inhibitor (H1152)	Calbiochem
RNeasy Mini Kit	Qiagen
Roswell Park Memorial Institute (RPMI) 1640 (+ 3000 mg/L L-glutamine + 25 mM HEPES)	Gibco
SYPRO® Ruby Protein Blot Stain	Life Technologies
T4 DNA ligase	New England Biolabs (NEB)
ThinCert™, 8 µm pore	Greiner bio-one
Trypsin/EDTA 0.05%	Gibco

2.1.2 Buffers and solutions

Table 2-2 Buffers and solutions

Buffers and solutions	Composition
Lysis buffer	50 mM Tris-HCl pH 8, 150 mM NaCl, 5 mM EGTA, 1% Triton X-100, supplemented with protease inhibitor cocktail (Roche), 25 mM NaF (Thr/Ser phosphatase inhibitor), 2 mM Na_3VO_4 (Tyr phosphatase inhibitor)
IP lysis buffer	1% Triton X-100, 20 mM Tris pH 8, 130 mM NaCl, 1 mM DTT supplemented with protease inhibitor cocktail (Roche), 10 mM NaF (Thr/Ser phosphatase inhibitor) and phosphatase inhibitor cocktails II and IV (Sigma)
Mg^{2+} lysis buffer (5x)	125 mM Hepes pH 7.5, 750 mM NaCl, 5% NP-40, 50 mM $MgCl_2$, 5 mM EDTA
Mg^{2+} lysis buffer (1x) – Pull down	5x Mg^{2+} buffer supplemented with protease inhibitor cocktail (Roche), 1 mM PMSF and 10% glycerol
Buffer 1	200 mM Na_2HPO_4, 1.3 M NaCl, 90 mM NaOH. Addition of buffer 1 to liquid collagen catalyses matrix polymerisation
Cell lysis buffer	2% SDS, 150 mM NaCl, 10 mM Tris-HCl, pH 8.0 supplemented with 2 mM Na_3VO_4, 50 mM NaF and protease inhibitor cocktail (Roche)
Dilution buffer	10 mM Tris-HCl, pH 8.0, 150 mM NaCl, 2 mM EDTA, 1% Triton X-100
Washing buffer	10 mM Tris-HCl, pH 8.0, 1 M NaCl, 1 mM EDTA, 1% NP-40
NuPAGE MES SDS Running Buffer (20x)	1 M MES, 1 M Tris, 69.3 mM SDS,

	20.5 mM EDTA
Transfer buffer	25 mM Tris-HCl pH 8.3, 192 mM glycine, 20% methanol
Tris-buffered saline (TBS)	5 mM Tris-HCl pH 7.6, 50 mM NaCl
Tris-buffered saline – 0.1% Tween (TBS-T)	TBS 1x + 0.1% Tween-20
Stripping buffer	1 mM Tris-HCl, 0.15 M NaCl. Adjust to pH 2.0
Tris-acetate-EDTA (TAE) (50x)	2 M Tris, 57.1 ml/l Glacial Acetic Acid, 0.05 M EDTA pH 8
GST beads lysis buffer	10 mM MgCl, 1 mM DTT, 1 mM PMSF complete volume with TBS
GST beads washing buffer	10 mM MgCl, 1 mM DTT, 1 mM PMSF complete volume with TBS. Supplemented with protease inhibitor cocktail (Roche)
Kinase assay buffer (2x)	40 mM $MgCl_2$, 4 mM $MnCl_2$, 60 mM Tris pH 7.4
Kinase assay fixing solution	8.75% acetic acid, 25% ethanol
Freezing solution	90% FCS, 10% dimethyl sulphoxide (DMSO)
Fix solution (Pro-Q®)	7% acetic acid, 10% methanol
Destain Solution (Pro-Q®)	50 mM sodium acetate, pH 4.0, 20% acetonitrile
Conjugation buffer	20 mM Hepes, pH 7.0, 1% Triton X-100
Kanamycin 100x stock	50 mg in 1 ml of ddH_2O
Ampicillin 100x stock	100 mg in 1 ml of ddH_2O
IPTG (1M)	238 mg in 1 ml of ddH_2O

2.1.3 Antibodies

Table 2-3 Primary antibodies

Antigen	Species	Dilution	Supplier
CD29 (β1 integrin)	mouse	WB (1:1000)	BD
p-cofilin (Ser3)	rabbit	WB (1:1000)	Cell Signalling Technologies
cofilin	rabbit	WB (1:1000)	Cell Signalling Technologies
cullin3	mouse	WB (1:1000)	BD
FLAG M2	rabbit	WB (1:1000)	Sigma
GFP (B-2)	mouse	WB (1:1000)	Santa Cruz
GFP (FL)	rabbit	WB (1:1000)	Santa Cruz
GAPDH	mouse	WB (1:10000)	Millipore
HA (3H10)	rat	WB (1:1000)	Roche
p-LIMK1/2	rabbit	WB (1:1000)	Cell Signalling Technologies
LIMK1	rabbit	WB (1:1000)	Cell Signalling Technologies
p-MLC2 (Thr18/Ser19)	rabbit	WB (1:1000)	Cell Signalling Technologies
MLC2	rabbit	WB (1:1000)	Cell Signalling Technologies
myc (9E10)	mouse	WB (1:1000	Santa Cruz
myc (A14)	rabbit	WB (1:1000)	Santa Cruz
PECAM-1 (CD31 – clone JC70A)	mouse	IF (1:100)	Dako
RhoA	rabbit	WB (1:1000)	Cell Signalling Technologies
ROCK1	mouse	WB (1:1000)	BD
ROCK2	mouse	WB (1:1000)	BD

WB: western blot; IF: immunofluorescence

Table 2-4 Secondary antibodies and reagents

Antigen	Species	Conjugate	Dilution	Supplier
mouse IgG	sheep	Horse radish peroxidase	1:5000	GE Healthcare
rabbit IgG	donkey	Horse radish peroxidase	1:5000	GE Healthcare
rat IgG	goat	Horse radish peroxidase	1:5000	GE Healthcare
mouse IgG (H+L)	goat	Alexa Fluor® 546	1:1000	Molecular Probes™
phalloidin		Alexa Fluor® 546	1/400	Molecular Probes™
phalloidin		Alexa Fluor® 633	1/40	Molecular Probes™
DAPI		N/A	1/10000	Molecular Probes™

2.1.4 Oligonucleotides

Table 2-5 siRNAs

Gene Symbol	Oligo number	Sequence
control	control siRNA	UUCUCCGAACGUGUCACG
cullin3	#3	CCGAACAUCUCAUAAAUAA
	#5	GAGAUCAAGUUGUACGUUA
RhoA	#1	AUGGAAAGCAGGUAGAGUU
	#2	GAACUAUGUGGCAGAUAUC
RhoBTB1	#1	AAAUGAAGCUGCCUGUUUA
	#2	GAACUUGGCUUACCAUACU
	#3	GGACGUGACAUUUAAAUUG
	#4	GAACACCCGUUAUCCUUGU
ROCK1	#2	GAAGAAACAUUCCCUAUUC
	#3	GAGAUGAGCAAGUCAAUUA
ROCK2	#5	GCAAAUCUGUUAAUACUCG
	#9	CAAACUUGGUAAAGAAUUG

Table 2-6 qPCR primers

Primer		Sequence 5'-3'
RhoBTB1	forward	CAAGCAGTATTGGATTATCTC
	reverse	TGGTCAACTCCTGAACGG
ROCK1	forward	CATGGTGATGGAATACATGC
	reverse	GTTATCAGGCTTCACATCTC
ROCK2	forward	GCATGGTACATTGTGATACAG
	reverse	CCCACTAGCATCTCATAAAG
GAPDH	forward	GTGAAGGTCGGAGTCAACG
	reverse	TGAGGTCAATGAAGGGGTC

Table 2-7 Mutagenesis primers

Mutagenesis primers		Sequences 5'-3'
S69A	forward	GAGGTCTTGGAGCGTGCTCGGGATGTTGTTG
	reverse	CAACAACATCCCGAGCACGCTCCAAGACCTC
T398A	forward	GGATGGGGCCCATGGCTGTGGTCAGGATG
	reverse	CATCCTGACCACAGCCATGGGCCCCATCC
S480A	forward	CGGATAAAAGAGTGTCTCGCCAAGGGAACGTTCTCGGA
	reverse	TCCGAGAACGTTCCCTTGGCGAGACACTCTTTTATCCG
T483A	forward	GTGTCTCAGCAAGGGAGCGTTCTCGGACGT
	reverse	ACGTCCGAGAACGCTCCCTTGCTGAGACAC
S480A T483A	forward	TCGGATAAAAGAGTGTCTCGCCAAGGGAGCGTTCGCGG ACGTGACATTTAAATT
S485A	reverse	AATTTAAATGTCACGTCCGCGAACGCTCCCTTGGCGAGA CACTCTTTTATCCGA

Table 2-8 Cloning primers

Cloning primers	Sequences 5'-3' (containing restriction enzyme site)
XhoI RhoBTB1 1-210/1-427 (Forward)	CCGCTCGAGATGGACGCTGACATGGACTAC
EcoRI RhoBTB1 1-210 (Reverse)	CGGAATTCTCAGGAAATCAGCGCTGCTCGG
EcoRI RhoBTB1 1-427 (Reverse)	CGGAATTCTCATTCCTTTTCATCCAGTTGTCCCG
HindIII RhoBTB1 266-696 (Forward)	CCGAAGCTTGCCGATGTTCTGTTCATCCTTCAG
HindIII RhoBTB1 485-696 (Forward)	CCGAAGCTTTCGGACGTGACATTTAAATTGGACG
BamHI RhoBTB1 266-696/485-696 (Reverse)	CGGGATCCTCAGGCCACTGCTGGAGATGAATTCC
HindIII BACURD1 (Forward)	CCGAAGCTTATGTCGGCGGAGGCCT
EcoRI BACURD1 (Reverse)	CGGAATTCTCATCAGTCCTTGAAGACAATTTGTTGGCC

Table 2-9 Sequencing primers

Sequencing primers	Sequences 5'-3'
RhoBTB1 forward 1	CACGCAGTATCAGCTGCTG
RhoBTB1 forward 2	CCACCGGTCATCAAATTCCAG
RhoBTB1 forward 4	GCACCACATCTGCACCAACT
RhoBTB1 forward 5	GAGAAGCAGAGCAGAGATTTC
RhoBTB1 reverse 1	GCCTGAGAGAAACACTCACTTC
BACURD1 forward 1	GAGGTTGGGTGCTGATTGAC

2.1.5 Plasmids

Table 2-10 Expression plasmids

Construct	Provided by
pCAG-myc-ROCK1	Professor Shuh Narumiya
pCAG-myc-ROCK1 1-1080	Professor Shuh Narumiya
pCAG-myc-ROCK1 1-727	Professor Shuh Narumiya
pCAG-myc-ROCK1 1-727 (K105A)	Dr Ritu Garg
pCAG-myc-ROCK1 1-540	Dr Ritu Garg
pCAG-myc-ROCK1 1-420	Dr Ritu Garg
pCAG-myc-ROCK1 1096-1354	Dr Ritu Garg
pCAG-myc-ROCK1 375-727	Dr Ritu Garg
pCAG-myc-ROCK2	Professor Shuh Narumiya
CB6-GFP-RhoA	Dr Ferran Valderrama
pEGFP-RhoA-V14	Dr Ferran Valderrama
pEGFP-RhoA-N19	Dr Ferran Valderrama
pCMV5-FLAG-RhoA-N19	Dr Giles Cory
pRK5-myc-RhoBTB1	Dr Pontus Aspenström
pGEX2T-RhoBTB1 1-301	Dr Brad McColl
pEGFP-RhoBTB2	Dr Ritu Garg
pCMV-HA-ubiquitin	Dr Matthias Krause

2.1.6 Restriction Enzymes

Table 2-11 Restriction enzymes

Restriction Enzyme	Restriction site 5'-3'	Supplier
BamHI	GGATCC	New England Biolabs (NEB)
BglII	AGATCT	NEB
EcoRI	GAATTC	NEB
HindIII	AAGCTT	NEB
NotI	GCGGCCGC	NEB
XhoI	CTCGAG	NEB

2.1.7 Software

Software	Supplier
Illustrator CS3	Adobe
ImageJ	National Institutes of Health (NIH)
LSM + Zen Software	Zeiss
Volocity	Perkin Elmer, Improvision
MxPro	Agilent Technologies
GraphPad Prism 4	GraphPad Software

2.2 Methods: molecular biology

2.2.1 Transformation of Escherichia coli (E. coli)

100 ng of plasmid DNA were added to 50 µl of competent DH5α in a 1.5 ml microtube and incubated on ice for 30 minutes. The bacterial suspension was heat-pulsed at 42°C for 45 seconds and then left on ice for 2 minutes. 800 µl of antibiotic-free L-Broth (LB) was added into the microtube and the cells were grown at 37°C for 1 hour. The microtubes were centrifuged and the pellet was resuspended in 100 µl. The cells were plated onto LB agar plates containing the appropriate antibiotic (100 µg/ml ampicillin or 50 µg/ml kanamycin) and incubated at 37°C overnight.

2.2.2 Extraction of plasmid DNA from bacteria

For small-scale production of plasmid DNA, Quantum Prep® Plasmid Miniprep Kits were used following the manufacturer's instructions. A single colony from an agar plate was transferred to 2 ml of LB medium containing 100 µg/ml ampicillin or 50 µg/ml

kanamycin. The culture was incubated overnight at 37°C. 1.5 ml of the overnight culture was transferred to a microtube and the cells were pelleted by centrifugation at 14,000 g for 30 secs. The supernatant was removed and 200 µl of cell resuspension solution was added. After mixing up and down until the cell pellet was completely resuspended, 250 µl of cell lysis solution was added and the microtube inverted gently. Immediately after 250 µl of neutralization solution was added and the cell debris was removed by centrifugation at 14,000 g for 5 minutes. The supernatant was transferred into a spin filter placed on a 2 ml tube. 200 µl of Quantum Prep matrix was added and solutions were mixed pippeting up and down. Tubes were centrifuged at 14,000 g for 30 secs. The filtrated was discarded and 500 µl of wash buffer was added into the spin filter. Tubes were centrifuged at 14,000 g for 30 secs. The filtrated was discarded and 500 µl of wash buffer was added again into the spin filter. Tubes were centrifuged at 14,000 g for 2 minutes. The spin filter was placed in a new 1.5 ml collection and 100 µl of TE were added into spin filter. Samples were centrifuged for 1 minute at 14,000 g to elute the DNA.

2.2.3 Determination of DNA concentration

DNA concentration was determined spectrophotometrically using a Nano-Drop system (ND-1000, www.nanodrop.com). 1.5 µl of sample was pipetted onto the end of a fibre optic cable and the optical density (OD) was measured at 260 nm. The DNA concentration in ng/µl was automatically determined using the following formula: concDNA = OD260 x 50 µg/ml (Sambrook and Russel, Molecular Cloning, 3rd Edition).

2.2.4 DNA amplification using Polymerase Chain Reaction (PCR)

The PCR reaction containing 20 ng of DNA template, Pfu DNA Polymerase 10x Reaction Buffer with $MgSO_4$, 25 pmol of each forward and reverse primers, 0.2 µM of each nucleotide (dATP, dTTP, dGTP and dCTP) was heated at 94ºC for 1 minute

before the Pfu DNA Polymerase was added. The PCR conditions were 94ºC for 45 secs, 50ºC for 1 minute and 72ºC for 2 minutes per kb for 35 cycles.

2.2.5 Ethanol precipitation of DNA

To purify and concentrate DNA, a 1:10 volume of 3 M sodium acetate pH 5.2 and a 2.5 volume of cold 100% ethanol were added to the PCR product (section 2.2.4). The solution was incubated overnight at -20ºC. To recover the precipitated DNA the sample was centrifuged at 17,000 g for 10 minutes. The supernatant was discarded and the DNA pellet was washed with 500 µl of 80% ethanol. The sample was centrifuged at 17,000 g for 10 minutes. The supernatant was discarded. The DNA pellet was air-dried and resuspended in distilled water.

2.2.6 Digestion of DNA using restriction enzymes

Plasmid DNA (0.5 to 2 µg) was digested using 1 unit/µg of restriction enzyme for 1 – 3 hours at 37°C. When necessary the restriction enzyme was inactivated for 20 minutes at 65°C or 80°C. NEBcutter V2.0 (http://tools.neb.com/NEBcutter2/) and Double Digest Finder (https://www.neb.com/tools-and-resources/interactive-tools/double-digest-finder) tools were used to determined suitable enzymes and the best conditions for each digestion, respectively. After each digestion, an amount of the restriction product and the undigested DNA were resolved on a 1% agarose gel.

2.2.7 Agarose gel electrophoresis

DNA fragments were separated depending on their molecular weight using 1% agarose gels. The gels were prepared dissolving agarose in 1x TAE buffer by boiling the mixture in a microwave oven. The solution was cooled down and poured into a gel tank containing a well comb. Ethidium bromide (0.5 µg/ml) was added before the gel was solid. Ethidium bromide binds to the DNA allowing the visualization of DNA fragments on a UV-transilluminator. After the gel solidified, DNA samples were diluted in 6x DNA

sample buffer and loaded into the wells. A 1 kb DNA ladder was run in parallel to identify the sizes of DNA fragments. Electrophoresis was carried out at 10-15 V/cm^2 until fragments were separated.

2.2.8 Extraction of DNA from agarose gels

Ethidium bromide-integrated DNA bands were visualised using UV light. Bands of interest were excised using a scalpel blade and the gel pieces were transferred to a 1.5 ml microtube. QIAEX II® Gel Extraction Kit was used to recover the DNA. Gel pieces containing DNA were incubated with 3 volumes (3 times the weight of the gel pieces) of Buffer QX1. 5 µl of QIAEX II beads were added to the microtube. Samples were incubated at 50ºC for 10 minutes (vortexing every 2 minutes) to solubilise the agarose and bind the DNA. Samples were centrifuged at 5,000 g for 30 secs. Supernatant was discarded and 500 µl of Buffer PE was added to wash the pellet (beads containing the DNA). Samples were centrifuged at 5,000 g for 30 secs. Supernatant was discarded and the pellet was air-dried for 15 minutes. To elute the DNA, 8 µl of distilled water was added. Samples were heated at 50ºC for 5 minutes (vortexing every 2.5 minutes). Samples were centrifuged at 17,000 g for 30 secs. The supernatant containing the DNA was transferred to a new microtube. The DNA was used immediately for the ligation reaction or stored at -20ºC.

2.2.9 DNA ligation

DNA fragments were ligated into the desired vector using 400 units of T4 DNA ligase in 1x T4 DNA Ligase Reaction Buffer at 16ºC for 16 hours. The ratio of insert and vector was 3:1. The following website was used to calculate the amount of insert that should be used considering the amount of vector was 25 ng: http://www.insilico.uni-duesseldorf.de/Lig_Input.html. DH5α competent cells were transformed with the product of the reaction (section 2.2.1). The next day 2-6 colonies from the agar plates were transferred to 2 ml of LB containing the appropriate antibiotic and incubated at

37ºC overnight. Plasmid DNA was extract from the bacteria (section 2.2.2) and the presence of the gene of interest was confirmed by sequencing (section 2.2.11).

2.2.10 Site-directed mutation

Single or multiple amino acid substitutions were introduced into myc-RhoBTB1 using QuikChange II XL Site-Directed Mutagenesis Kit following the manufacturer's instructions. Forward and reverse primers were designed using QuikChange Primer Design Program (http://www.genomics.agilent.com/). The primers were approximately 25 to 45 bases in length, contained the appropriated altered base, and had a minimum GC content of 40% and a predicted melting temperature (Tm) of > 78ºC. PCR reactions contained 10 ng of DNA template, 125 ng of each primer, 1 µl of dNTP mix, 5 µl of 10x reaction buffer and 3 µl of QuikSolution reagent in a total reaction volume of 50 µl. 1 µl of *PfuUltra* HF DNA polymerase (2.5 U/µl) was added to each sample reaction just before the PCR started. PCR conditions were 95ºC for 1 minute for 1 cycle; 95ºC for 50 secs, 60ºC for 50 secs, and 68ºC for 1 minute per kb of plasmid length for 18 cycles; 68ºC for 7 minutes for 1 cycle. 1 µl of Dpn I restriction enzyme (10 U/µl) was added to the PCR product to digest methylated wild-type parental DNA. The digestion was carried out at 37ºC for 1 hour. XL10-Gold ultracompetent cells were transformed with 2 µl of Dpn I-treated DNA (section 2.2.1). The next day 2-6 colonies from the agar plates were transferred to 2 ml of LB containing the appropriate antibiotic and incubated at 37ºC overnight. DNA was extract from the bacteria (section 2.2.2) and the correct mutational changes were confirmed by sequencing (section 2.2.11).

2.2.11 Sequencing

DNA sequencing was carried out by MWG-Biotech (http://www.mwg-biotech.com/). DNA template and primers were sent to the company and results were returned by e-mail.

2.2.12 GFP-RhoBTB1 and GFP-RhoBTB1 S3T2A subcloning

RhoBTB1 cDNA was subcloned from a myc-pRK5 to a pEGFP-C1 vector. pEGFP-C1 was digested using BglII and HindIII and pRK5-myc-RhoBTB1 or pRK5-myc-RhoBTB1 S69A/T398A/S480A/T483A/S485A (S3T2A) was digested using BamHI and HindIII. Fragments were separated on agarose gels (section 2.2.7). After extraction of DNA from the gels (section 2.2.8), RhoBTB1 cDNA was ligated into pEGFP-C1 (section 2.2.9). Competent DH5α cells were transformed (section 2.2.1) with 10 µl of ligation reaction. Clones were verified by sequencing (section 2.2.11).

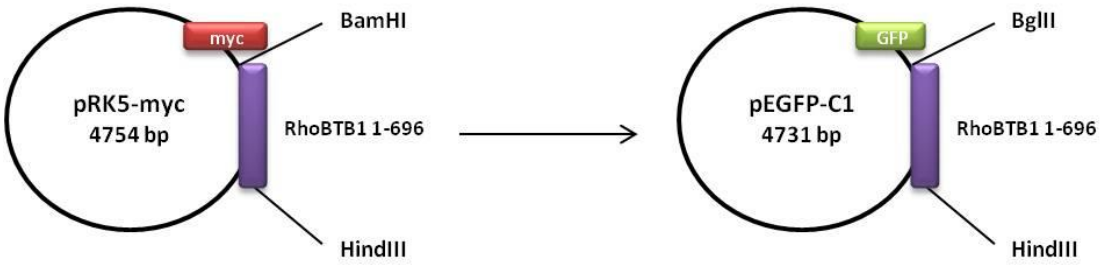

Figure 2.1 - Schematic diagram of RhoBTB1 subcloning into pEGFP-C1
pRK5-myc-RhoBTB1 was digested with BamHI and HindIII restriction enzymes; and pEGFP-C1 was digested with BglII and HindIII restriction enzymes. RhoBTB1 was ligated into pEGFP-C1 using T4 DNA ligase.

2.2.13 Cloning of KCTD13 (BACURD1) into N-GFP-CB6 vector

N-GFP-CB6-BACURD1 was prepared using PCR. pBlueScript-KCTD13 (GE Healthcare) was used as a template. BACURD1 was amplified by PCR using primers HindIII BACURD1 (Forward)/ EcoRI BACURD1 (Reverse). The PCR products were obtained as described in section 2.2.4. PCR products and N-GFP-CB6 vector were digested with HindIII and EcoRI (2.2.6). BACURD1 fragment was ligated into N-GFP-CB6 vector using T4 DNA ligase (2.2.9). Competent DH5α cells were transformed (section 2.2.1) with 10 µl of ligation reaction. Clones were verified by sequencing (section 2.2.11).

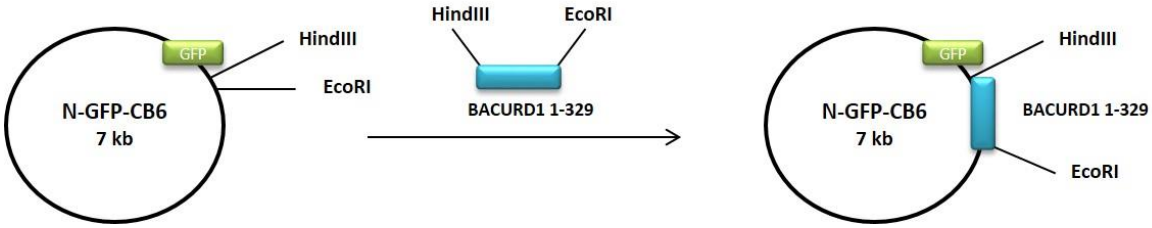

Figure 2.2 - Schematic diagram of BACURD1 cloning into N-GFP-CB6

BACURD1 fragment and N-GFP-CB6 were digested with HindII and EcoRI restriction enzymes. BACURD1 fragment was ligated into N-GFP-CB6 using T4 DNA ligase.

2.2.14 Construction of RhoBTB1 1-210, RhoBTB1 1-427, RhoBTB1 266-696 and RhoBTB1 485-696 fragments using N-GFP-CB6 vector

N-GFP-CB6-RhoBTB1 1-210, N-GFP-CB6-RhoBTB1 1-427, N-GFP-CB6-RhoBTB1 266-696 and N-GFP-CB6-RhoBTB1 485-696 constructs were prepared using PCR. pRK5-myc-RhoBTB1 was used as a template. RhoBTB1 1-210 and RhoBTB1 1-427 were amplified by PCR using primers XhoI RhoBTB1 1-210/1-427 (Forward)/ EcoRI RhoBTB1 1-210 (Reverse) and XhoI RhoBTB1 1-210/1-427 (Forward)/ EcoRI RhoBTB1 1-427, respectively. RhoBTB1 266-696 and RhoBTB1 485-696 were amplified by PCR using primers HindIII RhoBTB1 266-696 (Forward)/ BamHI RhoBTB1 266-696/485-696 (Reverse) and HindIII RhoBTB1 485-696 (Forward)/ BamHI RhoBTB1 266-696/485-696 (Reverse), respectively. The PCR products were obtained as described in section 2.2.4. For RhoBTB1 1-210 and RhoBTB1 1-427, PCR products and N-GFP-CB6 vector were digested with XhoI and EcoRI (section 2.2.6). For RhoBTB1 266-696 and RhoBTB1 485-696, PCR products and N-GFP-CB6 vector were digested with HindIII and BamHI (section 2.2.6). RhoBTB1 fragments were ligated into N-GFP-CB6 vector using T4 DNA ligase (section 2.2.9). Competent DH5α cells were transformed (section 2.2.1) with 10 µl of ligation reaction. Clones were verified by sequencing (section 2.2.11).

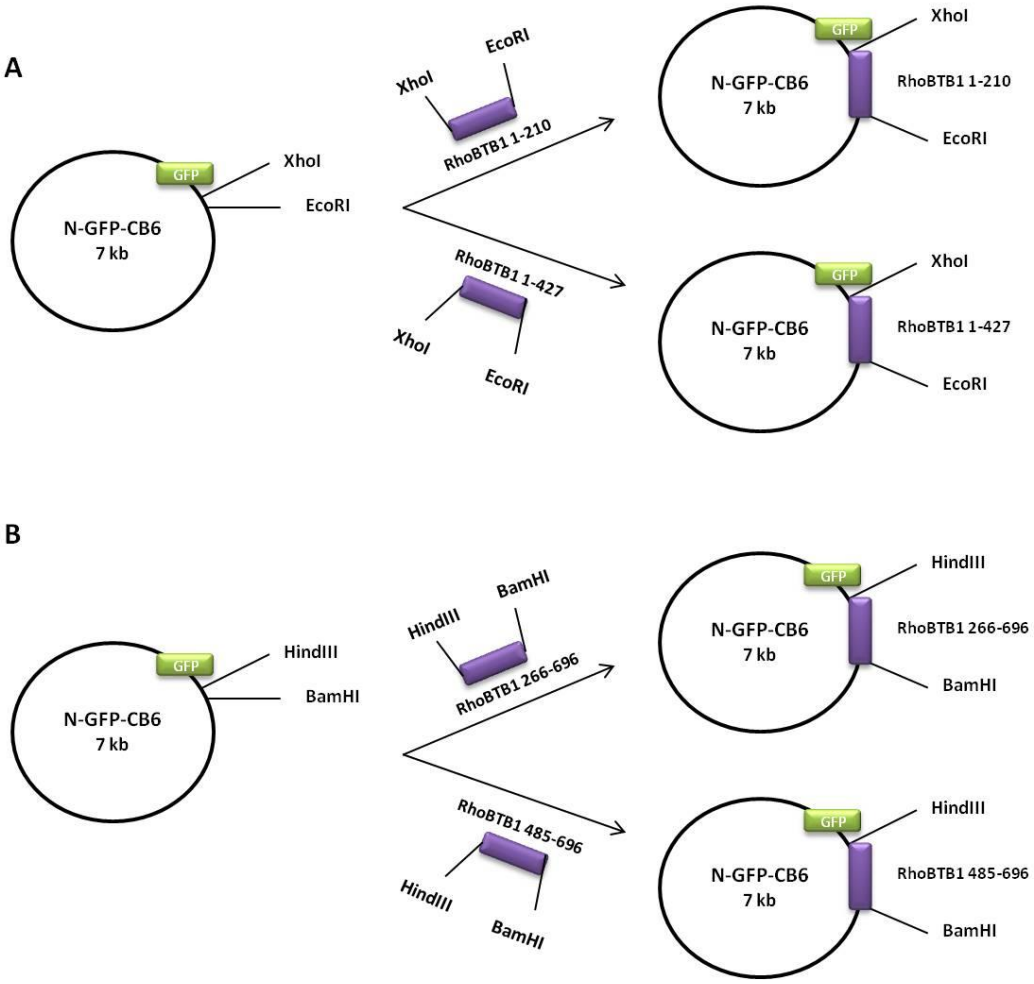

Figure 2.3 - Schematic diagram of RhoBTB1 cloning into N-GFP-CB6

A) RhoBTB1 fragments and N-GFP-CB6 were digested with XhoI and EcoRI restriction enzymes. B) RhoBTB1 fragments and N-GFP-CB6 were digested with HindIII and BamHI restriction enzymes. RhoBTB1 fragments were ligated into N-GFP-CB6 using T4 DNA ligase.

2.2.15 Extraction of total RNA from mammalian cells

Extraction of total RNA from cells was performed using the RNeasy Mini Kit following the manufacturer's instructions. After 72 hours of siRNA transfection cells were washed twice with cold $PBS^{-/-}$ and 350 µl of RLT buffer were added to each well. Cells were scraped and lysates were transferred to a 1.5 ml microtube. 350 µl of 70% ethanol were added to each tube and samples were homogenized by pipetting. The total 700 µl was transferred to an RNeasy spin column placed on a 2 ml collection tube. Samples were centrifuged for 15 s at 8,000 g. The filtrated was discarded and 700 µl of RW1

buffer were added to the spin column. Samples were centrifuged for 15 secs at 8,000 g. In this step there is enrichment in mRNA, since RNAs smaller than 200 nucleotides are excluded from the silica-based membrane. The filtrated was discarded and 500 µl of RPE buffer were added to the spin column. Samples were centrifuged for 15 secs at 8,000 g to wash the spin column membrane. The filtrated was discarded and the spin column membrane was washed again with 500 µl of RPE buffer. Samples were centrifuged for 2 min at 8,000 g. The spin column was placed in a new 1.5 ml collection tube and 30 µl of RNase-free water were added directly to the spin column membrane. Samples were centrifuged for 1 minute at 8,000 g to elute the RNA.

RNA was purified using a DNA-free™ DNAse Treatment Kit, in order to remove contaminating DNA. 0.1 volume of 10x DNAse1 buffer and 1 µl of DNAse1 were added to the RNA. Samples were gently mixed and incubated at 37ºC for 30 minutes. 0.1 volume of DNA Inactivation Reagent beads were added and samples were incubated for another 2 minutes at 37ºC. Samples were centrifuged for 1 minute at 10,000 g. The supernatant was transferred into a new 1.5 ml microtube. RNA concentration was determined using a Nano-Drop spectrophotometer by determining the absorbance at 260 nm. Samples were stored at -80ºC or immediately used.

2.2.16 qPCR

Extraction of mRNA (section 2.2.15) from the cells was performed 72 hours after siRNA transfection (section 2.3.1.3). qPCR was carried out using Brilliant III Ultra-Fast SYBR® Green QRT-PCR Master Mix. qPCR reactions contained 100 ng of experimental RNA, 2x SYBR Green QRT-PCR master mix, 300 mM of each primer, 1 mM DTT and 1 µl of RT/RNase block. Each condition was carried out in triplicate and GAPDH was used as a reference gene (internal control). The assay was carried out using the Stratagene MX3500P™ sequence detection system and the amplification cycles were carried out following the manufacturer's instructions: 50ºC for 10 minutes for 1 cycle (cDNA

synthesis); 95ºC for 3 minutes for 1 cycle; 95ºC for 10 secs and 60ºC for 20 secs for 40 cycles; 95ºC for 15 secs, 60ºC for 20 secs and 95ºC for 15 secs for 1 cycle (dissociation stage). The dissociation stage was added in order to obtain the dissociation curve and confirm that each primer pair amplified only one single product. For the analysis of raw data the MxPro software was used. Quantification of the amplified cDNA was achieved by comparing the number of amplification cycles (Ct) after which the fluorescent signal crossed a threshold level. The following formula was applied to quantify the results:

$$2^{-\Delta\Delta CT} = [(\text{Ct gene of interest} - \text{Ct internal control}) \text{ sample A} - (\text{Ct gene of interest} - \text{Ct internal control}) \text{ sample B})]$$

2.3 Methods: cell biology

2.3.1 Cell culture

2.3.1.1 Thawing and freezing cells

To thaw cells, a cryovial was taken from liquid nitrogen and thawed at 37ºC in a waterbath. The cells were then transferred to a 75 cm^2 tissue culture flask and 10 ml of the appropriate cell culture medium was added. The medium was changed the next day. In the case of cell lines, cells were passaged at least two times before being used for experiments. In the case of primary human umbilical vein endothelial cells (HUVECs), cells were used between passage 1-4.

To freeze cells, cells were detached using trypsin and pelleted at 800 g for 5 minutes. Cells from a 75 cm^2 flask were resuspended in 1 ml of freezing solution and aliquoted into cryovials. Cryovials were inserted into a cryo freezing container and stored at -80ºC to allow slow freezing overnight. The cells were then transferred to liquid nitrogen for long-term storage.

2.3.1.2 Growing and passaging cells

Cells were grown using different protocols depending on the cell type. HUVECs were grown on fibronectin-coated flasks (10 µg/ml in $PBS^{+/+}$ for 1 hour at 37ºC) in EBM-2 at 37ºC and 5% CO_2. Medium was replaced 24 hours after thawing. HUVECs were passaged by removing the medium from the flask and washing cells with $PBS^{-/-}$. Cells were detached with 1 ml of trypsin/EDTA at 37ºC for 3 minutes and 9 ml of medium were added to the flask to inactivate the trypsin. Cells were diluted to the desired concentration and added to a new flask with fresh medium. Cells were not diluted more than 1:4 during passage. PC3 cells (kind gift from Prof John Masters) and HCC1954 (kind gift from Prof Joy Burchell) were grown in RPMI containing 10% FCS and penicillin (100 IU/ml)/ streptomycin (100 µg/ml); MDA-MB-231, MCF-7, Cos7, Hela (kind gift from Prof Ulrike Eggert) and HEK293 cells were grown in DMEM containing 10% FCS, penicillin (100 IU/ml)/ streptomycin (100 µg/ml) and 1% pyruvate; and Cal51 cells were grown in DMEM containing 20% FCS, penicillin (100 IU/ml)/ streptomycin (100 µg/ml) and 1% pyruvate. Cells were grown at 37ºC and 5% CO_2. For passaging, cells were washed with $PBS^{-/-}$ and incubated with 1 ml of trypsin/EDTA at 37ºC until they detached. 9 ml of growth medium were added to inactivate trypsin and cells were diluted 1/10 or 1/5, according to their growth rate. Cells were passaged every 3-4 days, depending on their confluence.

2.3.1.3 Synthetic siRNA transfection using Oligofectamine™

Cells were transfected on a 6-multiwell plate with different siRNA oligonucleotides using Oligofectamine™ (following the manufacturer's instructions). The desired volume of siRNA from a 20 µM stock solution was diluted in 200 – 500 µl of Opti-MEM (solution A) while the desired volume of Oligofectamine™ (1.3 times the volume of siRNA) was added to 200 – 500 µl of Opti-MEM (solution B). The final concentration of siRNA used was 50 nM. Solutions were incubated for 5 minutes at room temperature (RT). Solution

B was mixed into solution A and incubated for 20 minutes. The medium of the cells was replaced by medium without antibiotics and immediately after the mixture of solution A and B was added drop wise to the well. After 6 hours, the transfection medium was replaced for a fresh complete medium. After 48 or 72 hours of transfection, cells were either used for the motility assays, or lysed for mRNA extraction or for cell lysate preparation.

2.3.1.4 DNA transfection using Lipofectamine™2000

MDA-MB-231 and Hela cells were transfected on a 6-multiwell plate or on a 10 cm dish with different DNA plasmids using Lipofectamine™2000 (following the manufacturer's instructions). The desired amount of DNA plasmid was diluted in 200 – 500 µl of Opti-MEM (solution A) while the desired volume of Lipofectamine™2000 (ratio 1 µg of DNA: 2 µl of Lipofectamine™2000) was added to 200 – 500 µl of Opti-MEM (solution B). Solutions were incubated for 5 minutes at RT. Solution B was mixed into solution A and incubated for 20 minutes. The medium of the cells was replaced by medium without antibiotics and immediately after the mixture of solution A and B was added drop wise to the well or dish. After 6 hours, the transfection medium was replaced for a fresh complete medium. After 24 or 48 hours of transfection, cells were either lysed for cell lysate preparation or fixed for immunostaining.

2.3.1.5 DNA transfection using PEI

Cos7 cells were transfected on a 10 cm dish with different DNA plasmids using polyethylenimine (PEI). The desired amount of DNA plasmid was diluted in 1 ml of Opti-MEM together with PEI in a ratio of 1 µg of DNA: 4 µl of PEI. The mixture was incubated for 20 minutes and added drop wise to the dish. After 24 hours, cells were lysed for cell lysate preparation.

2.3.2 Treatment of cells with inhibitors

MLN4924 treatment: Cells were treated for 2 hours with 1 µM or 2 µM of MLN4924 (dissolved in DMSO) diluted in complete medium. As control, cells were treated in parallel with same volume of DMSO.

H1152 treatment: Cells were treated for 4 hours with 5 µM H1152 (dissolved in ddH_2O) diluted in complete medium.

Cycloheximide treatment: Cells were treated for 6 hours with 50 µg/ml cycloheximide (dissolved in DMSO) diluted in complete medium.

MG132 treatment: Cells were treated for 4 hours with 10 µM MG132 inhbitor (dissolved in DMSO) diluted in complete medium.

2.3.3 Morphology assay

2.3.3.1 3D-Morphology-Based assay

The protocol was based on an assay established in the laboratory (Colomba and Ridley, 2014; Reymond et al., 2012). A 96-well plate was coated with 40 µl of a 7.5 mg/ml Matrigel solution. The plate was incubated at 37°C for 1 hour. Cancer cells transfected with siRNA oligonucleotides 48 hours before the assay were detached using trypsin, counted and re-suspended in the appropriated medium without FCS in a final concentration of 5 x 10^6 cells/ml. For each well, 100 µl of cancer cells and 100 µl of a 7 mg/ml Matrigel solution were mixed by pipetting up and down. The 200 µl of cells mixed with the Matrigel was transferred into one of the wells in the Matrigel-coated plate. The plate was incubated at 37°C. After 2 hours, 100 µl of appropriated medium without FCS was added to each well. The plate was kept in the incubator at 37°C for 24 hours. Images were acquired using a Nikon TE2000-E microscope with a Plan Fluor 10x objective (Nikon) and a Hamamatsu Orca-ER digital camera.

2.3.4 Motility and Transmigration assays

2.3.4.1 Adhesion assay

The protocol was based on an assay established in the laboratory (Borda D'Agua, 2012; Reymond et al., 2012). 96-well plates were coated with collagen I (50 µg/ml for 1 hour at 37ºC) and HUVECs were seeded to form a monolayer one day before the experiment. Cancer cells labelled with CFSE (10 µM)/$PBS^{+/+}$ solution were detached using non-enzymatic dissociation solution and seeded so that each condition could be tested in triplicate. Some extra wells were left without cancer cells to allow HUVEC auto-fluorescence to be determined. Cancer cells were incubated with endothelial cells for 5, 10, 15 and 30 minutes or only for 15 minutes. Adhesion was stopped by aspirating the medium carefully and the remaining cells were washed with $PBS^{+/+}$. Wells containing only cancer cells, kept to determine the total number of cancer cells added per condition, were not aspirated. Fluorescence levels of the attached cells were measured, as well as the wells containing just cancer cells or just HUVECs, using a plate reader (Fusion αFP plate reader). The background fluorescence of HUVECs alone was subtracted from each value and then each value was normalized by the total number of cells that was added per condition (cancer cells alone).

2.3.4.2 Intercalation assay – fixed cell imaging

The protocol was based on an assay established in the laboratory (Borda D'Agua, 2012; Reymond et al., 2012). HUVECs were seeded on coverslips coated with collagen type I (50 µg/ml for 1 hour at 37ºC), one or two days before the experiment, to form a monolayer. Cancer cells were staining using a CFSE (10 µM)/$PBS^{+/+}$ solution, detached using non-enzymatic dissociation solution, counted and re-suspended in 0.1% FCS-containing DMEM or RPMI medium at $2.5x10^4$/100 µl. Cells were kept in suspension for about 30 minutes before starting the intercalation assay, to allow them to recover from the CFSE staining. Cancer cells were allowed to interact with the

HUVECs for 60 minutes. Cells were aspirated carefully and washed with $PBS^{+/+}$. Cells were fixed for 15 minutes at RT with 4% paraformaldehyde (PFA) and immunostained (section 2.3.5). Images were acquired using Zeiss LSM510 confocal laser-scanning microscope.

2.3.4.3 Intercalation assay – live cell imaging

The protocol was based on an assay established in the laboratory (Borda D'Agua, 2012; Reymond et al., 2012). HUVECs were seeded on a 24-well plate coated with collagen type I (50 µg/ml for 1 hour at 37ºC), one or two days before the experiment, to form a monolayer. The 24-well plate was inserted into a humidified chamber (37ºC and 5% CO_2) on the timelapse microscope at least 30 minutes before the beginning of the assay. Several fields of acquisition were chosen based on the confluence and appearance of the endothelial cells before adding the cancer cells, and saved for subsequent recording during cancer cell interaction. Cancer cells, labelled or not with CFSE, were detached using a non-enzymatic dissociation solution, counted and added against the multi-well walls without disturbing or shaking the plate to avoid changes to the pre-established positions and focus. Timelapse movies were acquired over a period of up to 6-7 hours using a Nikon TE2000-E microscope with a Plan Fluor 10x objective (Nikon), a Hamamatsu Orca-ER digital camera and Volocity software. Cancer cells in the movies were subsequently tracked on top of the endothelial cells using ImageJ software. A cancer cell was considered intercalated when it changed from phase bright to phase dark, and the cell shape was no longer rounded but spread between endothelial cells.

2.3.4.4 Transwell-based 3D invasion assay

A 3D model for cancer cell invasion analysis was adapted by Barbara Borda D'Agua from the protocol established in the laboratory for leukocyte 3D transendothelial migration (TEM) analysis (Cain et al., 2010). Collagen type I gels were prepared mixing

9 parts of PureCol® with 1 part of cold Buffer 1. The final concentration of collagen I in the gel was 2 mg/ml. To obtain the desired concentration, collagen I at a concentration of 2.7 mg/ml was diluted with cold EGM-2 medium. Around 250 µl of the liquid matrix was added to a transwell where a hydrophobic barrier was manually drawn inside the upper insert (ThinCert™) using a pen (Dako Pen, S2002): the ink provides a barrier to liquids, avoiding meniscus formation. The matrix was incubated at 37ºC in the absence of CO_2 for at least 4 hours. The gel became opaque when totally polymerized. After polymerization, gels were hydrated with warm cell medium for at least 6 hours before performing the invasion assays. Cancer cells were stained using a (CFSE, 10 µM)/$PBS^{+/+}$ solution, detached using a non-enzymatic dissociation solution, counted and re-suspended in 0.1% FCS-containing DMEM or RPMI medium at $2.5x10^4$/100 µl. Before seeding the cells, 400 µl of fresh medium was added on top of the gel. DMEM or RPMI containing 10% FCS was added to the bottom, in order to create a gradient of FCS to act as a chemoattractant for cancer cells. Cancer cells were added on top of the gel and allowed to invade for 24 hours. To measure invasion, cells were fixed with 4% PFA, permeabilised with 0.1% Triton X-100 in $PBS^{+/+}$ and stained with DAPI (nucleus). The samples were imaged using Zeiss LSM510 confocal laser-scanning microscope.

2.3.4.5 Transwell-based 3D TEM assay

The assay was performed as described in section 2.3.4.4, except that before adding the CFSE-labelled cancer cells, a HUVEC monolayer was established on top of the collagen I gels. The whole experiment was performed using EBM-2 medium. To evaluate TEM of cancer cells, samples were fixed and stained following the protocol described in section 2.3.4, with the exception that the HUVECs were stained for PECAM-1. Samples were analysed with a Zeiss LSM510 confocal laser-scanning microscope.

2.3.5 Immunofluorescence

Cells were fixed in 4% PFA for 15 minutes at RT. Fixed cells were washed with $PBS^{+/+}$ and then permeabilised in 0.1% Triton X-100/$PBS^{+/+}$ for 5 minutes at 4ºC. After washing with $PBS^{+/+}$, cells were blocked in 3% BSA/$PBS^{+/+}$ for 30 minutes at RT. Primary antibodies were diluted in 3% BSA/$PBS^{+/+}$ and incubated for 2 hours at RT. Fluorophore-conjugated secondary antibodies, phalloidin (to label F-actin) and DAPI (nuclei) were prepared in the same way as primary antibodies and incubated for 45-60 minutes at RT. Coverslips were then washed and mounted onto glass slides using fluorescent mounting medium.

2.3.6 Confocal microscopy

A Zeiss LSM510 confocal laser-scanning microscope and the ZEN software were used to take images of fluorescently stained cells. Images were taken with 512x512 pixels resolution and objectives EC Plan-Neofluar 20x/0.50 M27 and Plan-Aprochromat 63x/1.40 Oil DIC M27 were used depending on the type of experiment. Laser and appropriate filters were used as shown in Table 2-12. All images were acquired using the range indicator in ZEN software to avoid saturation and high background when adjusting gain and amplification.

Table 2-12 Lasers and filters used for confocal microscopy

Fluorophore	Laser	Excitation (nm)	Emission (nm)
GFP/Alexa 488	Argon	488/494	520/517
Alexa 546	Helium/Neon	556	573
Alexa 633	Helium/Neon	632	647
DAPI	Diode 405/30	405	430

2.4 Methods: cell biochemistry

2.4.1 Preparation of cell lysates

Cells were washed with cold $PBS^{-/-}$ and lysed on ice with a cell scraper after adding lysis buffer. Lysates were collected and transferred to a fresh 1.5 ml microtube. Samples were centrifuged at 8,000 g at 4ºC for 10 minutes. NuPAGE® LDS Sample Buffer (4x) containing 5% β-mercaptoethanol was added to each sample and samples were boiled for 5 minutes. Samples were used immediately or stored at -20ºC.

2.4.2 SDS-PAGE and western blot

Samples were resolved in 4-12% SDS-polyacrylamide gels and electrophoretically transferred to nitrocellulose membranes of 0.45 µm pore. Membranes were blocked for 1 hour at RT in 5% (w/v) dried skimmed milk powder in TBS-T. Membranes were incubated overnight at 4ºC with primary antibodies. Membranes were washed 3 times for 10 minutes with TBS-T before incubation with the secondary horseradish peroxidise-conjugated anti-mouse or anti-rabbit antibodies for 1 hour at RT. Membranes were washed again for three times, 10 minutes each; and developed using enhanced chemiluminescence (ECL) western blotting detection reagent. Protein levels on the immuno-blots were analysed by densitometry using ImageJ.

2.4.3 Stripping of western blot

Nitrocellulose membranes were washed three times for 10 minutes with stripping buffer at RT. To remove any residual stripping buffer, membranes were washed with TBS-T for 10 minutes at RT. Blots were re-blocked with 5% dried skimmed milk powder in TBS-T for 1 hour at RT and then the protocol was carried out as described in section 2.4.2.

2.4.4 Preparation of GST-fusion proteins

Competent DH5α cells were transformed with pGEX-2T-RhoBTB1 1-301 and plated onto LB agar plates containing 100 µg/ml ampicillin. One colony was transferred to 50 ml LB containing 100 µg/ml ampicillin and grown overnight at 37ºC. The overnight culture was diluted 1/10 into 500 ml of fresh LB containing 100 µg/ml ampicillin and grown for 3 hours at 37ºC. To induce protein expression, 0.3 mM of isopropyl β-D-1-thiogalactopyranoside (IPTG) was added and the culture incubated at 37ºC for 3 hours. Cells were pelleted in 50 ml tubes by centrifugation at 1,500 g for 20 minutes at 4ºC and cells were immediately lysed or stored at -40ºC for future use. Cells were lysed to extract GST-fused proteins with GST beads lysis buffer. After all the pellets were resuspended, the lysate was sonicated (SONICS Vibracell VCX130 Ultrasonic Cell Disrupter) on ice for 10 minutes (70% intensity with 10s pulses). Subsequently 1% Triton X-100 was added and the lysate was incubated for 30 minutes at 4ºC with gentle mixing. The lysate was then centrifuged at 3,500 g for 30 minutes at 4ºC. The supernatant was incubated with glutathione sepharose beads (previously washed with GST beads washing buffer) for 1 hour at 4ºC under rotation. The supernatant was removed and the beads washed three times with GST beads washing buffer. The beads were resuspended in GST beads washing buffer and kept at 4ºC for up to two weeks. GST-fusion proteins were used for pull down assays.

2.4.5 Pull down

For the pull down using GST-RhoBTB1 1-301, Cos7 cells in 10 cm dishes were transfected with full length myc-ROCK1 and myc-ROCK1 deletion mutants (section 2.3.1.5). After 24 hours, cells were washed with $PBS^{-/-}$ and 1x Mg^{2+} lysis buffer was added to the dishes. Cells were lysed on ice with a cell scraper. The lysate was transferred to a 1.5 ml microtube and centrifuged at 17,000 g for 10 minutes at 4ºC. A small aliquot of the total lysate was kept to check total protein levels by immunoblotting.

The lysates were incubated with 40 µl of GST-RhoBTB1 1-301 for 2 hours at 4ºC under rotation. Beads were washed three times with 1x Mg^{2+} lysis buffer. Proteins were eluted by boiling the samples after addition of NuPAGE® LDS Sample Buffer (2x) containing β-mercaptoethanol. Pull down samples and loading control samples were analysed by western blotting (section 2.4.2).

2.4.6 Immunoprecipitation and co-immunoprecipitation

Cells in a 10 cm dish were transfected with one or more plasmids containing the gene(s) of interest. After 24 hours, cells were washed with $PBS^{+/+}$ and 1 ml of IP lysis buffer was added to each dish. After 10 minutes of incubation, cells were scraped and lysates were collected into 1.5 ml microtubes. Samples were centrifuged at 8,000 g at 4ºC for 10 minutes and the supernatant transferred to a new microtube. A small aliquot of the total lysate was kept to check total protein levels by immunoblotting. Cell lysates were incubated with 10 µl of anti-myc agarose beads, GFP-Trap®, anti-FLAG agarose beads or anti-HA agarose beads (pre-washed with IP lysis buffer) per sample for 2 hours at 4ºC with rotation. Beads were washed three times with IP lysis buffer. After the last wash, immunocomplexes were dissociated from the beads by boiling with NuPAGE® LDS Sample Buffer (2x) containing β-mercaptoethanol. The samples analysed by western blot (section 2.4.2), or processed further as needed.

2.4.7 Ubiquitination assay *in vivo*

The assay was performed as described in Choo and Zhang (2009). Briefly, cells transfected with vectors encoding GFP, HA-ubiquitin, GFP-RhoA-N19, GFP-RhoBTB1, GFP-RhoBTB2 and myc-RhoBTB1 were treated with MG132 inhibitor for 4 hours (section 2.3.2). Cells were lysed with cell lysis buffer and then transferred to a 1.5 ml microtube. Samples were boiled for 10 minutes and sonicated (SONICS Vibracell VCX130 Ultrasonic Cell Disrupter) for 15 secs. Dilution buffer was added to each tube

and samples were incubated at 4ºC for 30 minutes with rotation. Diluted samples were centrifuged at 17,000 g for 30 minutes and the supernatant was transferred to a new microtube. A small aliquot of the total lysate was kept to check total protein levels by immunoblotting. Cell lysates were incubated with 10 µl of anti-myc agarose beads or anti-HA agarose beads (pre-washed with dilution buffer) per sample at 4ºC overnight with rotation. Samples were centrifuged at 5,000 g for 5 minutes and supernatant was aspirated. Beads were washed twice with washing buffer. After the last wash, immunocomplexes were dissociated from the beads by boiling with NuPAGE® LDS Sample Buffer (2x) containing β-mercaptoethanol. The samples analysed by western blotting (section 2.4.2).

2.4.8 *In vitro* kinase assay with radiolabeled ATP

myc-RhoBTB1, myc-ROCK1 1-727, myc-ROCK1 1-727 (K105A), myc-ROCK1 1-540, GFP, GFP-RhoBTB1, GFP-RhoBTB1 S3T2 were expressed in Cos7 cells (section 2.3.1.5) and purified by immunoprecipitation using anti-myc-agarose beads or GFP-binding protein coupled to agarose (GFP-trap®) (section 2.4.6). Beads were combined depending on the conditions of the experiment (e.g. myc-RhoBTB1 beads were combined with myc-ROCK1 1-727 beads). Samples were washed five times with IP lysis buffer and twice in kinase buffer 1x. Beads were then pelleted by centrifugation and resuspended in 29 µl of kinase mix (kinase buffer 2x, 30 µM ATP, 0.1 µCi/µl [^{32}P] γATP). 1 µl of recombinant GST-ROCK1 17-535 was added in some of the conditions. Samples were incubated at 30ºC for 30 minutes with gently vortexing every 15 minutes. 30 µl of NuPAGE® LDS Sample Buffer (2x) containing β-mercaptoethanol was added and samples were boiled for 5 minutes. Samples were resolved in 4-12% SDS-polyacrylamide gels and fixed in kinase assay fixing solution for 30 minutes. Gels were dried for 2 hours at 70ºC and analysed by autoradiography.

2.4.9 Pro-Q

Samples were resolved in 4-12% SDS-polyacrylamide gels and electrophoretically transferred to Immobilon-FL PVDF membranes (low fluorescence). After electroblotting, membranes were allowed to dry completed before proceeding with the Pro-Q® Diamond Phosphoprotein Blot Stain Kit. Following the manufacturer's instructions, membranes were pre-wet in methanol and proteins on membranes were fixed by incubation with Fix Solution for 10 minutes. Membranes were washed 4 times for 5 minutes with distilled water. Phosphoproteins were stained by incubating the membranes with Pro-Q® Diamond reagent diluted 1/1000 in Pro-Q® Diamond blot stain buffer for 15 minutes. Membranes were washed 3 times for 5 minutes in Destain solution. After the final wash, membranes were allowed to dry completely before visualising the phosphoproteins in the blot with a UV-transilluminator.

2.4.10 DSS crosslinking

Cos7 cells were transfected with empty vector or vector encoding myc-RhoBTB1 (section 2.3.1.5). After 24 hours, cells were washed with $PBS^{-/-}$ and lysed with conjugation buffer. Samples were centrifuged at 8,000 g at 4ºC for 10 minutes. Clarified lysates were transferred to fresh tubes and disuccinimidyl suberate (DSS) crosslinker was added to final concentrations of 0.05 mM, 0.1 mM and 0.25 mM. Samples were incubated for 30 minutes with rotation at RT. Reactions were stopped by adding 20 mM Tris-HCl (pH 7.5) and incubation for 15 minutes at room temperature. NuPAGE® LDS Sample Buffer (4x) containing 5% β-mercaptoethanol was added to each sample and cross-linked products were detected by western blotting (section 2.4.2).

3 RhoBTB1 and cancer cell interaction with endothelial cells

3.1 Introduction

According to the World Health Organization (WHO), metastasis is the most common cause of death for cancer patients. It is a multi-step process in which cancer cells need to detach from the primary tumour, interact and invade into the surrounding tissue to reach the vessels, intravasate, survive the shear stress, extravasate and grow in a new site of the body (Sahai, 2007; Steeg, 2006). Most of the cells that disseminate from the primary tumour are resistant to existing therapeutic agents, making metastatic disease incurable in most cases. Successful cancer treatment is highly dependent on the capacity of new treatments to affect metastatic cells (Valastyan and Weinberg, 2011). One of the key steps of metastasis is the exit of cancer cells from the blood vessels into new tissues. The cells can either disrupt the walls of the vessels after a micro-colony of cancer cells is formed on top of the endothelium; or the cancer cells can cross the endothelium individually and reach the stromal microenvironment. The latter step is known as extravasation (Sahai, 2007; Valastyan and Weinberg, 2011). Extravasation is a well-studied process in leukocytes, due to its importance in the inflammatory response, but less is known in cancer cells. *In vitro*, cancer cells have been observed to adhere to endothelial cells, intercalate between endothelial cells and transmigrate (Figure 3.1). The firm adhesion between the cancer cells and the endothelium followed by the diapedesis through the endothelial monolayer is part of a complex process called transendothelial migration (TEM) (Miles et al., 2008).

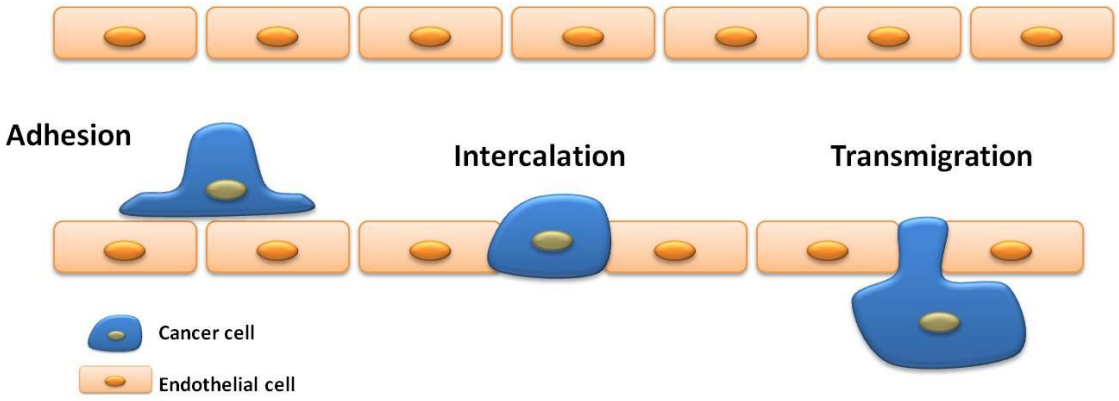

Figure 3.1 - Cancer cell extravasation

In vitro, cancer cells under fluid flow are able to adhere, intercalate between endothelial cells and transmigrate.

Relatively little is known regarding signalling pathways involved in TEM. One group of proteins that has been linked to this process is the Rho GTPase family. Because TEM involves dynamic shape changes (Reymond et al., 2012), it is not surprising that Rho GTPases play an important role in this step. Some classic Rho GTPases have been described to regulate TEM *in vitro*. For example, RNAi-mediated depletion of RhoA in T cells decreases TEM (Heasman et al., 2010). However, the opposite effect is observed in PC3 prostate cancer cells, in which cells expressing shRNA targeting RhoA have increased invasion and TEM (Sequeira et al., 2008). Rac1 in endothelial cells has been shown to be important in regulating endothelial permeability and leukocyte TEM (Cain et al., 2010).

Breast cancer is the most commonly diagnosed cancer in women worldwide (World Health Organization - WHO). Metastatic breast cancer is incurable in most cases and conventional therapy has only a palliative effect on metastases (Mego et al., 2010). Breast cancer is a heterogeneous disease. Based on gene expression profile and immuno-histochemical expression of oestrogen receptor (ER), progesterone receptor (PR) and human epidermal growth factor receptor (HER2), breast cancer is classified into at least five subtypes: luminal A, luminal B, $HER2^{+}$, basal and claudin-low. As

shown in Table 3-1, each subtype responds differently to treatment and has a different prognosis (Eckhardt et al., 2012; Holliday and Speirs, 2011).

Table 3-1 Molecular classification of breast cancers

Subtype	Marker expression	Characteristics
Luminal A	$ER^+/PR^+/HER2^-$	Endocrine responsive*, often chemotherapy responsive
Luminal B	$ER^+/PR^{+/-}/HER2^{+/-}$	Usually endocrine responsive, variable to chemotherapy, $HER2^+$ is trastuzumab** responsive
Basal	$ER^-/PR^-/HER2^-$	Endocrine nonresponsive, often chemotherapy responsive
Claudin-low	$ER^-/PR^-/HER2^-$	Intermediate response to chemotherapy
$HER2^+$	$ER^-/PR^-/HER2^+$	Trastuzumab responsive, chemotherapy responsive

ER: oestrogen receptor; PR: progesterone receptor; HER2: human epidermal growth factor receptor 2. * Hormone therapy, e.g. tamoxifen; ** Trastuzumab: monoclonal antibody that interferes with HER2 receptor.

Recently, the atypical Rho GTPase RhoBTB1 was one of several hits in a siRNa screen performed to determine the effect of Rho GTPases on the adhesion of cancer cells to endothelial cells. Using a pool of siRNAs, RhoBTB1 depletion led to decrease of more than 25% in adhesion of PC3 prostate cancer cells to endothelial cells (Reymond et al., 2012). Depletion of RhoBTB1 using two different siRNAs led to a decrease in TEM of MDA-MB-231 breast cancer and PC3 prostate cancer cells (Borda D'Agua, 2012). In addition, a decrease in expression of β1 integrin and reduced expression and acitivity of RhoA was observed following RhoBTB1 depletion in MDA-MB-231 cells (Borda D'Agua, 2012). However, most of these results were only observed in a single cell line, and thus it is important to determine whether they are reproducibly observed in other cell lines. RhoBTB1 could have an important role in breast cancer progression, since RhoBTB2, also a member of the RhoBTB subfamily, was first described as a gene deleted in breast cancer (Hamaguchi et al., 2002).

To explore more the role of RhoBTB1 in breast cancer cell TEM, other breast cancer cell lines were selected to be used in 2D and 3D models to study cell adhesion, intercalation and transmigration into a monolayer of endothelial cells. Because of the number of breast cancer subtypes, cell lines were selected based on their profile of marker expression, in order to compare the effects of RhoBTB1 depletion on breast cancer cell lines derived from different subtypes (Figure 3.2). Each cell line was first tested for their behaviour in several assays, and subsequently one cell line that behaved similarly to MDA-MB-231 cells was selected to analyse the effects of RhoBTB1 depletion.

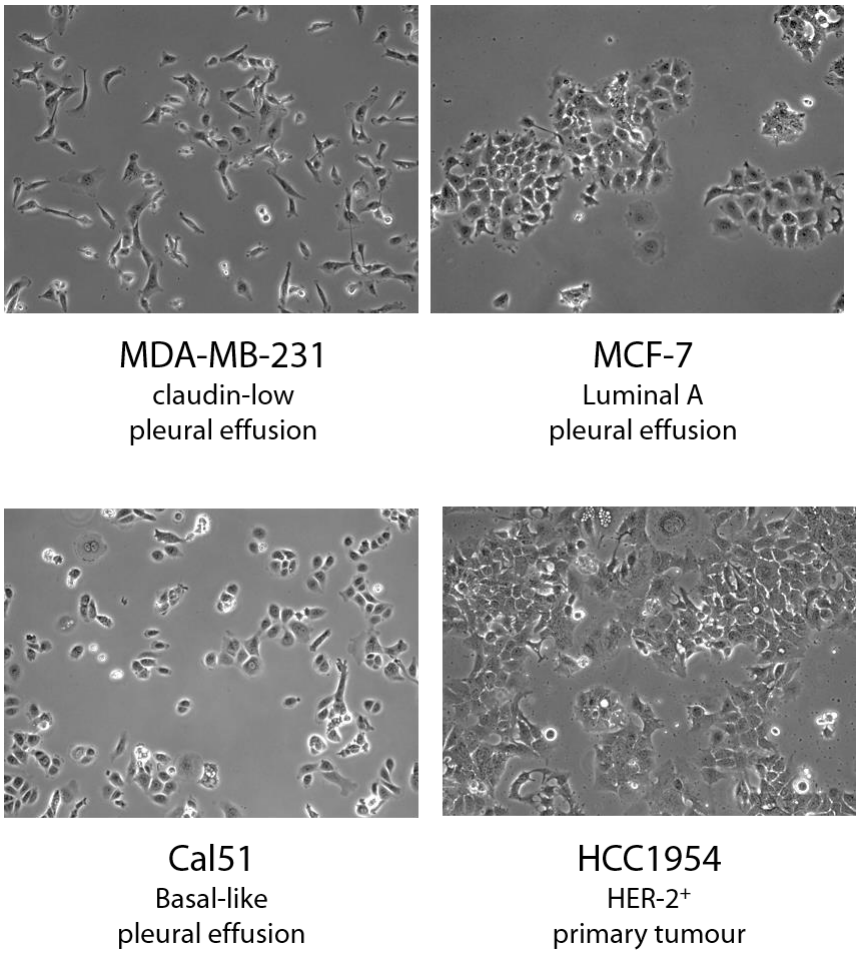

Figure 3.2 – Morphology of breast cancer cell lines

MDA-MB-231 cell line is a claudin-low subtype, MCF-7 cell line is luminal A subtype, Cal51 cell line is basal-like subtype and HCC1954 cell line is HER2 positive (Koochekpour et al., 2014; Neve et al., 2006; Sharpe et al., 2011).

3.2 Interaction of MCF-7, Cal51 and HCC1954 breast cancer cells with a matrix of collagen I

One important step during metastasis is the ability of the cancer cells to interact with the surrounding environment (Reymond et al., 2013). Collagen I is one of the major components of the stromal environment that surrounds both primary and secondary tumours (Hooper et al., 2006; Sabeh et al., 2009). To evaluate if MCF-7, Cal51 and HCC1954 cells could invade into a 3D collagen I matrix, cells stained with the fluorescent dye carboxyfluorescein succinimidyl ester (CFSE) were added on top of collagen I matrices and left for 24 hours. FCS was used as a chemoattractant (Figure 3.3).

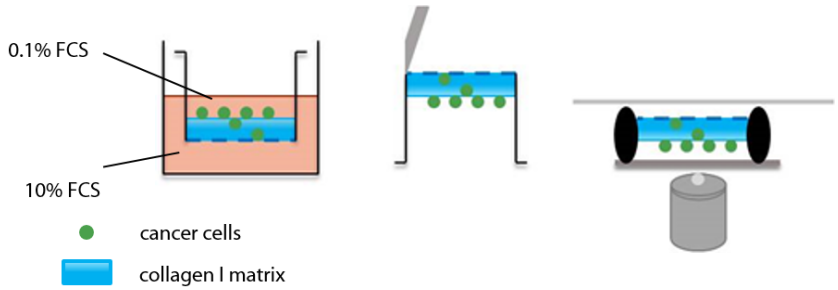

Figure 3.3 - Diagram of transwell 3D invasion assay

CFSE-stained cells are added to a 2.0 mg/ml collagen I matrix in a transwell. FCS is used as a chemoattractant (0.1% FCS in the top chamber and 10% FCS in the bottom chamber). Cells are left to invade for 24 hours. The collagen I matrix is removed from the transwell, stained for DAPI (nuclei) and analysed in a confocal microscope (section 2.3.4.4).

MDA-MB-231 cells were used as a control, because it is known that these cells can invade collagen I (Mierke et al., 2011). Cells from all four different cell lines could adhere to collagen I. However, only HCC1954 and MDA-MB-231 cells invaded into the collagen I within 24 hours (Figure 3.4).

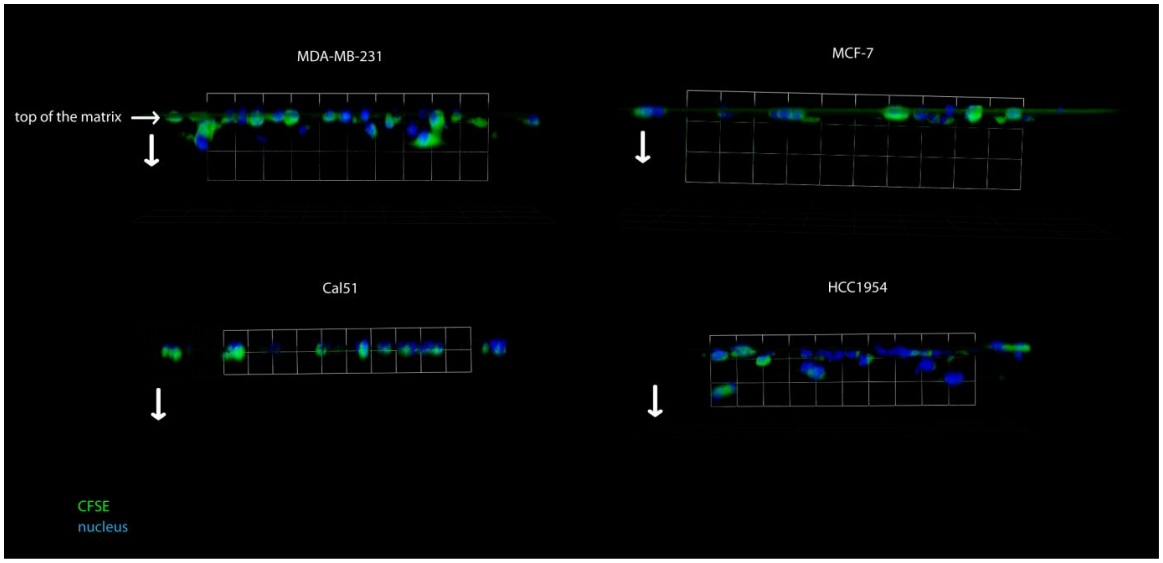

Figure 3.4 - Invasion of breast cancer cell lines into collagen I

CFSE-labelled cancer cells were seeded on top of 2.0 mg/ml of collagen I in transwells. Gels were fixed after 24 hours and stained with DAPI to label the nuclei. XYZ projections of the cancer cells on the 3D matrices were obtained from confocal microscopy z-stacks using Volocity software. Images are representative of two independent experiments. Scale bar = 1 unit = 45.7µm.

3.3 Optimization of adhesion, intercalation and transendothelial migration with MCF-7, Cal51 and HCC1954 cell lines

3.3.1 MCF-7, Cal51 and HCC1954 breast cancer cells intercalate between confluent human umbilical endothelial cells

The ability of MCF-7, Cal51 and HCC1954 cells to adhere and intercalate between endothelial cells (HUVECs) was then investigated using an intercalation assay with live cell imaging (Reymond et al., 2012). Timelapse acquisition for 6 hours showed that MCF-7, Cal51 and HCC1954 cells adhered to the HUVECs. A cancer cell is considered adhered when the cell body is really rounded and phase-bright and stays at one specific position on the endothelial cells (Figure 3.5), contrasting with the phase-dark and flat monolayer of HUVECs. When the cancer cells intercalate, they become phase-dark and as flat as the endothelial cells.

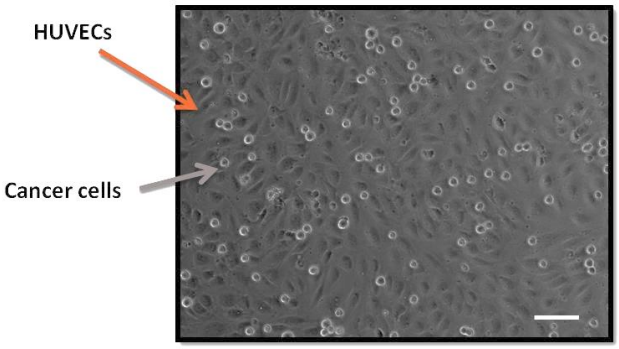

Figure 3.5 - Intercalation assay - live cell imaging

Cancer cells were added on top of an endothelial monolayer (time point = 0 minutes). Orange arrow: monolayer of HUVECs; grey arrow: cancer cells. Scale bar = 100 µm.

MDA-MB-231 cells were used as a control, since this cell line was previously used in our laboratory to identify a role of RhoBTB1 in intercalation (Chapter 3.1). After 1 hour, almost 50% of MDA-MB-231 cells had intercalated and by the end of 6 hours approximately 80% of cells had intercalated (Figure 3.6A and 3.6B, movies 3.1). The only cell line that had a similar pattern of intercalation to MDA-MB-231 cells was Cal51. Almost 80% of Cal51 cells intercalated after 6 hours (Figure 3.6C and 3.6D, movie 3.2).

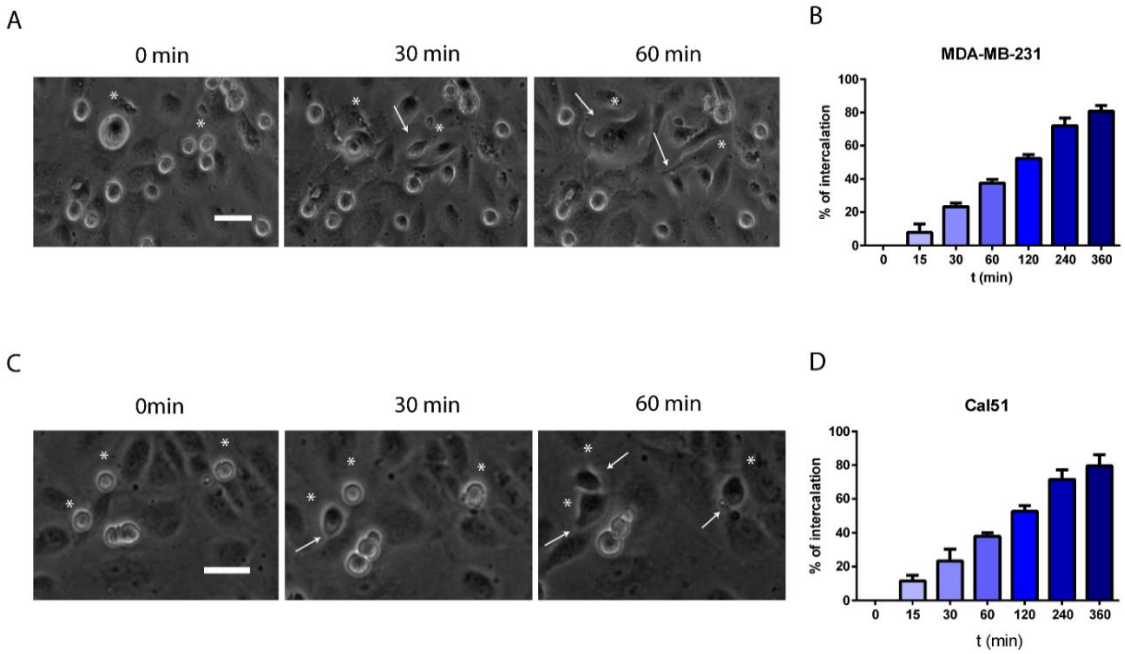

Figure 3.6 - Intercalation of MDA-MB-231 and Cal51 cells into HUVECs

MDA-MB-231 and Cal51 cells were monitored by timelapse microscopy acquiring an image every 3 to 5 min over 6 hours. A) and C) Zoomed images of representative time points (0, 30 and 60 minutes). White stars indicate examples of cells that intercalate. White arrows indicate the cells at the time of intercalation. Intercalation rates were analysed using ImageJ software. B) and D) Quantification of intercalated cells at the indicated time points from two independent experiments. Nine different fields of each condition were analysed per experiment (~30 cells per field). Values represent mean ± SD. Scale bar = 50 µm.

Analysis of HCC1954 cells indicated that almost 90% of cells had flattened and become phase-dark after 6 hours (Figure 3.7B). However, when the movies were analysed more closely, it was clear that not all of these cells intercalated. Instead, some cells were spread on top of the HUVECs (Figure 3.7A, movie 3.3). It was difficult to quantify the percentage of intercalated and spread cells separately. Once the cancer cells become part of the monolayer, it is difficult to differentiate all the cells from the endothelial cells. To try to overcome this problem, HCC1954 cells were stained with CFSE. However, when these cells spread and intercalate, they become very flat, so that is difficult to detect the CFSE fluorescence (Figure 3.8). Modifications in the protocol are necessary to study this cell line.

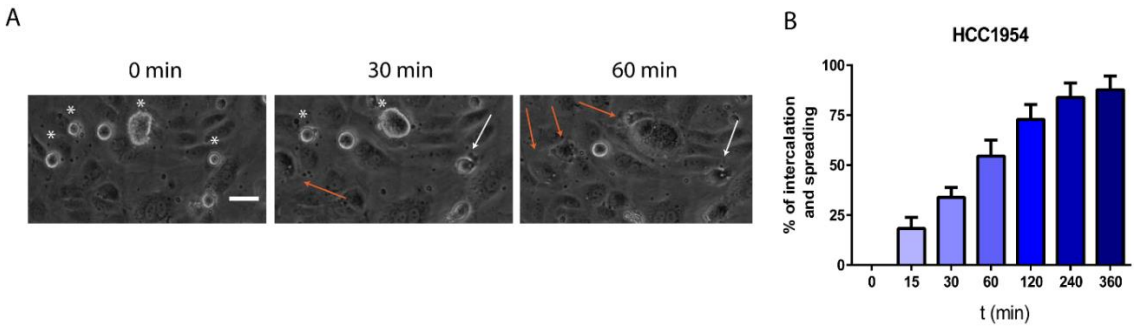

Figure 3.7 - Spreading and intercalation of HCC1954 cells into HUVECs

HCC1954 cells were monitored by timelapse microscopy acquiring an image every 3 min over 6 hours. A) Zoomed images of representative time points (0, 30 and 60 minutes). White stars indicate cells that intercalate or spread. White arrow indicates the moment of intercalation and orange arrows indicate the moment of spreading. Intercalation rates were analysed using ImageJ software. B) Quantification of intercalated and spread cells at the indicated time points from two experiments. Nine different fields were analysed in the experiment (~30 cells per field). Values represent mean ± SD. Scale bar = 50 µm.

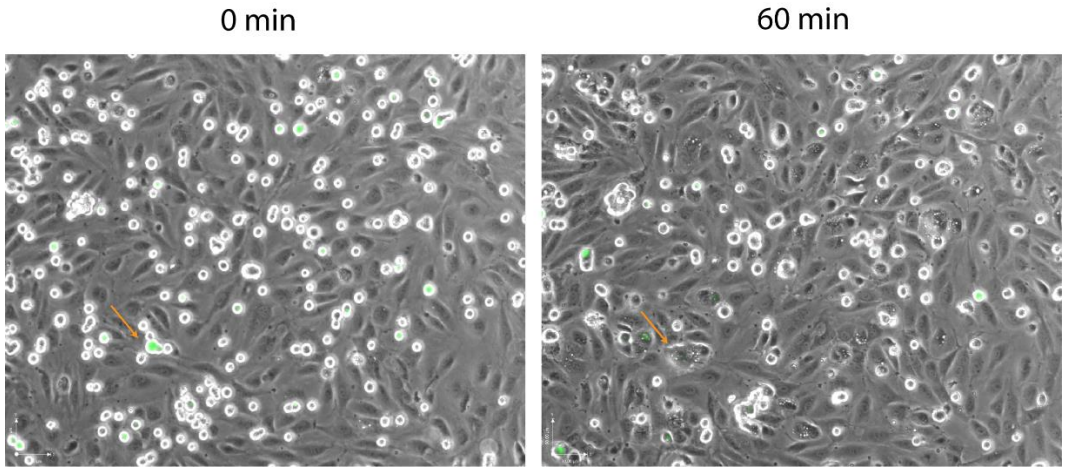

Figure 3.8 - Spreading and intercalation of HCC1954 cells stained with CFSE into HUVECs

HCC1954 cells stained with CFSE were monitored by timelapse microscopy acquiring an image every 3 min over 6 hours. Images are representative of the time points in the beginning and middle of the experiment. Orange arrow indicates a cell for which CFSE staining is no longer detectable after spreading/intercalating.

MCF-7 cells have a luminal A subtype phenotype (Neve et al., 2006) and grow in groups (Figure 3.2). When added to the endothelial monolayer, the groups pushed away the endothelial cells, making large gaps in the monolayer (Figure 3.9). Nevertheless, when an MCF-7 cell was not in a group, it intercalated in the same way as MDA-MB-231 and Cal51 cells (Figure 3.6 - white arrow). It was difficult to quantify the intercalation of MCF-7 cells because there were so many groups of cells, therefore the images were not analysed.

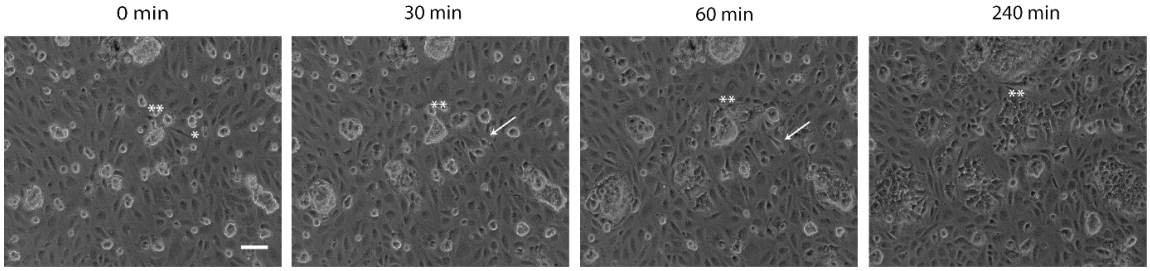

Figure 3.9 - Intercalation of MCF-7 cells into HUVECs

MCF-7 cells were monitored by timelapse microscopy acquiring an image every 3 min over 6 hours. Images are representative of the time points in the beginning, middle and end of the experiment. One white star indicates a single cell that will intercalate. White arrow indicates the timepoint of intercalation. Two white stars indicate a group of cells that will spread and form a hole in the endothelial monolayer. Nine different fields were analysed in the experiment. Scale bar = 100 μm.

3.3.2 Breast cancer cell morphology on endothelial cells

To investigate in more detail how each breast cancer cell line interacts with endothelial cells, CFSE-stained cancer cells were added to HUVECs and then fixed after 1 hour, stained for PECAM-1 (endothelial cell junctions) (Muller et al., 2002) and F-actin and analysed by confocal microscopy. Orthogonal projections show the side view of migrating cells, allowing cancer cells below the endothelial monolayer to be observed.

Unexpectedly, Cal51 cells were observed to cross the endothelial cells either through paracellular migration or transcellular migration (Figures 3.10 and 3.11). There are two routes that cells can transmigrate across endothelial cells: between the endothelial cells, which is known as paracellular migration and involves disruption of endothelial

cell-cell junctions; or through the endothelial cells, called transcellular migration (Figure 3.12). Leukocytes can transmigrate either by paracellular or transcellular migration (Carman, 2009), but whether cancer cells can take a transcellular route *in vivo* is unclear.

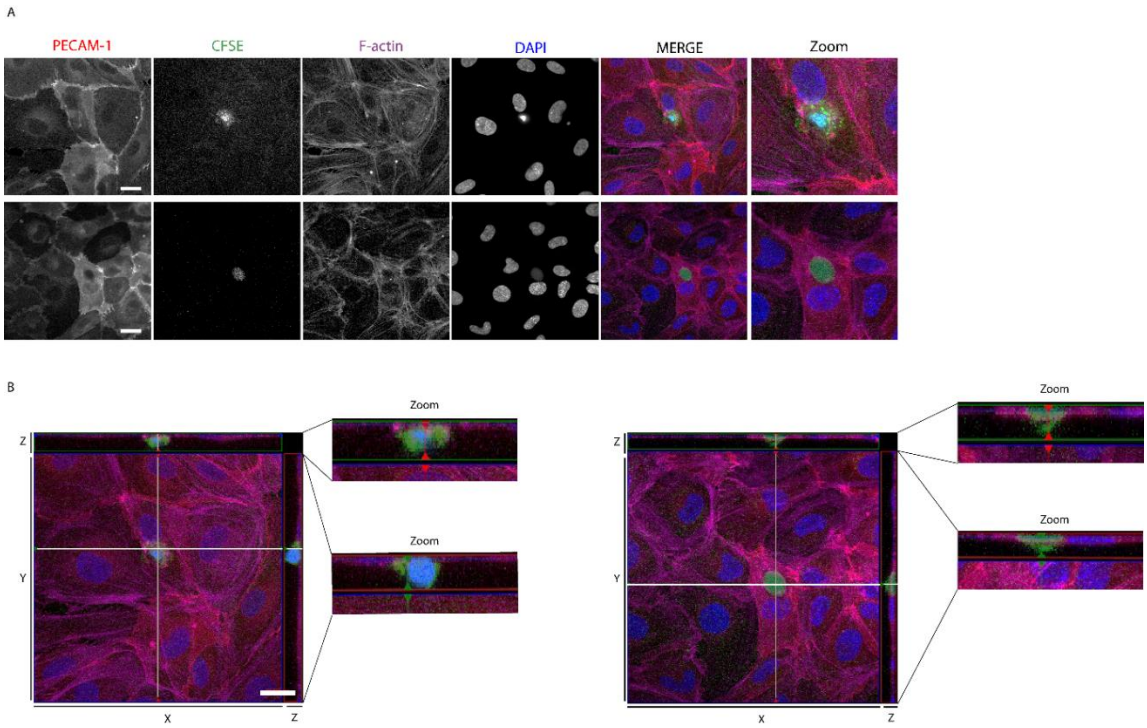

Figure 3.10 - Interaction of Cal51 cells with HUVECs - transcellular migration

HUVECs were grown to confluency on collagen I-coated glass coverslips. CFSE-labelled Cal51 cells were added to the monolayer for 1 hour. Non-adherent cells were washed off and the cells that remained adhered were fixed and permeabilized. Cells were stained for F-actin, PECAM-1 and nuclei (DAPI). Images were acquired by confocal microscopy using Zen software (Zeiss) with a 63x oil immersion objective and are representative of random fields from three independent experiments. A) xy view of the 3D projection of a z-stack of 20 images. Scale bar = 20 µm. B) xy and orthogonal projections of the same fields shown in (A). The beige and white lines across x-y are the regions in the image that are represented in the z-projection. Scale bar = 20 µm.

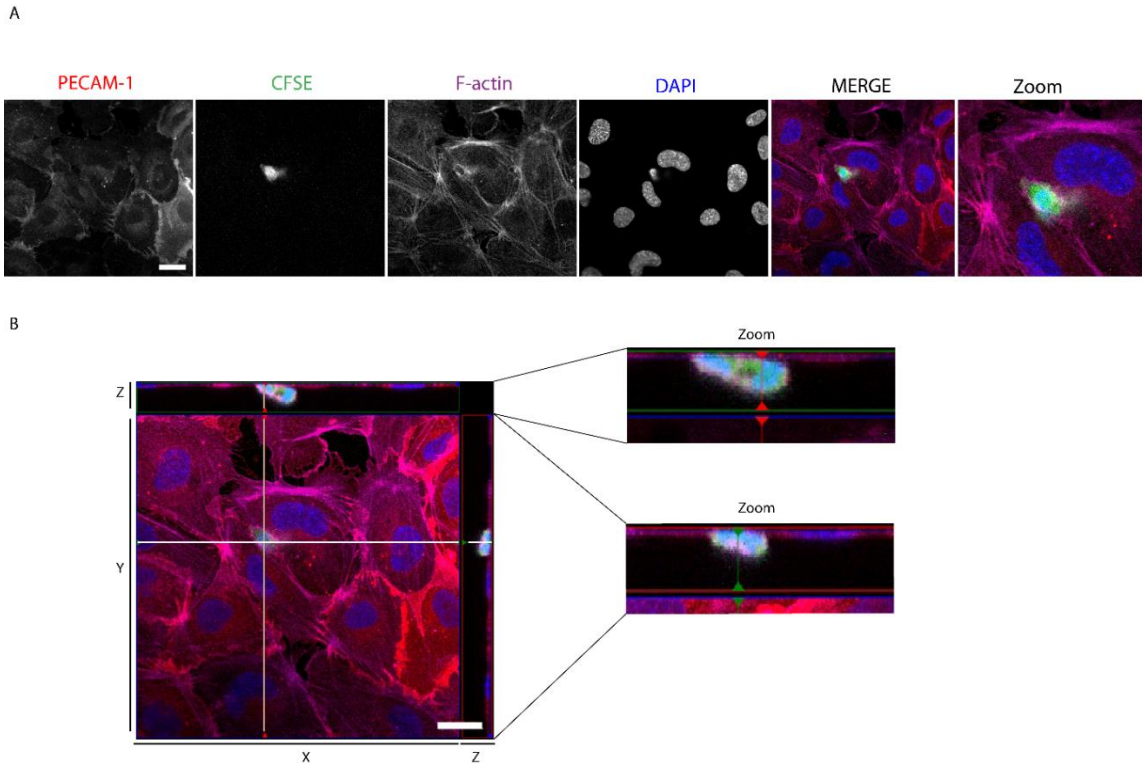

Figure 3.11 - Interaction of Cal51 cells with HUVECs - paracellular migration

HUVECs were grown to confluency on collagen I-coated glass coverslips. CFSE-labelled Cal51 cells were added to the monolayer for 1 hour. Non-adherent cells were washed off and the cells that remained adhered were fixed and permeabilized. Cells were stained for F-actin, PECAM-1 and nuclei (DAPI). Images were acquired by confocal microscopy using Zen software (Zeiss) with a 63x oil immersion objective and are representative of random fields from three independent experiments. A) xy view of the 3D projection of a z-stack of 30 images. Scale bar = 20 µm; B) xy and orthogonal projections of the same field shown in (A). The beige and white lines across x-y are the regions in the image that are represented in the z-projections. Scale bar = 20 µm.

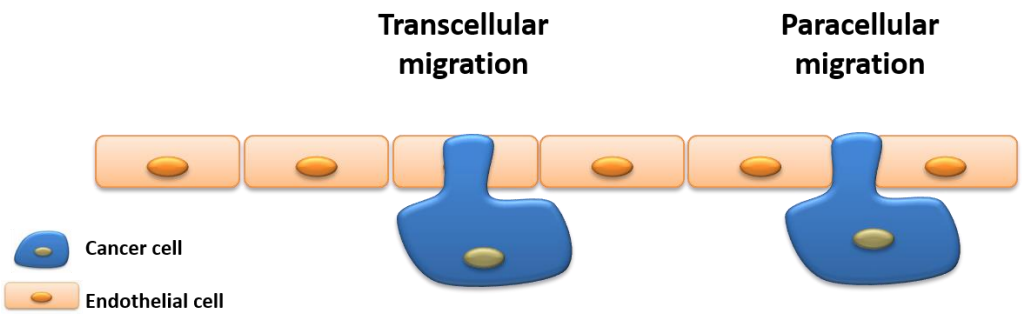

Figure 3.12 - Routes of transendothelial migration

Cells can transmigrate across endothelial cells using two routes: paracellular migration and trancellular migration. Paracellular migration involves disruption of endothelial cell-cell junctions and cells migrate between endothelial cells. In transcellular migration, cells cross the endothelium through the endothelial cells.

Quantification of Cal51 cells that underwent paracellular or transcellular migration through the endothelial monolayer at 1 hour (~ 40% cells intercalated – Figure 3.6D) showed that most cells used the paracellular route to migrate (~75%) (Figure 3.13).

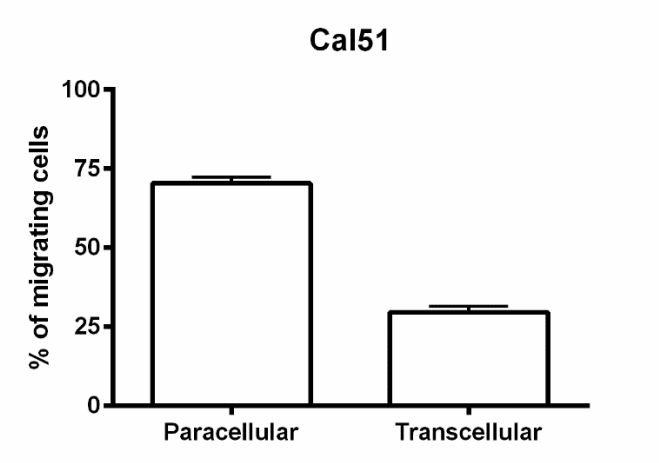

Figure 3.13 - Quantification of Cal51 cell paracellular migration versus transcellular migration

Graph shows data from three independent experiments. At least 100 cells that were transmigrating at 1 hour after addition of HUVECs were counted in each experiment. Values represent mean ± SEM.

Although in movies some HCC1954 cells spread on top of endothelial cells, it was possible to observe intercalating HCC1954 cells when they were fixed and analysed by confocal microscopy. After 1 hour, HCC1954 cells were either spread on top of endothelial cells or intercalated (Figure 3.14).

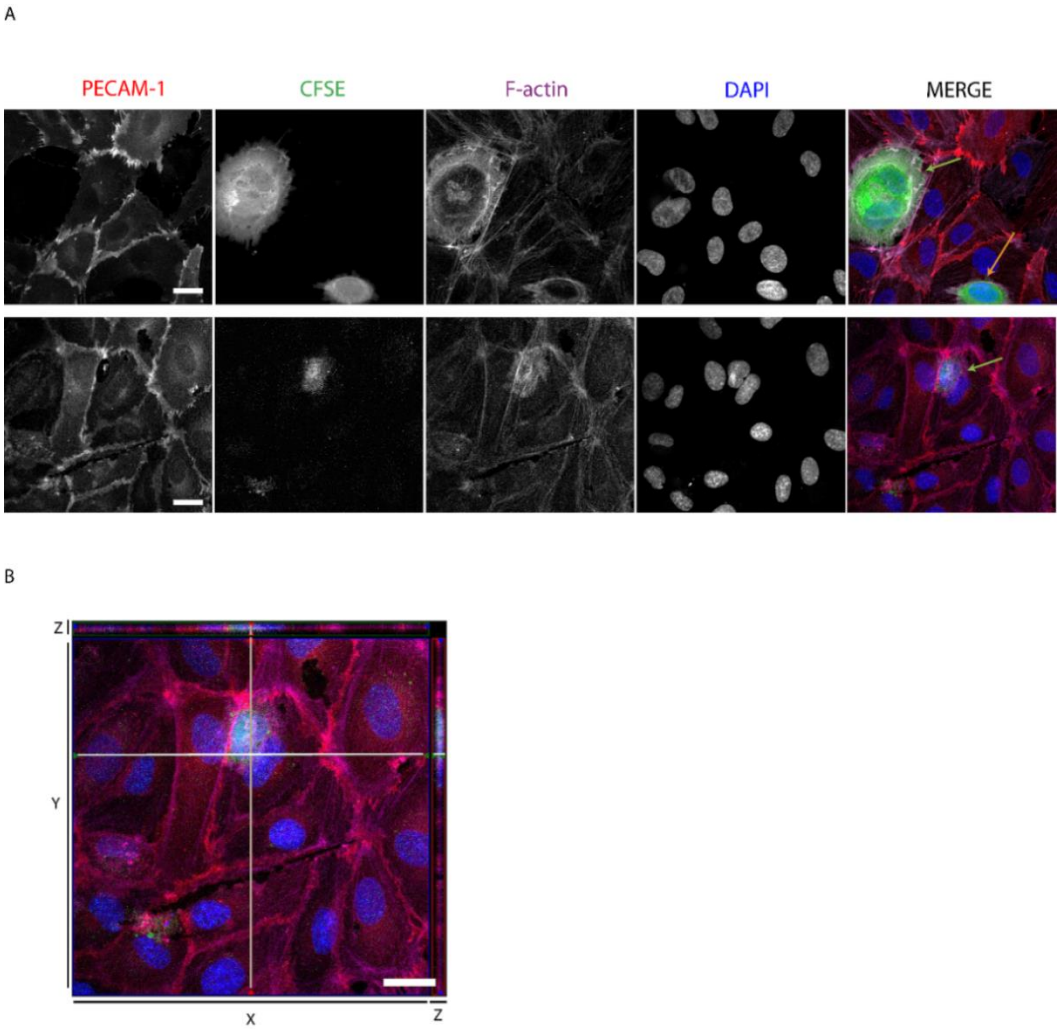

Figure 3.14 - Interaction of HCC1954 cells with HUVECs

HUVECs were grown to confluency on collagen I-coated glass coverslips. CFSE-labelled HCC1954 cells were added to the monolayer for 1 hour. Non-adherent cells were washed off and the cells that remained adhered were fixed and permeabilized. Cells were stained for F-actin, PECAM-1 and nuclei (DAPI). Images were acquired by confocal microscopy using Zen software (Zeiss) with a 63x oil immersion objective and are representative of random fields from three independent experiments. A) xy view of the 3D projection of a z-stack of 11 images. Green arrows indicate cells that intercalated and orange arrow indicates a cancer cell on top of an endothelial cell. Scale bar = 20 µm; B) xy and orthogonal projections of the same field shown in (A). The beige and white lines across x-y are the regions in the image that are represented in the z-projections. Scale bar = 20 µm.

MCF-7 cells, as observed in the movies (Figure 3.9, movie 3.3), formed holes in the endothelial monolayer when they remained in groups (Figure 3.15).

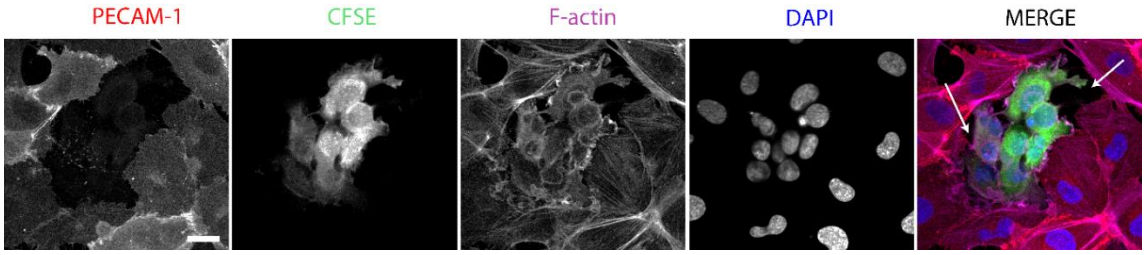

Figure 3.15 - Interaction of MCF-7 cells with HUVECs

HUVECs were grown to confluency on collagen I-coated glass coverslips. CFSE-labelled MCF-7 cells were added to the monolayer for 1 hour. Non-adherent cells were washed off and the cells that remained adhered were fixed and permeabilized. Cells were stained for F-actin, PECAM-1 and nuclei (DAPI). Images were acquired by confocal microscopy using Zen software (Zeiss) with a 63x oil immersion objective and are representative of random fields from three independent experiments. White arrows indicate the holes formed by the cancer cells. Scale bar = 20 µm.

To obtain as many single cells as possible, MCF-7 cells were treated with EGTA before being added to the monolayer of HUVECs. EGTA was added to the cell media in a final concentration of 5 nM and left to act for 1 hour. Cells were resuspended in fresh media and added to the monolayer of endothelial cells. EGTA chelates calcium, which is important for cell-cell junction formation (Gonzalez-Mariscal et al., 1990). Treatment with EGTA breaks the cell-cell junctions, making it easier to separate the cells. When single MCF-7 cells interacted with the endothelial monolayer, they could intercalate (Figure 3.16).

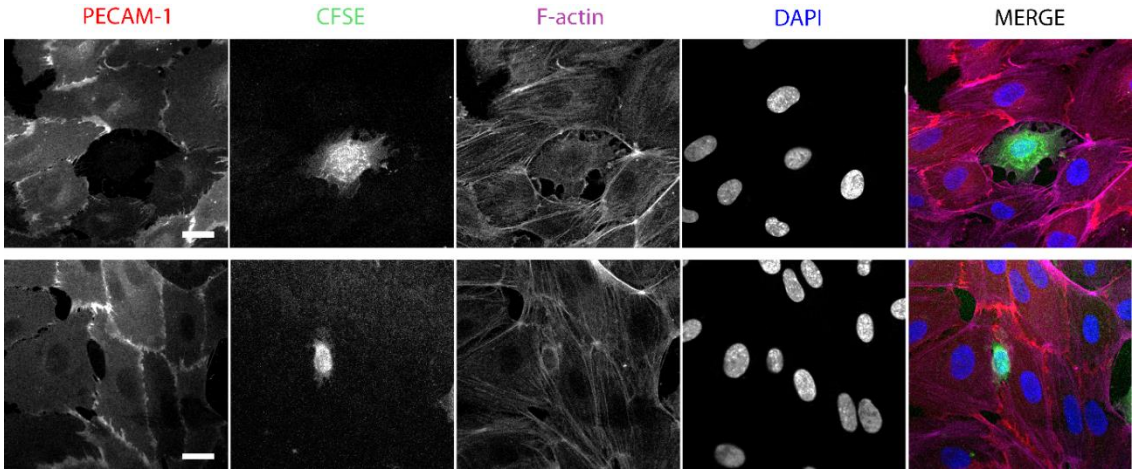

Figure 3.16 - Interaction of EGTA-treated MCF-7 cells with HUVECs

HUVECs were grown to confluency on collagen I-coated glass coverslips. Before CFSE-labelled MCF-7 cells were added to the monolayer for 1 hour, 5 nM of EGTA was added to the cells. Non-adherent cells were washed off and the cells that remained adhered were fixed and permeabilized. Cells were stained for F-actin, PECAM-1 and nuclei (DAPI). Images were acquired by confocal microscopy using Zen software (Zeiss) with a 63x oil immersion objective and are representative of random fields from two independent experiments. Scale bars = 20 µm.

3.3.3 Adhesion timecourse of HCC1954 and Cal51 cells to endothelial cells

All 3 types of breast cancer cells were able to adhere to endothelial cells as observed in the movies. Adhesion of cells to endothelial cells is one of the earlier steps of TEM (Reymond et al., 2013). This step involves proteins that are expressed on the cell surface and are not necessarily the same ones involved in other steps of this process. To determine the best time point to evaluate adhesion of cancer cell lines to HUVECs, a timecourse experiment was performed. The adhesion assay is based on the comparison of the fluorescence of total CFSE-labelled cells versus fluorescence of remaining cells after washing (Figure 3.17).

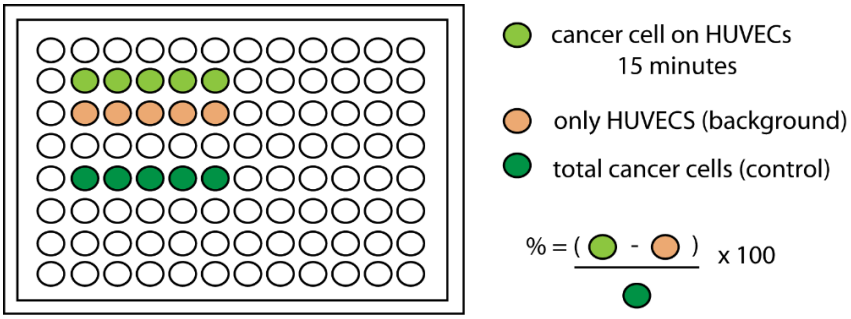

Figure 3.17 - Diagram of adhesion assay

CFSE-stained cancer cells are added to a monolayer of HUVECs and washed off after 15 minutes. Wells with only a monolayer of HUVECs were used to subtract the background fluorescence. Percentage of adhesion was calculated subtracting the fluorescence of HUVEC background from the fluorescence of cancer cells after washing. Then, this value was divided by the fluorescence of total cancer cells and multiplied by 100 (section 2.3.4.1).

Because MCF-7 cells grow in groups and it is difficult to prepare the solutions with the desired number of cells, the fluorescence signal was too strong, and it was difficult to obtain reliable results. MCF-7 cells were therefore not used in this assay (Figure 3.18).

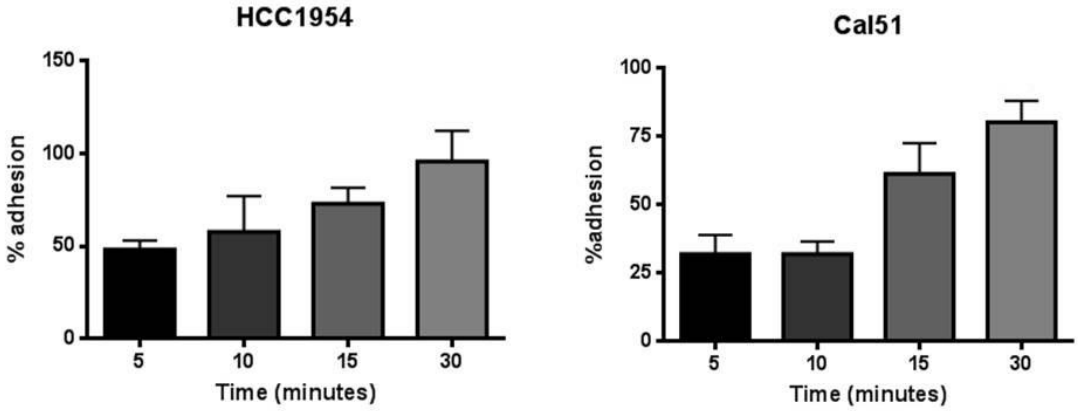

Figure 3.18 - Adhesion timecourse of HCC1954 and Cal51 cells to HUVECs

HUVECs were grown to confluence on collagen I-coated plates. CFSE-labelled cancer cells were added to the HUVECs and allowed to adhere for 5, 10, 15 and 30 minutes. Non-adherent or loosely adherent cells were washed off and the levels of fluorescence were measured on a plate reader. Graphs show data from three independent experiments, each carried out in triplicate. Values represent mean ± SEM. 100% corresponds to the signal of total number of cells in the wells that were not washed.

Although Cal51 and HCC1954 cells showed a tendency to increase adhesion over time, only at 30 minutes did Cal51 cells have a significant increase in adhesion compared to 5 minutes. The results were quite variable, as indicated by the large error bars. A possible reason for this variability between experiments is that the CFSE staining varies between each experiment. However, the results were used to choose the best time point to perform adhesion assays. The 15 minute time point was chosen because more than 50% of the cells have adhered but only around 10% have intercalated (Figure 3.6D).

3.3.4 Breast cancer cell interaction with endothelial cells on a thick layer of collagen

The behaviour of the MDA-MB-231, MCF-7, Cal51 and HCC1954 cells was investigated in a 3D TEM model (Cain et al., 2011) which includes all the steps of transendothelial migration (adhesion, intercalation and transmigration). Transmigration under the endothelium was observed for MDA-MB-231, Cal51 and HCC1954 cells (Figure 3.19, 3.20 and 3.21).

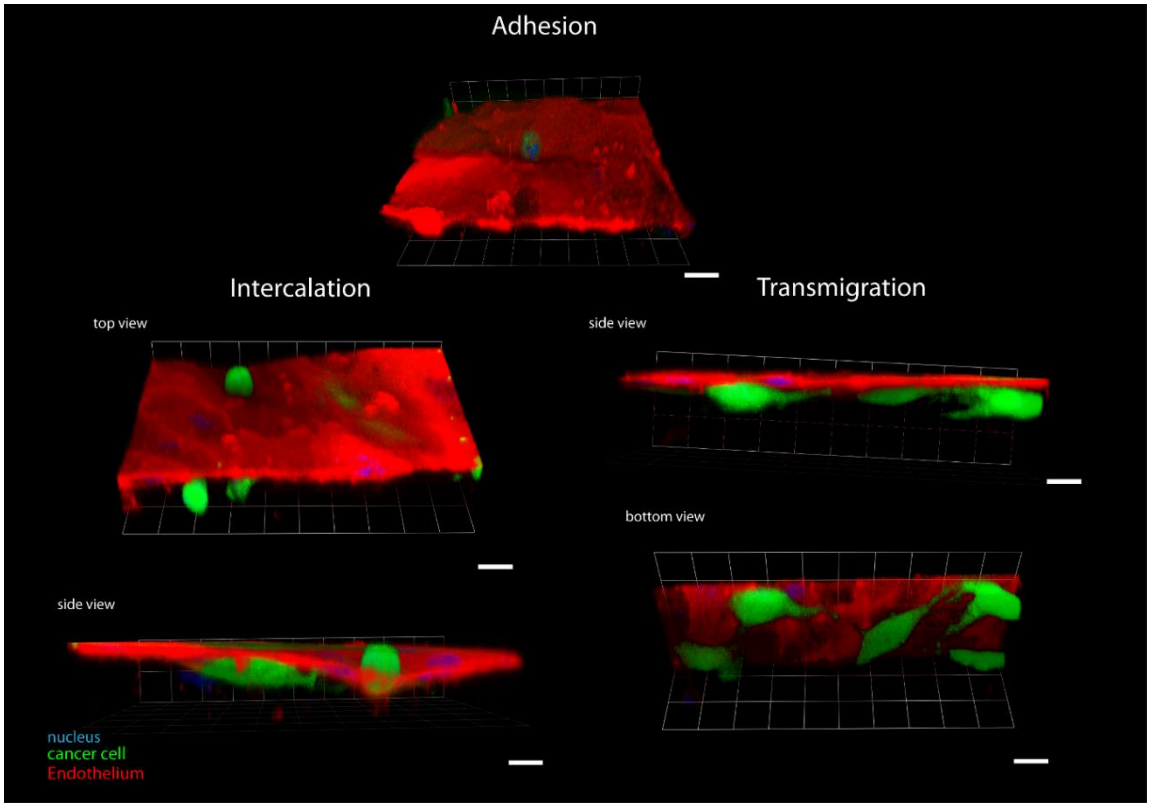

Figure 3.19 - Interaction of MDA-MB-231 cells with endothelial cells on a thick collagen I layer

CFSE-labelled cancer cells were added to a confluent monolayer of HUVECs seeded on top of a thick 2 mg/ml collagen I matrix. After 24 hours, cells were fixed and stained for PECAM-1 (red) and with DAPI (blue). Images of four different fields were acquired by confocal microscopy using Zen software. xyz projections of a z-stack of 40 images of the cancer cells on the 3D matrices were obtained using Volocity software. Images on the left represent the top and side views of xyz projections during intercalation. Images on the right represent the side and bottom views of xyz projections after transmigration. Scale bar = 1 unit = 45.7 µm. Images are from one experiment.

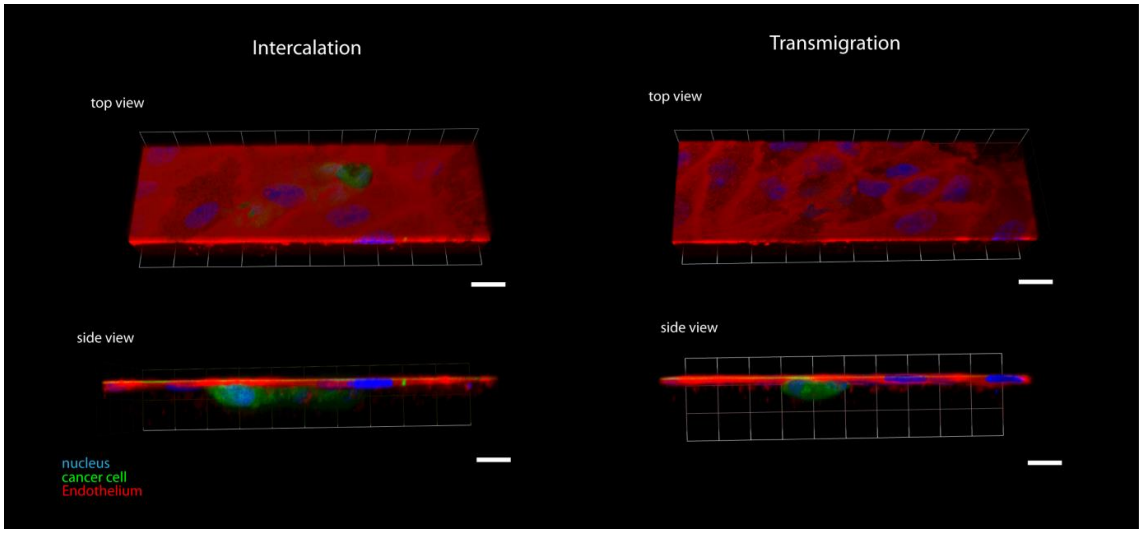

Figure 3.20 - Interaction of Cal51 cells with endothelial cells on a thick collagen I layer

CFSE-labelled cancer cells were added to a confluent monolayer of HUVECs seeded on top of a thick 2 mg/ml collagen I matrix. After 24 hours, cells were fixed and stained for PECAM-1 (red) and with DAPI (blue). Images of four different fields were acquired by confocal microscopy using Zen software. xyz projections of a z-stack of 40 images of the cancer cells on the 3D matrices were obtained using Volocity software. Images on the left represent the top and side views of xyz projections during intercalation. Images on the right represent the top and side views of xyz projections after transmigration. Scale bar = 1 unit = 45.7 µm. Images are from one experiment.

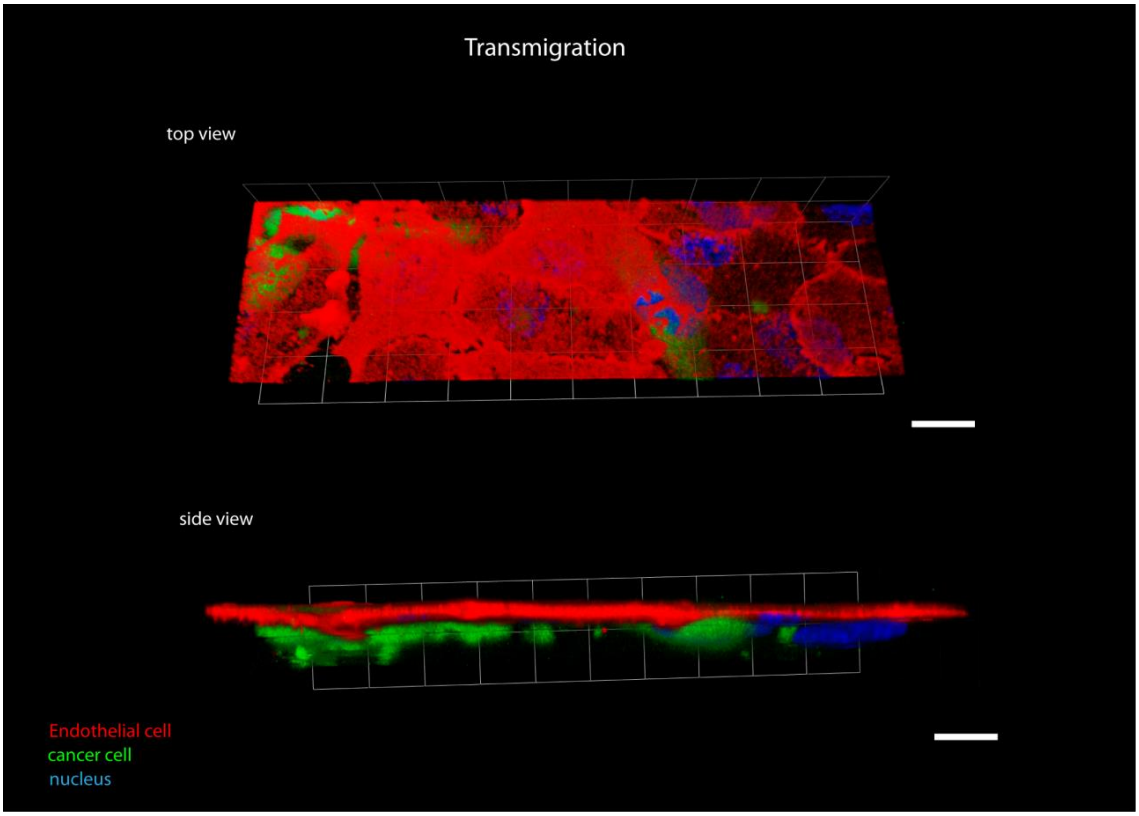

Figure 3.21 - Interaction of HCC1954 cells with endothelial cells on a thick collagen I layer

CFSE-labelled cancer cells were added to a confluent monolayer of HUVECs seeded on top of a thick 2 mg/ml collagen I matrix. After 24 hours, cells were fixed and stained for PECAM-1 (red) and with DAPI (blue). Images of four different fields were acquired by confocal microscopy using Zen software. xyz projections of a z-stack of 40 images of the cancer cells on the 3D matrices were obtained using Volocity software. Images represent the top and side views of xyz projections after transmigration. Scale bar = 1 unit = 45.7 µm. Images are from one experiment.

Due to the formation of holes in the monolayer of endothelial cells by the MCF-7 cells, it was difficult to assess if the cancer cells were transmigrating (Figure 3.22).

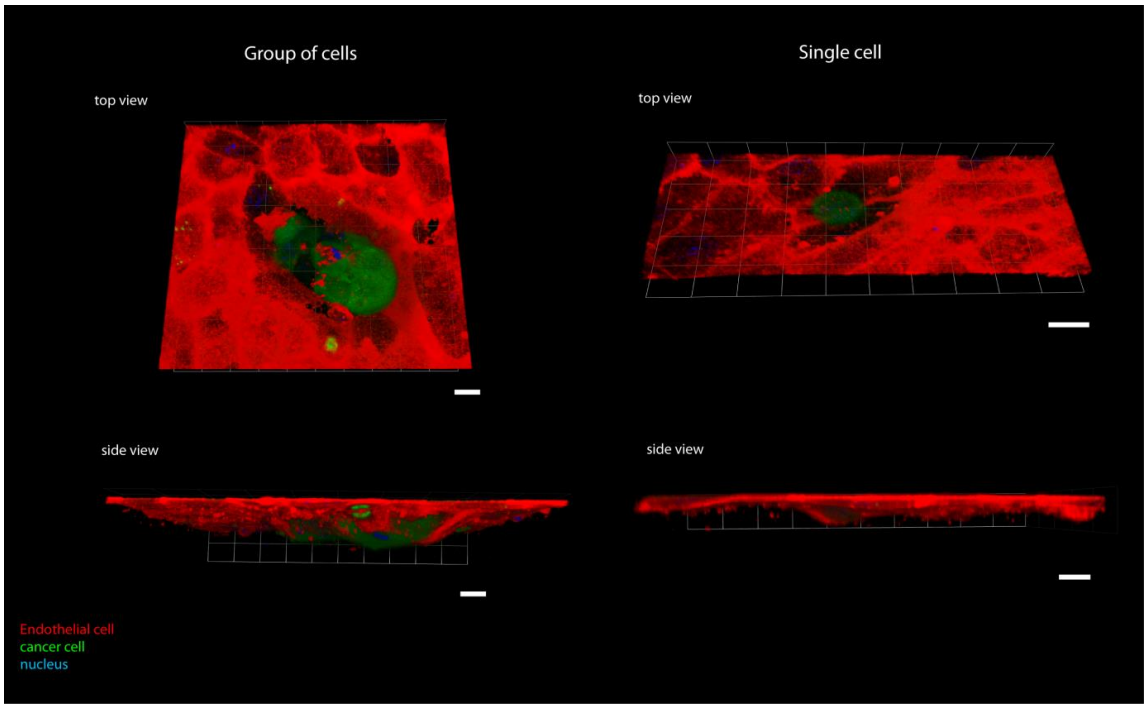

Figure 3.22 - Interaction of MCF-7 cells with endothelial cells on a thick collagen I layer

CFSE-labelled cancer cells were added to a confluent monolayer of HUVECs seeded on top of a thick 2 mg/ml collagen I matrix. After 24 hours, cells were fixed and stained for PECAM-1 (red) and with DAPI (blue). Images of four different fields were acquired by confocal microscopy using Zen software. xyz projections of a z-stack of 40 images of the cancer cells on the 3D matrices were obtained using Volocity software. Images on the left represent the top and side views of xyz projections of a group of cells. Images on the right represent the top and side views of xyz projections of a single cell. Scale bar = 1 unit = 45.7 µm. Images are from one experiment.

3.4 Effects of RhoBTB1 depletion in Cal51 cells on endothelial interaction

To determine how RhoBTB1 depletion affected breast cancer cell interaction with endothelial cells, Cal51 cells were chosen. Both MDA-MB-231 and Cal51 cell lines are triple negative (ER^-, PR^-, $HER2^-$, Table 3.1), but they do not belong to the same subtype (Figure 3.2). Although the morphology of MDA-MB-231 and Cal51 cells is not similar in 2D culture, these cells behaved in a similar way when added on top of endothelial cells. Almost 80% of MDA-MB-231 and Cal51 cells were intercalated after 6 hours. These cells intercalate as single cells and they do not damage the endothelium during intercalation and TEM (Figure 3.6, 3.19 and 3.20).

RhoBTB1 was depleted in Cal51 cells using four different siRNA oligos targeting RhoBTB1. RhoBTB1 mRNA levels in Cal51 cells were reduced by around 50% using oligos #1, #2 and #3 at 72 hours after siRNA transfection, similar to the results obtained in MDA-MB-231 cells (Figure 3.23). Since oligos #1 and #2 were used for functional assays with MDA-MB-231 cells (Borda D'Agua, 2012), these oligos were also used for Cal51 cells. Protein levels were not analysed because there is no antibody available that can detect endogenous RhoBTB1 in these cell lines.

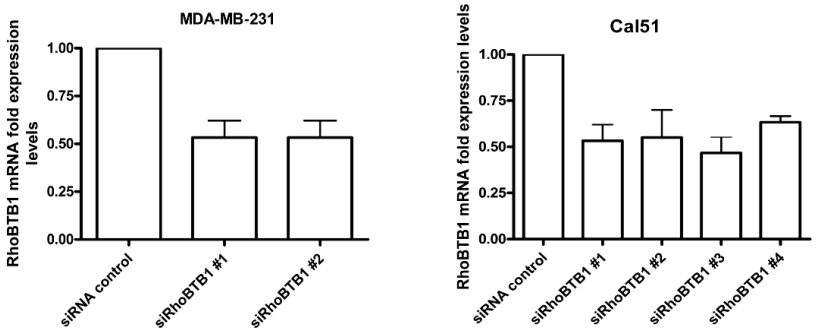

Figure 3.23 - RhoBTB1 depletion in MDA-MB-231 and Cal51 cells

MDA-MB-231 and Cal51 cells were transfected with siRNA control or siRNA oligos #1 and #2 and oligos #1, #2, #3 and #4 targeting RhoBTB1, respectively. After 72 hours, the relative amount of RhoBTB1 mRNA was determined by quantitative PCR. Graphs show data from three independent experiments. All values were normalized to siRNA control. Values represent mean ± SEM.

Adhesion and intercalation of Cal51 cells into a monolayer of HUVECs was analysed after depletion of RhoBTB1. Adhesion was affected only by depletion of RhoBTB1 using oligo #2 (Figure 3.24A). Intercalation of Cal51 cells appeared to be slightly reduced at early time points, but there was no significant different between the conditions at any time point (Figure 3.24B).

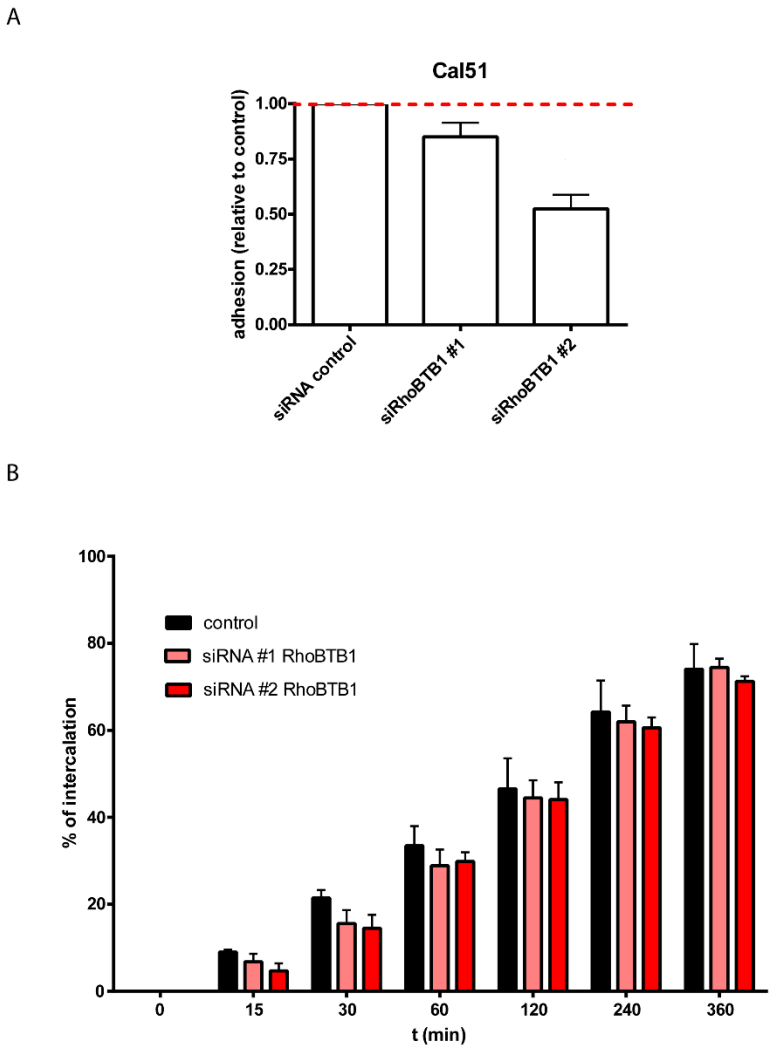

Figure 3.24 - Adhesion and intercalation of Cal51 cells into endothelial cells

A) HUVECs were grown to confluence on collagen I-coated plates. CFSE-labelled Cal51 cells were added to the HUVECs and allowed to adhere for 15 minutes. Non-adherent or loosely adherent cells were washed off and the levels of fluorescence were measured. Graphs show data from four independent experiments, each carried out in quintuplicate. Values represent mean ± SEM. B) Cal51 cells were monitored by timelapse microscopy acquiring an image every 3-5 min over 6 hours. The graph shows the percentage of intercalated cells at the indicated time points from three independent experiments. Nine different fields of each condition were analysed per experiment (~ 30 cells per field). Values represent mean ± SEM.

3.4.1 RhoBTB1 effects on β_1 integrin and RhoA levels

One of the proteins affected by RhoBTB1 depletion in MDA-MB-231 cells was β_1 integrin. β_1 integrin is known to be involved in adhesion of PC3 prostate cancer cells to endothelial cells (Reymond et al., 2012). Integrin receptors are heterodimers of α and β subunits that are well-known to bind to extracellular matrix ligands, connecting the extracellular matrix to the actin cytoskeleton (Campbell and Humphries, 2011). Integrins have also been shown to bind receptors on other cells. For example, VCAM-1 in the endothelial cell can interact with $\alpha_4\beta_1$ in cancer cells (Miles et al., 2008). Depletion of RhoBTB1 in MDA-MB-231 cells led to a decrease in β_1 integrin levels, which in turn, could be the cause of the decrease in adhesion of cancer cells to endothelial cells (Figure 3.25 – Results from Borda D'Agua (2012)).

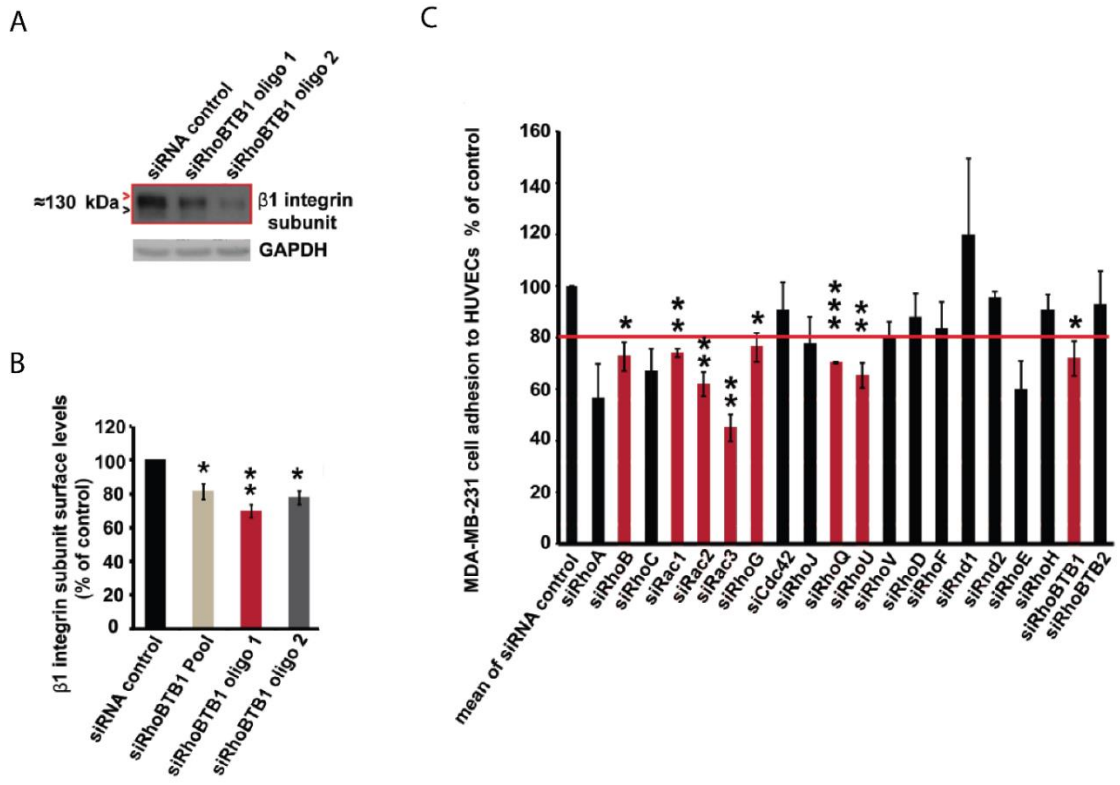

Figure 3.25 - Effects of RhoBTB1 depletion in β_1 integrin expression and cancer cell adhesion to endothelial cells in MDA-MB-231 cells

A) MDA-MB-231 cells were siRNA transfected and 72 hours after cells were lysed and equal amounts of protein analysed by immunoblotting with antibody to β_1 integrin subunit. Blot was re-probed for GAPDH. Blot is representative of three independent experiments. B) siRNA- transfected MDA-MB-231 cells were detached 72 hours after transfection and stained for β_1 integrin subunit surface levels with a specific antibody. The background levels were detected by including a second population of control and depleted cells labelled with mouse Alexa-488. Levels were measured by flow cytometry from three independent experiments. β_1 integrin subunit surface levels were quantified. Results are expressed relative to IgG secondary antibody. Values represent mean ± SEM. **p<0.01, *p<0.05, compared to siRNA control, determined by unpaired Student's t-test. C) HUVECs were grown to confluence on collagen I-coated plates. CFSE-labelled cancer cells were added to the HUVECs and allowed to adhere for 15 minutes. Non-adherent or loosely adherent cells were washed off and the levels of fluorescence were measured. Graphs show data from three independent experiments, each carried out in triplicate. Red bars represent the hits. Values represent mean ± SEM. ***p<0.001, **p<0.01, *p<0.05, compared to siRNA control, determined by unpaired Student's t-test. Results from Borda D'Agua (2012).

Endogenous levels of β_1 integrin were compared in different breast cancer cell lines. MDA-MB-231 cells had the highest levels, followed by Cal51 cells. MCF-7, T47D and HCC1954 cells had similar levels of β_1 integrin (Figure 3.26). MDA-MB-231 and HCC1954 cells had only one band while MCF-7, T47D and Cal51 cells have two bands. The two bands could be differentially glycosylated forms of β_1 integrin, or and alternatively spliced isoforms (de Melker and Sonnenberg, 1999; Zhao et al., 2008). T47D cell line was included to analyse if cell lines from the same subtype (luminal A) have similar β_1 integrin band pattern. In this case, both T47D and MCF-7 cells had two bands for β_1 integrin (Figure 3.26).

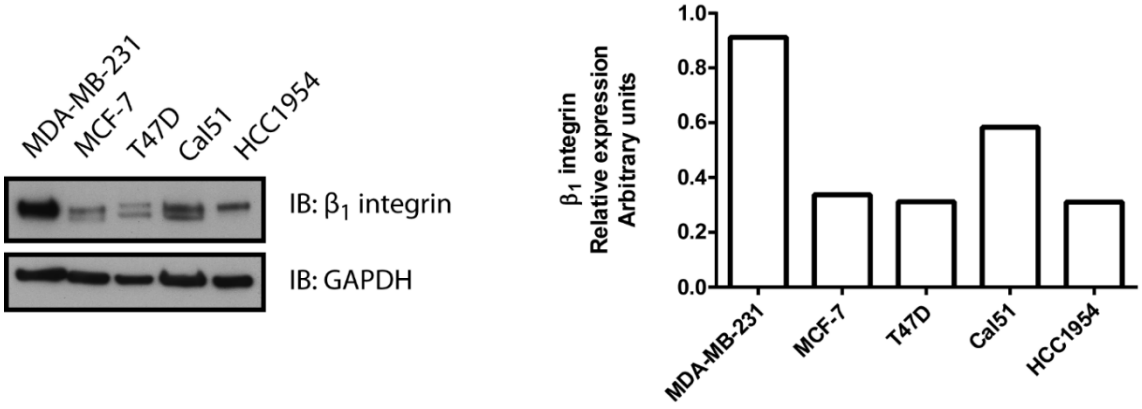

Figure 3.26 - Expression of β_1 integrin in breast cancer cell lines

Breast cancer cells were lysed and protein expression was analysed by western blotting. GAPDH is used as a loading control. Graph shows the quantification of the band density of β_1 integrin normalised to GAPDH. Blots are from one experiment.

Levels of β_1 integrin in Cal51 cells after RhoBTB1 depletion were analysed. A decrease in β_1 integrin expression was significant only for oligo #2 (Figure 3.27).

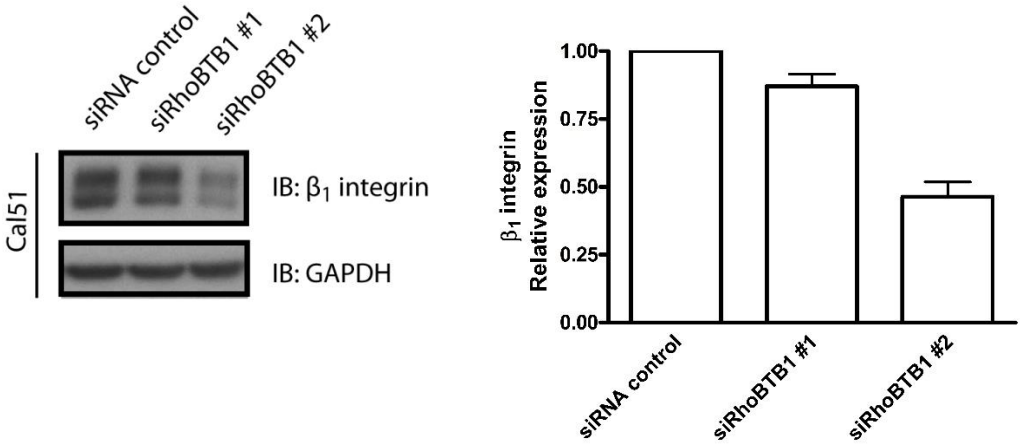

Figure 3.27 - Expression of β_1 integrin in Cal51 cells after RhoBTB1 depletion

Cal51 cells were transfected with siRNA control or siRNA oligos #1 and #2 targeting RhoBTB1. After 72 h, cells were lysed and protein expression was analysed by western blotting. GAPDH is used as a loading control. Graph shows the quantification of the bands density of three independent experiments, normalised to GAPDH and relative to siRNA control. Values represent mean ± SEM.

Another protein that was affected by RhoBTB1 depletion in MDA-MB-231 cells was RhoA. Depletion of RhoBTB1 led to a decrease in RhoA levels and depletion of RhoA decreased intercalation of cancer cells into endothelial cells (Figure 3.28 – Results from Borda D'Agua (2012)). The hypothesis is that RhoA is involved in cancer cell/endothelial cell interaction during intercalation. RhoA is known to be involved in actin cytoskeleton rearrangement, affecting cell motility (Wheeler and Ridley, 2004) (Chapter 1, section 1.1.2).

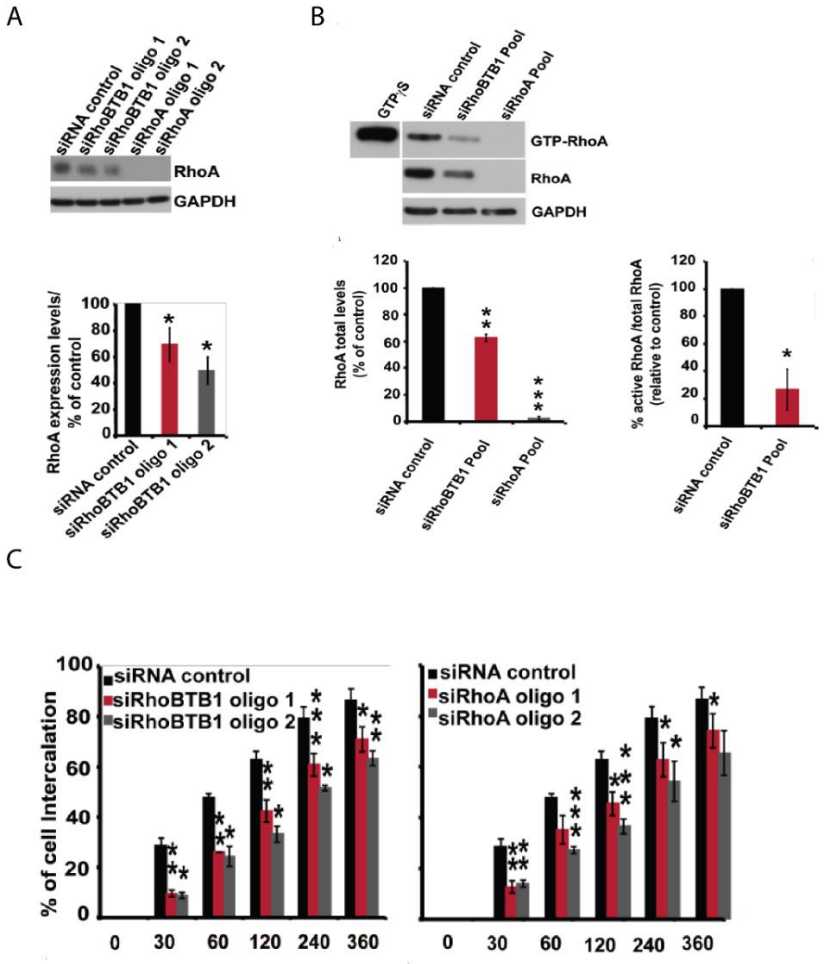

Figure 3.28 - Effects of RhoBTB1 depletion in RhoA expression and activity; and cancer cell intercalation into endothelial cells in MDA-MB-231 cells

A) MDA-MB-231 cells were siRNA transfected and after 72 hours cells were lysed and equal amounts of protein were analysed by immunoblotting with antibody to RhoA. Blot was re-probed for GAPDH. Blots are representative of three independent experiments. Graph show RhoA levels relative to GAPDH. Value represent mean ± SEM. *p<0.05, compared to siRNA control, determined by unpaired Student's t-test. B) MDA-MB-231 cells were siRNA transfected for RhoBTB1 and RhoA. 72 hours after transfection cells were lysed and incubated with GST-Rhotekin-RBD beads to pull down active RhoA. Immunoblots were probed for RhoA and total lysates membranes were rre-probed for GAPDH. Total lysate of siRNA control sample was used for pull down positive control, using pre-loading of GTPases in lysate with GTPγS. Blots are representative of three independent experiments. Graphs show total RhoA levels relative to GAPDH and active RhoA levels relative to total RhoA. Values represent mean ± SEM. ***p<0.001, **p<0.01, *p<0.05, compared to siRNA control, determined by unpaired Student's t-test. C) siRNA-transfected MDA-MB-231 cells were monitored acquiring an image every 3 minutes for 6 hours. Graphs show data from three independent experiments. Three different fields of each condition were analysed per experiment (100-150 cell per experiment; ~ 50 cells per field). Values represent mean ± SEM. ***p<0.001, **p<0.01, *p<0.05, compared to siRNA control, determined by unpaired Student's t-test. Results from Borda D'Agua (2012).

Levels of RhoA in Cal51 cells after RhoBTB1 depletion were analysed. There was no significant difference in RhoA expression between the conditions (Figure 3.29).

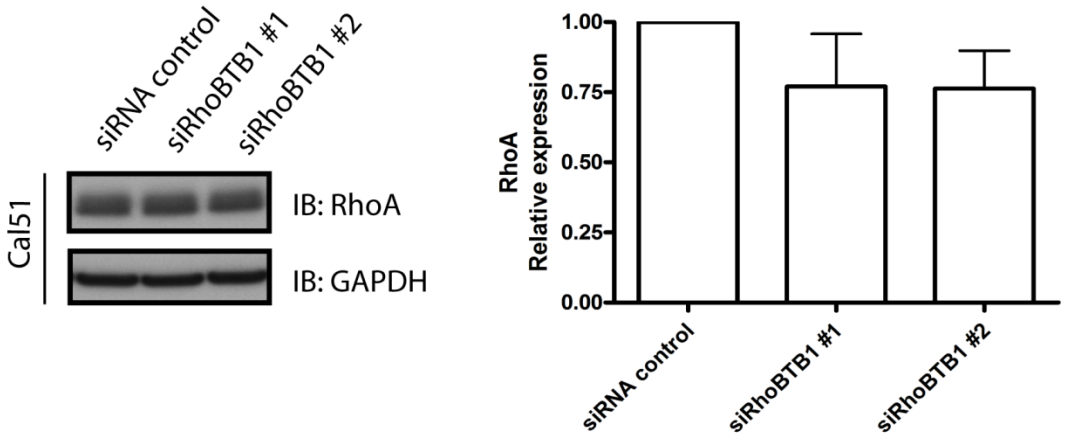

Figure 3.29 - Expression of RhoA in Cal51 cells after RhoBTB1 depletion

Cal51 cells were transfected with siRNA control or siRNA oligos #1 and #2 targeting RhoBTB1. After 72 h, cells were lysed and protein expression was analysed by western blotting. GAPDH is used as a loading control. Graph shows the quantification of the band density of three independent experiments, normalised to GAPDH and relative to siRNA control. Values represent mean ± SEM.

3.5 Discussion

To investigate whether RhoBTB1 affected cancer cell invasion or cancer cell interaction with endothelial cells, functional assays were performed using breast cancer cell lines. After optimization of three breast cancer cell lines using the 2D and 3D models in our laboratory to study adhesion, intercalation and transmigration, Cal51 cells were chosen to be used in the RhoBTB1 depletion experiments.

3.5.1 Characterization of breast cancer cell lines with endothelial cells

Depletion of RhoBTB1 in MDA-MB-231 cells decreases cell adhesion and intercalation into an endothelial monolayer (Figure 3.25 and 3.28 from Borda D'Agua (2012)). To determine whether RhoBTB1 could affect the interaction of other breast cancer cell lines with endothelial cells, three cell lines (MCF-7, Cal51 and HCC1954) were first tested regarding their ability to interact with collagen I matrix and endothelial monolayers. The results with MCF-7, Cal51 and HCC1954 cell lines showed promising and interesting results indicating that they could be used in studies of cancer cell interaction with endothelial cells. All three cell lines were able to interact with a collagen I matrix and endothelial cells. However, modifications in the protocol are necessary for some of the cell lines.

The Cal51 cell line was the one that showed the most interesting and unexpected results. In the live cell imaging intercalation assay, this cell line showed a similar behaviour to MDA-MB-231 cells. Although the two cell lines are not from the same breast cancer cell subtype (Figure 3.2), they are both triple negative, were isolated from pleural effusions and are highly tumorigenic (Cailleau et al., 1974; Gioanni et al., 1990; Neve et al., 2006). These common characteristics could be important during the cancer cell intercalation step. In addition, in the confocal images it was possible to observe that Cal51 cells could cross the endothelial monolayer using either a

paracellular or transcellular migration route. The transcellular route is quite difficult to observe for cancer cells *in vitro*, but for this cell line almost 25% of the cells transmigrated through the transcellular route. Transcellular migration is still not well understood. In leukocytes, there seems to be more than one mechanism that these cells use to cross through the endothelial cell. One mechanism is using "invadosome-like protrusions" that are fused with intracellular vesicular structures similar to caveolae and vesiculo-vacuolar organelles (VVOs) (Carman, 2009; Feng et al., 2002; Millán and Ridley, 2005). Another one is the transcellular migration mediated by the lateral border recycling compartment (LBRC) of the endothelial cells. A membrane containing PECAM, JAM-A and CD99 is recruited from the LBRC and surrounds the leukocyte that is transmigrating (Mamdouh et al., 2009). Although these mechanisms differ in some aspects, they both require an enrichment of ICAM-1 and PECAM-1 around the cell that is transmigrating (Carman, 2009; Mamdouh et al., 2009; Millan et al., 2006). In cancer cells, E-selectin and MLCK have been implicated in transcellular extravasation and transcellular intravasation, respectively (Khuon et al., 2010; Tremblay et al., 2008). It would be interesting to study if any of these molecules is involved in transcellular migration of Cal51 cells. Moreover, Cal51 cells could transmigrate between endothelial cells cultured on top of thick collagen, but it was not possible to observe any invasion into the collagen I matrix after 24 hours. Cal51 cells have not been reported to invade collagen I matrices. Perhaps these cells interact more with other components of the stroma such as fibronectin or other types of collagen (Psaila and Lyden, 2009).

The HCC1954 cell line was able to transmigrate across the endothelial cells and invade into the collagen I matrix in the 3D model after 24 hours. However, in the intercalation assay using fixed cells, some cells spread on top of the endothelial cells. It is not known whether this affects the transmigration or if it is a different way that the cells use to transmigrate. One possible explanation is that HCC1954 cells express different receptors from the other cell lines analysed that are important for stable cancer cell-

endothelial cell adhesion. HCC1954 cell line is the only one studied that is originated from a primary tumour (Neve et al., 2006). Several receptors have been implicated in the stable cancer cell-endothelial cell adhesion, including integrins, CD44 and MUC1 (Reymond et al., 2013). Therefore, it would be interesting to test the roles of these receptors through RNAi screening in the future. Further experiments are necessary to study better the behaviour of HCC1954 cells.

MCF-7 cells caused more problems during the experiments. Most of the cells grow as groups which made it difficult to analyse the transmigration of single cells. During the live imaging intercalation assay, it was possible to see that the cell groups form holes in the monolayer, pushing away the endothelial cells. It is known that MCF-7 cells secret a lipid (12(s) hydroxyeicosatetraenoic acid – HETE) that induces retraction of the endothelial monolayer (Uchide et al., 2007). This could explain the effect of MCF-7 cells in the monolayer observed in the intercalation images and in the 3D TEM images. Because there are many cell groups, it was difficult to control the exact number of cells that were in each well. Trying to work with as many single cells as possible, cells were treated with EGTA before performing the experiment. However, the fluorescence values obtained were too low. To study this cell line, changes in the protocol are necessary.

3.5.2 Effects of RhoBTB1 depletion in Cal51 cells on endothelial interaction

Based on the characterization of the breast cancer cell lines with endothelial cells, Cal51 cells were chosen to be used in additional functional assays to study the effects of RhoBTB1 depletion in these cells. Cal51 cell line is a basal-like breast cancer subtype obtained from a pleural effusion. Cal51 cells are triple negative (ER^-, PR^- and $HER2^-$) similar to MDA-MB-231 cells. Both cell lines form experimental metastasis in the lung when injected in the tail vein of mice. However, MDA-MB-231 cells have been used more than Cal51 cells in studies *in vitro* and *in vivo*.

Initial functional assays have shown that adhesion of Cal51 cells to endothelial cells were affected only by one oligo targeting RhoBTB1 (oligo #2). A decrease of around 50% was observed. According to previous studies in MDA-MB-231 cells, depletion of RhoBTB1 leads to a decrease in cancer cell adhesion to endothelial cells of around 30% and β_1 integrin is one of the proteins that might be involved in cancer cell/endothelial cell interaction in this model (Figure 3.25 from Borda D'Agua (2012)). Decrease in β_1 expression after Cdc42 depletion has also shown to affect adhesion of PC3 cells to endothelial cells, causing a decrease in approximately 40% of cancer cell adhesion (Reymond et al., 2012). For that reason, levels of β_1 integrin were analysed in different breast cancer cell lines. Expression of this protein in MDA-MB-231 cells is higher than in Cal51 cells. This could indicate that β_1 integrin might have a more important role in MDA-MB-231 cells than in Cal51 cells. However, when the levels of β_1 integrin were analysed after RhoBTB1 depletion, there was a decrease only with siRhoBTB1 #2, the same siRNA that decreased Cal51 cell adhesion to endothelial cells. These results could indicate that there is an off-target effect of oligo #2 targeting RhoBTB1. Other siRNA oligos need to be tested in the future. In addition, it seems that RhoBTB1 has no effect in the levels of β_1 integrin in Cal51 cells. It would be interesting to investigate whether β_1 integrin depletion reduces adhesion or intercalation of Cal51 cells to endothelial cells.

Intercalation of Cal51 cells into a monolayer of endothelial cells was also analysed. Studies with MDA-MB-231 cells have shown that depletion of RhoBTB1 significantly reduces cancer cell intercalation into a monolayer of endothelial cells in the first 2 hours of experiment. Depletion of RhoA is also able to decrease intercalation of MDA-MB-231 cells into endothelial cells (Figure 3.28 from Borda D'Agua (2012)). Based on these findings, expression and activity of RhoA in MDA-MB-231 cells were analysed after depletion of RhoBTB1. Both expression and activity of RhoA are reduced after knockdown of RhoBTB1 in these cells (Figure 3.28 from Borda D'Agua (2012)).

Interaction of RhoA and RhoBTB1 will be further explored in Chapter 5. The lack of phenotype in Cal51 cells could mean that RhoBTB1 is not able to regulate RhoA in these cells. And in fact, depletion of RhoBTB1 in Cal51 cells does not affect total RhoA levels. Because no phenotype was observed in the adhesion and intercalation assays, the transmigration assay was not performed with the Cal51 cell line.

Problems in RhoBTB1 knockdown in Cal51 cells could be one possible explanation for the fact that depletion of RhoBTB1 does not affect adhesion and intercalation of these cells into endothelial cells. The efficiency of RhoBTB1 mRNA knockdown (approximately 50% decrease in mRNA levels) obtained in Cal51 cells is similar MDA-MB-231 cells. However, the protein levels could be different. Another possible explanation is that the signalling by RhoBTB1 in MDA-MB-231 cells is different in Cal51 cells, so that RhoBTB1 is not important for endothelial interaction. More experiments are necessary to explore this possibility. It is also important in the future to repeat some experiments comparing directly MDA-MB-231 and Cal51 cells.

4 Characterization of RhoBTB1

4.1 Introduction

Since RhoBTB1 depletion in Cal51 breast cancer cells did not reproduce the results described for MDA-MB-231 cells concerning interaction with endothelial cells (as reported in Chapter 3), the focus of the project changed to characterise RhoBTB1 signalling, based initially on what has been reported for RhoBTB2 and RhoBTB3. These three proteins share a similar domain organization: a GTPase domain which is followed by a proline-rich region, a tandem of two BTB domains and a conserved C-terminal region (Berthold et al., 2008a). However, only RhoBTB1 and RhoBTB2 are considered part of the Rho GTPase family, since the GTPase domain of RhoBTB3 shows very low similarity to the other Rho GTPase proteins (Boureux et al., 2007; Wennerberg and Der, 2004). RhoBTB3 is considered a separate member of the Ras superfamily (Boureux et al., 2007).

In this chapter, some already known properties of RhoBTB1 were tested such as interaction with cullin3 and localisation to vesicles. All three RhoBTB proteins are known to bind cullin3 (Berthold et al., 2008a) and RhoBTB2 has been shown to be a substrate of a cullin3 ubiquitin ligase complex (Wilkins et al., 2004). RhoBTB3 seems to act as a BTB adaptor protein, since it forms a complex with cullin3 which mediates ubiquitination of cyclin E on the Golgi (Lu and Pfeffer, 2013). However, it has also been shown that RhoBTB3 protects 5-HT7a receptor from proteasomal degradation (Matthys et al., 2012). Apart from the interaction with cullin3, there is no evidence that RhoBTB1 is either a substrate or a BTB adaptor protein of cullin3 ubiquitin ligase complexes.

Overexpressed myc-epitope tagged RhoBTB1 and RhoBTB2 have been shown to localise to vesicles, with almost no effect on the actin cytoskeleton in PAE cells (Aspenstrom et al., 2004). As mentioned in Chapter 1 (section 1.1.7), RhoBTB2 is involved in transporting VSVG in a microtubule-dependent manner (Chang et al.,

2006). This suggests that the localisation of RhoBTB proteins to vesicles could be related to their cellular functions.

It has been reported that RhoBTB2 and RhoBTB3 can form homodimers and heterodimers through their BTB domains (Berthold et al., 2008a). However, this has not been tested for RhoBTB1. The physiological relevance of RhoBTB dimerisation is still unknown. One possible role for these dimers would be as part of the cullin3 complex, since it is known that some BTB adaptor proteins dimerise to interact with either cullin3 or the substrate (McMahon et al., 2006). Regulation of RhoBTB proteins is poorly understood. These proteins do not cycle between an active GTP-bound form and an inactive GDP-bound form (Berthold et al., 2008a), and therefore are not regulated by GAPs and GEFs. They are not prenylated and so do not interact with GDIs (Rivero et al., 2001). To better understand how RhoBTB1 could be regulated, some post-translational modifications were tested including ubiquitination and phosphorylation.

4.2 RhoBTB1 homodimerises and heterodimerises

To test whether RhoBTB1 can form dimers, RhoBTB1 tagged with either GFP or myc at the N-terminus was used, because there is no commercially available antibody that detects endogenous RhoBTB1. Cos7 cells were co-transfected with vectors encoding myc-RhoBTB1 and GFP-RhoBTB1. myc-RhoBTB1 and GFP-RhoBTB1 co-immunoprecipitated, suggesting that RhoBTB1 can homodimerise (Figure 4.1).

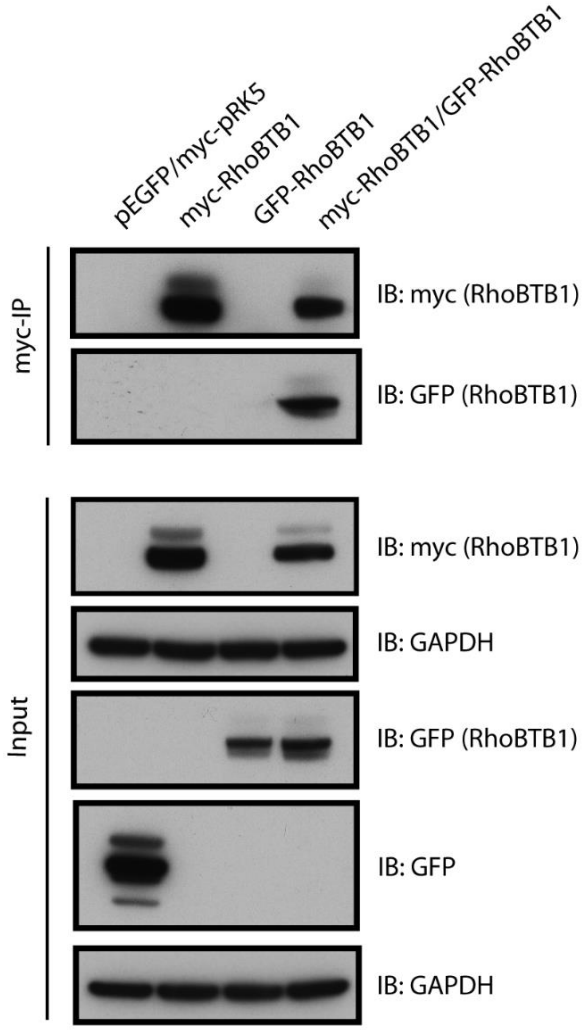

Figure 4.1 - Interaction of GFP-RhoBTB1 with myc-RhoBTB1

Cos7 cells were transfected with empty pEGFP and myc-pRK5 or vectors encoding myc-RhoBTB1 and/or GFP-RhoBTB1. After 24 hours, cells were lysed and incubated with anti-myc-agarose beads. Total lysates (input) and immunoprecipitates (myc-IP) were probed with anti-myc and anti-GFP antibodies to show levels of myc-RhoBTB1 and GFP-RhoBTB1. The interaction between myc-RhoBTB1 and GFP-RhoBTB1 is shown in the immunoprecipitates. GAPDH is used as a loading control. Blots are representative of three independent experiments.

As an alternative method to detect dimerisation, cells lysates were treated with the crosslinker disuccinimidyl suberate (DSS) after transfection with vector encoding myc-RhoBTB1. DSS contains two N-hydroxysuccinimide esters that are reactive towards primary amines and it is used to crosslink proteins (Leitner et al., 2010). This allows the detection of protein complexes that are not normally retained under denaturing conditions. Dimers (~ 150 kDa) and tetramers (~ 300 kDa) of myc-RhoBTB1 were detected following DSS treatment (Figure 4.2). The crosslinking assay is a good tool to observe protein complexes, but it does not distinguish between homodimers and interactions with other proteins. If RhoBTB1 forms a complex with other proteins apart from itself, these interactions would also be detected by DSS crosslinking.

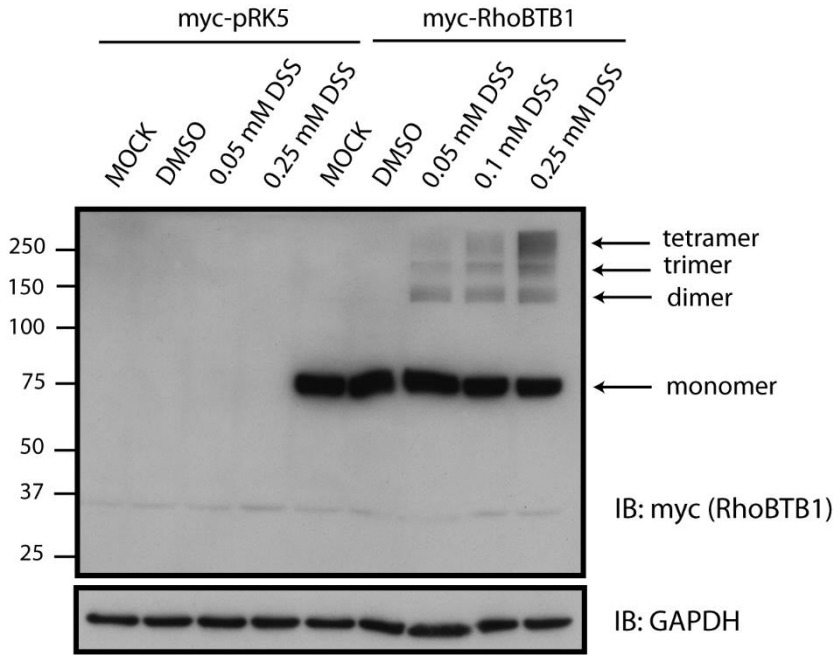

Figure 4.2 - RhoBTB1 can form homodimers and homotetramers

Cos7 cells were transfected with empty myc-pRK5 or vector encoding myc-RhoBTB1. After 24 hours, cells were lysed and treated with different concentrations (0.05, 0.1 and 0.25 mM) of disuccinimidyl suberate (DSS) crosslinker or DMSO as a control. Total lysates were probed with anti-myc antibody. GAPDH is used as a loading control. Blots are representative of two independent experiments. MOCK: untreated cells.

To determine the region of RhoBTB1 that is important for the formation of homodimers, RhoBTB1 from myc-RhoBTB1 was subcloned into a pEGFP-C1 vector (section 2.2.12) and RhoBTB1 deletion mutants were cloned into a GFP-CB6 vector (section 2.2.14) (Figure 4.3). The deletion mutants were first cloned into a pEGFP-C1 vector. However, no protein expression was observed for any of the mutants, because the sequences were not in frame. The deletion mutants were therefore cloned into a GFP-CB6 vector.

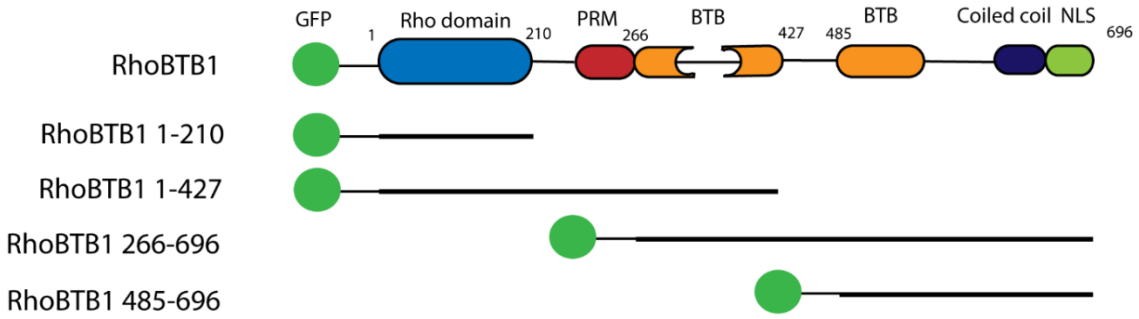

Figure 4.3 - Domain structure of GFP-RhoBTB1 and GFP-RhoBTB1 deletion mutants

RhoBTB1 1-210 = Rho domain; RhoBTB1 1-427 = Rho domain and first BTB domain; RhoBTB1 266-696 = first BTB domain, second BTB domain and C-terminus; RhoBTB1 485-696 = second BTB domain and C-terminus.

Cos7 cells were co-transfected with vectors encoding myc-RhoBTB1, full length GFP-RhoBTB1 and GFP-RhoBTB1 deletion mutants. Only GFP-RhoBTB1 1-210 was not able to interact with myc-RhoBTB1 (Figure 4.4). This is the only construct that does not encode a protein with at least one BTB domain, suggesting that BTB domains are necessary for RhoBTB1 dimerisation. This experiment needs repeating to confirm the results.

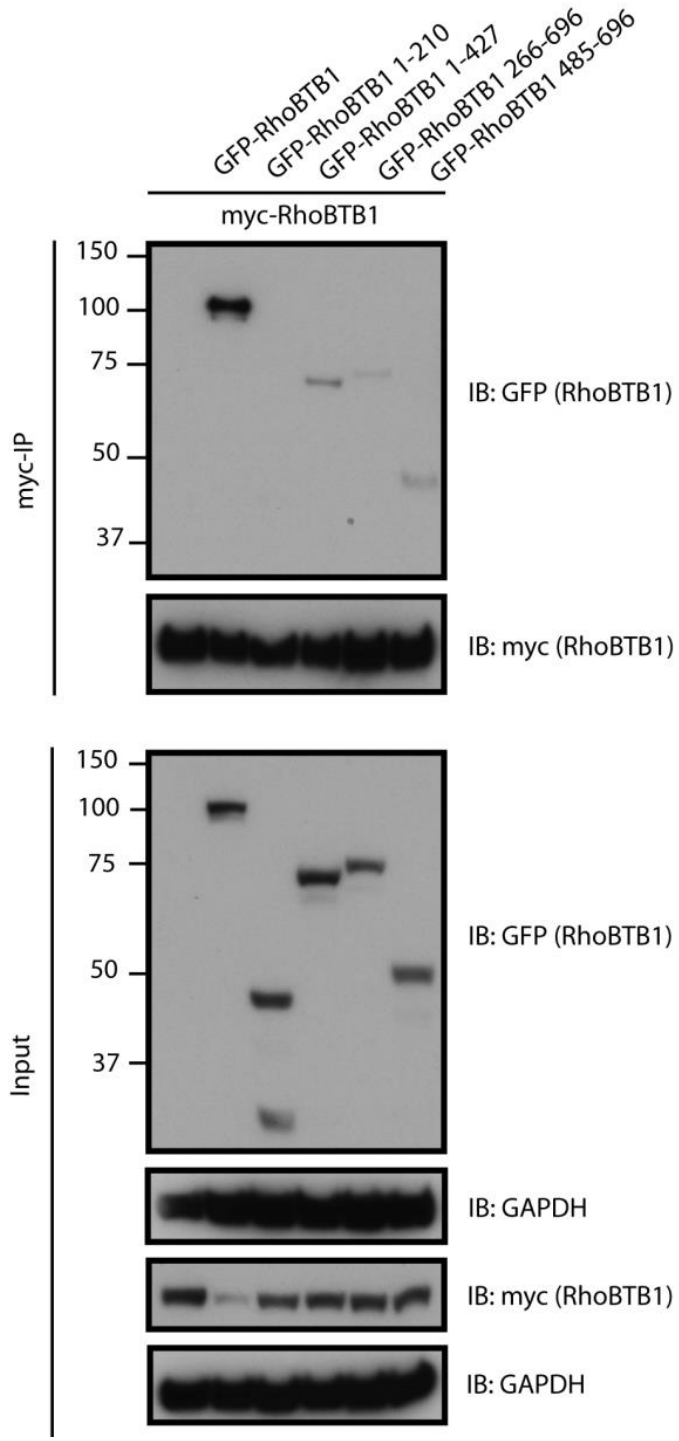

Figure 4.4 - Interaction of RhoBTB1 with RhoBTB1 deletion mutants

Cos7 cells were transfected with vectors encoding myc-RhoBTB1, GFP-RhoBTB1 and GFP-RhoBTB1 deletion mutants. After 24 hours, cells were lysed and incubated with anti-myc-agarose beads. Total lysates (input) and immunoprecipitates (myc-IP) were probed to show levels of myc-RhoBTB1 and endogenous cullin3. The interaction between myc-RhoBTB1 and GFP-RhoBTB1 deletion mutants is shown in the immunoprecipitates. GAPDH is used as a loading control. Blots are from one experiment.

Interaction of RhoBTB1 with RhoBTB2 was also studied to test the formation of heterodimers. Cos7 cells were co-transfected with vectors encoding myc-RhoBTB1 and GFP-RhoBTB2. myc-RhoBTB1 was able to immunoprecipitate with GFP-RhoBTB2 (Figure 4.5). These initial results suggest that RhoBTB1 could form homodimers and heterodimers. However, more experiments are necessary to prove these observations.

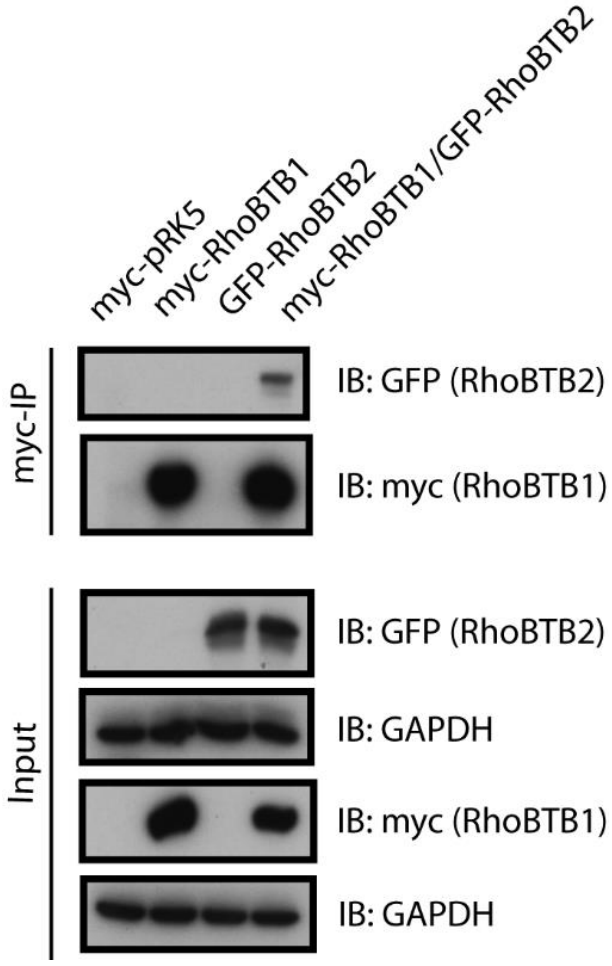

Figure 4.5 - Interaction of RhoBTB1 with RhoBTB2

Cos7 cells were transfected with empty myc-pRK5 or vectors encoding myc-RhoBTB1 and/or GFP-RhoBTB2. After 24 hours, cells were lysed and incubated with anti-myc-agarose beads. Total lysates (input) and immunoprecipitates (myc-IP) were probed to show levels of myc-RhoBTB1 and GFP-RhoBTB2. The interaction between myc-RhoBTB1 and GFP-RhoBTB2 is shown in the immunoprecipitates. GAPDH is used as a loading control. Blots are from one experiment.

4.3 Interaction of RhoBTB1 with cullin3

It has been shown that RhoBTB proteins can interact with cullin3, a scaffold protein in ubiquitin ligase complexes (Berthold et al., 2008a). To confirm this interaction, Cos7 cells were transfected with a vector encoding myc-RhoBTB1 and lysates immunoprecipitated with anti-myc-agarose beads. myc-RhoBTB1 was able to interact with endogenous cullin3 (Figure 4.6). As mentioned in section 1.2.2, the activity of CRLs can be regulated by NEDD8, an ubiquitin-like polypeptide which covalently binds to a conserved lysine residue in cullins (Wu et al., 2005). The higher molecular weight band for cullin3 in the blot corresponds to cullin3 covalently modified by NEDD8 (see Figure 4.8).

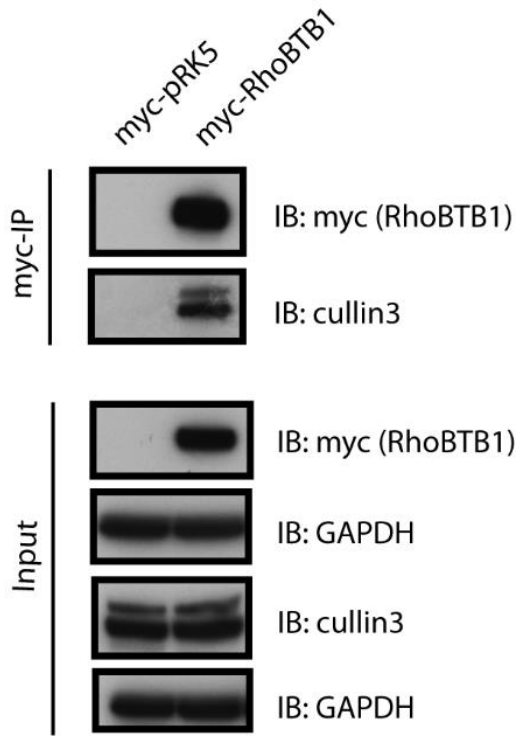

Figure 4.6 - Interaction of RhoBTB1 and cullin3

Cos7 cells were transfected with empty myc-pRK5 or vector encoding myc-RhoBTB1. After 24 hours, cells were lysed and incubated with anti-myc-agarose beads. Total lysates (input) and immunoprecipitates (myc-IP) were probed to show levels of myc-RhoBTB1 and endogenous cullin3. The interaction between myc-RhoBTB1 and cullin3 is shown in the immunoprecipitates. GAPDH is used as a loading control. Blots are representative of three independent experiments.

To determine the region of RhoBTB1 that is important for the interaction with cullin3, Cos7 cells were transfected with vectors encoding full length GFP-RhoBTB1 and GFP-RhoBTB1 deletion mutants. Endogenous cullin3 was only able to interact with full length GFP-RhoBTB1 and more weakly with GFP-RhoBTB1 266-696. This is consistent with what has been observed for other proteins where cullin3 is able to interact with these proteins through their BTB domain (Pintard et al., 2004). These two constructs are the only ones that encode proteins with the two BTB domains, suggesting that both BTB domains of RhoBTB1 are necessary for its interaction with cullin3 (Figure 4.7).

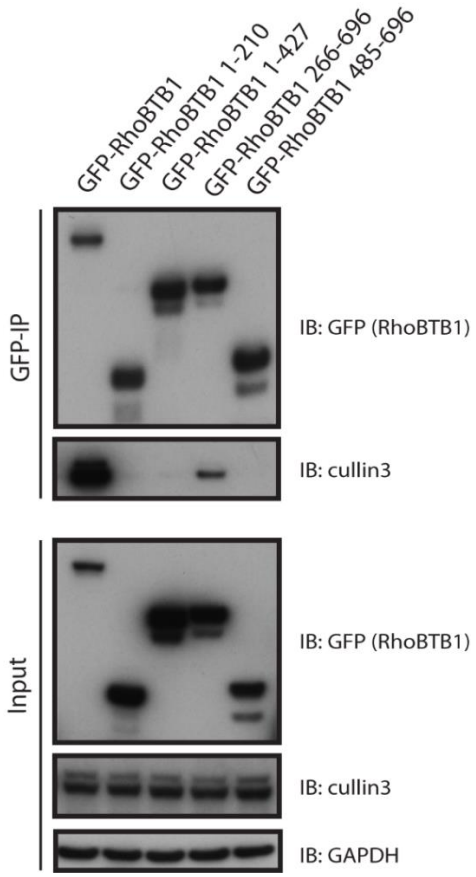

Figure 4.7 - Interaction of RhoBTB1 deletion mutants and cullin3

Cos7 cells were transfected with vectors encoding GFP-RhoBTB1 and GFP-RhoBTB1 deletion mutants. After 24 hours, cells were lysed and incubated with GFP-binding protein coupled to agarose (GFP-trap®). Total lysates (input) and immunoprecipitates (GFP-IP) were probed to show levels of GFP-RhoBTB1 and endogenous cullin3. The interaction between GFP-RhoBTB1 and cullin3 is shown in the immunoprecipitates. GAPDH is used as a loading control. Blots are representative of two independent experiments.

As neddylation of cullin3 is important for its activity (Wu et al., 2005), its role in cullin3 interaction with RhoBTB1 was tested. Neddylation was inhibited by the addition of MLN4924, an inhibitor of NAE which adds NEDD8 to lysine of cullins (Zhao et al., 2012). The efficiency of the treatment is measured by the decrease in the intensity of the higher molecular weight band of cullin3. Inhibition of cullin3 neddylation did not prevent the interaction between myc-RhoBTB1 and endogenous cullin3 (Figure 4.8).

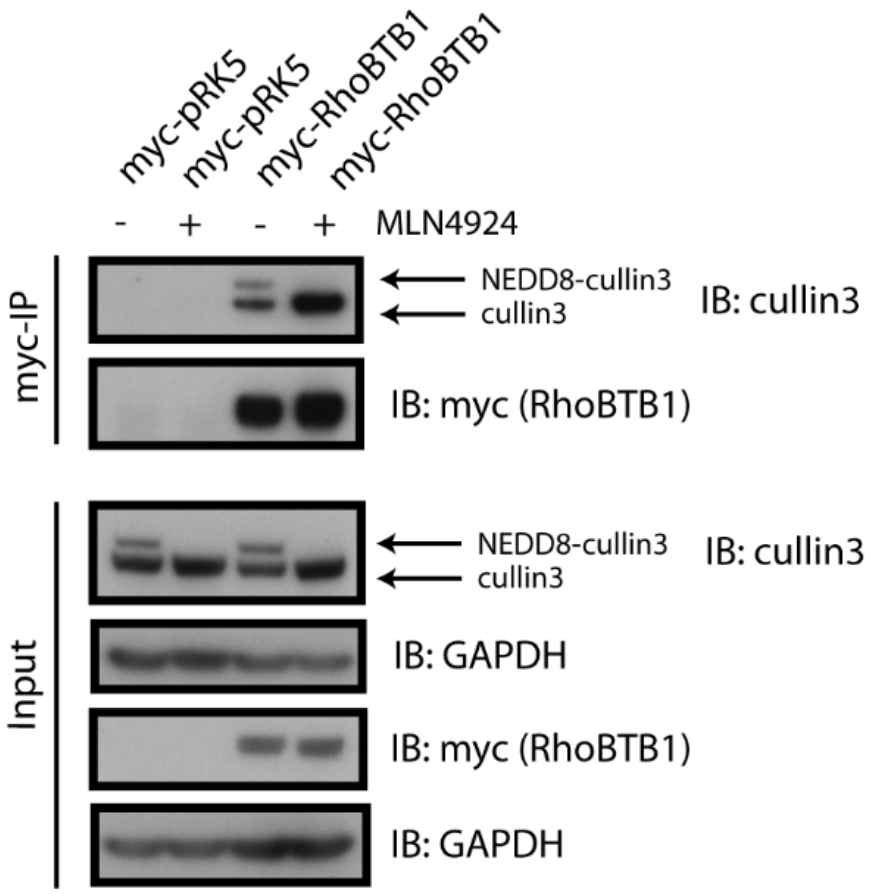

Figure 4.8 - Interaction of RhoBTB1 and cullin3 after MLN4924 treatment

Cos7 cells were transfected with empty myc-pRK5 or vector encoding myc-RhoBTB1. After 24 hours, cells were treated with 1 μM of MLN4924 (+) or DMSO (-) for 2 hours. Cells were lysed and incubated with anti-myc-agarose beads. Total lysates (input) and immunoprecipitates (myc-IP) were probed to show levels of myc-RhoBTB1 and endogenous cullin3. The interaction between myc-RhoBTB1 and cullin3 is shown in the immunoprecipitates. GAPDH is used as a loading control. Blots are representative of three independent experiments.

4.4 Ubiquitination of RhoBTB1

One of the post-translational modifications that Rho GTPases can undergo is ubiquitination (Chapter 1, section 1.1.1). RhoBTB2 has already been shown to be ubiquitinated and it is known to be a substrate for cullin3-RING ubiquitin ligases (Wilkins et al., 2004). However, the ubiquitination site has not been identified yet. Ubiquitination of RhoBTB1 has not been studied, although it also interacts with cullin3. Using the GG Base website (https://ggbase.hms.harvard.edu/) and the PhosphoSite Plus website (www.phosphosite.org), it was found that RhoBTB1 has a potential ubiquitination site in its Rho domain (K119). The ubiquitination of RhoBTB1 was therefore analysed. Cos7 cells were transfected with vectors encoding HA-ubiquitin and GFP-RhoBTB1 or myc-RhoBTB1. GFP-RhoA-N19, a dominant negative mutant, and GFP-RhoBTB2 were used as controls, since it is known that GDP-RhoA and RhoBTB2 can be ubiquitinated (Chen et al., 2009; Wang et al., 2003; Wilkins et al., 2004). HA-ubiquitin was immunoprecipitated using anti-HA-agarose beads. GFP-RhoBTB1 was able to associate with ubiquitin (Figure 4.9A). Although there are multiple RhoBTB1 bands (lane 6), there was not a molecular-weight ladder as observed in RhoA-N19 (lane 8) which suggests the presence of polyubiquitinated proteins. Bands for RhoBTB2 were not very clear, probably due to the low expression of GFP-RhoBTB2. The strongest band observed for RhoBTB1 (lane 6) is around 112 kDa. Since GFP-RhoBTB1 is 100 kDa and ubiquitin is 8.5 kDa, this increase in molecular weight could indicate the presence of RhoBTB1 bound to one ubiquitin molecule (Figure 4.9A, orange arrow). RhoBTB1 ubiquitination was also investigated by immunoprecipitating myc-RhoBTB1 and blotting for HA-ubiquitin. Several bands for RhoBTB1 were observed by this method (Figure 4.9B). However, a band around 87 kDa was present which could indicate the presence of RhoBTB1 bound to one ubiquitin molecule (myc-RhoBTB1 is 79 kDa) (Figure 4.9B, red arrow). The different band sizes observed in each experimental approach could represent different types of

ubiquitination on RhoBTB1 (reviewed in Chapter 1). Another possibility is that other ubiquitinated proteins bind to RhoBTB1 (e.g. RhoBTB2) and are detected in the blots.

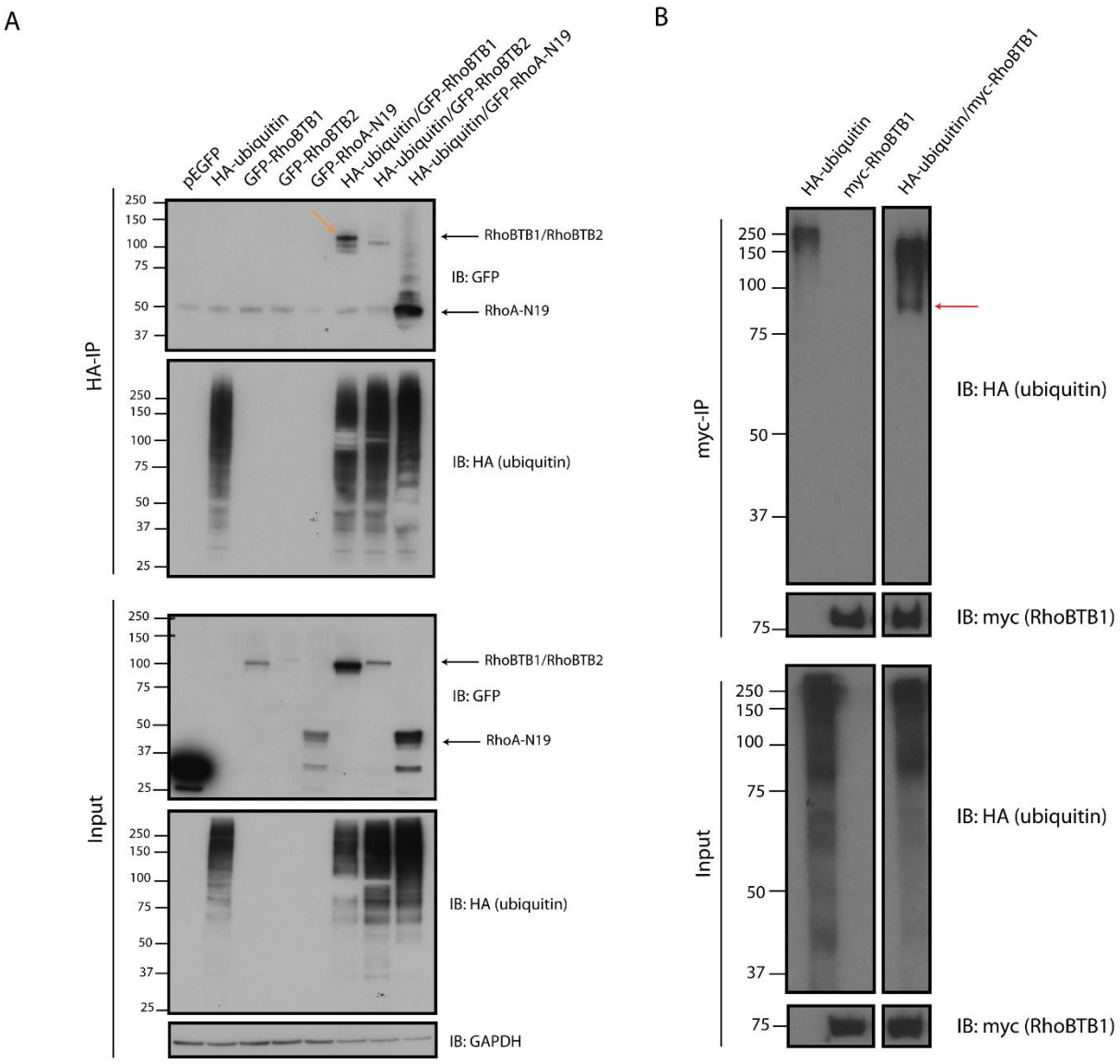

Figure 4.9 - Ubiquitination of RhoBTB1

A) Cos7 cells were transfected with empty pEGFP or vectors encoding HA-ubiquitin, GFP-RhoBTB1, GFP-RhoBTB2 or GFP-RhoA-N19. After 24 hours, cells were lysed and incubated with anti-HA-agarose beads. Total lysates (input) and immunoprecipitates (HA-IP) were probed to show levels of HA-ubiquitin, GFP-RhoBTB1, GFP-RhoBTB2 and GFP-RhoA-N19. GAPDH is used as a loading control. Blots are from one experiment. B) Cos7 cells were transfected with empty vector or vectors encoding HA-ubiquitin and myc-RhoBTB1. After 24 hours, cells were lysed and incubated with anti-myc-agarose beads. Total lysates (input) and immunoprecipitates (myc-IP) were probed to show levels of HA-ubiquitin and myc-RhoBTB1. Blots are representative of three experiments. Lanes are from the same blot.

4.5 Phosphorylation of RhoBTB1

Using the PhosphoSite Plus website (www.phosphosite.org) which shows data from high-throughput mass spectrometry analysis (Hornbeck et al., 2015), seven phosphorylation sites were reported in the RhoBTB1 protein (Figure 4.10).

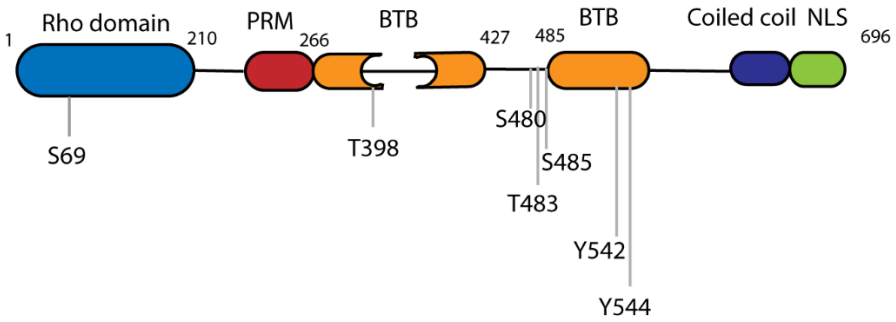

Figure 4.10 - Possible phosphorylation sites on RhoBTB1
Possible phosphorylation sites on RhoBTB1 obtained from www.phosphosite.org website (data from high-throughput mass spectrometry analysis).

To determine whether RhoBTB1 could be phosphorylated, the ProQ® Diamond dye was used. The dye is described to bind directly and selectively to the phosphate moiety (Patent number: US 7,102,005 B2). It is possible to detect phosphoserine-, phosphothreonine- and phosphotyrosine-containing proteins with this reagent. This reagent has previously been used in our laboratory for Rnd3 (Riou et al., 2013). myc-RhoBTB1 was immunoprecipitated using anti-myc-agarose beads, and phosphorylated RhoBTB1 was detected using ProQ® Diamond (Figure 4.11). Phosphorylation of RhoBTB1 is explored more in Chapter 6.

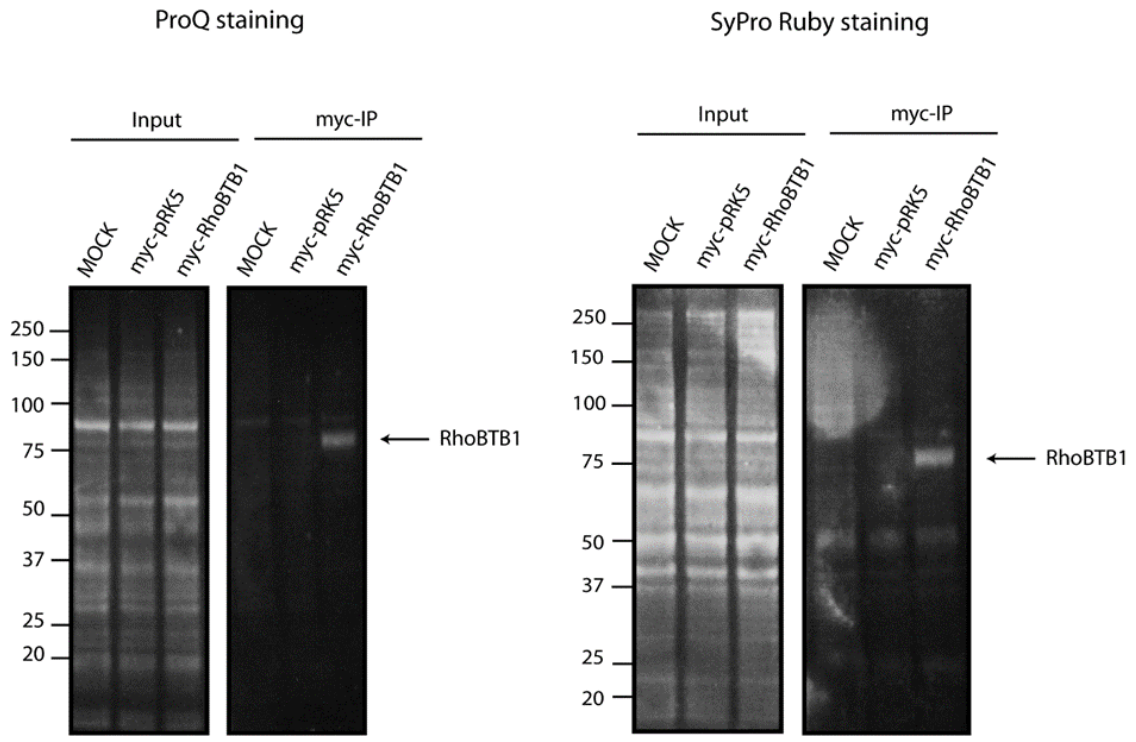

Figure 4.11 - Phosphorylation of RhoBTB1

Cos7 cells were transfected with empty myc-pRK5, or vector encoding myc-RhoBTB1. After 24 hours, cells were lysed and incubated with anti-myc-agarose beads. Total lysates and immunoprecipitated lysates were resolved on a 4-12% polyacrylamide gel and transferred to a low fluorescence PVDF membrane. Membrane was incubated with ProQ Diamond reagent followed by incubation with SyPro Ruby (total protein). Images were taken using a dual intensity ultraviolet transilluminator. Blots are from one experiment. MOCK: untransfected cells.

4.6 Localisation of RhoBTB1

To investigate the localisation of RhoBTB1 and whether it alters the actin cytoskeleton, Hela cells were used, because they are well spread in 2D culture conditions and have stress fibres. These cells have been used before to study changes in actin cytoskeleton (Ishizaki et al., 2001). Hela cells were transfected with vector encoding GFP-RhoBTB1. After 24 hours, cells were fixed and stained for F-actin to observe stress fibres (Figure 4.12A). In approximately 60% of the transfected cells (Figure 4.12B), GFP-RhoBTB1 was localised mainly in the cytoplasm. The rest of the cells had GFP-RhoBTB1 localised either in the cytoplasm and punctate localisation (~ 25%) or mainly with a punctate localisation (~ 15%) (Figure 4.12B). This punctate localisation could suggest the association of RhoBTB1 with vesicles. Because some cells with punctate GFP-RhoBTB1 localisation had abundant stress fibres, the percentage of cells with stress fibres was determined in control and RhoBTB1-overexpressing cells. However, no significant changes were observed (Figure 4.12C). More experiments are necessary to study this effect because the number of cells analysed was low.

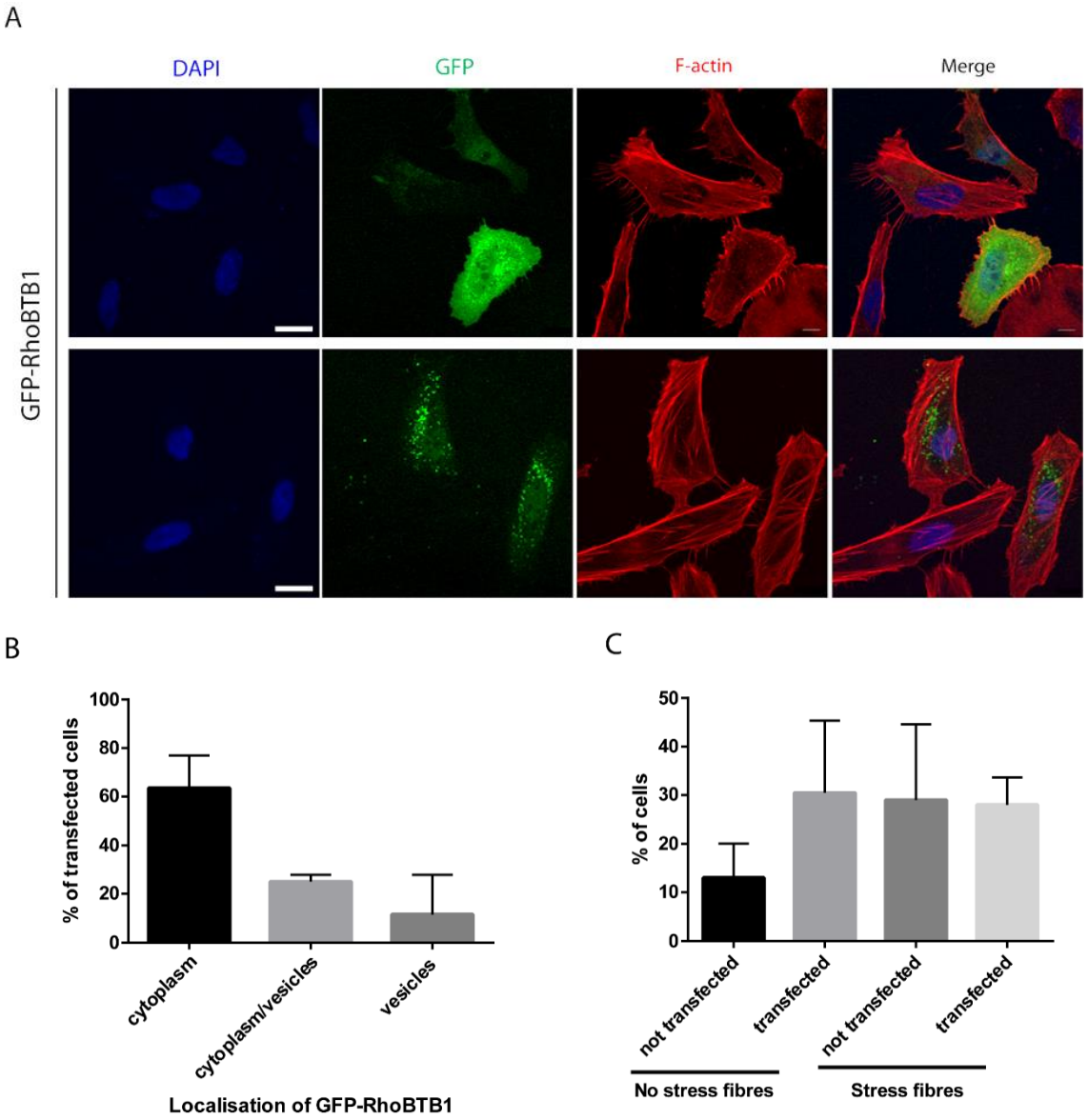

Figure 4.12 - Localisation of RhoBTB1

A) Hela cells were transfected with a vector encoding GFP-RhoBTB1. After 24 hours, cells were fixed and stained for F-actin and nuclei (DAPI). Images are representative of two independent experiments. Scale bar = 20 μm. B) Quantification of localisation of GFP-RhoBTB1 in transfected Hela cells. Graph shows data from two independent experiments. Around 10 cells that were expressing GFP-RhoBTB1 were counted in each experiment. Values represent mean ± SD. C) Quantification of stress fibres in transfected and untransfected Hela cells. Graph shows data from two independent experiments. 20 cells were counted in each experiment. Values represent mean ± SD.

To explore the effect of RhoBTB1 domains on protein localisation, Hela cells were transfected with vectors encoding GFP-RhoBTB1 and GFP-RhoBTB1 deletion mutants. After 24 hours, cells were fixed and stained for F-actin to observe stress fibres (Figure 4.13). GFP-RhoBTB1 1-427, GFP-RhoBTB1 266-696 and GFP-RhoBTB1 485-696 mutants were found mainly in the cytoplasm and in some cells, had a punctate localisation that might represent vesicles. Moreover, GFP-RhoBTB1 1-210 predominantly had a punctate localisation. Whether these are vesicles, or other structures, needs to be determined, since these structures could also be protein aggregates. Another interesting observation is the presence of full length RhoBTB1 and RhoBTB1 deletion mutants in the nucleus. However, GFP-RhoBTB1 1-427 lacks the C-terminal domain where the potential NLS region of RhoBTB1 is found (Figure 1.9). Therefore, it is possible that another region of RhoBTB1 could be responsible for its localisation in the nucleus.

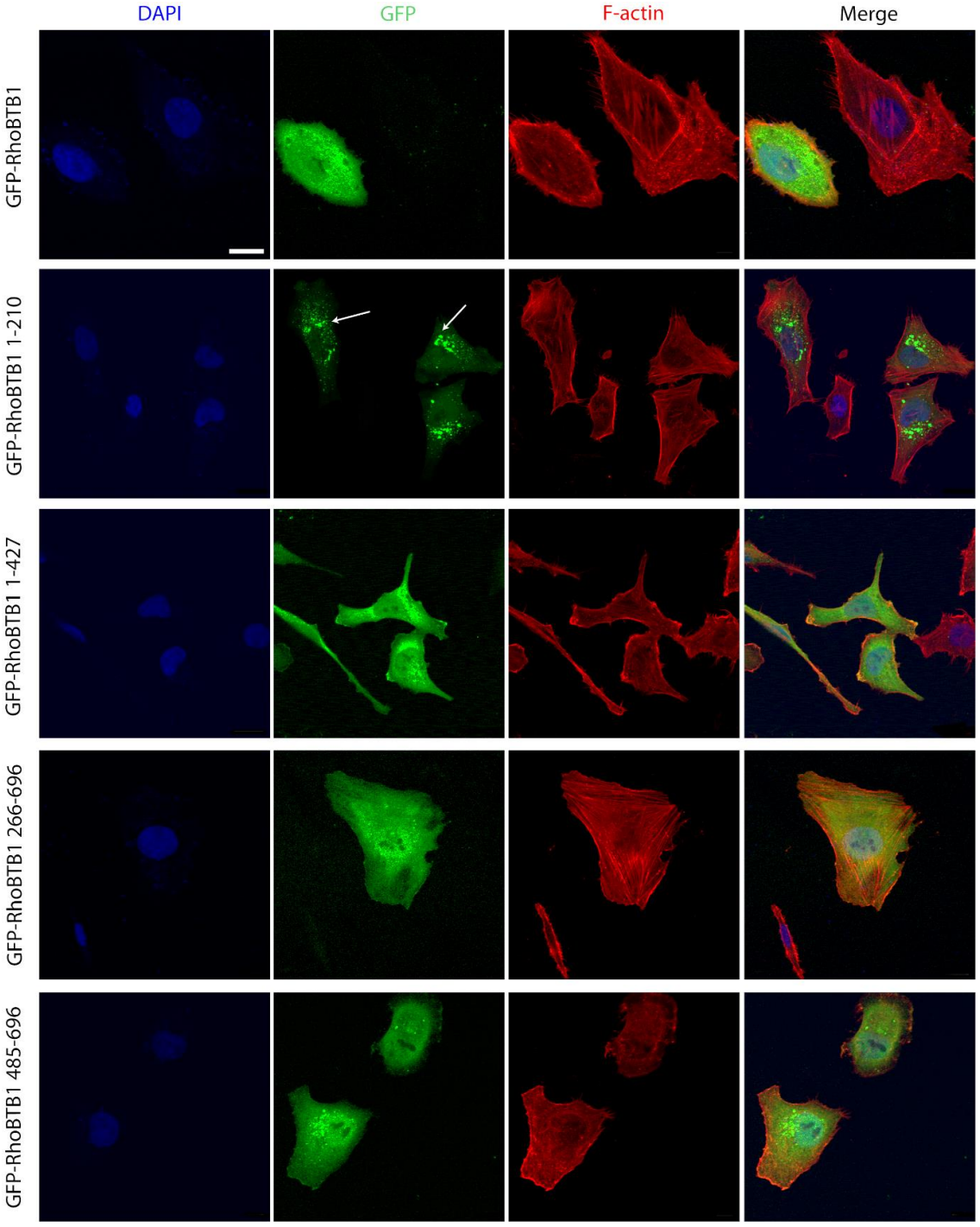

Figure 4.13 - Localisation of RhoBTB1 and RhoBTB1 deletion mutants

Hela cells were transfected with a vector encoding GFP-RhoBTB1, GFP-RhoBTB1 1-210, GFP-RhoBTB1 1-427, GFP-RhoBTB1 266-696 and GFP-RhoBTB1 485-696. After 24 hours, cells were fixed and stained for F-actin and nuclei (DAPI). Images are representative of two independent experiments. White arrows indicate punctate structures. Scale bar = 20 μm.

4.7 Discussion

Within the Rho family, RhoBTB1 is one of the least studied member. Apart from its interaction with cullin3, there are no other interacting partners or effector proteins known for RhoBTB1 and little is known about its regulation. In addition to GEFs, GAPs and GDIs, expression and activity of Rho GTPases can be controlled by transcriptional, post-transcriptional and post-translational regulations (Liu et al., 2012). RhoBTB1 expression has been shown to be regulated by the microRNA-31 in human colon cancer (Xu et al., 2013) and by PPARγ in a mouse model (Pelham et al., 2012). In this chapter, the interaction between cullin3 and RhoBTB1 was further explored, as well as the formation of RhoBTB1 homodimers. Possible mechanisms for RhoBTB1 regulation were also studied.

Initially, the interaction between RhoBTB1 and cullin3 was confirmed. RhoBTB2 is known to interact with cullin3 through its first BTB domain. Using different RhoBTB1 deletion mutants, it was observed that RhoBTB1 needs both of its two BTB domains to interact with endogenous cullin3. It is possible that RhoBTB1 containing only one BTB domain is still able to interact with cullin3, but in a weaker manner so that endogenous cullin3 was not detected under the conditions used here. The experiment for RhoBTB2 was performed overexpressing cullin3 which could facilitate the interaction of the first BTB domain with cullin3, even if the binding was weaker. Another possible explanation is that RhoBTB1 and RhoBTB2 interact with cullin3 in a slightly different manner: RhoBTB1 needs both BTB domains while RhoBTB2 interacts only with the first BTB domain. The identity between the first BTB domain of RhoBTB1 and RhoBTB2 is 38% while for the second BTB domain it is 68%.

Another condition analysed for RhoBTB1 and cullin3 interaction was the importance of cullin3 activation. As mentioned in section 1.2.2, one of the mechanisms to activate cullin proteins is through covalent addition of NEDD8. Treatment with the neddylation

inhibitor MLN4924 completely depletes the higher molecular weight form (cullin3-NEDD8) of cullin3. However, RhoBTB1 was still able to interact with the unneddylated form. It has been reported before that interaction of cullin3 with its adaptor proteins does not require cullin3 activation. For example, neddylation of cullin3 is not important for its interaction with the BTB adaptor protein Keap1 (Chew et al., 2007).

Some proteins containing BTB domain have been shown to form homodimers and heterodimers through their BTB domains (Stogios et al., 2005). The formation of BTB protein homodimers in some cases is important for the assembly of the ubiquitin ligase complex (Canning et al., 2013). Results shown here suggest that RhoBTB1 was able to homodimerise and heterodimerise with RhoBTB2. Similarly, RhoBTB2 can form homodimers and heterodimers with RhoBTB3 (Berthold et al., 2008a). The use of a crosslinker implied the presence of RhoBTB1 tetramers. However, the presence of these structures could be either due to the high amount of ectopic RhoBTB1 in cells or the detection of a protein complex that RhoBTB1 is part of. The BTB domains are essential for the dimerisation of RhoBTB1 since their deletion (GFP-RhoBTB1 1-210) prevented the formation of homodimers. More experiments using recombinant RhoBTB1 are necessary to confirm these results. Solving the crystal structure of RhoBTB proteins would be very useful to study the dimerisation of these proteins. The relevance of these findings for RhoBTB1 function is still unclear. One possible role for dimer formation could be related to the potential involvement of RhoBTB proteins in the ubiquitination of substrates through their interaction with cullin3 (Figure 4.14) as shown for other BTB adaptor proteins (Figure 1.12).

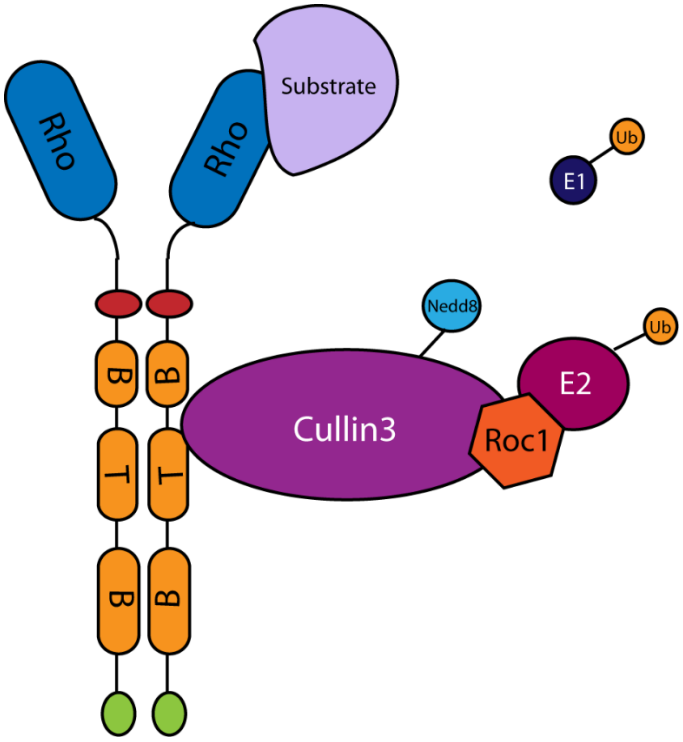

Figure 4.14 - Model of interaction between RhoBTB1 homodimer and cullin3
RhoBTB1 dimer interacts with the substrate through its Rho domain and with cullin3 through its BTB domains.

Exogenous expression of GFP-RhoBTB1 in Hela cells has shown that this protein is localised mainly in the cytoplasm and nucleus and in some cells, it is also observed to vesicles. These results are in agreement with other studies using PC3, Cos7 and PAE cells (Aspenstrom et al., 2004; Borda D'Agua, 2012). The lack of a CAAX box or the report of any lipid modification in RhoBTB1 are good indicators that this protein is likely to be found in the cytosol and not on membranes. The presence of RhoBTB1 on vesicle-like structures only in some cells could reflect different functions depending on protein localisation. If RhoBTB1 is on vesicles, it will associate indirectly unless there is a previously unrecognised lipid modification or lipid-binding domain. Data generated in our laboratory (not published) indicates that RhoBTB1 might have a role in β_1 integrin recycling and it is able to associate with some endosomal markers. RhoBTB2 has

already been shown to be involved in transporting VSVG from the endoplasmic reticulum to the Golgi apparatus (Chang et al., 2006). Using GFP-RhoBTB1 deletion mutants, the role of each of the domains of RhoBTB1 on its localisation was analysed. The only mutant that had a striking difference when compared to the full length protein was GFP-RhoBTB1 1-210. This mutant encodes only the Rho domain of RhoBTB1 and the protein was mainly localised to punctate structures. Because the expression of the protein is high, the structures could be protein aggregates. Co-staining using vesicle markers (e.g. EEA1, LAMP1, Rab4, Rab11) is necessary to determine the localisation of GFP-RhoBTB1 1-210. If it is on vesicles, this would indicate that the Rho domain of RhoBTB1 is important for its localisation.

No clear differences in cell morphology or actin cytoskeleton were observed in RhoBTB1-overexpressing cells. However, the number of cells analysed was too low to draw any conclusions. In addition, as shown in Chapter 5, RhoBTB1 depletion in MDA-MB-231 and PC3 cells led to elongation of these cells when embedded in Matrigel, suggesting a role for RhoBTB1 in regulating the actin cytoskeleton. This is discussed in more detail in Chapter 5.

Possible mechanisms for RhoBTB1 regulation include post-translational modifications, since these proteins do not cycle between an active GTP-bound form and an inactive GDP-bound form (Berthold et al., 2008a). On websites with high throughput mass spectrometry data, potential phosphorylation and ubiquitination sites were observed for RhoBTB1. Based on these data, preliminary assays were performed to determine whether RhoBTB1 could be phosphorylated and/or ubiquitinated. Using immunoprecipitation assays, it was possible to observe ubiquitination of RhoBTB1. However, depending on the protein being immunoprecipitated, the pattern of the bands in the blots was different. One possible explanation for these two different results is that RhoBTB1 can be both monoubiquitinated and polyubiquitinated. The lack of a molecular-weight ladder in the ubiquitin immunoprecipitated assay could mean that

there is more monoubiquitinated than polyubiquitinated RhoBTB1 which would then appear stronger in the blot. Different ubiquitin modifications can lead to different outcomes. As mentioned in Chapter 1, monoubiquitinated proteins are involved in endocytosis, endosomal sorting, histone regulation, DNA repair, virus budding and nuclear export while polyubiquitinated protein are targeted to DNA repair, endocytosis and activation of protein kinases (lysine 63) or protein degradation (lysine 48). Therefore, ubiquitination of RhoBTB1 could mean that this protein could be involved in very different processes in cells. Phosphorylation of RhoBTB1 was initially analysed using the reportedly phosphospecific protein stain ProQ® Diamond. A band for RhoBTB1 was observed, and thus it could be phosphorylated on one or more sites. Further analysis of RhoBTB1 phosphorylation is described in Chapter 6.

Although more experiments are necessary to confirm the findings in this chapter, it is possible to speculate that some of the results could be linked to each other. For example, localisation of RhoBTB1 could be influenced by ubiquitination and/or phosphorylation. Phosphorylation could also affect RhoBTB1 ubiquitination, if phosphorylation is necessary for interaction between RhoBTB1 and cullin3. In addition, dimerisation of RhoBTB1 might be important for cullin3 interaction which in turn would affect RhoBTB1 ubiquitination and this could lead to changes in RhoBTB1 localisation or degradation.

5 Role of RhoBTB1 in RhoA regulation

5.1 Introduction

Depletion of RhoBTB1 in MDA-MB-231 cells was described to lead to a decrease in RhoA expression (Borda D'Agua, 2012). However, the mechanisms linking RhoBTB1 to RhoA are unknown. One option that was explored in this chapter is the possible role of RhoBTB1 in the degradation of RhoA mediated by thecullin3 ubiquitin ligase complex. RhoA is known to be a substrate of the BACURD/cullin3 complex (Chen et al., 2009), which leads to ubiquitination of RhoA and consequent degradation by the proteasome. Since RhoBTB1 binds to cullin3, the possibility that RhoBTB1 interacts with RhoA and affects its degradation was analysed.

RhoA is one of the best-studied members of the Rho GTPase family. RhoA is closely related to RhoB and RhoC. The *RhoA, RhoB* and *RhoC* genes were identified in 1985 (Madaule and Axel, 1985) and since then, a great volume of knowledge has been generated. RhoA is a 21 kDa protein and it is ubiquitously expressed (Narumiya, 1996). It is localised to the plasma membrane and the cytoplasm (Adamson et al., 1992), and as a classic Rho GTPase, RhoA is a molecular switch which cycles between an active GTP-bound form and an inactive GDP-bound form (Hall, 2012). The N-terminal region is the part of the protein involved in GTP binding and hydrolysis (Wheeler and Ridley, 2004). This cycling is controlled by GAPs, GEFs and GDIs (Cherfils and Zeghouf, 2013). RhoA has a CAAX box near its C-terminus which undergoes prenylation (addition of a geranylgeranyl group). This lipid modification allows the protein to translocate between the plasma membrane and the cytosol (Adamson et al., 1992). RhoGDIs control the localisation of RhoA, since they bind to the prenyl group, preventing the protein localising to the membrane. Once in the membrane, RhoA is activated and is able to interact with several effectors (Aspenström, 1999; Bishop and Hall, 2000). The GTP-bound form of RhoA interacts with at least 11 proteins that are

involved in many different cellular processes including regulation of the actin cytoskeleton, gene transcription, cell-cell contacts, G1 cell-cycle progression and cell transformation (Braga, 1999; Hill et al., 1995; Qiu et al., 1995b; Ridley and Hall, 1992; Welsh et al., 2001)

5.1.1 RhoA effectors

The main effectors involved in the ability of RhoA to control cytoskeletal rearrangement and cell morphology are Rho-associated kinase (ROCK) and mammalian homolog of Drosophila diaphanous (mDia). ROCKs are serine/threonine kinases: mammals have two ROCKs, ROCK1 and ROCK2. Both ROCK1 and ROCK2 have been shown to bind to active RhoA (Ishizaki et al., 1996; Matsui et al., 1996). This interaction leads to activation of ROCKs and phosphorylation of their downstream targets including myosin phosphatase and myosin light chain (MLC) (Amano et al., 1996a; Kimura et al., 1996). Phosphorylation of myosin phosphatase inhibits this enzyme, allowing MLC to be phosphorylated which increases actin-activated ATPase activity of myosin II (Amano et al., 1996a; Tan et al., 1992). Myosin interacts with actin in an ATP-dependent manner to generate movement, leading to cell contraction (Citi and Kendrick-Jones, 1987). However, it has recently been proposed that RhoA is not involved in activation of ROCK (Truebestein et al., 2015). mDia1 is a member of the formin protein family, and has two close relatives in mammals, mDia2 and mDia3. These proteins consist of a Rho GTPase-binding domain (RBD), three formin homology domains (FH1-3), two coiled-coil domains and an intramolecular interaction domain at the C-terminal region that can interact with the N-terminal region to inhibit mDia activity (Krebs et al., 2001). mDia1 is able to interact with active-RhoA and profilin (Watanabe et al., 1997). RhoA binds to the N-terminal region of mDia1 and releases it from the intramolecular inhibitory interaction with the C-terminal region. Once active, mDia1 interacts with profilin through the FH1 domain and induces actin polymerization via the FH2 domain (Breitsprecher and Goode, 2013; Higashida et al., 2004; Krebs et al., 2001). The FH2

domain of mDia1 has been shown to be important for microtubule orientation and coordination with actin filaments. However, the mechanism for this process remains unknown (Ishizaki et al., 2001). ROCKs and mDia1 appear to cooperate with each other during Rho-mediated stress fibre formation. The balance of these two proteins can influence the thickness and density of stress fibres (Watanabe et al., 1999). G1 progression mediated by RhoA is also dependent on the ROCK/mDia1 activation balance. Inhibition of ROCK activity leads to an increase in mDia1 function which promotes G1 progression (Mammoto et al., 2004).

RhoA can interact and activate other kinases including protein kinase N (PKN), citron kinase and phosphatidylinositol-4-phosphate 5-kinase (PIP5K). PKN1, PKN2 and PKN3 are also serine/threonine kinases that can interact with RhoA (Amano et al., 1996b; Vincent and Settleman, 1997; Watanabe et al., 1996). The N-terminal region of these proteins interacts with active RhoA (Flynn et al., 1998; Maesaki et al., 1999). PKN proteins are involved in several cellular processes including cytoskeletal regulation, cell adhesion, vesicle transport, glucose transport and transcriptional activation (Mukai, 2003).

Initially, active RhoA was found to interact with citron, a protein very similar to the ROCK family of kinases apart from the lack of a kinase domain (Madaule et al., 1995). However, a splice variant of citron was identified with a kinase domain in its N-terminal domain. Citron kinase is found in the midbody between two dividing daughter cells and it is important for cytokinesis (Madaule et al., 1998). This kinase has been shown to also phosphorylate MLC but not myosin phosphatase, and this phosphorylation could be involved in citron kinase role during cytokinesis (Yamashiro et al., 2003).

PIP5K is another kinase regulated by RhoA (Chong et al., 1994). This kinase catalyses the last step in phosphatidylinositol (4,5)-bisphosphate (PIP2) synthesis (Oude Weernink et al., 2004). PIP2 is a membrane phospholipid and it is a substrate of two

important enzymes, PI-phospholipase C (PI-PLC) and type I PI3-kinases. In addition, PIP2 is able to bind to a large number of effector domains that are involved in the regulation of actin polymerization, endocytosis and exocytosis, turnover of focal adhesions and activity of potassium channels (Downes et al., 2005). PIP5K binds RhoA regardless of whether it is in the active or inactive form. However, the activation of PIP5K is mediated only by GTP-bound RhoA with involvement of ROCK as well (Ren et al., 1996; Weernink et al., 2004; Weernink et al., 2000). The role of other RhoA effectors including rhotekin and rhophilin is less well understood.

5.1.2 RhoA in transendothelial migration

As mentioned in Chapter 3, TEM is one of the steps of cell extravasation from blood vessels. RhoA has been implicated in this process in both leukocytes and cancer cells. In leukocytes, Rho/ROCK signalling was initially described as being important for monocyte tail retraction during transmigration into an endothelial monolayer (Worthylake et al., 2001). Later, it was shown that depletion of RhoA in T-cells leads to loss of polarization and defects in the ability of the cells to crawl on endothelial cells and transmigrate. In this study, RhoA was found to be active not only in the rear of transmigrating cells but also in the cell front (Heasman et al., 2010). RhoA has also been implicated in the transmigration of cancer cells into an endothelial monolayer. Inhibition of RhoA prenylation affects transendothelial migration of MDA-MB-231 cells into a monolayer of calf pulmonary arterial endothelial cells (Kusama et al., 2006). RhoA lacking the lipid modification is not able to translocate to the membrane and be activated. In the prostate cancer cell line PC3, RhoA/ROCK signalling is also involved in transendothelial migration *in vitro* (Brown et al., 2014).

5.1.3 Regulation of RhoA

As a classic Rho GTPase, RhoA is regulated by several GEFs, GAPs and GDIs. These proteins control the activity and localisation of Rho GTPases inside the cell. In addition,

levels of total protein can be regulated by expression and degradation. As described in Chapter 1, RhoA is a target of miRNAs and it can also undergo ubiquitination with consequent proteasomal degradation. Moreover, post-translational modifications can influence the fate of proteins. For example, phosphorylation of RhoA by PKA leads to increase in binding to RhoGDIs, protecting RhoA from ubiquitination (Rolli-Derkinderen et al., 2005) while phosphorylation of RhoA by Erk2 facilitates ubiquitination mediated by SCF^{FBXL19} E3 ubiquitin ligase (Wei et al., 2013). Therefore, regulation of RhoA is a complex network that can be controlled in many different ways.

5.2 Depletion of cullin3 and RhoBTB1 leads to a decrease in RhoA total levels

Cullin3 and RhoBTB1 were depleted in MDA-MB-231 cells and the levels of RhoA expression were analysed with and without cycloheximide treatment (6 hours). Cycloheximide is a protein synthesis inhibitor in eukaryotes, allowing the analysis of protein levels at specific time points without new expression. Depletion of cullin3 increased levels of RhoA consistent with results obtained by Chen et al. (2009), but when protein synthesis was blocked, RhoA levels remained at basal levels (siRNA control) (Figure 5.1). This indicates that new protein synthesis is required for RhoA levels to increase following cullin3 depletion.

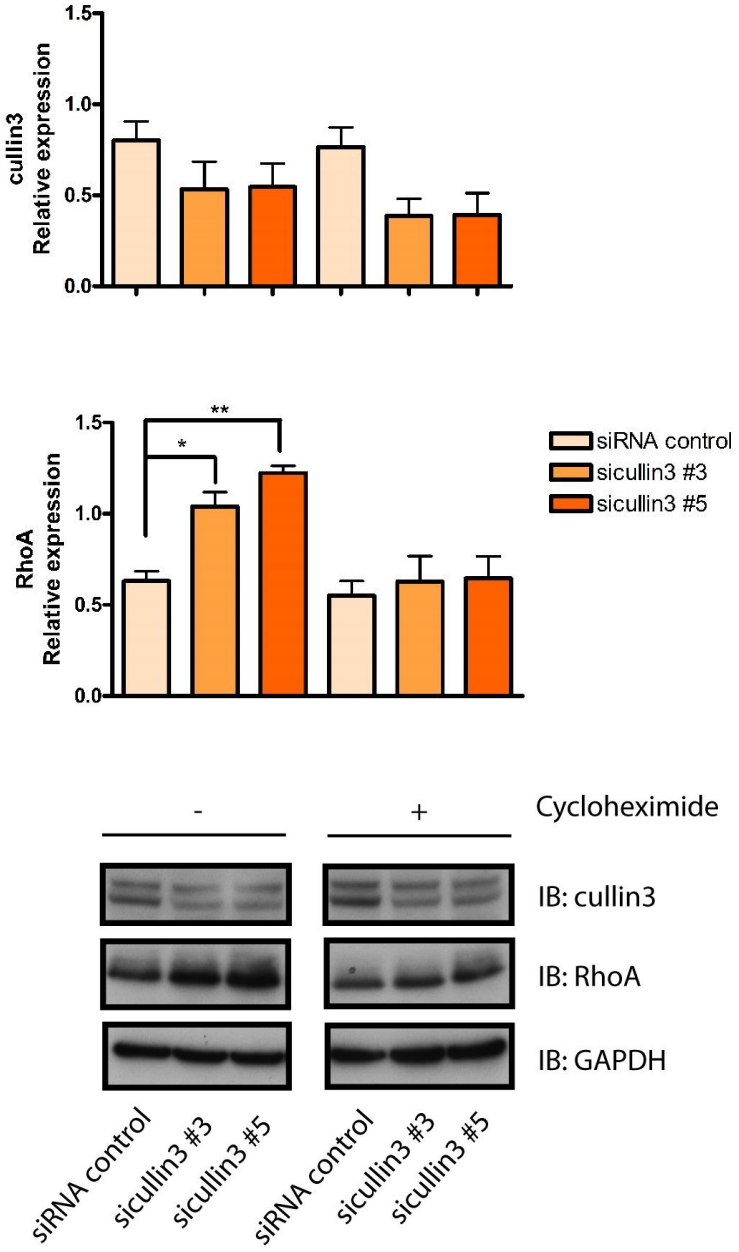

Figure 5.1 - Expression of RhoA in MDA-MB-231 cells after cullin3 depletion

Cells were transfected with siRNA control or siRNA oligos #3 and #5 targeting cullin3. After 48 hours, cells were treated with cycloheximide (50 µg/ml) for 6 hours. Cells were then lysed and protein expression was analysed by western blotting. GAPDH is used as a loading control. Graph shows the quantification of the band density of five independent experiments. Values represent mean ± SEM. *p<0.05, **p<0.01 compared to siRNA control (- cycloheximide), determined by unpaired one-way ANOVA, followed by Dunnett´s test.

In addition, inhibition of cullin3 activity with MLN4924 also affected levels of RhoA as expected (Figure 5.2). Inhibition of cullin3 activity led to an increase in RhoA total protein levels.

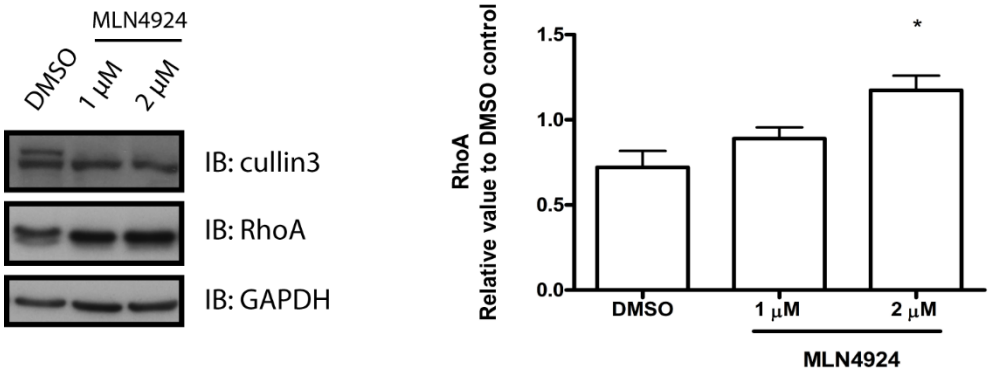

Figure 5.2 - Inhibition of cullin3 affects RhoA total protein levels in MDA-MB-231 cells

MDA-MB-231 cells were treated with 1 μM or 2 μM of MLN4924 or DMSO for 2 hours. Cells were lysed and protein expression was analysed by western blotting. GAPDH is used as a loading control. Graph shows the quantification of the band density of three independent experiments, normalised to GAPDH and relative to DMSO. Values represent mean ± SEM. *p<0.05, compared to DMSO, determined by unpaired one-way ANOVA, followed by Dunnett´s test.

Borda D'Agua (2012) observed that depletion of RhoBTB1 in MDA-MB-231 cells led to a decrease in activity and expression of RhoA (Figure 3.28). However, under the conditions used here, depletion of RhoBTB1 did not affect RhoA levels in untreated cells. Only when cells were treated for 6 hours with cycloheximide was it possible to observe a decrease in RhoA levels. Treatment with cycloheximide did not affect levels of RhoA in the siRNA control (Figure 5.3).

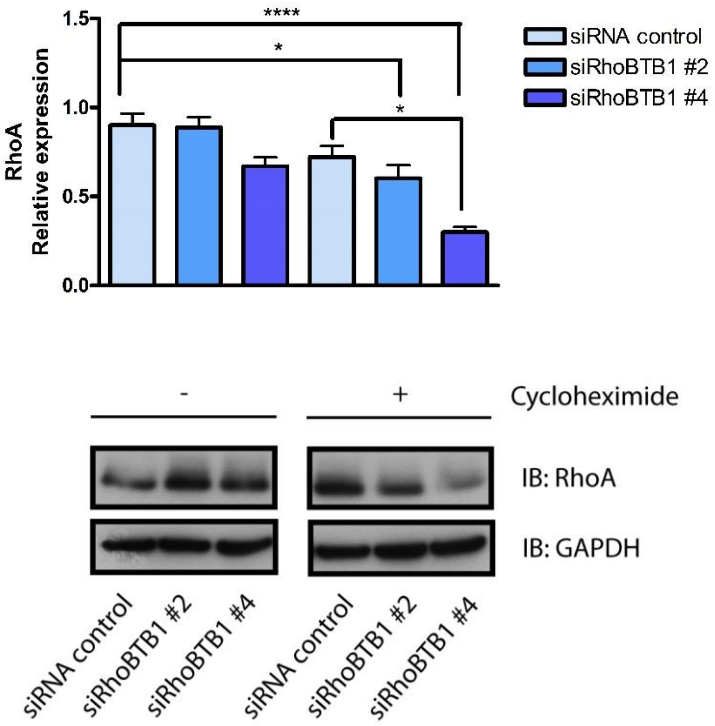

Figure 5.3 - Expression of RhoA in MDA-MB-231 cells after RhoBTB1 depletion

Cells were transfected with siRNA control or siRNA oligos #2 and #4 targeting RhoBTB1. After 72 hours, cells were treated with cycloheximide (50 µg/ml) for 6 hours. Cells were then lysed and protein expression was analysed by western blotting. GAPDH is used as a loading control. Graph shows the quantification of the band density of five independent experiments. Values represent mean ± SEM. *p<0.05, ****p<0.0001, compared to siRNA control (- cycloheximide) and *p<0.05, compared to siRNA control (+ cycloheximide), determined by unpaired one-way ANOVA, followed by Dunnett´s test.

It has been shown that GDP-RhoA can be ubiquitinated by the BACURD/cullin3 ubiquitin ligase complex and degraded by proteasomal degradation (Chen et al., 2009). BACURDs are BTB adaptor proteins that bind to substrates and bring them to the cullin3 complex to be ubiquitinated. Like BACURDs, RhoBTB proteins have BTB domains and they could potentially act in a similar way, bringing substrates to be ubiquitinated by the cullin3 ubiquitin ligase complex. As shown above, depletion of RhoBTB1 reduces levels of RhoA in the presence of cycloheximide, suggesting that RhoBTB1 normally protects RhoA from degradation rather than stimulating its degradation.

To test whether RhoBTB1 interacted with RhoA, the two proteins were co-overexpressed in Cos7 cells, followed by immunoprecipitation. myc-RhoBTB1 was co-transfected with three different constructs encoding RhoA: GFP-RhoA, GFP-RhoA-N19 (threonine to arparagine, dominant negative) (Coso et al., 1995) and GFP-RhoA-V14 (glycine to valine, constitutively active) (Ihara et al., 1998; Ridley and Hall, 1992). RhoBTB1 interacted only with the dominant-negative form of RhoA (GFP-RhoA-N19). Cullin3 was used as a control to confirm the efficiency of the immunoprecipitation (Figure 5.4). Total expression of GFP-RhoA-N19 is lower than GFP-RhoA and GFP-RhoA-V14 probably because RhoA-N19 is more targeted for degradation. Co-transfection of myc-RhoBTB1 and GFP-RhoA leads to lower total expression of both proteins when compared to single transfection. This could be caused by competition for expression. However, levels of myc-RhoBTB1 in the myc-IP are consistent in all the conditions.

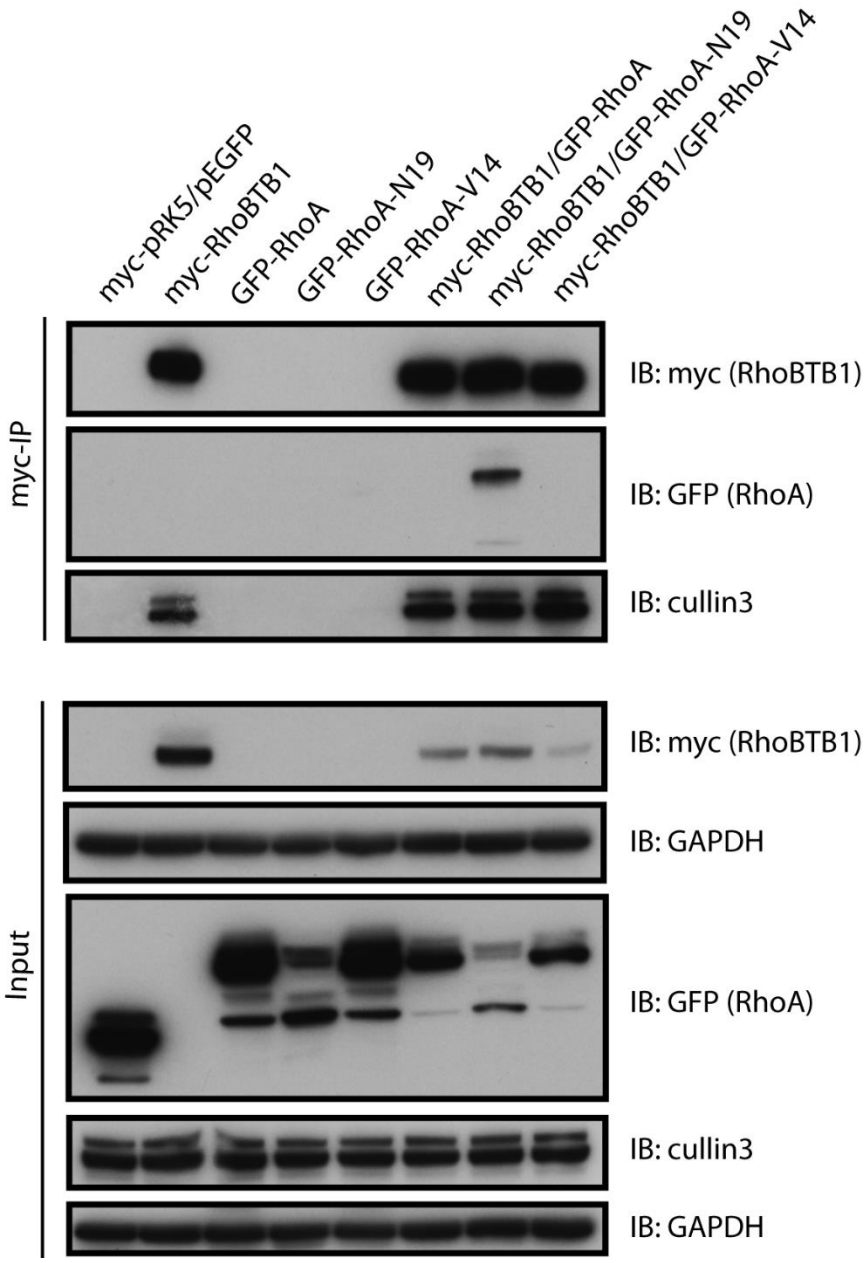

Figure 5.4 - Interaction of RhoBTB1 and RhoA mutants

Cos7 cells were co-transfected with empty myc-pRK5 and pEGFP or vector encoding myc-RhoBTB1, GFP-RhoA, GFP-RhoA-N19, GFP-RhoA-V14, myc-RhoBTB1/GFP-RhoA, myc-RhoBTB1/GFP-RhoA-N19 or myc-RhoBTB1/GFP-RhoA-V14. After 24 hours, cells were lysed and incubated with anti-myc-agarose beads. Total lysates (input) and immunoprecipitates (myc-IP) were probed to show expression of myc-RhoBTB1, GFP-RhoA, GFP-RhoA-N19, GFP-RhoA-V14. The interaction between myc-RhoBTB1 and GFP-RhoA-N19 is shown in the immunoprecipitates (myc-IP). GAPDH is used as a loading control. Blots are representative of two independent experiments.

To determine the region of RhoBTB1 that is important for the interaction with RhoA, Cos7 cells were co-transfected with vectors encoding full length GFP-RhoBTB1, GFP-RhoBTB1 deletion mutants (Figure 5.5A) and FLAG-RhoA-N19. Only constructs encoding proteins containing the Rho domain of RhoBTB1 were able to interact with FLAG-RhoA-N19 (Figure 5.5B). It was also observed that the presence of RhoBTB1 constructs led to an increase in FLAG-RhoA-N19 expression. This effect could be a result of RhoBTB1 protection over RhoA degradation. However, it is important to observe that RhoBTB1 deletion constructs were cloned into a different plasmid from the full length RhoBTB1.

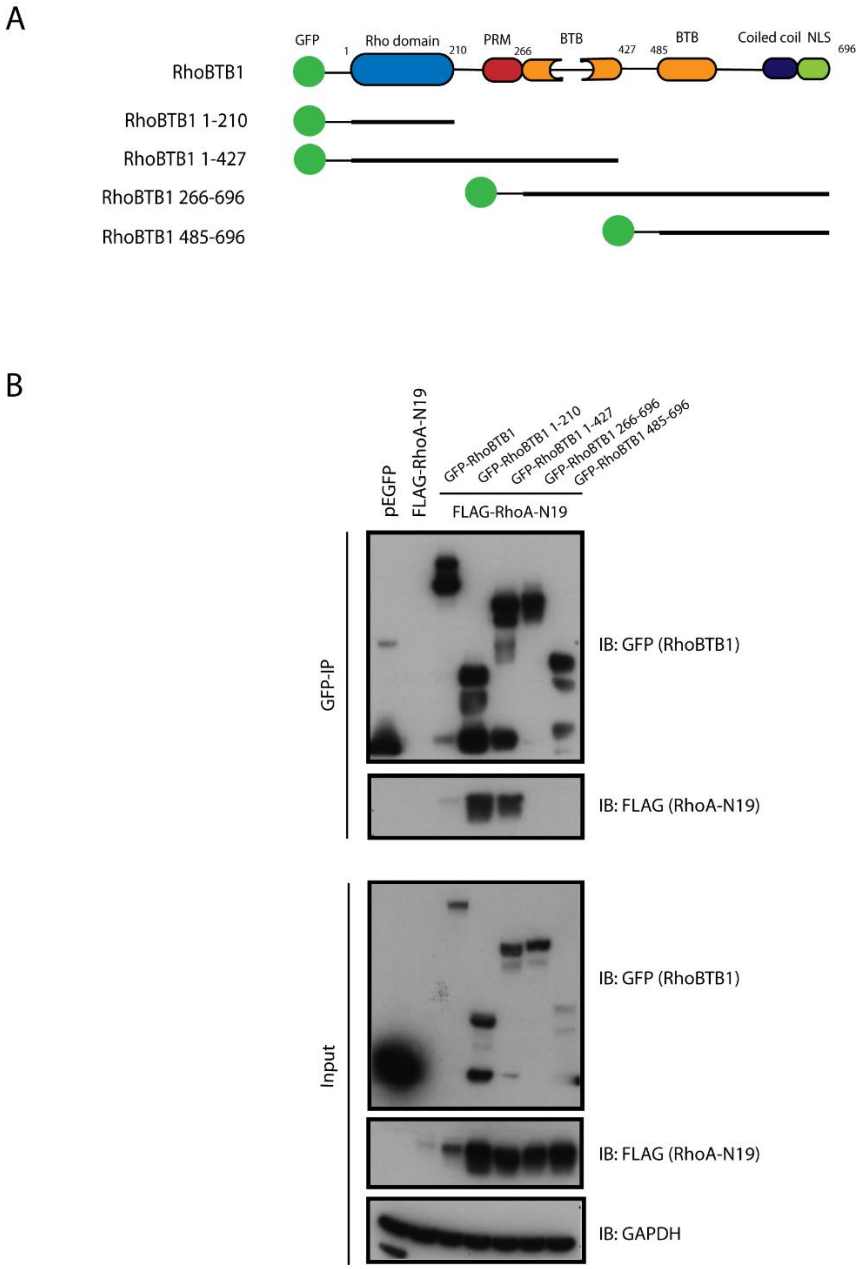

Figure 5.5 - Interaction of RhoBTB1 deletion mutants and RhoA dominant negative mutant (RhoA-N19)

A) Domain structure of GFP-RhoBTB1 and GFP-RhoBTB1 deletion mutants B) Cos7 cells were co-transfected with empty pEGFP or vector encoding FLAG-RhoA-N19, GFP-RhoBTB1 and GFP-RhoBTB1 deletion mutants. After 24 hours, cells were lysed and incubated with GFP-binding protein coupled to agarose (GFP-trap®). Total lysates (input) and immunoprecipitates (GFP-IP) were probed to show expression of FLAG-RhoA-N19, GFP-RhoBTB1 and GFP-RhoBTB1 deletion mutants. The interaction between FLAG-RhoA-N19 and GFP-RhoBTB1, FLAG-RhoA-N19 and GFP-RhoBTB1 1-210, and FLAG-RhoA-N19 and GFP-RhoBTB1 1-427 are shown in the immunoprecipitates (GFP-IP). GAPDH is used as a loading control. Blots are representative of three independent experiments.

As shown above (Figure 5.3), RhoBTB1 interacts with dominant negative RhoA-N19, which is believed to mimic the GDP-bound form of RhoA. Since RhoBTB1 interacts with cullin3 (Chapter 4) (Berthold et al., 2008a) and with RhoA, as well as BACURD1, RhoBTB1 could be competing with BACURD1 for RhoA binding in the cullin3 ubiquitin ligase complex.

To study the hypothesis that RhoBTB1 and BACURD1 could compete for GDP-RhoA binding, BACURD1 was subcloned into a GFP-vector (section 2.2.13). To test if RhoA-N19 was able to interact with BACURD1, Cos7 cells were co-transfected with vectors encoding FLAG-RhoA-N19, myc-RhoBTB1 and GFP-BACURD1. Both RhoBTB1 and BACURD1 interacted with RhoA-N19 (Figure 5.6).

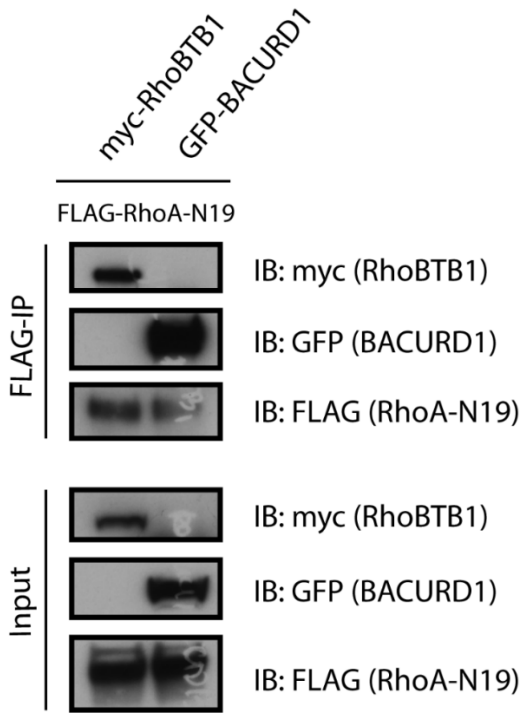

Figure 5.6 - Interaction of BACURD1 with RhoA-N19

Cos7 cells were co-transfected with vector encoding FLAG-RhoA-N19 and myc-RhoBTB1 or GFP-BACURD1. After 24 hours, cells were lysed and incubated with anti-FLAG-agarose beads. Total lysates (input) and immunoprecipitates (FLAG-IP) were probed to show expression of FLAG-RhoA-N19, myc-RhoBTB1 and GFP-BACURD1. The interactions between FLAG-RhoA-N19 and myc-RhoBTB1, and FLAG-RhoA-N19 and GFP-BACURD1 are shown in the immunoprecipitates (FLAG-IP). Blots are from one experiment.

A competition assay was performed transfecting constant amounts of vectors encoding FLAG-RhoA-N19 and GFP-BACURD1, and different amounts of the vector encoding GFP-RhoBTB1. It was observed a decrease in the expression of GFP-BACURD1 and FLAG-RhoA-N19 in the presence of GFP-RhoBTB1. One possible explanation is a competition between the plasmids which is commonly observed when two or more plasmids are transfected at the same time in the cell. Even with this difference in expression, a decrease in the amount of BACURD1 which interacted with RhoA-N19 was observed when RhoBTB1 was co-transfected (Figure 5.7). More repeats are necessary to confim that, since the results are not statistically significant. In addition, an unspecific binding between FLAG-beads and GFP-BACURD1 was observed. However, the presence of RhoA-N19 increased the amount of BACURD in the FLAG-IP.

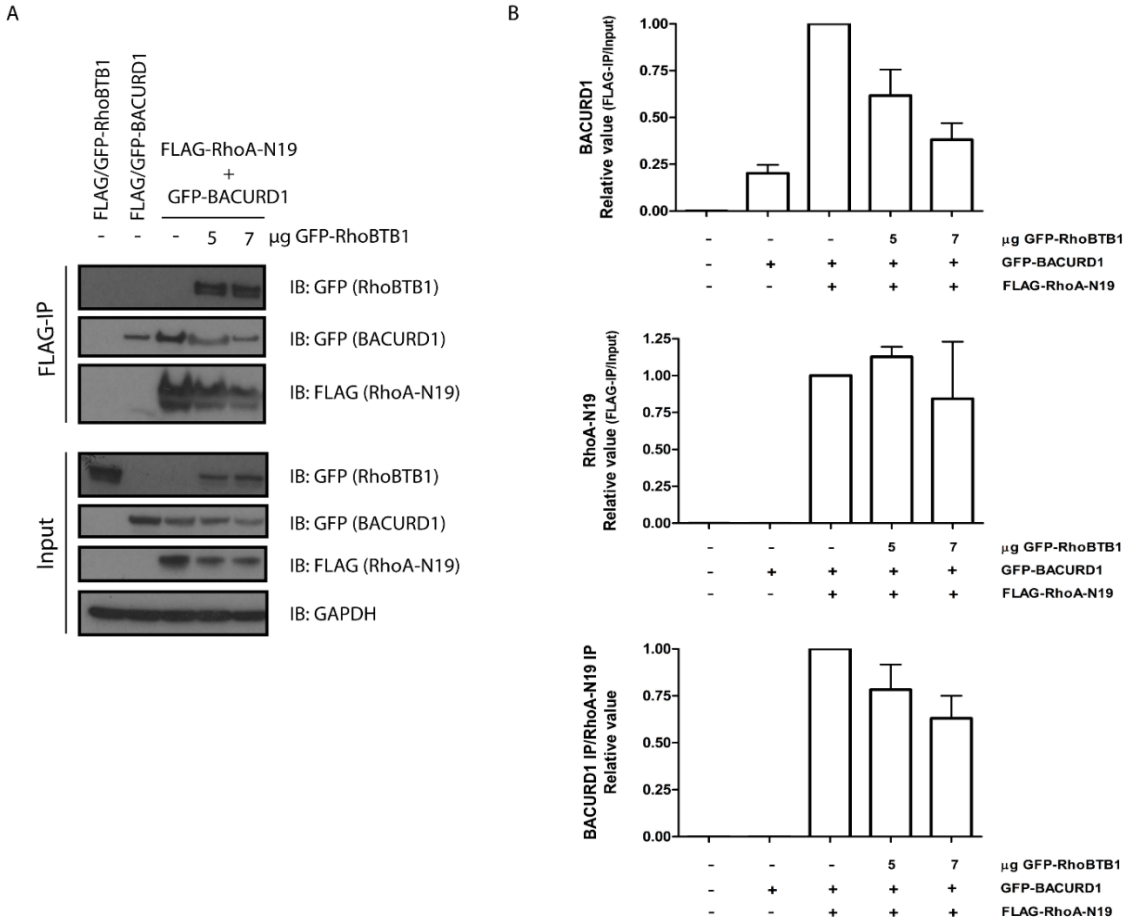

Figure 5.7 - Competition between RhoBTB1 and BACURD1 to interact with RhoA-N19

A) Cos7 cells were co-transfected with empty pFLAG-CMV-2 or vector encoding FLAG-RhoA-N19 and GFP-BACURD1. Vector encoding GFP-RhoBTB1 is co-transfected with increasing amounts of DNA. After 24 hours, cells were lysed and incubated with anti-FLAG-agarose beads. Total lysates (input) and immunoprecipitates (FLAG-IP) were probed to show expression of FLAG-RhoA-N19, GFP-RhoBTB1 and GFP-BACURD1. The interaction between FLAG-RhoA-N19 and GFP-RhoBTB1, and FLAG-RhoA-N19 and GFP-BACURD1 are shown in the immunoprecipitates (FLAG-IP). GAPDH is used as a loading control. Blots are representative of three independent experiments. B) Graphs show the quantification of the band density of three independent experiments. All values were normalized by FLAG-RhoA-N19/GFP-BACURD1 condition. Values represent mean ± SEM.

5.3 RhoBTB1 depletion alters cancer cell morphology in 3D

Although depletion of RhoBTB1 do not seem to affect cell morphology in 2D in MDA-MB-231 breast cancer cells (Figure 5.8, results from Borda D'Agua (2012)), the effect of RhoBTB1 depletion has not been tested in a 3D culture system. However, RhoBTB1 could affect the morphology in 2D in other cell types. It is well known that 2D cultures are not the best representation of the environment that surrounds cells in organisms. Cells that grow on flat and hard plastic lose tissue-specific architecture, and have different mechanical and biochemical signals, and cell-cell communication to 3D systems (Pampaloni et al., 2007). 3D cultures have been shown to mimic better the situation *in vivo*, and these cultures are able to decrease the gap between *in vitro* and *in vivo* cancer models (Pampaloni et al., 2007). One of the most obvious differences between cells grown in 2D and 3D cultures is their morphology. Cells in a monolayer are able to adhere and spread horizontally. Once in a 3D environment, cells have the option to spread vertically which allows them to acquire a different morphology from in 2D culture. Changes in cell geometry and organization can affect cell function including apoptosis, proliferation and migration (Baker and Chen, 2012).

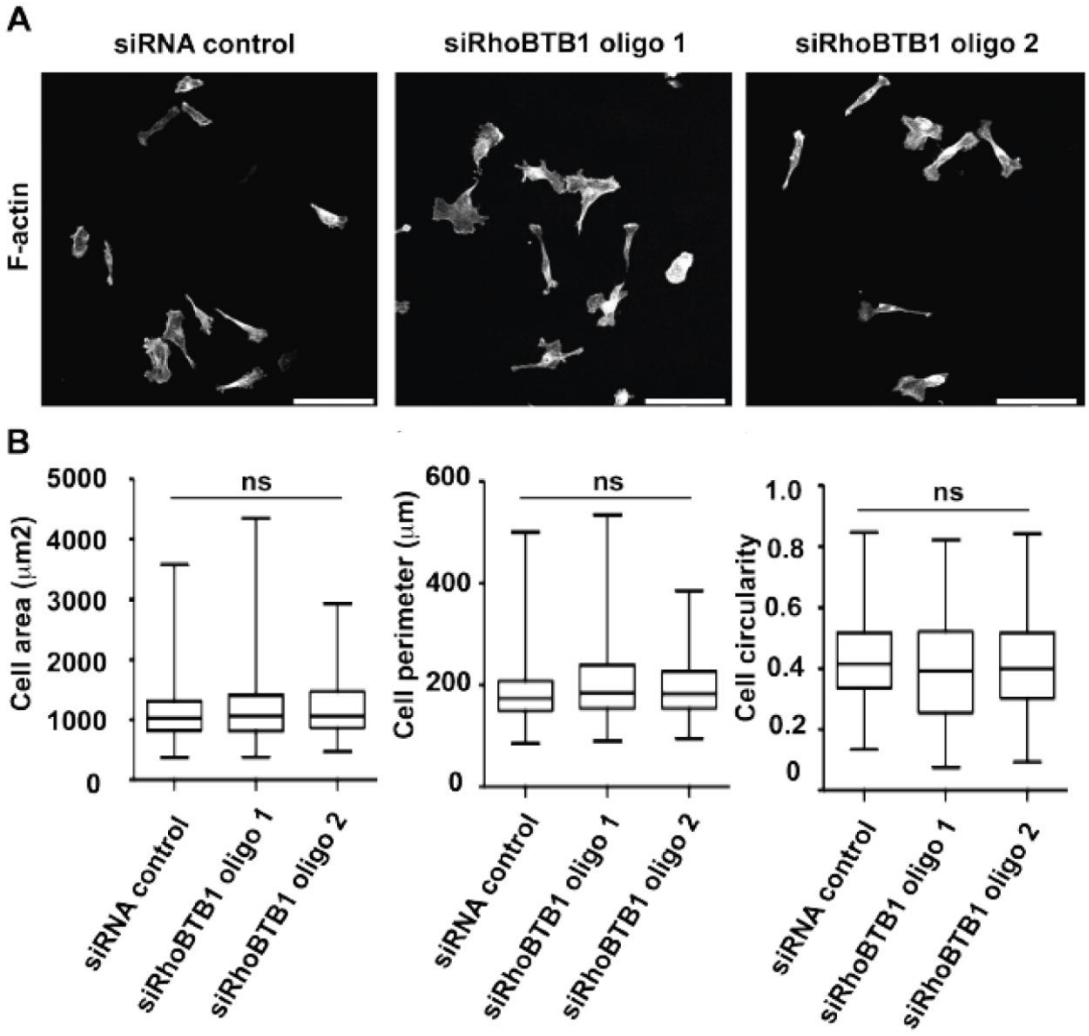

Figure 5.8 - RhoBTB1 depletion does not affect the actin cytoskeleton of MDA-MB-231 cells

A) siRNA-transfected MDA-MB-231 cells were detached from the transfection plate 24 hours after transfection, seeded on collagen I-coated coverslips and allowed to adhere and spread for 48 hours. Cells were fixed and stained for F-actin. B) Graphs show quantification of 100 cells, from three independent experiments using Image J software. Box plots show the medians, 25th and 75th percentiles and whiskers show the 5th and 95th percentiles. Scale bars = 100 µm. ns = not significant, compared to siRNA control, determined by one-way ANOVA analysis of variance followed by a Dunnett´s multiple comparison. Results were generated by Barbara Borda D'Agua.

To study the effects of RhoBTB1 depletion on cancer cell morphology in a 3D environment, MDA-MB-231 and PC3 cells were embedded in a Matrigel matrix using a method stablished in our laboratory using PC3 cells (Colomba and Ridley, 2014). MDA-

MB-231 and PC3 cells were transfected with siRNA oligos targeting RhoBTB1 and after 48 hours, cells were embedded in Matrigel and incubated at 37ºC. Phase-contrast images of all the conditions were taken after 24 hours. Depletion of RhoA was used as a control because it is known that RhoA-depleted cells become elongated in a 3D Matrigel matrix. Both MDA-MB-231 and PC3 cells had a more rounded morphology when embedded in Matrigel, compared to 2D culture (Figure 5.9). However, when RhoBTB1 was depleted, the cells had a more elongated phenotype, similar to the phenotype observed for RhoA depletion (Figure 5.10 and 5.11). The effects on cell elongation are higher in PC3 cells, since these cells have a more rounded phenotype when compared to MDA-MB-231 cells (Figure 5.10 and 5.11). Because RhoBTB1 depletion had similar results as RhoA depletion, this suggests that the effects observed following RhoBTB1 depletion could be caused by reduced RhoA signalling.

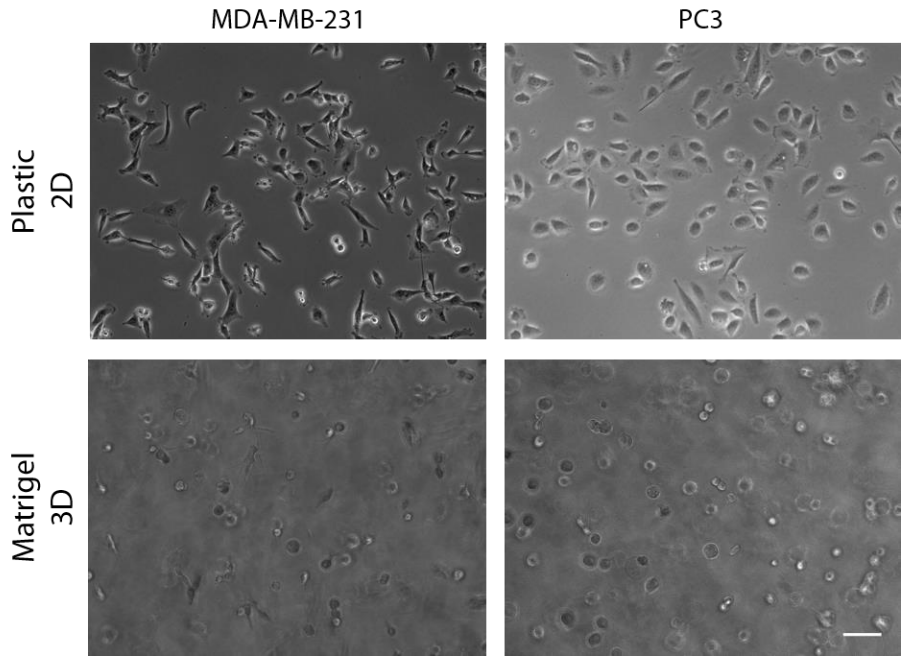

Figure 5.9 - Morphology of MDA-MB-231 and PC3 cells in 2D and 3D cultures

MDA-MB-231 and PC3 cells were grown on plastic or embedded in 3.5 mg/ml of Matrigel. Scale bar = 100 µm.

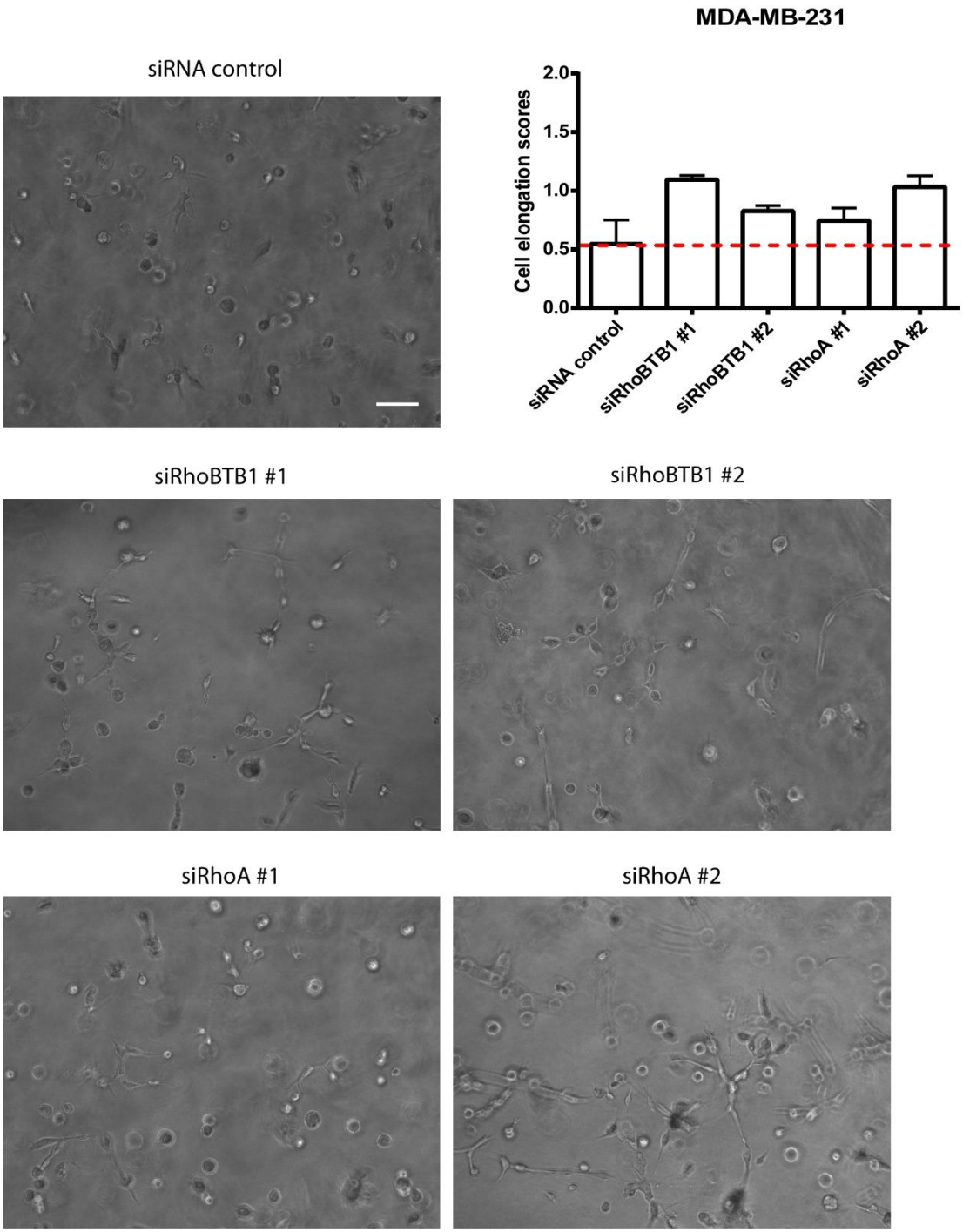

Figure 5.10 - Morphology of MDA-MB-231 cells in Matrigel

MDA-MB-231 cells transfected with siRNA oligos targeting RhoBTB1 or RhoA, or siRNA control. After 48 hours, cells were embedded in 3.5 mg/ml of Matrigel in a 96-well plate coated with 7 mg/ml of Matrigel. Phase-contrast images were taken after 24 hours. Images are representative of two independent experiments. Cells were scored based on their elongation: 0 = rounded morphology and 3 = elongated morphology. Graph shows quantification of cell elongation scores from two independent experiments. Ten different fields of each condition were analysed per experiment. Values represent mean ± SD. Scale bar = 100 μm.

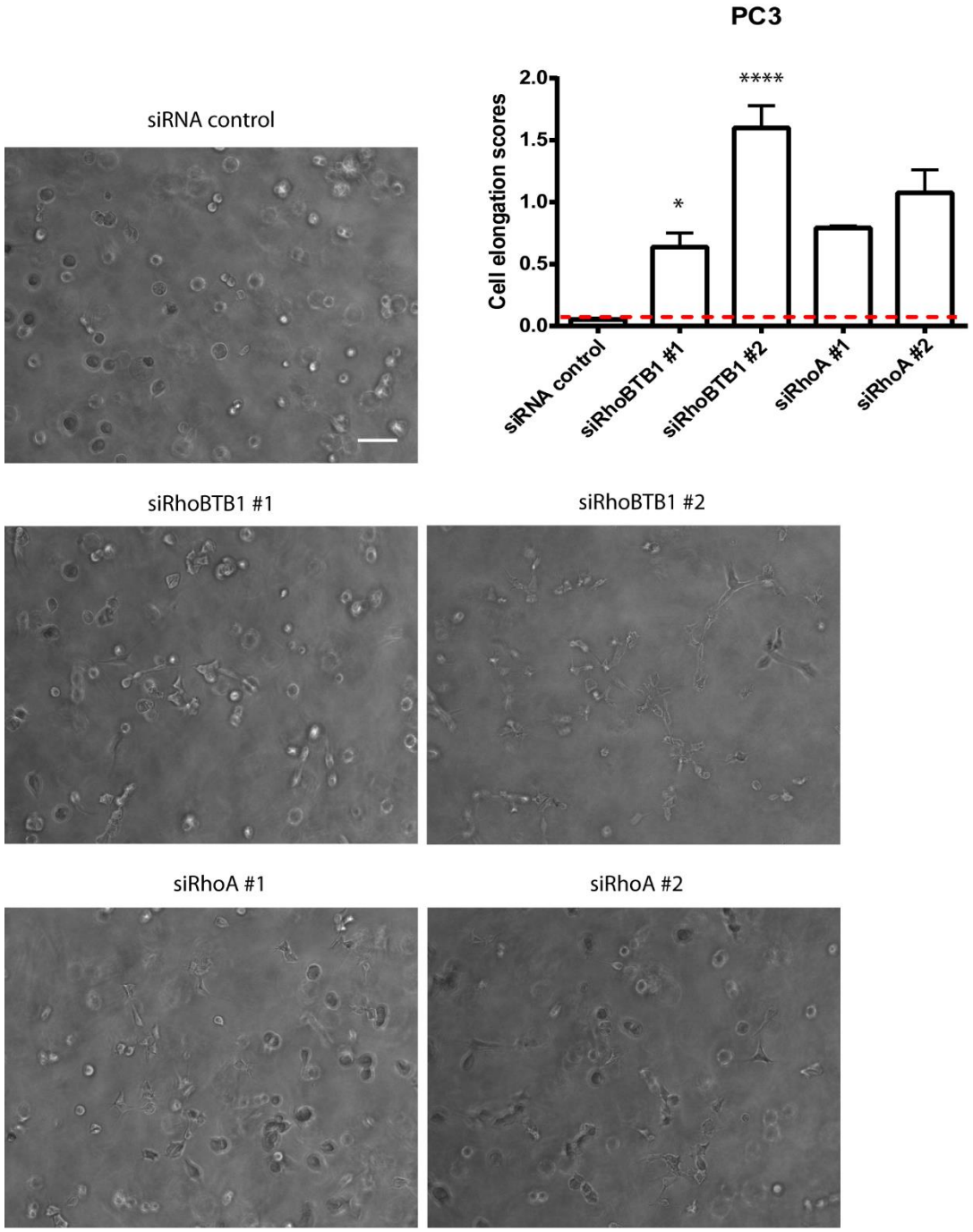

Figure 5.11 - Morphology of PC3 cells in Matrigel

PC3 cells transfected with siRNA oligos targeting RhoBTB1 or RhoA, or siRNA control. After 48 hours, cells were embedded in 3.5 mg/ml of Matrigel in a 96-well plate coated with 7 mg/ml of Matrigel. Phase-contrast images were taken after 24 hours. Images are representative of three independent experiments. Cells were scored based on their elongation: 0 = rounded morphology and 3 = elongated morphology. Graph shows quantification of cell elongation scores from three independent experiments. Ten different fields of each condition were analysed per experiment. Values represent mean ± SEM. *p<0.05, ****p<0.0001, compared to siRNA control, determined by one-way ANOVA analysis of variance followed by a Dunnett´s multiple comparison. Scale bar = 100 µm.

5.4 Discussion

In order to investigate at a molecular level the effects of RhoBTB1 depletion, Borda D'Agua (2012) analysed whether RhoBTB1 depletion altered the expression or activity of the Rho GTPases RhoA, Rac1 and Cdc42. Only RhoA was affected by RhoBTB1 depletion in MDA-MB-231 cells. siRNA-transfected cells showed a decrease in expression and activity of RhoA, without changes in the mRNA levels. This suggests that RhoBTB1 could be involved somehow in inhibiting RhoA degradation. It is known that RhoA is targeted for degradation after ubiquitination by at least three different complexes (Chen et al., 2009; Wang et al., 2003; Wei et al., 2013). As RhoBTB1 consists of 2 BTB domains and it is able to bind cullin3, it is most likely that it affects ubiquitination of RhoA by the BACURD/cullin3 complex (Chen et al., 2009). The hypothesis is that RhoBTB1 is a cullin3-interacting BTB adaptor protein. RhoBTB1 could compete with BACURD, a BTB adaptor protein, for the binding to GDP-RhoA, and thereby, inhibit RhoA degradation mediated by BACURD/cullin3 complex. It is known that Rho GTPases can regulate each other at different levels. The classic example is the crosstalk between RhoA and Rac as mentioned in Chapter 1 (section 1.1.4).

First, to confirm the effects of RhoBTB1 depletion on RhoA levels, MDA-MB-231 cells were transfected with siRNA oligos targeting cullin3 and RhoBTB1. Depletion of cullin3 led to increase in RhoA protein levels as expected (Chen et al., 2009). However, after 6 hours of treatment with cycloheximide, RhoA levels returned to basal levels (control). One possible explanation is that the remaining cullin3 (only 50% of knockdown) is able to degrade RhoA under these conditions. A decrease in RhoA levels was observed in RhoBTB1-depleted cells after 6 hours of cycloheximide treatment, but not without cycloheximide. In contrast, Borda D'Agua (2012) observed that RhoA levels were reduced by RhoBTB1 depletion even without cycloheximide treatment. One possible reason for this difference could be the efficiency of transfection. If the efficiency in

RhoBTB1 depletion in Borda D'Agua's experiments was higher than in this study, less RhoBTB1 protein would be available in cells, leading to stronger effects on RhoA degradation. Because there is no antibody available which detects endogenous RhoBTB1 in these cells, this can not be tested directly.

After showing that RhoBTB1 had an effect on RhoA levels, a possible interaction between these two proteins was explored. Based on the hypothesis that RhoBTB1 is a BTB adaptor protein for cullin3 and protects RhoA from proteasomal degradation, the interaction of RhoBTB1 and RhoA was analysed, using vectors encoding GFP-RhoA, GFP-RhoA-V14 (constitutively active) and GFP-RhoA-N19 (dominant negative). It is known that the BACURD/cullin3 ubiquitin ligase complex binds preferentially to GDP-RhoA (Chen et al., 2009). It was observed that BACURD1/2 interacted with recombinant GDP-bound RhoA but not with recombinat GTP-RhoA. BACURD1/2 could also interact more with RhoA-N19 when compared to wild-type RhoA (Chen et al., 2009). Interestingly, RhoBTB1 interacted with RhoA-N19 and not with RhoA-V14. The RhoA-N19 mutant is to be either the GDP-bound or free-nucleotide (Coso et al., 1995). Because RhoBTB1 interacted only with this mutant, and not RhoA-V14 which is mostly GTP-bound in cells, it is likely to assume that RhoBTB1 does not interact with the GTP-bound form of RhoA. If RhoBTB1 interacts with GDP-RhoA, similar to BACURD (Chen et al., 2009), then it should also associate with wild-type RhoA. However, this was not observed in the immunoprecipitation. One possible explanation is that wild-type RhoA was predominantly GTP-bound in cells. The interaction of RhoBTB1 with GTP-RhoA versus GDP-RhoA could be tested using recombinant RhoA protein. Using RhoBTB1 deletion mutants, it was observed that RhoA-N19 interacts with the Rho domain of RhoBTB1. Therefore, the model for RhoBTB1 interactions is that it associates with RhoA through its Rho domain and cullin3 through its BTB domains (Figure 5.12). Another interesting result from this experiment is the fact that the levels of FLAG-RhoA-

N19 were higher in the total lysate in the presence of RhoBTB1. This supports a model where RhoBTB1 protect RhoA-N19 from degradation.

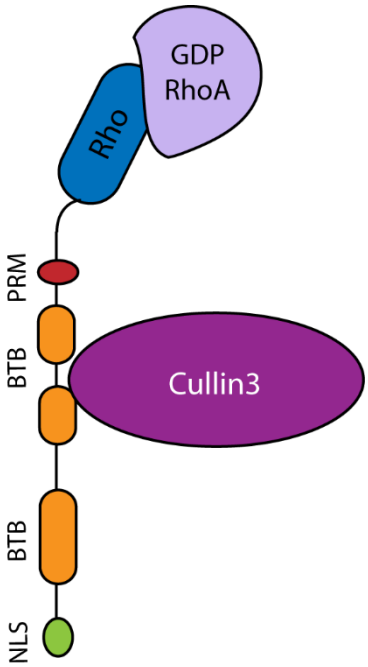

Figure 5.12 - Model of interaction between RhoBTB1, RhoA and cullin3
RhoBTB1 interacts with RhoA through its Rho domain and with cullin3 through its BTB domains.

Since BACURD1 and RhoBTB1 can both interact with RhoA and cullin3, it was hypothesised that these proteins could compete for RhoA binding. The presence of exogenous RhoBTB1 decreased the interaction between BACURD1 and RhoA-N19. This suggests that RhoA degradation could be regulated by the level of RhoBTB1 expression. When levels of RhoBTB1 are high, this protein binds preferentially to RhoA and cullin3, inhibiting RhoA ubiquitination or allowing a different type of ubiquitination that is not targeted for degradation. Therefore, when levels of RhoBTB1 are low, BACURD1 can bind to the complex, leading to increased RhoA degradation (Figure 5.13). However, more experiments are necessary to confirm this hypothesis. For

example, an ubiquitination assay to analyse the levels of RhoA ubiquitination after RhoBTB1 depletion would demonstrate if RhoBTB1 affects RhoA ubiquitination.

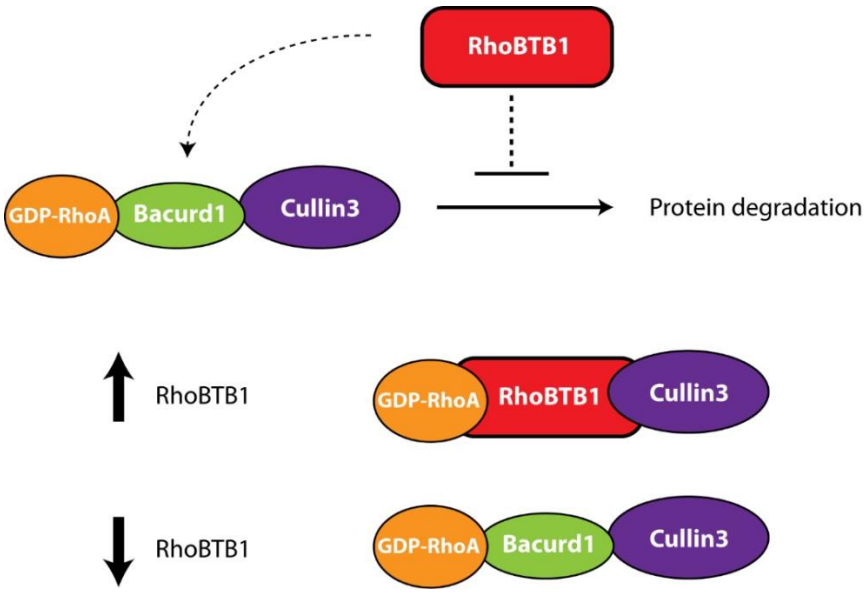

Figure 5.13 - Model of competition between RhoBTB1 and BACURD1

High levels of RhoBTB1 lead to preferential binding to RhoA and cullin3, inhibiting RhoA degradation. When levels of RhoBTB1 are low, BACURD1 is the BTB adaptor protein in the complex, leading to RhoA degradation.

Depletion of RhoBTB1 does not affect cell morphology of MDA-MB-231 cells in 2D culture (Borda D'Agua, 2012). However, in a 3D environment, RhoBTB1 depletion caused changes in the morphology of MDA-MB-231 and PC3 cells. These cells had a rounded morphology when embedded in a 3D Matrigel matrix. Depletion of RhoBTB1 led to elongation of cancer cells, similar to the phenotype observed for RhoA depletion (Vega et al., 2011). As mentioned above (section 5.3), cells in a 3D environment are often able to interchange between two modes of migration: amoeboid and mesenchymal. During amoeboid movement, cells have a rounded morphology and require activation of Rho/ROCK signalling to increase levels of actomyosin contractility. On the other hand, during mesenchymal movement, cells have an elongated

morphology and are dependent on Rac1-mediated cell migration. Therefore, the cross-talk between Rho and Rac is important to control these different cell shapes (Parri and Chiarugi, 2010; Sailem et al., 2014). Because RhoBTB1 depletion causes elongation of cells and a decrease in RhoA levels, it is possible that RhoBTB1 regulates the actin cytoskeleton through RhoA signalling. One hypothesis is that RhoBTB1 protects RhoA from degradation which allows this protein to activate effectors that increase cell contractility, making the cells round up. It would be interesting to test the effects of RhoBTB1 depletion on the close relatives of RhoA, RhoB and RhoC (Wheeler and Ridley, 2004). Another possibility is that RhoBTB1 could reduce Rac1 signalling and lamellipodial extension, but there is no evidence so far that supports this hypothesis.

RhoBTB1/RhoA-N19 interaction and changes in cell morphology in 3D culture after RhoBTB1 deletion are good indicators that RhoBTB1 might have an indirect role in controlling the actin cytoskeleton. Our model suggests that this could be through inhibiting RhoA degradation mediated by the BACURD/cullin3 complex. More experiments are necessary to elucidate the exact mechanism. It is necessary to confirm that RhoA and cullin3 interact with RhoBTB1 in the same complex and that RhoA binds directly to RhoBTB1. It would be important to study these interactions using recombinant proteins. An ubiquitination assay *in vitro* would be really interesting to analyse the real effects of RhoBTB1 in RhoA ubiquitination (Choo and Zhang, 2009). This approach could be also used to study more directly a potential competition between RhoBTB1 and BACURD in the cullin3 ubiquitin ligase complex.

6 Interaction of RhoBTB1 and ROCK1

6.1 Introduction

Based on the interaction of RhoBTB1 with RhoA observed in Chapter 5, the effects of RhoBTB1 depletion on RhoA effectors was analysed. It was predicted that RhoBTB1 would affect the activity of the RhoA effectors ROCK1 or ROCK2 indirectley through its interaction with RhoA. Surprisingly, an interaction between RhoBTB1 and ROCK1 was observed and explored in this chapter. As mentioned in Chapter 1, there is a complex crosstalk between Rho GTPases that can involve not only their regulators but also their effectors. The interaction between RhoBTB1 and ROCK1 could be part of one of these crosstalks.

Rho-associated kinases (ROCKs) are serine/threonine kinases that are part of the AGC family of protein kinases (Amano et al., 2010). These proteins have a kinase domain at their N-terminus, a long amphipathic α-helix that forms a coiled-coil structure in the middle, and a cysteine-rich zinc finger-like motif and a pleckstrin-homology (PH) region in their C-terminus (Ishizaki et al., 1997). Both N- and C-terminal regions are important for ROCK protein activity (Amano et al., 2010). In mammals, there are two ROCKs, ROCK1 and ROCK2, that were first identified as RhoA-binding proteins (Ishizaki et al., 1996; Leung et al., 1995; Matsui et al., 1996). The amino-acid sequences of ROCK1 and ROCK2 show 65% of overall identity with 92% identity of their kinase domain in humans (Figure 6.1A) (Amano et al., 2010; Riento and Ridley, 2003). The consensus phosphorylation sequence for ROCKs is R/KXS/T or R/KXXS/T (where R is arginine, K is lysine, X is any amino acid, S is serine and T is threonine) (Kawano et al., 1999; Sumi et al., 2001). However, some substrates are phosphorylated on sites that do not conform to the consensus phosphorylation sequence. One example is Rnd3/RhoE which is phosphorylated on serine 222 (HMP**S**R) by ROCK1 (Riento et al., 2005). Crystal structure and biochemical studies

have shown that ROCKs dimerise through two different regions: the N-terminal region and the coiled-coil region (Figure 6.1B) (Jacobs et al., 2006; Shimizu et al., 2003; Yamaguchi et al., 2006).

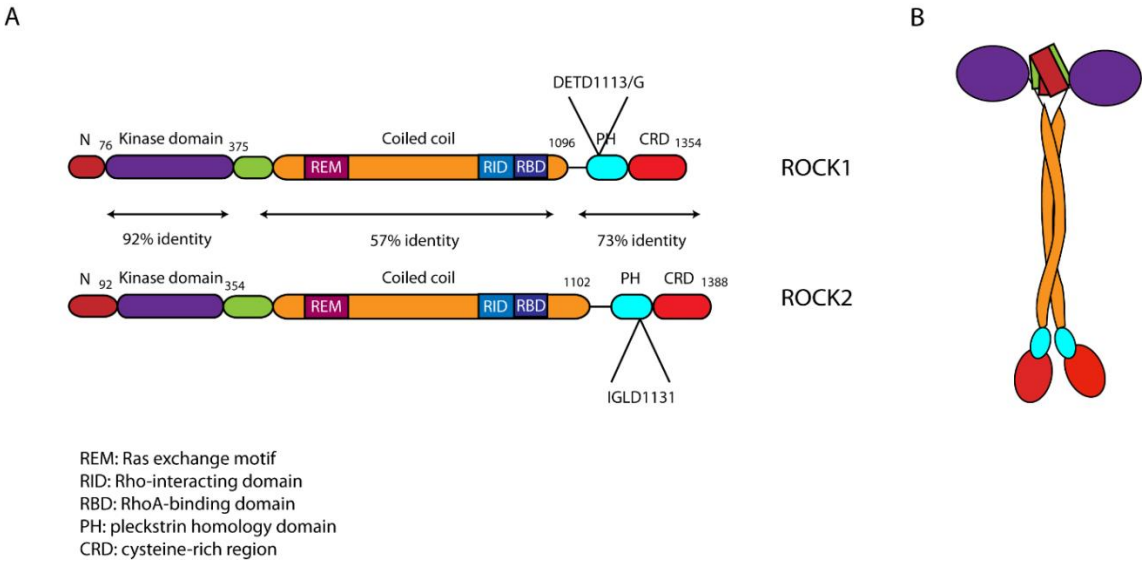

Figure 6.1 - ROCK1 and ROCK2

A) Domain organization of ROCK1 and ROCK2 in humans. DETD1113/G: conserved sequence in ROCK1 cleaved by caspase 3. IGLD1131: conserved sequence in ROCK2 cleaved by granzyme B. B) Diagram of the dimer structure of ROCKs. ROCKs form parallel dimers through the N-terminal and central coiled-coil regions.

6.1.1 ROCK effectors

ROCKs induce the formation of stress fibres and focal adhesions in a variety of cell lines (Amano et al., 1997; Ishizaki et al., 1997; Leung et al., 1996). They phosphorylate the myosin-binding subunit (MBS, also known as myosin phosphatase-targeting subunit, MYPT) of myosin phosphatase which inhibits its activity, leading to an increase in phosphorylated myosin light chain 2 (MLC2) (Kawano et al., 1999; Kimura et al., 1996). ROCKs can also directly phosphorylate MLC2 (Amano et al., 1996a). Phosphorylated MLC2 promotes the assembly of myosin II filaments and then their interaction with F-actin to form stress fibres (Ridley, 1999). It is believed that ROCK1

and ROCK2 have the same role in regulating MLC2 phosphorylation. Knock out of both ROCK1 and ROCK2 is necessary to affect pMLC (Kumper et al., 2016). ROCK1 and ROCK2 knockout mice have indicated the two kinases have redundant roles in cell proliferation and tumorigenesis (Kumper et al., 2016). However, in some models, ROCK1 and ROCK2 have distinct roles. For example, in rat embryo fibroblasts only depletion of ROCK1 affects assembly of stress fibres and focal adhesions while ROCK2 seems to be involved in phagocytosis (Yoneda et al., 2005). ROCKs can also control the actin cytoskeleton through LIM kinase (LIMK)/cofilin pathway. LIMK is phosphorylated by ROCK which leads to phosphorylation of cofilin-induced and inhibition of actin depolymerisation. This stabilizes F-actin and contributes to increased actomyosin contractility (Maekawa et al., 1999).

Adducin, a membrane-associated actin-interacting protein, is another ROCK substrate. ROCK2 phosphorylates adducin which increases its interaction with F-actin (Kimura et al., 1998). As well as affecting the actin cytoskeleton, ROCKs phosphorylate many other substrates involved in a range of cellular processes (Amano et al., 2010; Morgan-Fisher et al., 2013). For example, vimentin and glial fibrillary acidic protein (GFAP) are intermediate filaments that are phosphorylated during cytokinesis by ROCK1 and ROCK2, respectively, which prevents filament formation (Goto et al., 1998; Kosako et al., 1997).

6.1.2 Regulation of ROCKs

ROCKs can be regulated by protein interactions, phosphorylation and proteolysis. The C-terminal region containing the Rho-binding domain and the PH region interacts with the kinase domain, inhibiting ROCK activity (Amano et al., 1999). Interaction of GTP-bound RhoA with Rho-binding domain (RBD) in the coiled-coil region, is believed to release the kinase domain from this inhibition (Amano et al., 1999; Fujisawa et al., 1996; Riento and Ridley, 2003). However, recent data suggest that ROCK2 is present

in cells in an extended conformation which would be incompatible with intramolecular autoinhibition. The authors propose that ROCK2 is constitutively active, based on an *in vitro* activity assay (Truebestein et al., 2015). The activity to ROCK2 is instead suggested to be regulated by the length of its coiled-coil region and not by binding to membranes, RhoA or phosphorylation (Truebestein et al., 2015).

Another way of activating ROCKs is through proteolytic cleavage of the C-terminal region. During apoptosis, caspase-3 cleaves ROCK1 at a conserved DETD1113/G sequence (Figure 6.1), leading to constitutive kinase activity and cell blebbing (Coleman et al., 2001; Sebbagh et al., 2001). ROCK2 is also activated during apoptosis, but in a caspase-independent manner. Granzyme B, a potent proapoptotic protease contained in cytotoxic granules released by natural killer cells or cytotoxic T lymphocytes (Lord et al., 2003), cleaves ROCK2 at the IGLD1131 sequence (Figure 6.1), which is not found in ROCK1 (Sebbagh et al., 2005).

ROCK can be negatively regulated by small GTP binding proteins. Gem and Rad have been shown to bind to ROCK and inhibit MLC phosphorylation. This leads to a reduction in stress fibre and focal adhesion formation, neurite retraction and Rho-dependent transformation (Ward et al., 2002).

ROCKs can be autophosphorylated (Ishizaki et al., 1996; Leung et al., 1995) and phosphorylated by other kinases. Phosphorylation does not seem necessary for kinase activity of ROCK, but it could regulate ROCK signalling through the phosphorylation of other regions (Julian and Olson, 2014). Autophosphorylation of ROCK1 on Ser1333 and of ROCK2 on Ser1336 are markers of kinase activation but these modifications do not regulate the catalytic activity (Chuang et al., 2013; Chuang et al., 2012; Julian and Olson, 2014). Phosphorylation might affect binding of ROCK to RhoA. For example, phosphorylation of ROCK2 on Tyr722 decreases binding to RhoA while dephosphorylation of ROCK2 by Shp-2 on the same site increases RhoA/ROCK2

signalling (Lee and Chang, 2008; Lee et al., 2010). However, the mechanistic basis of these observations is unclear. ROCK2 is also a substrate of polo-like kinase-1 (Plk1) and these proteins co-localise during cytokinesis. *In vitro*, Plk1 and RhoA cooperate to increase the kinase activity of ROCK2 (Lowery et al., 2007).

ROCKs have been shown to be regulated by microRNAs in some cancers. For example, transfection of microRNA-584 into clear renal cell adenocarcinoma cell lines leads to a decrease in cell motility and expression of ROCK1 (Ueno et al., 2011). In hepatocellular carcinoma cells, ectopic expression of microRNA-124 reduces ROCK2 expression and decreases formation of stress fibres, filopodia and lamellipodia (Zheng et al., 2012).

6.1.3 ROCKs in cancer

ROCKs have been shown to be involved in several steps of cancer progression (Narumiya et al., 2009; Schofield and Bernard, 2013). Somatic mutations that encode constitutively active forms of both ROCK proteins are found in some human cancers (Kale et al., 2015; Morgan-Fisher et al., 2013). In addition, high expression of ROCK1 and ROCK2 has been associated with a more aggressive behaviour of cancer cells (Kale et al., 2015; Morgan-Fisher et al., 2013).

6.2 Effects on RhoA downstream effectors after RhoBTB1 depletion in MDA-MB-231 cells

As shown in Chapter 5 and by Borda D'Agua (2012), depletion of RhoBTB1 in MDA-MB-231 cells can decrease RhoA expression. To determine whether RhoBTB1 affected signalling downstream of RhoA, levels of phosphorylated MLC2, phosphorylated cofilin, phosphorylated LIMK1/2, ROCK1 and ROCK2 were evaluated by western blotting (Figure 6.2 and Figure 6.3). Unexpectedly, only expression of ROCK1 and ROCK2 was reduced following RhoBTB1 depletion (Figure 6.3).

RhoBTB1 depletion did not appear to affect phosphorylation or expression of known RhoA/ROCK effectors (e.g. MLC, cofilin and LIMK). These results could indicate that the decrease in ROCK levels is not sufficient to cause detectable effect on these effectors, and indeed other kinases (e.g. PAK) are able to phosphorylate the same substrates (Edwards et al., 1999). However, this experiment was performed only once and more repeats are necessary.

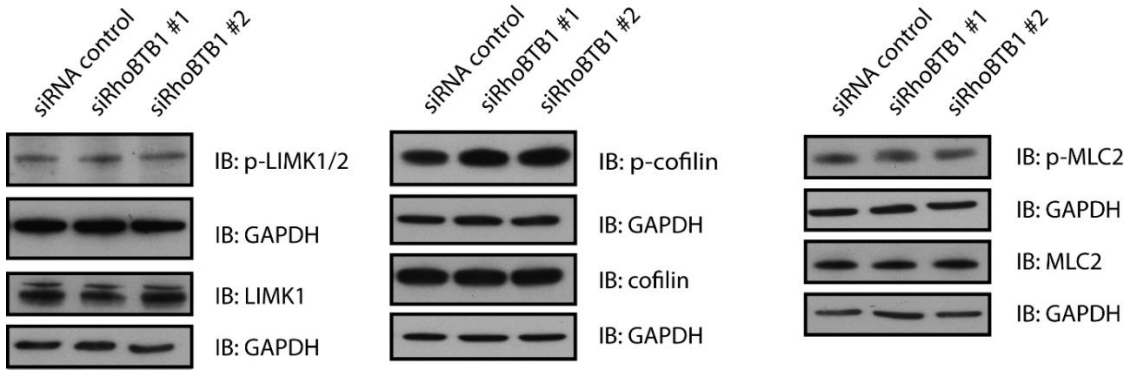

Figure 6.2 - RhoBTB1 depletion does not affect levels of p-LIMK1/2, p-cofilin and p-MLC2 in MDA-MB-231 cells

MDA-MB-231 cells were transfected with siRNA control or siRNA oligos #1 and #2 targeting RhoBTB1. After 72 hours, cells were lysed and protein expression was analysed by western blotting. GAPDH is used as a loading control. Blots are from one experiment.

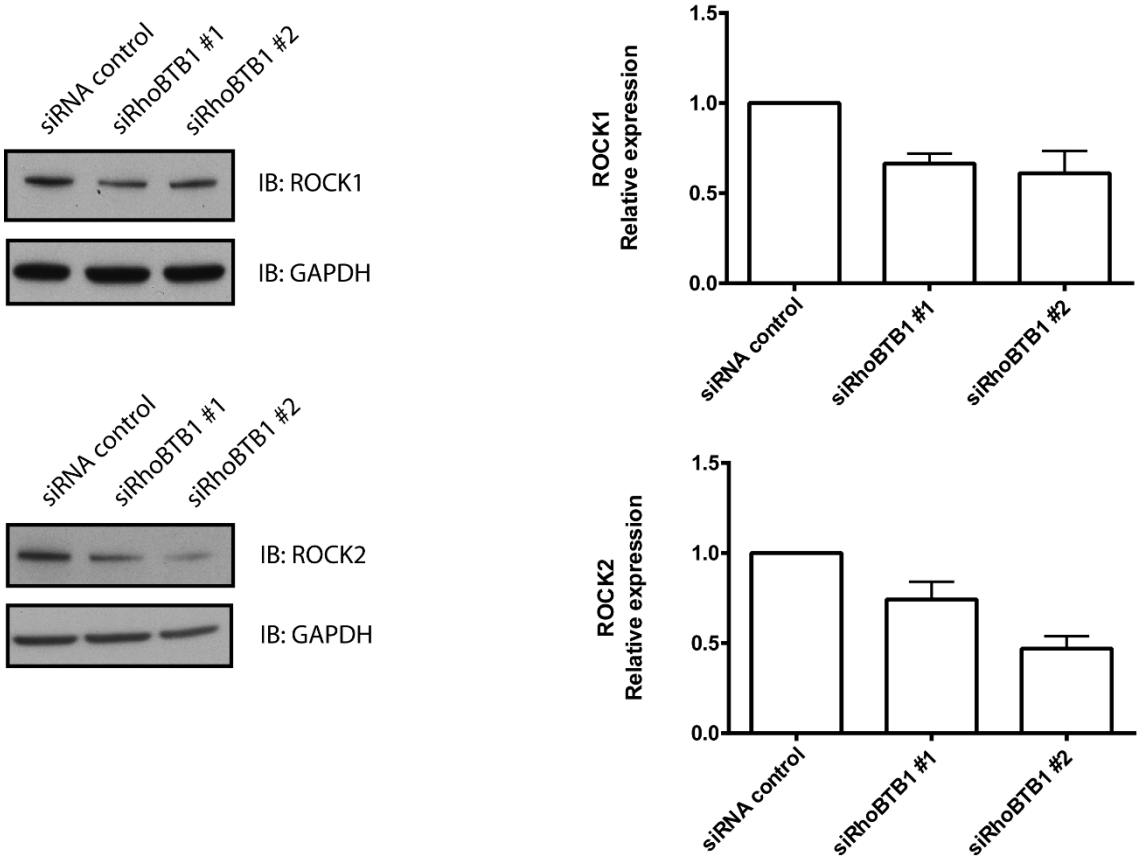

Figure 6.3 - RhoBTB1 depletion reduces levels of ROCK1 and ROCK2 proteins in MDA-MB-231 cells

MDA-MB-231 cells were transfected with siRNA control or siRNA oligos #1 and #2 targeting RhoBTB1. After 72 hours, cells were lysed and protein expression was analysed by western blotting. GAPDH is used as a loading control. Graphs show the quantification of the band density of five independent experiments, normalised to GAPDH and relative to siRNA control.

To determine whether RhoBTB1 regulates ROCK1 and ROCK2 expression at the transcriptional level, the mRNA levels of ROCK1 and ROCK2 were quantified by qPCR after RhoBTB1 knockdown. No significant difference in the mRNA levels of ROCK1 or ROCK2 were observed (Figure 6.4).

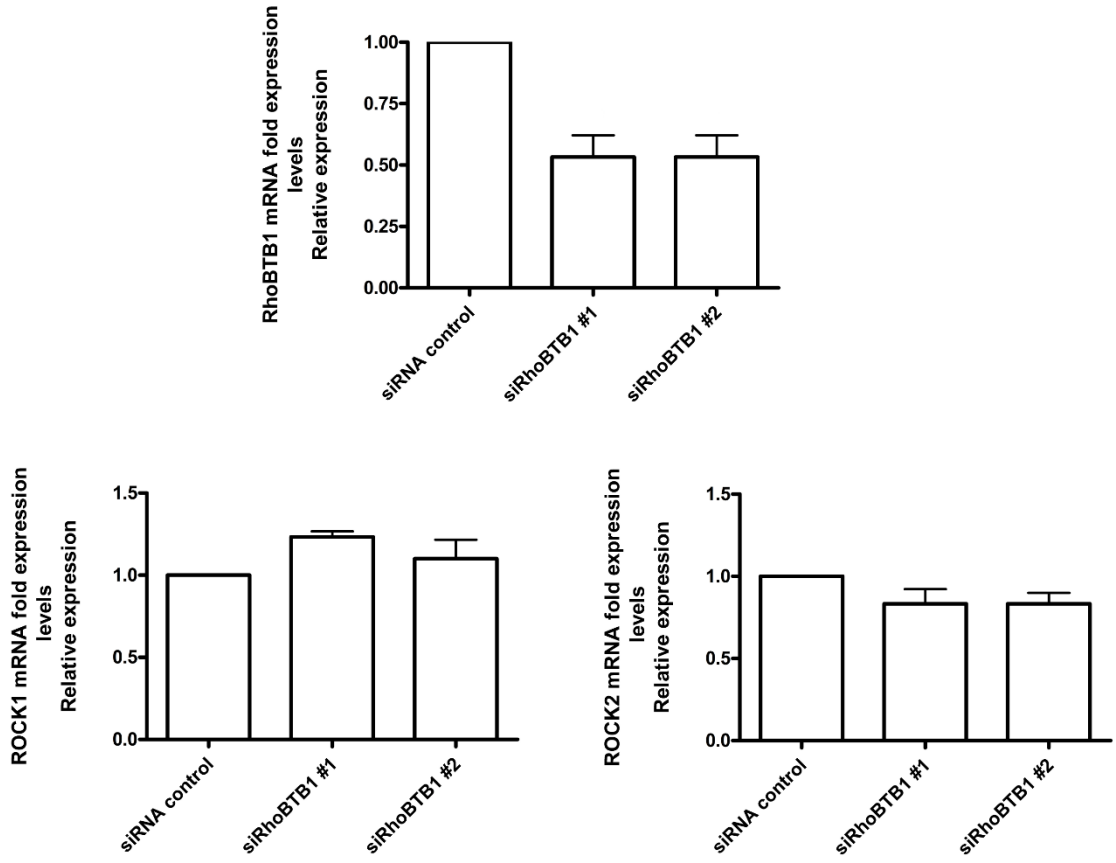

Figure 6.4 - mRNA levels of ROCK1 and ROCK2 after RhoBTB1 depletion in MDA-MB-231 cells

MDA-MB-231 cells were transfected with siRNA control or siRNA oligos #1 and #2 targeting RhoBTB1. After 72 hours, mRNA was isolated and the amount of RhoBTB1, ROCK1 and ROCK2 cDNA was determined by quantitative PCR. Graphs show data of three independent experiments. All values were normalized to siRNA control.

6.3 Effects of ROCK1 and ROCK2 depletion in MDA-MB-231 cells on endothelial interaction

In an attempt to correlate the effects of RhoBTB1 knockdown on cancer cell extravasation and ROCK1/2 expression, MDA-MB-231 cells were transfected with siRNAs targeting ROCK1, ROCK2 or both ROCK1 and ROCK2 together (Figure 6.5A). Adhesion and intercalation of these cells into endothelial cells were analysed. Depletion of ROCK1/2 together or separately increased adhesion (Figure 6.5B) which is the opposite of what is reported for RhoBTB1 depletion (Borda D'Agua, 2012). In contrast, intercalation was not significantly affected (Figure 6.5C), indicating that the

reduction in MDA-MB-231 cell intercalation following RhoBTB1 depletion is unlikely to be related to lower ROCK1/2 levels.

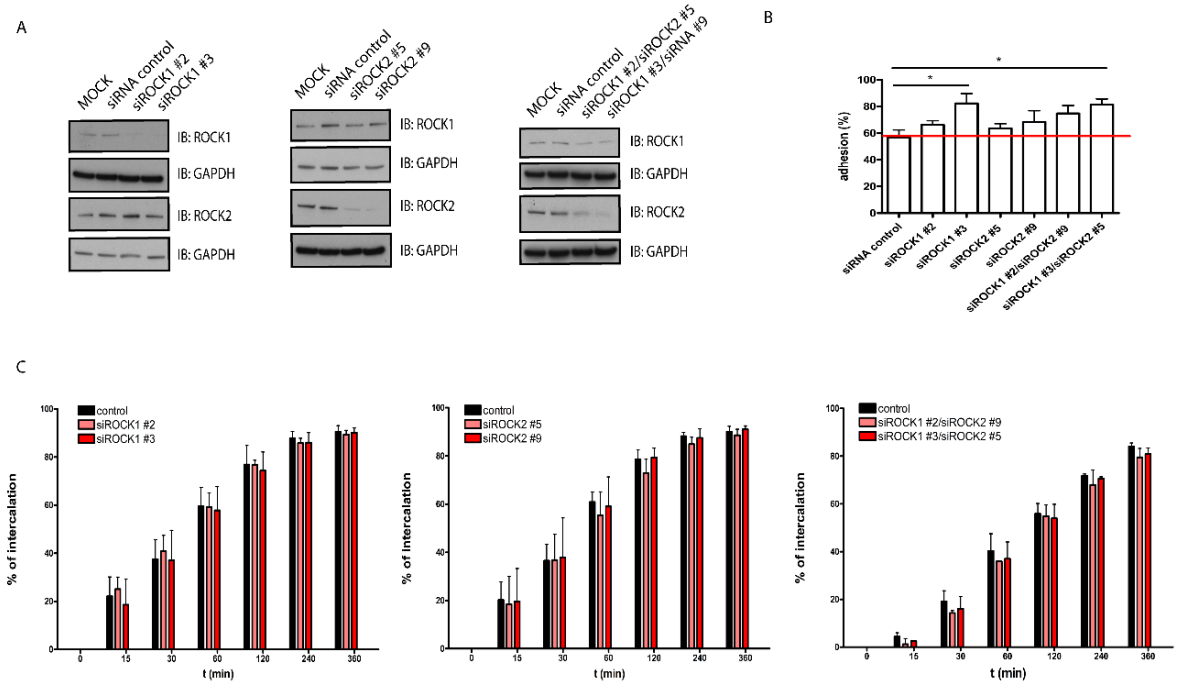

Figure 6.5 - Effects of ROCK1/2 knockdown on adhesion and intercalation of MDA-MB-231 cells into endothelial cells

A) Blots show the expression of ROCK1 and ROCK2 after siRNA transfection with oligos targeting ROCK1, ROCK2 and ROCK1/2 together, or control siRNA. B) HUVECs were grown to confluence on collagen I-coated plates. CFSE-labelled cancer cells were added and allowed to adhere 15 minutes. Not-adherent or loosely adherent cells were washed of and the levels of fluorescence were measured. Graphs show data from at least three independent experiments, each carried out in quintuplicate. All values were normalized to siRNA control. Values represent mean ± SEM. *p<0.05, compared to siRNA control, determined by unpaired one-way ANOVA, followed by Dunnett´s test. C) MDA-MB-231 cells were monitored by timelapse microscopy acquiring an image every 3-5 min over 6 hours. The graph shows the percentage of intercalated cells at the indicated time points from two independent experiments. Nine different fields from each condition were analysed per experiment (~ 30 cells per field). Values represent mean ± SD. MOCK is the condition where the cells are not transfected.

6.4 RhoBTB1 interacts with ROCK1

To investigate how RhoBTB1 regulates the expression of ROCK proteins, the possibility that RhoBTB1 interact with ROCK1 was tested. GFP-RhoBTB1 was co-

expressed with myc-ROCK1 and the interaction of the proteins was evaluated after immunoprecipitation. RhoBTB1 co-immunoprecipitated with ROCK1 1-727 (Figure 6.6).

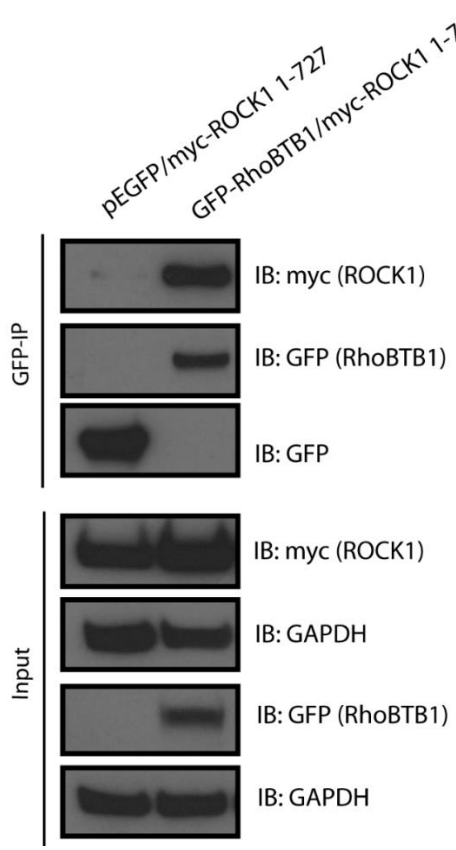

Figure 6.6 - RhoBTB1 interacts with ROCK1

Cos7 cells were transfected with empty pEGFP or vectors encoding myc-ROCK1 1-727 and GFP-RhoBTB1. After 24 hours, cells were lysed and incubated with GFP-binding protein coupled to agarose (GFP-trap®). Total lysates (input) and immunoprecipitates (GFP-IP) were probed to show levels of myc-ROCK1 1-727 and GFP-RhoBTB1. The interaction between myc-ROCK1 1-727 and GFP-RhoBTB1 is shown in the immunoprecipitates (GFP-IP). GAPDH is used as a loading control. Blots are representative of two independent experiments.

To determine which region of ROCK1 interacted with RhoBTB1, Cos7 cells we transfected with vectors encoding RhoBTB1 and different regions of ROCK1 (Figure 6.7A). RhoBTB1 interacted with full length ROCK1, ROCK1 1-1080, ROCK1 1-727 and ROCK1 1-540 but not with ROCK1 1-420 and ROCK1 1096-1394 (Figure 6.7B).

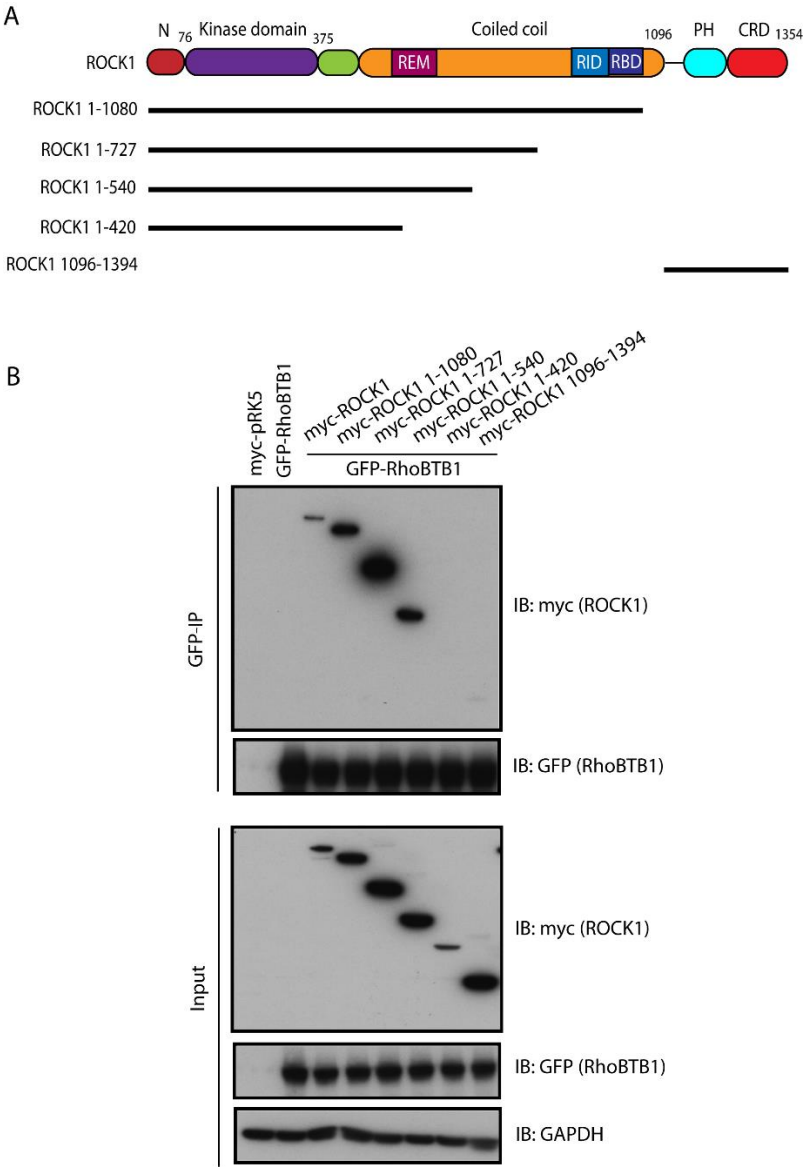

Figure 6.7 - RhoBTB1 interaction with ROCK1 deletion mutants

A) Domain structure of ROCK1 and ROCK1 deletion mutants. B) Cos7 cells were transfected with empty myc-pRK5 or vectors encoding GFP-RhoBTB1, myc-ROCK1 and myc-ROCK1 deletion mutants. After 24 hours, cells were lysed and incubated with GFP-binding protein coupled to agarose (GFP-trap®). Total lysates (input) and immunoprecipitates (GFP-IP) were probed to show levels of GFP-RhoBTB1, myc-ROCK1 and myc-ROCK1 deletion mutants. The interaction between GFP-RhoBTB1 and myc-ROCK1 deletion mutants is shown in the immunoprecipitates (GFP-IP). GAPDH is used as a loading control. Blots are representative of two independent experiments.

To determine if the Rho domain of RhoBTB1 was involved in ROCK1 interaction, a pull down assay using the recombinant GST-RhoBTB1 1-301 (Figure 6.8A) was performed with lysates of Cos7 cells transfected with vectors encoding different regions of

ROCK1. RhoBTB1 1-301 was able to interact with full length ROCK1, ROCK1 1-1080, ROCK1 1-727 and ROCK1 1-540 (Figure 6.8B). Weak bands were observed for both ROCK1 1-420 and ROCK1 1096-1394 (Figure 6.8B). However, these bands could be only background. To confirm this, a condition with only GST should be included. More repeats are necessary to confirm these results.

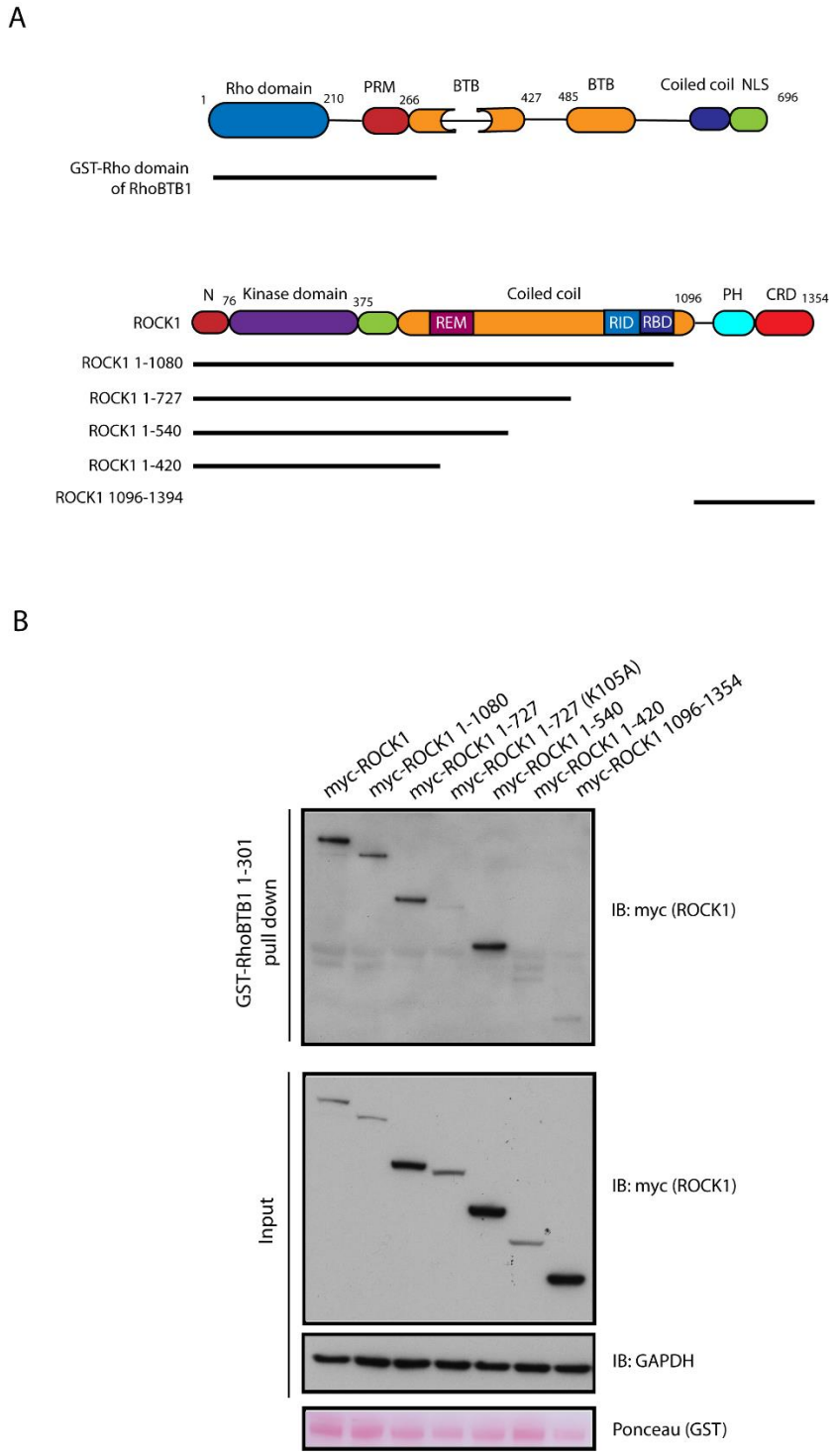

Figure 6.8 - GST-RhoBTB1 1-301 interaction with ROCK1 deletion mutants

A) Domain structure of RhoBTB1, RhoBTB1 1-301, ROCK1 and ROCK1 deletion mutants. B) Cos7 cells were transfected with vectors encoding myc-ROCK1 and myc-ROCK1 deletion mutations. After 24 hours, cells were lysed and incubated with GST-RhoBTB1 1-301 beads. Total lysates (input) and pull down were probed to show levels of myc-ROCK1 and myc-ROCK1 deletion mutants. The interaction between GST-RhoBTB1 1-301 and myc-ROCK1 deletion mutants is shown in the pull down. GAPDH is used as a loading control. Ponceau staining of the western blot was used to verify GST-RhoBTB1 1-301 protein levels. Blots are from one experiment.

Based on the results obtained with the recombinant RhoBTB1 1-301 and ROCK1 deletion mutants (Figure 6.8), it appears that the RhoBTB1 1-301 is sufficient for the interaction with ROCK1. Interestingly, the two ROCK1 deletion mutants (ROCK1 1-420 and ROCK1 1096-1394) that did not interact with RhoBTB1 lack a region of ROCK1 where the REM (Ras exchange motif, also known as HR1 domain) domain is located (Figure 6.9).

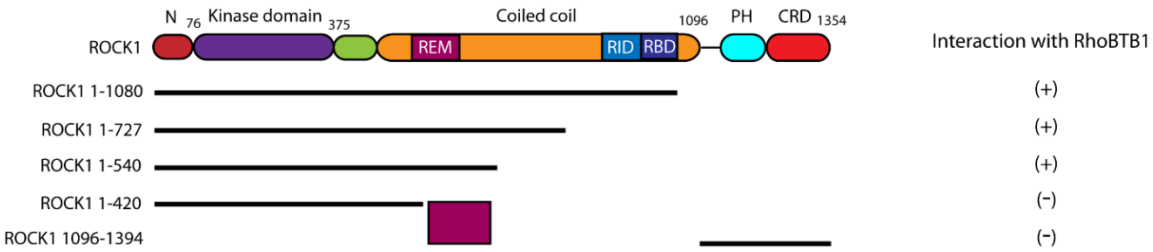

Figure 6.9 - Domain structure of ROCK1 deletion mutants

The magenta rectangle shows the region of ROCK1 that is missing in both ROCK1 1-420 and ROCK1 1096-1394.

To confirm that the region between amino acids 420 and 540 is important for ROCK1 and RhoBTB1 interaction, another co-immunoprecipitation was performed using a construct encoding ROCK1 375-727 (Figure 6.10A) (Garg et al., 2008). RhoBTB1 interacted with ROCK1 375-727 but not with ROCK1 1-420, as shown previously (Figure 6.10B).

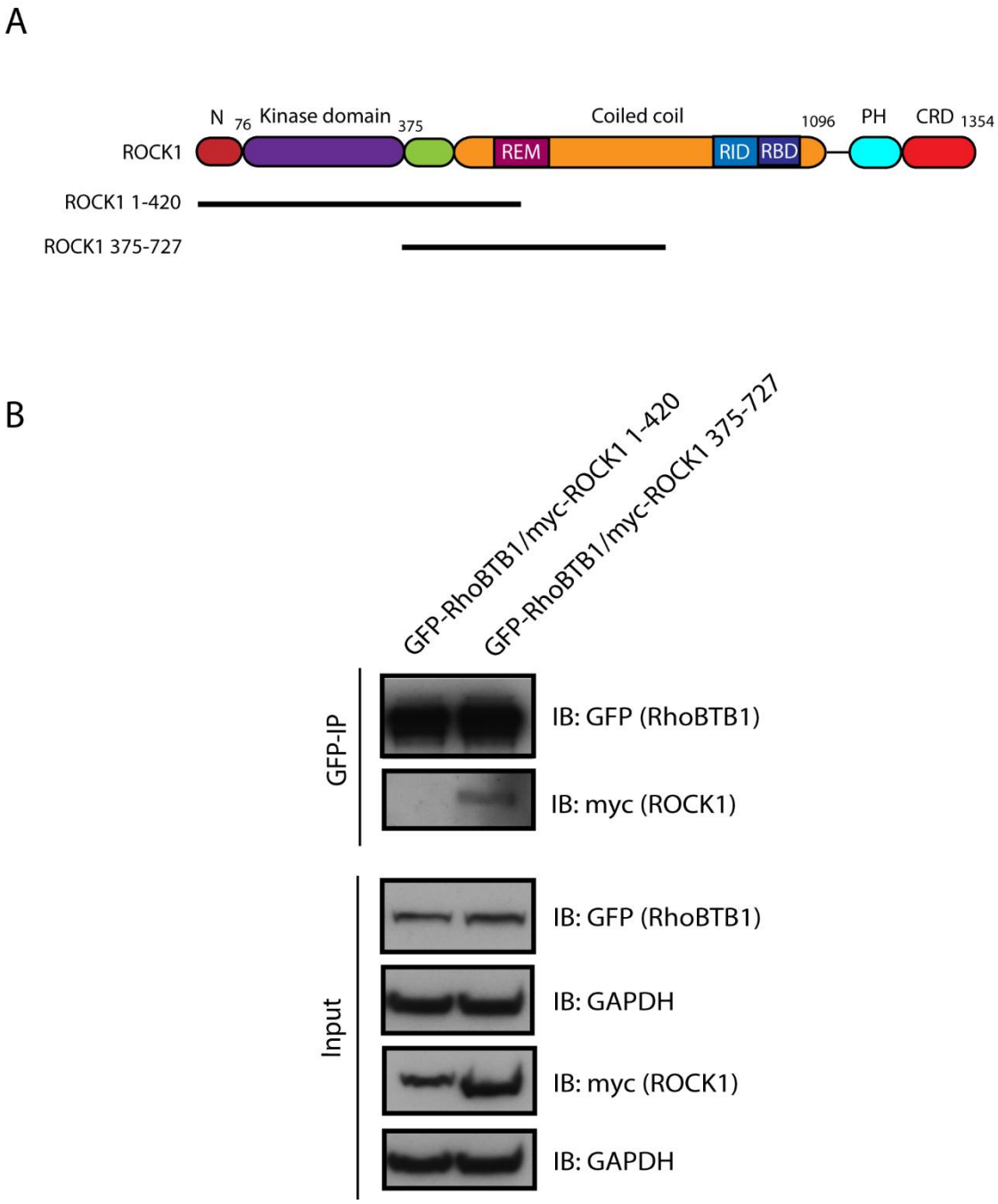

Figure 6.10 - RhoBTB1 interacts with ROCK1 375-727 but not with ROCK1 1-420

A) Domain structure of ROCK1 and ROCK1 deletion mutants. B) Cos7 cells were transfected with vectors encoding GFP-RhoBTB1 and myc-ROCK1 deletion mutants. After 24 hours, cells were lysed and incubated with GFP-binding protein coupled to agarose (GFP-trap®). Total lysates (input) and immunoprecipitates (GFP-IP) were probed to show levels of GFP-RhoBTB1 and myc-ROCK1 deletion mutants. The interaction between GFP-RhoBTB1 and myc-ROCK1 deletion mutants is shown in the immunoprecipitates (GFP-IP). GAPDH is used as a loading control. Blots are from one experiment.

Taken together, these results suggest that the interaction of RhoBTB1 and ROCK1 might be mediated through the Rho domain of RhoBTB1 and the REM domain of ROCK1.

Since RhoBTB1 and ROCK1 interact, one possible pathway that could be involved in the regulation of ROCK1 expression is proteasomal degradation after ubiquitination by RhoBTB1/cullin3 ubiquitin ligase complex. To test this hypothesis, MDA-MB-231 cells were treated with the neddylation inhibitor MLN4924 for 2 hours. Inhibition of cullin3 activity did not affect total protein levels of ROCK1 (Figure 6.11). This suggests that RhoBTB1 affects the expression of ROCK1 through another pathway. However, it would be important to repeat the experiment after RhoBTB1 depletion. Because RhoBTB1 could be protecting ROCK1 from degradation, depletion of RhoBTB1 could potentiate the effects of MLN4924 inhibitor on the total levels of ROCK1.

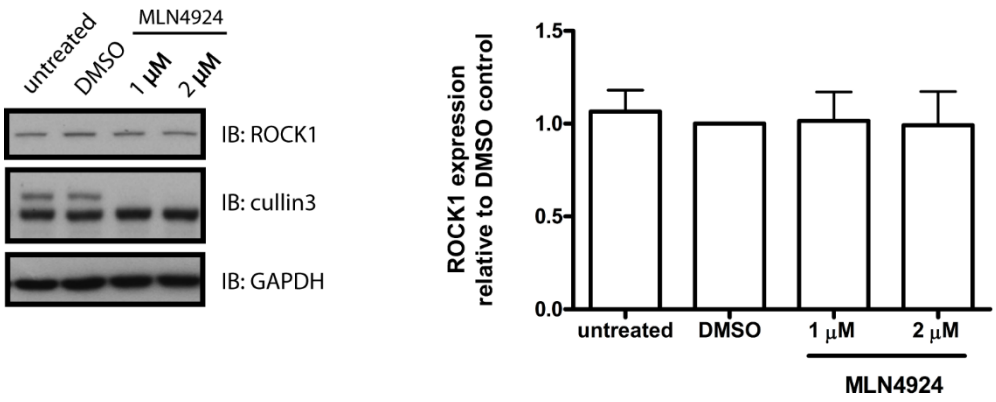

Figure 6.11 - Inhibition of cullin3 does not affect ROCK1 total protein levels in MDA-MB-231 cells

MDA-MB-231 cells were treated with 1 μM or 2 μM of MLN4924 or DMSO as solvent control for 2 hours. Cells were lysed and protein expression was analysed by western blotting. GAPDH is used as a loading control. Graph shows the quantification of the band density of five independent experiments, normalised to GAPDH and relative to DMSO. All values were normalized to DMSO condition. Values represent mean ± SEM.

6.5 Phosphorylation of RhoBTB1 by ROCK1

ROCK1 is a serine/threonine kinase that can interact with RhoBTB1 and could therefore potentially phosphorylate it. To investigate whether ROCK1 might phosphorylate RhoBTB1, cells expressing myc-RhoBTB1 were treated with the ROCK inhibitor H1152 (Sasaki et al., 2002). Treatment with ROCK inhibitor decreased levels of phosphorylated RhoBTB1 at 4 hours after addition (Figure 6.12). These were preliminary results and more repeats are necessary.

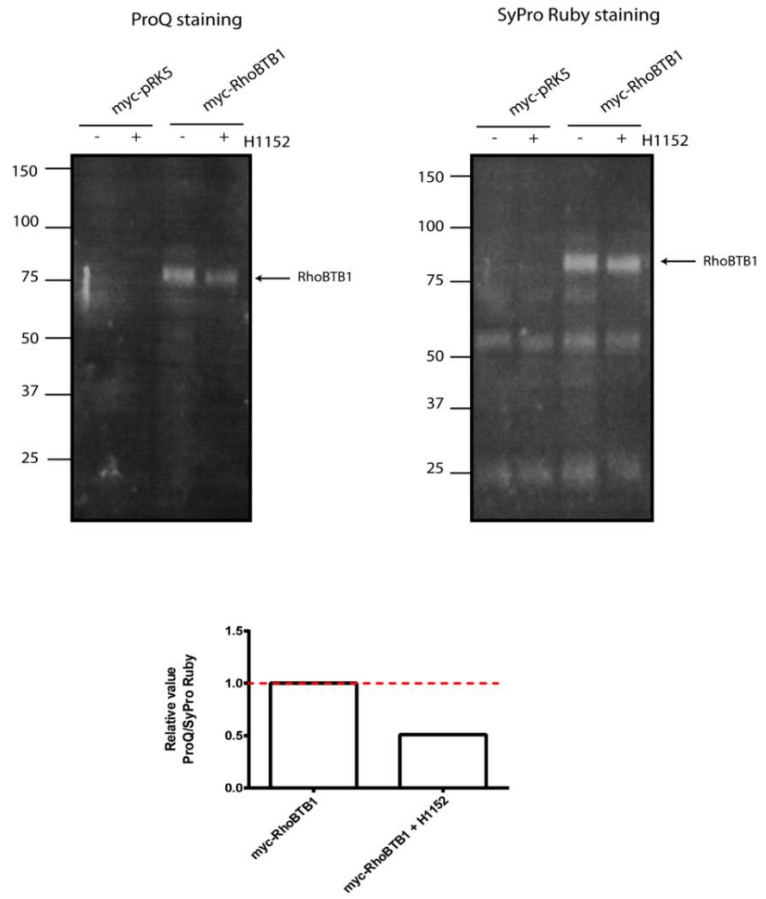

Figure 6.12 - ROCK inhibitor reduces RhoBTB1 phosphorylation

Cos7 cells were transfected with myc-pRK5 and myc-RhoBTB1. After 24 hours, cells were treated with 5 μM H1152 (ROCK inhibitor) for 4 hours. Cells were then lysed and incubated with anti-myc-agarose beads. Immunoprecipitated lysates were resolved in a 4-12% SDS-polyacrylamide gel and transferred to a low fluorescence PVDF membrane. The membrane was incubated with ProQ Diamond stain (phosphorylated protein) followed by incubation with SyPRO Ruby (total protein). Blots are from one experiment. Graph shows the relative value of phosphorylated protein/total protein, normalized to myc-RhoBTB1 without H1152 treatment.

Since these preliminary data suggest that inhibition of ROCK1/2 activity decreases RhoBTB1 phosphorylation, a kinase assay using ^{32}P-ATP was performed to analyse phosphorylation of RhoBTB1 by ROCK1. ROCK1 was able to phosphorylate RhoBTB1 (Figure 6.13A) and the Rho domain of RhoBTB1 (RhoBTB1 1-210) (Figure 6.13B). The kinase dead ROCK1 (ROCK1 1-727 (K205A)) was not able to phosphorylate RhoBTB1 (Figure 6.13A).

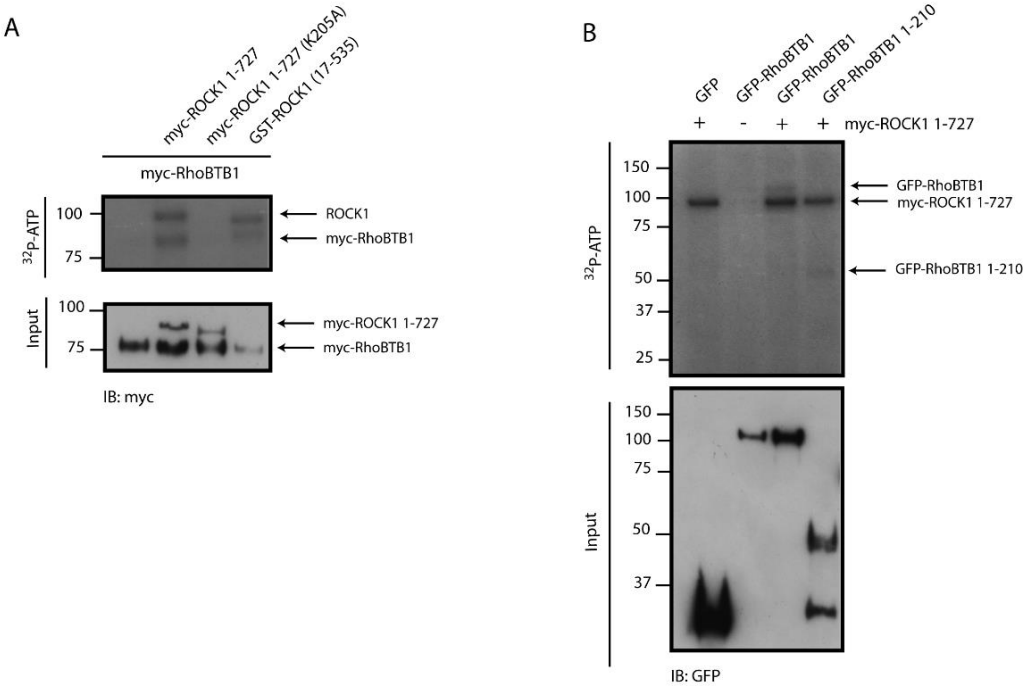

Figure 6.13 - Phosphorylation of RhoBTB1 by ROCK1

A) Cos7 cells were transfected with vectors encoding myc-RhoBTB1, myc-ROCK1 1-727 or myc-ROCK1 1-727 (K205A). After 24 hours, cells were lysed and incubated with anti-myc-agarose beads. Immunoprecipitated lysates were combined as indicated (myc RhoBTB1 alone, myc-RhoBTB1 and myc-ROCK1 1-727, myc-RhoBTB1 and myc-ROCK1 1-727 (K205A) (kinase dead), and myc-RhoBTB1 and recombinant GST-ROCK1 (17-535)). Samples were incubated in a kinase buffer containing ^{32}P-ATP for 30 minutes and then resolved in a 4-12% SDS polyacrylamide gel. Bands show the phosphorylated proteins. Results are representative of three independent experiments. B) Cos7 cells were transfected with vectors encoding GFP, GFP-RhoBTB1, GFP-RhoBTB1 1-210 and myc-ROCK1 1-727. After 24 hours, cells were lysed and incubated with either GFP-binding protein coupled to agarose (GFP-trap®) or anti-myc-agarose beads. Immunoprecipitated lysates were combined as indicated (GFP and myc-ROCK1 1-727, GFP-RhoBTB1 alone, GFP-RhoBTB1 and myc-ROCK1 1-727, and GFP-RhoBTB1 1-210 and myc-ROCK1 1-727). Samples were incubated in a kinase buffer containing ^{32}P-ATP for 30 minutes and then resolved in a 4-12% SDS polyacrylamide gel. Bands (top) show the phosphorylated proteins. Results are representative of two independent experiments.

To determine whether any of the sites on PhosphoSite Plus website (www.phosphosite.org) (Hornbeck et al., 2015) is phosphorylated by ROCK1, all 5 possible phosphorylation sites were mutated to alanine (S69A/T398A/S480A/T483A/S485A = RhoBTB1 S3T2A) (section 2.2.10) (Table 6-1). The PhosphoSite Plus website contains data from low- and high-throughput (LTP and HTP) studies. A kinase assay using ^{32}P-ATP was performed to analyse phosphorylation of the RhoBTB1 mutant by ROCK1. ROCK1 was still able to phosphorylate RhoBTB1-S3T2A (lane 4) (Figure 6.14). This suggests that there are other phosphorylation sites on RhoBTB1 that are not on the PhosphoSite Plus website. This mutant seems to be less stable than wild-type RhoBTB1 because there is less of this protein in the input. ROCK 1-540 was used in the assays to try to have a better separation between RhoBTB1 and ROCK1 bands.

Table 6-1 Possible phosphorylated sites on RhoBTB1 (PhosphoSite Plus database)

Amino acid	Sequence	Conserved in multiple species*	Mutation
S69	CQEVLER**S**RDVVD	**CQEVLERSRDVVD**	S69A
T398	RMGPM**T**VVRMDA	RMGPM**T**VVRM**D**A	T398A
S480	KECL**S**KGTFSDV	**KECL**S**K**GT**F**S**DV**	S480A
T483	KECLSKG**T**FSDV	**KECL**S**K**GT**F**S**DV**	T483A
S485	KECLSKGTF**S**DV	**KECL**S**K**GT**F**S**DV**	S485A

*bold: conversed residues. Homo sapiens, Pan troglodytes, Macaca mulatta, Lupus familis, Mus musculus, Rattus norvegicus, Ornithorhyncus anatinus, Gallus gallus, Xenopus laevis, Brachydanio rerio.

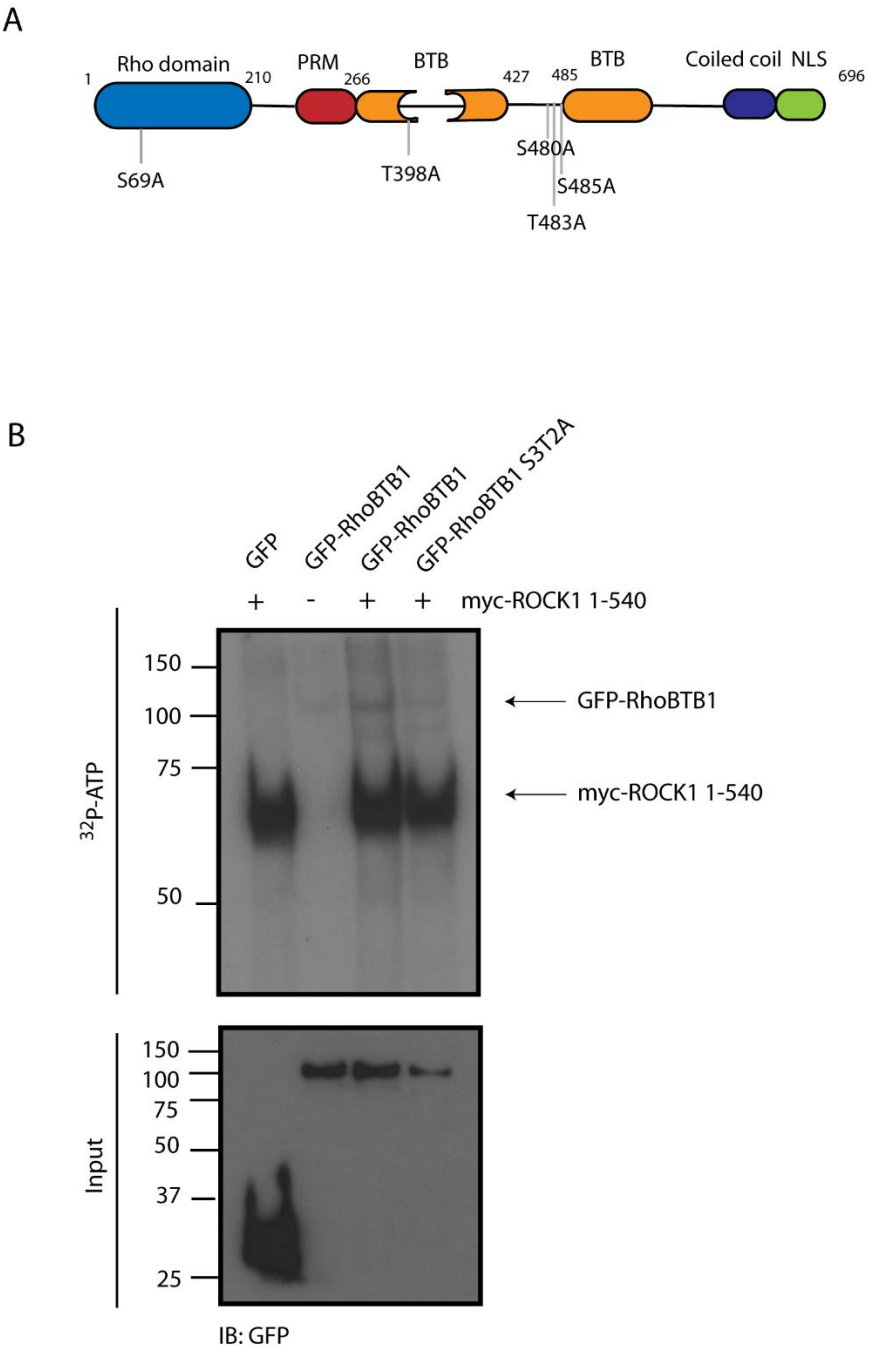

Figure 6.14 - Mutation of possible phosphorylation sites does not prevent phosphorylation of RhoBTB1

A) Mutation of 5 possible phosphorylation sites on RhoBTB1 B) Cos7 cells were transfected with vectors encoding GFP, GFP-RhoBTB1, GFP-RhoBTB1 S3T2A or myc-ROCK1 1-540. After 24 hours, cells were lysed and incubated with either GFP-binding protein coupled to agarose (GFP-trap®) or anti-myc-agarose beads. Immunoprecitated lysates were combined as indicated (GFP and myc-ROCK1 1-540, GFP-RhoBTB1 alone, GFP-RhoBTB1 and myc-ROCK1 1-540, and GFP-RhoBTB1 S3T2A and myc-ROCK1 1-540). Samples were incubated in a kinase buffer containing ^{32}P-ATP for 30 minutes and then resolved in a 4-12% SDS polyacrylamide gel. Bands

show the phosphorylated proteins. Results are representative of three independent experiments.

The role of RhoBTB1 phosphorylation is unknown. Phosphorylation can affect different aspects of a protein including activity, stability, conformation and localisation which in turn could influence protein-protein interactions (Nishi et al., 2011). RhoBTB1 mutants were therefore used to study the possible effects of phosphorylation on RhoBTB1 interaction with other proteins. Several different point mutations were introduced in the 5 phosphorylation sites on RhoBTB1 (Figure 6.14A).

Because RhoBTB1 interacts with RhoA through its Rho domain (Chapter 5), the serine 69 (S69) localised in the Rho domain (Figure 6.14A) was mutated to an alanine and this mutant was used in a co-immunoprecipitation assay with myc-RhoBTB1 and GFP-RhoA-N19. RhoA-N19 interacted with both RhoBTB1 and RhoBTB1 S69A (Figure 6.15), suggesting that the phosphorylation of this residue is not necessary for this interaction. These are only preliminary results and more repeats are necessary.

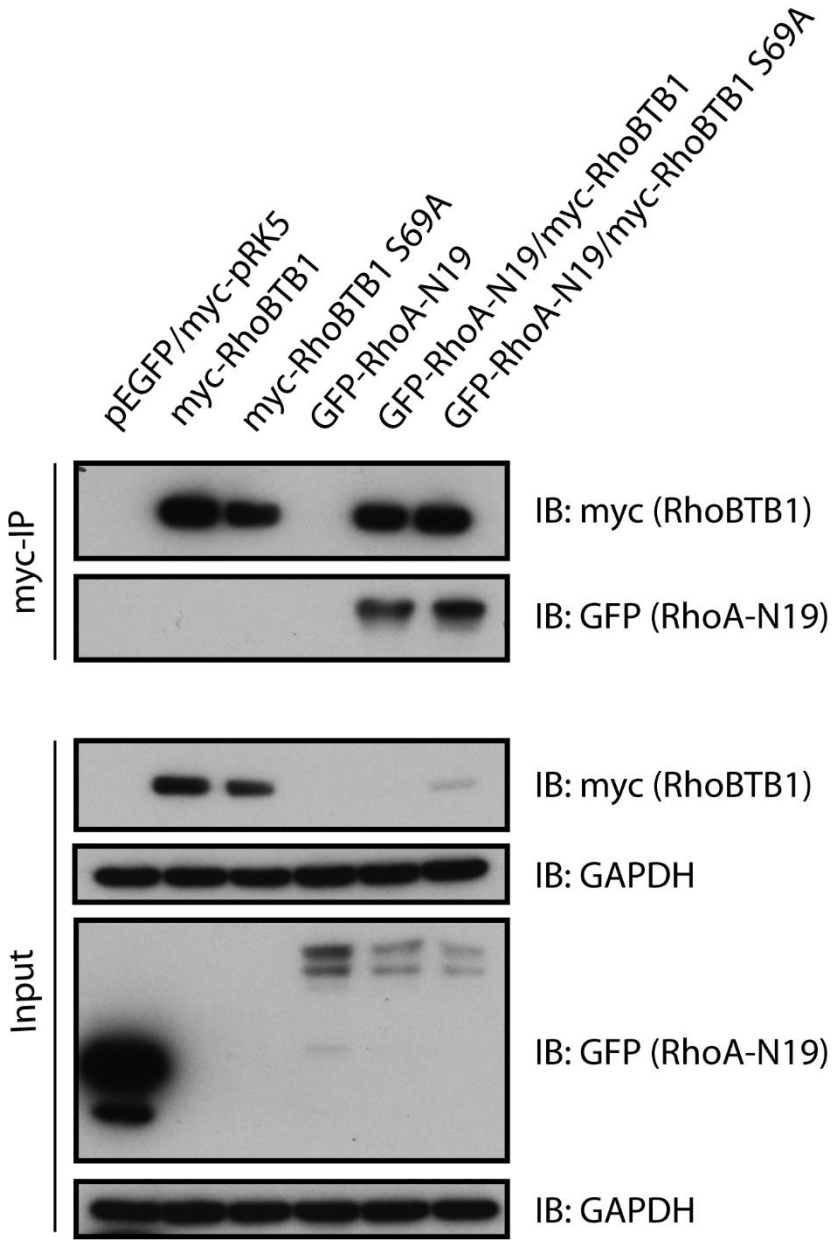

Figure 6.15 - Mutation of serine 69 does not affect RhoBTB1 interaction with RhoA-N19

Cos7 cells were transfected with empty myc-pRK5 and pEGFP or vectors encoding myc-RhoBTB1, myc-RhoBTB1 S69A and GFP-RhoA-N19. After 24 hours, cells were lysed and incubated with anti-myc-agarose beads. Total lysates (input) and immunoprecipitates (myc-IP) were probed to show levels of myc-RhoBTB1, myc-RhoBTB1 S69A and GFP-RhoA N19. The interaction between myc-RhoBTB1 and GFP-RhoA-N19, and myc-RhoBTB1 S69A and GFP-RhoA-N19 is shown in the immunoprecipitates (myc-IP). GAPDH is used as a loading control. Blots are from one experiment.

It is known that cullin3 interacts with RhoBTB1 (Chapter 4) (Berthold et al., 2008a) but not whether phosphorylation regulates this interaction. To study if phosphorylation is involved in the interaction between cullin3 and RhoBTB1, two different approaches were used: single point mutations of phosphorylation sites and multiple point mutations of the 5 possible phosphorylation sites.

Serine 480 (S480) and threonine 483 (T483), localised close to the second BTB domain, were mutated to alanine and these mutants were used in an immunoprecipitation assay. Cullin3 and RhoA-N19 were able to interact with RhoBTB1, RhoBTB1 S480A and RhoBTB1 T483A (Figure 6.16). However, mutation of T483 seemed to increase interaction with cullin3 and mutation of S480 seemed to decrease interaction with RhoA-N19. More experiments are necessary to confirm these results.

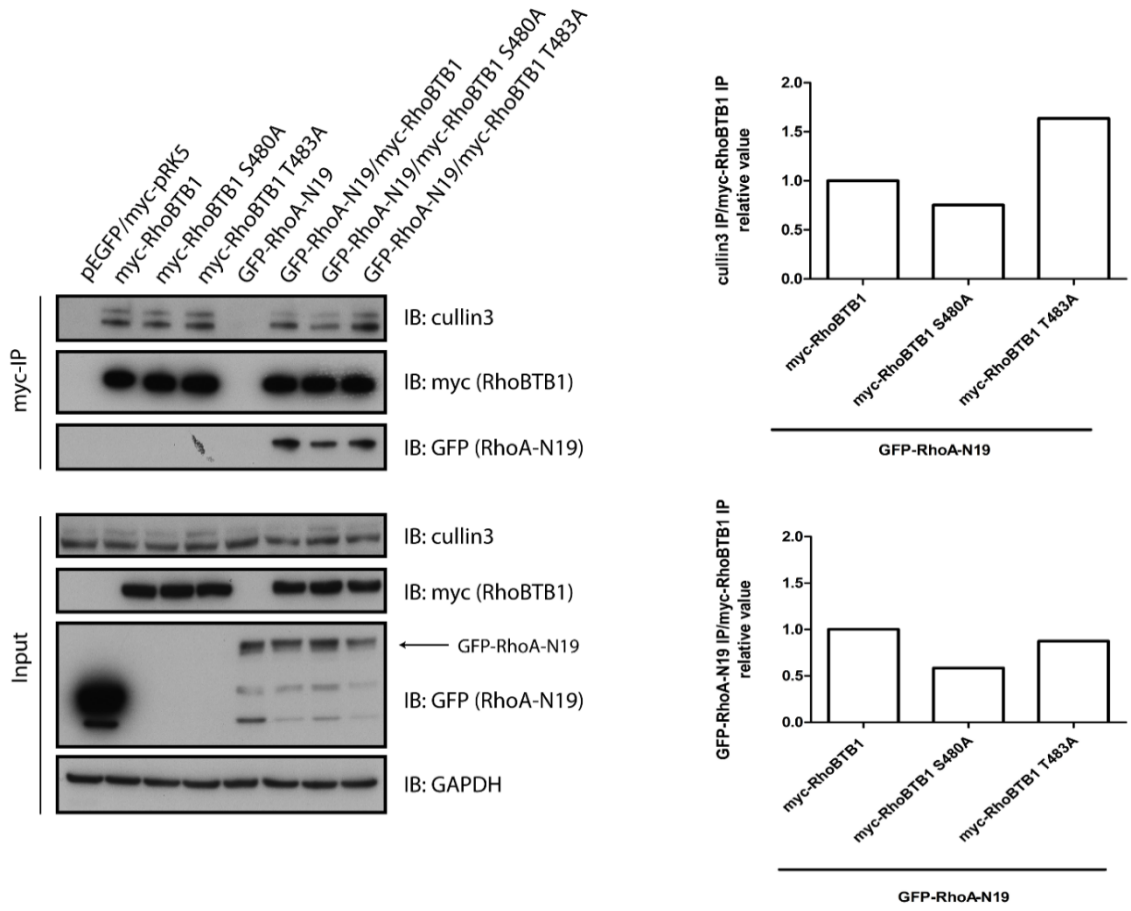

Figure 6.16 - Mutation of serine 480 or threonine 483 affects RhoBTB1 interaction with RhoA-N19 and cullin3

Cos7 cells were transfected with empty myc-pRK5 and pEGFP or vectors encoding myc-RhoBTB1, myc-RhoBTB1 S480A, myc-RhoBTB1 T483A and GFP-RhoA-N19. After 24 hours, cells were lysed and incubated with anti-myc-agarose beads. Total lysates (input) and immunoprecipitates (myc-IP) were probed to show levels of myc-RhoBTB1, myc-RhoBTB1 S480A, myc-RhoBTB1 T483A, GFP-RhoA-N19 and cullin3. The interaction between myc-RhoBTB1 and GFP-RhoA-N19, myc-RhoBTB1 and cullin3, myc-RhoBTB1 S480A and GFP-RhoA-N19, myc-RhoBTB1 S480A and cullin3, myc-RhoBTB1 T483A and GFP-RhoA-N19, and myc-RhoBTB1 T483A and cullin3 is shown in the immunoprecipitates (myc-IP). GAPDH is used as a loading control. Graphs show the quantification of the band density from one experiment. Band density of cullin3 (myc IP) or GFP-RhoA-N19 was normalized by myc-RhoBTB1 (myc IP). All values were normalized to myc-RhoBTB1/GFP-RhoA-N19 condition.

In addition to the single point mutations, interaction of RhoBTB1 and cullin3 was analysed using RhoBTB1 containing multiple point mutations. Multiple mutations could lead to a stronger effect on RhoBTB1 and cullin3 interaction. Mutation of 4 sites together, serine 69 (S69), serine 480 (S480), threonine 483 (T483) and serine 485 (S485) to alanine (RhoBTB1 S3T1A), seemed to increase binding of RhoBTB1 to cullin3 (lane 4) (Figure 6.17). However, when threonine 398 (T398) was also mutated to an alanine (RhoBTB1 S3T2A), the interaction was decreased (lane 5) (Figure 6.17). The single mutation of serine S69 (S69) to alanine also seemed to decrease interaction between RhoBTB1 and cullin3. RhoBTB1 S3T1 and RhoBTB1 S3T2 seems to be less stable than wild-type RhoBTB1 due to reduced levels of these mutants in the input.

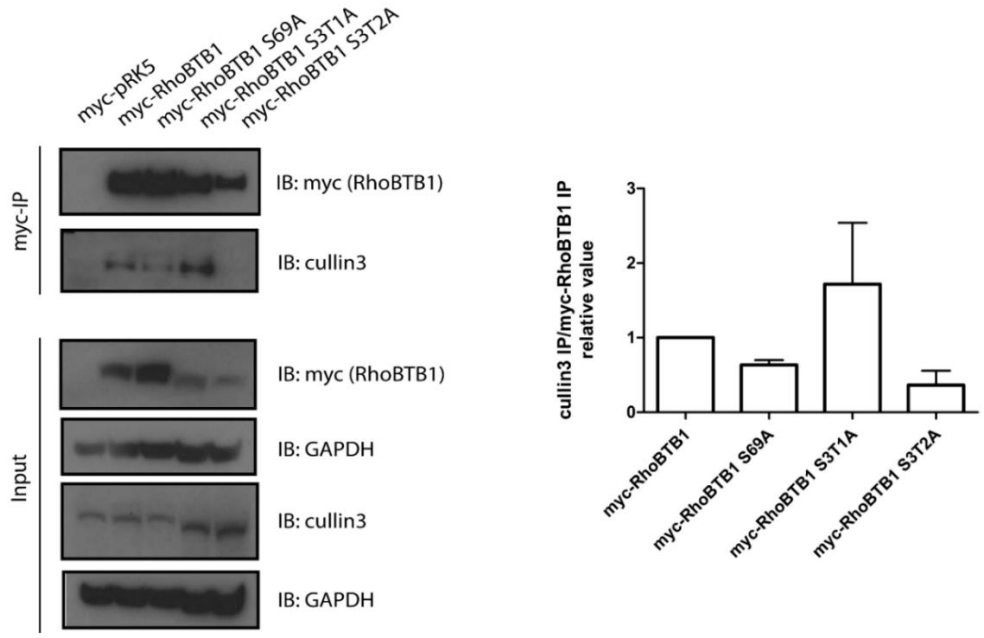

Figure 6.17 - Effect of different RhoBTB1 residues on cullin3 interaction

Cos7 cells were transfected with empty myc-pRK5 or vectors encoding myc-RhoBTB1, myc-RhoBTB1 S69A, myc-RhoBTB1 S3T1A and myc-RhoBTB1 S3T2A. After 24 hours, cells were lysed and incubated with anti-myc-agarose beads. Total lysates (input) and immunoprecipitates (myc-IP) were probed to show levels of myc-RhoBTB1, myc-RhoBTB1 S69A, myc-RhoBTB1 S3T1A, myc-RhoBTB1 S3T2A and cullin3. The interaction between myc-RhoBTB1 and cullin3, myc-RhoBTB1 S69A and cullin3, myc-RhoBTB1 S3T1A and cullin3, and myc-RhoBTB1 S3T2A and cullin3 is shown in the immunoprecipitates (myc-IP). GAPDH is used as a loading control. Graph shows the quantification of the band density from two independent experiments. Band density of cullin3 (myc IP) was normalized by myc-RhoBTB1 (myc IP). All values were normalized to myc-RhoBTB1 condition. Values represent mean ± SD.

6.6 Discussion

Depletion of RhoBTB1 reduced protein levels of ROCK1 and ROCK2, without changing their mRNA levels. This suggests that RhoBTB1 could protect ROCKs from degradation, similar to RhoA (Chapter 5). So far, ROCKs have not been reported to be targets for proteasomal degradation. In contrast to RhoA levels (Chapter 5), inhibition of cullin3 activity did not affect protein levels of ROCK1. RhoBTB1 could be protecting ROCK1 from degradation by other ubiquitin ligases, instead of cullin3-associated ubiquitin ligase complexes. Another possible explanation for the apparent decrease in ROCK expression is that RhoBTB1 affects localisation of ROCKs between soluble and insoluble fractions of cells rather than total levels. It has been shown that serum-starvation and/or stimulation with thrombin cause translocation of a small percentage of ROCKs to the Triton X-100 insoluble fraction (Fujita et al., 1997; Sahai et al., 2001). When RhoBTB1 is depleted, there is a decrease in ROCK levels in the blot (Figure 6.3) which corresponds only to the soluble fraction. To confirm this hypothesis, a fractionation assay should be performed to compare the levels of ROCKs in soluble and insoluble fractions with or without RhoBTB1 depletion.

To investigate if the effect of depleting RhoBTB1 on ROCK1 and ROCK2 levels could be involved in its effect in decreasing MDA-MB-231 cell adhesion to and intercalation into endothelial cells (Borda D'Agua, 2012), ROCK1 and ROCK2 were depleted in MDA-MDA-231 cells. Although double depletion of ROCK1 and ROCK2 led to an increase in cancer cell adhesion to endothelial cells, the levels were similar to only depletion of ROCK1, suggesting that the phenotype observed is a consequence of a decrease in ROCK1 protein levels. This is the opposite of what was observed for RhoBTB1 depletion, and therefore it is unlikely that this RhoBTB1 effect is related to the decrease in ROCK1 levels. It has been shown that depletion of ROCK1 and ROCK2 can affect cell adhesion in different ways. For example, depletion of ROCK1, but not ROCK2, decreases adhesion of keratinocytes to fibronectin (Shi et al., 2013).

The reasons for this difference are still unknown, but the activation of distinct receptors by ROCK1 and ROCK2 is a possible explanation. These results suggest that the phenotype of RhoBTB1 depletion does not involve the decrease in ROCK1 or ROCK2 levels. No difference in cancer cell intercalation into endothelial cells was observed after ROCK1 and/or ROCK2 depletion.

The interaction discovered here between RhoBTB1 and ROCK1 is new and unexpected. Using different vectors encoding deletion mutants for ROCK1, it was possible to map a potential binding region in ROCK1 for RhoBTB1, to a site including the REM domain. This domain is found in some Ras and Rho GEFs (Bos et al., 2007) and it has been shown to be important for binding of RhoA to PKNs, rhotekin and rhophilin (Bishop and Hall, 2000; Blumenstein and Ahmadian, 2004; Flynn et al., 1998). It was also observed that the Rho domain of RhoBTB1 was sufficient for the interaction with ROCK1. To determine whether there is a direct interaction between RhoBTB1 and ROCK1 recombinant protein domains should be used. Since both RhoBTB1 and ROCK1 are high molecular weight proteins (79 kDa and 160 kDa, respectively), it would be necessary to use isolated domains, for example, the Rho domain of RhoBTB1 and ROCK1 375-727 which includes the REM domain and part of the coiled-coil region. ROCK2 should also be tested in the future, since it has a REM domain which is 56% identical to the REM domain of ROCK1. The results in this chapter also show that RhoBTB1 is phosphorylated by ROCK1 *in vitro*. However, the specific sites that were phosphorylated were unknown.

ROCK1 was able to phosphorylate RhoBTB1 1-210. The phosphorylated site in this region could be serine 69 (Table 6-1). Furthermore, mutation of all 5 potential phosphorylation sites reported in PhophoSite Plus website did not prevent phosphorylation of RhoBTB1. Other serine(s) and/or threonine(s) on RhoBTB1 might be phosphorylated by ROCK1. At least eight consensus phosphorylation sequences for ROCK are present in RhoBTB1 (R/KXS/T or R/KXXS/T, where R is arginine, K is

lysine, X is any amino acid, S is serine and T is threonine) (Figure 6.18). Only one of the 5 sites tested here, threonine 483 (T483), is among them. Because RhoBTB1 have many serines and threonines, it would be interesting to use mass spectrometry to map the sites phosphorylated by ROCK1 *in vitro*. In addition to ROCK1, other kinases could phosphorylate RhoBTB1.

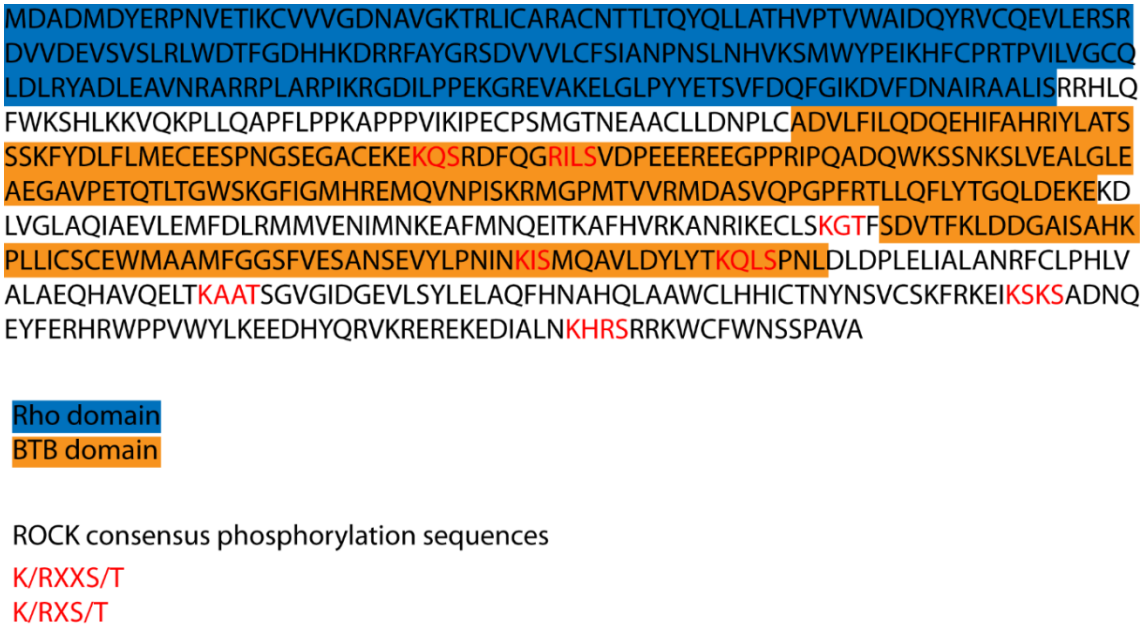

Figure 6.18 - Potential phosphorylation sites for ROCKS
ROCK consensus phosphorylation sequences in RhoBTB1 are shown in red.

Even without knowing which sites are phosphorylated on RhoBTB1 in Cos7 cells, RhoBTB1 phosphosite-mutants were used to study the effects that these sites might have in the interaction of RhoBTB1 with other proteins. I hypothesised that phosphorylation could regulate RhoBTB1 interaction with cullin3 or RhoA. As suggested in Chapter 5, RhoBTB1 could be a BTB adaptor in cullin3 ubiquitin ligase complexes. Adaptor proteins in E3 ubiquitin ligase complexes can undergo post-translational modifications that affect their activity or affinity for the substrate (Chapter 1, section 1.2.2). Phosphorylation could play an important role in regulating binding of RhoBTB1 to cullin3. Indeed, mutation of some potential phosphorylation sites seemed to affect RhoBTB1 and cullin3 interaction. Mutation of serine 69 to alanine led to a

decrease while mutation of threonine 483 led to an increase in RhoBTB1 association with cullin3. Serine 69 is located in the Rho domain of RhoBTB1 and its mutation could perhaps stabilise an inactive conformation in which the Rho domain of RhoBTB1 interacts with the first BTB domain (Figure 6.19) (Berthold et al., 2008a).

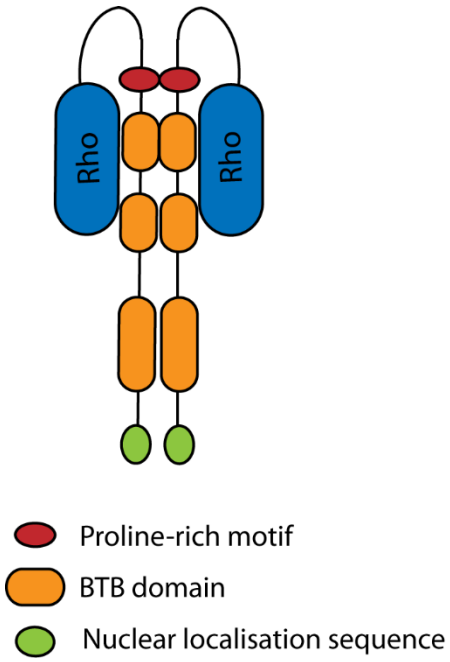

Figure 6.19 - Model of RhoBTB1 inactive conformation
Rho domain of RhoBTB1 interacts with the first BTB domain, keeping RhoBTB1 in an inactive conformation (adapted from Berthold et al. (2008a)).

Threonine 483 is located close to the second BTB domain (Figure 6.13A). Mutation of this site could affect binding of cullin3 and RhoBTB1 since it seems that the second BTB domain is also involved in this interaction (Chapter 4). In addition, mutation of serine 69, serine 480, threonine 483 and serine 485 altogether led to an increase in RhoBTB1 and cullin3 co-immunoprecipitation. However, when threonine 398 was also mutated, the association decreased more than two fold. This suggests that threonine 398 is important for RhoBTB1 and cullin3 interaction. An additional experiment with only threonine 398 mutated in RhoBTB1 is necessary to confirm this hypothesis. Although these results are interesting, more repetitions are necessary to confirm them,

since some experiments were performed only once. RhoA-N19 interaction with RhoBTB1 was also affected by mutation of serine 480. Because this site is close to the second BTB domain and RhoA-N19 interacts with the Rho domain of RhoBTB1 (Chapter 5), it is possible that this mutation leads to a change in conformational in RhoBTB1, affecting interaction with RhoA. However, more repeats are necessary to confirm this.

These results show that RhoBTB1 can be phosphorylated by ROCK1 and probably by other kinases as well. Phosphorylation of RhoBTB1 could be a way of regulating its interaction with other proteins. Phosphorylation could also be involved in RhoBTB1 localisation and degradation which could affect the activity and expression of other proteins and thus it would be interesting to investigate the localisation of mutants tested in this chapter.

7 Concluding remarks

7.1 RhoBTB1 and potential functions in cancer

RhoBTB1 is an atypical Rho GTPase which does not have any known function. Initially, *RhoBTB1* was considered a candidate tumour suppressor gene because *RhoBTB2* was identified as homozygously deleted in breast cancer (Hamaguchi et al., 2002). RhoBTB1 has been shown to be downregulated in some cancers such as head and neck, breast and kidney cancers, but it has also been reported to be upregulated in some cancer cell lines (Beder et al., 2006; Berthold et al., 2008b; Ramos et al., 2002).

Since cancer is among the leading causes of morbidity and mortality in the world, causing more than 8 million deaths in 2012 (World Health Organization – WHO), it is important to investigate how putative tumour suppressors such as RhoBTB1 contribute to cancer progression. Metastasis is one of the main reasons for the aggressive course of this disease. Two main steps during metastasis are invasion and transendothelial migration. During intravasation and extravasation from the blood vessels, cancer cells attach to the endothelium and transmigrate (Reymond et al., 2013). Rho GTPases are known to be involved in this process (Ridley, 2015). It was found that RhoBTB1 depletion affected adhesion and intercalation of MDA-MB-231 and PC3 cells to endothelial cells *in vitro* (Borda D'Agua, 2012). This suggested that RhoBTB1 might promote cancer cell metastasis, having a role in the extravasation of cancer cells from the blood vessels. However, this phenotype in MDA-MB-231 and PC3 cells was not observed here in Cal51 cells. This could mean that the effects of RhoBTB1 are cell line specific or that it is necessary to inhibit RhoBTB1 above a certain threshold to observe effects on cell adhesion and intercalation. More experiments are necessary with a larger panel of cell lines to determine if a threshold knockdown of RhoBTB1 is important to obtain the depletion phenotype observed by Borda D'Agua (2012). An antibody that detects endogenous levels of RhoBTB1 would be very useful for this

purpose. In addition, generation of stable cell lines that do not express RhoBTB1 using CRISPR/Cas9 approaches would be useful to avoid variations in siRNA transfection (Ran et al., 2013).

The changes in cancer cell morphology after RhoBTB1 depletion in a 3D Matrigel matrix assay presented here indicate that RhoBTB1 might have a role in cancer progression. RhoBTB1 depletion in MDA-MB-231 and PC3 cells leads to cell elongation which indicates that RhoBTB1 promotes cell rounding. RhoA depletion in MDA-MB-231 cells also led to cell elongation with a consequent increase in cell invasion (Vega et al., 2011). If this is true for other types of tumours, the fact that RhoBTB1 might be involved in cell rounding could also mean that RhoBTB1 promotes a decrease in cancer cell invasion. It would be interesting in the future to test the role of RhoBTB1 in invasion assays into different matrices (e.g. collagen I and Matrigel) and study the effects of RhoBTB1 depletion in an *in vivo* model such as experimental metastasis in mice or human-mouse xenograft models (Khanna and Hunter, 2005), using a panel of cancer cell lines. This would give clues of how much RhoBTB1 is involved in this process.

7.2 RhoBTB1-interacting partners and Rho function

Identifying RhoBTB1-interacting proteins could provide clues to its function. Cullin3 is the only protein known to associate with RhoBTB1 and therefore, it has been hypothesized that RhoBTB1 could be involved in targeting proteins for degradation (Berthold et al., 2008b). It is still unclear whether RhoBTB1 is an adaptor protein in cullin3 ubiquitin ligase complexes that presents its binding proteins for ubiquitination. However, results presented here and by Borda D'Agua (2012) suggest that RhoBTB1 might have a protective role towards RhoA, inhibiting its degradation. There are other similar cases where the interaction between two proteins protects one of them from

degradation. For example, RhoA binding to RhoGDIs protects it from proteasomal degradation (Boulter and Garcia-Mata, 2010).

Initial results show that RhoBTB1 is able to interact preferentially with a dominant negative RhoA mutant, possibly through its Rho domain region. In addition, RhoBTB1 depletion leads to a decrease in total RhoA protein levels after treatment with cycloheximide. Preliminary data suggest that RhoBTB1 might compete with BACURD1 for RhoA-N19 binding. Altogether, these results suggest a potential role for RhoBTB1 as protector of RhoA degradation (Figure 7.1). This hypothesis needs to be confirmed using additional experiments. For example, it would be interesting to confirm preferential interaction of RhoBTB1 with GDP-RhoA rather than GTP-RhoA, using recombinant RhoA, and to solve the crystal structure of Rho domain of RhoBTB1. An *in vitro* ubiquitination assay would be useful to either test competition between RhoBTB1 and BACURD or ubiquitination of RhoA in the presence of RhoBTB1 (Choo and Zhang, 2009). RhoBTB1 could still bring GDP-RhoA to the cullin3 ubiquitin ligase complex, but promote other forms of ubiquitination (Figure 1.10) which do not lead to degradation. This would be possible to observe by changes in migration of RhoA in western blots or by using mass spectrometry (Kaiser and Wohlschlegel, 2005).

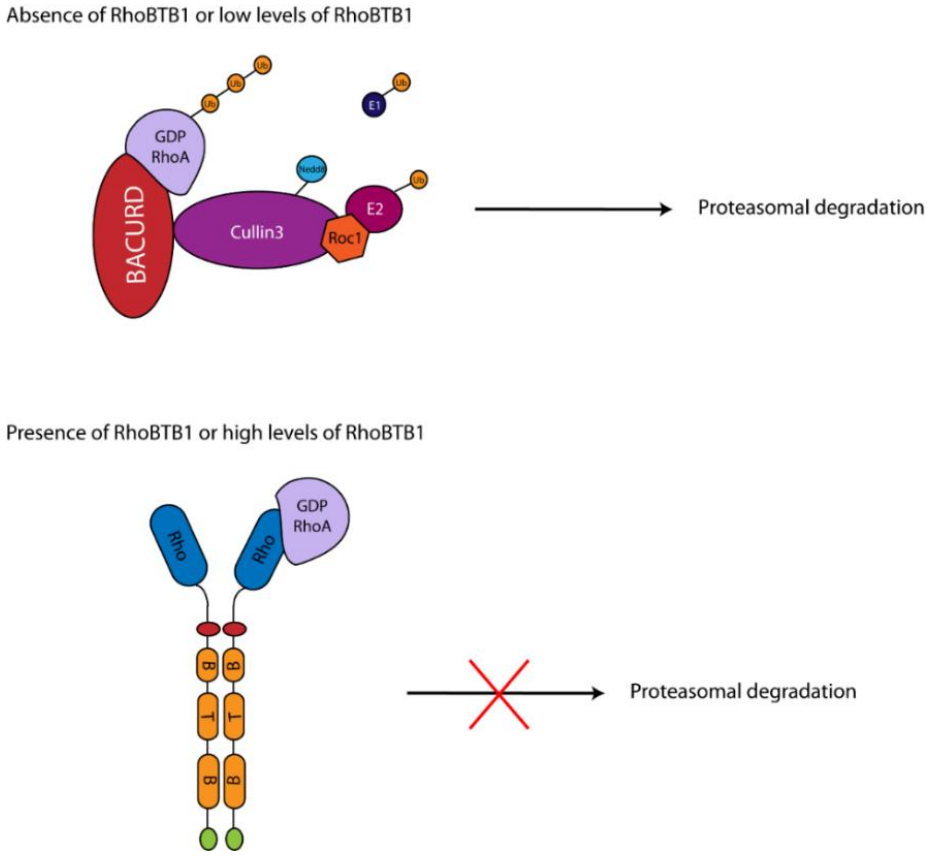

Figure 7.1 - RhoBTB1 and RhoA model of interaction

In the absence or low levels of RhoBTB1, BACURD binds preferentially to GDP-RhoA and brings it to be ubiquitinated by the cullin3 ubiquitin ligase complex. Polyubiquitination (K48) of RhoA leads to proteasomal degradation. In the presence or high levels of RhoBTB1, GDP-RhoA binds preferentially to RhoBTB1 and it is protected from polyubiquination (K48) which targets protein to proteasomal degradation.

RhoBTB1 is reported here for the first time to interact with ROCK1 and to be phosphorylated by this kinase. It would be interesting to test if ROCK2 could also phosphorylate RhoBTB1, since Rnd3 is only phosphorylated by ROCK1 (Riento et al., 2005). The relevance of RhoBTB1 phosphorylation is still unclear, but it could affect the interaction of RhoBTB1 with other proteins (e.g. cullin3 and RhoA). This could occur directly, through changes in RhoBTB1 conformation which would increase or decrease its interaction with other proteins; or indirectly, through changes in RhoBTB1 localisation which would bring the proteins close together. The specific site(s) on RhoBTB1 which is phosphorylated by ROCK1 is still unknown. It is possible that

RhoBTB1 is phosphorylated by other kinases, since there is only one possible phosphorylated site from the five obtained from PhosphoSite Plus database that matches the consensus for ROCKs. Preliminary data suggest that RhoBTB1 could also affect ROCK1/2 degradation. However, it does not seem that this involves cullin3 ubiquitin ligase complexes. Proteasomal degradation of ROCKs has never been described before, and thus it would be interesting to test other ubiquitin ligases in future experiments to identify ROCK1/2-specific ligases such as using siRNA screens.

In summary, the data presented in this thesis show new and unexpected protein-protein interactions involving RhoBTB1, and suggest a role in cancer cell invasion. To confirm these interactions and identify new ones, an unbiased proteomic screen using different domains of RhoBTB1 should be performed. The presence of several clearly distinct domains in RhoBTB1 is an indicator that this protein could be involved in different cellular processes to classic Rho GTPases, as well as have overlapping functions through its interactions with RhoA and ROCK1.

8 References

Abo, A., Pick, E., Hall, A., Totty, N., Teahan, C.G., and Segal, A.W. (1991). Activation of the NADPH oxidase involves the small GTP-binding protein p21rac1. Nature *353*, 668-670.

Adamson, P., Paterson, H.F., and Hall, A. (1992). Intracellular localization of the P21rho proteins. The Journal of Cell Biology *119*, 617-627.

Alan, J.K., Berzat, A.C., Dewar, B.J., Graves, L.M., and Cox, A.D. (2010). Regulation of the Rho family small GTPase Wrch-1/RhoU by C-terminal tyrosine phosphorylation requires Src. Mol Cell Biol *30*, 4324-4338.

Alan, J.K., and Lundquist, E.A. (2013). Mutationally activated Rho GTPases in cancer. Small GTPases *4*, 159-163.

Amano, M., Chihara, K., Kimura, K., Fukata, Y., Nakamura, N., Matsuura, Y., and Kaibuchi, K. (1997). Formation of Actin Stress Fibers and Focal Adhesions Enhanced by Rho-Kinase. Science *275*, 1308-1311.

Amano, M., Chihara, K., Nakamura, N., Kaneko, T., Matsuura, Y., and Kaibuchi, K. (1999). The COOH Terminus of Rho-kinase Negatively Regulates Rho-kinase Activity. Journal of Biological Chemistry *274*, 32418-32424.

Amano, M., Ito, M., Kimura, K., Fukata, Y., Chihara, K., Nakano, T., Matsuura, Y., and Kaibuchi, K. (1996a). Phosphorylation and Activation of Myosin by Rho-associated Kinase (Rho-kinase). Journal of Biological Chemistry *271*, 20246-20249.

Amano, M., Mukai, H., Ono, Y., Chihara, K., Matsui, T., Hamajima, Y., Okawa, K., Iwamatsu, A., and Kaibuchi, K. (1996b). Identification of a Putative Target for Rho as the Serine-Threonine Kinase Protein Kinase N. Science *271*, 648-650.

Amano, M., Nakayama, M., and Kaibuchi, K. (2010). Rho-Kinase/ROCK: A Key Regulator of the Cytoskeleton and Cell Polarity. Cytoskeleton (Hoboken, Nj) *67*, 545-554.

Ananthakrishnan, R., and Ehrlicher, A. (2007). The Forces Behind Cell Movement. International Journal of Biological Sciences *3*, 303-317.

Ardley, H.C., and Robinson, P.A. (2005). E3 ubiquitin ligases. Essays In Biochemistry *41*, 15-30.

Aronheim, A., Broder, Y.C., Cohen, A., Fritsch, A., Belisle, B., and Abo, A. (1998). Chp, a homologue of the GTPase Cdc42Hs, activates the JNK pathway and is implicated in reorganizing the actin cytoskeleton. Current Biology *8*, 1125-1129.

Aspenström, P. (1999). Effectors for the Rho GTPases. Current Opinion in Cell Biology *11*, 95-102.

Aspenstrom, P., Fransson, Å., and Saras, J. (2004). Rho GTPases have diverse effects on the organization of the actin filament system. Biochemical Journal *377*, 327-337.

Aspenstrom, P., Ruusala, A., and Pacholsky, D. (2007). Taking Rho GTPases to the next level: the cellular functions of atypical Rho GTPases. Exp Cell Res *313*, 3673-3679.

Bade, D., Pauleau, A.L., Wendler, A., and Erhardt, S. (2014). The E3 ligase CUL3/RDX controls centromere maintenance by ubiquitylating and stabilizing CENP-A in a CAL1-dependent manner. Dev Cell *28*, 508-519.

Baker, B.M., and Chen, C.S. (2012). Deconstructing the third dimension – how 3D culture microenvironments alter cellular cues. Journal of Cell Science *125*, 3015-3024.

Bamburg, J.R., and Bernstein, B.W. (2010). Roles of ADF/cofilin in actin polymerization and beyond. F1000 Biol Rep *2*, 62.

Beder, L.B., Gunduz, M., Ouchida, M., Gunduz, E., Sakai, A., Fukushima, K., Nagatsuka, H., Ito, S., Honjo, N., Nishizaki, K.*, et al.* (2006). Identification of a candidate tumor suppressor gene RHOBTB1 located at a novel allelic loss region 10q21 in head and neck cancer. J Cancer Res Clin Oncol *132*, 19-27.

Benitah, S.A., Valeron, P.F., van Aelst, L., Marshall, C.J., and Lacal, J.C. (2004). Rho GTPases in human cancer: an unresolved link to upstream and downstream transcriptional regulation. Biochim Biophys Acta *1705*, 121-132.

Berthold, J., Schenkova, K., Ramos, S., Miura, Y., Furukawa, M., Aspenstrom, P., and Rivero, F. (2008a). Characterization of RhoBTB-dependent Cul3 ubiquitin ligase complexes--evidence for an autoregulatory mechanism. Exp Cell Res *314*, 3453-3465.

Berthold, J., Schenkova, K., and Rivero, F. (2008b). Rho GTPases of the RhoBTB subfamily and tumorigenesis. Acta Pharmacol Sin *29*, 285-295.

Berzat, A.C., Buss, J.E., Chenette, E.J., Weinbaum, C.A., Shutes, A., Der, C.J., Minden, A., and Cox, A.D. (2005). Transforming activity of the Rho family GTPase, Wrch-1, a Wnt-regulated Cdc42 homolog, is dependent on a novel carboxyl-terminal palmitoylation motif. J Biol Chem *280*, 33055-33065.

Bijkerk, R., Bruin, R.G.d., Solingen, C.v., Duijs, J.M.G.J., Kobayashi, K., Veer, E.P.v.d., Dijke, P.t., Rabelink, T.J., Goumans, M.J., and Zonneveld, A.J.v. (2012). MicroRNA-155 Functions as a Negative Regulator of RhoA Signaling in TGF-β-induced Endothelial to Mesenchymal Transition. MicroRNA *1*, 2-10.

Bishop, A.L., and Hall, A. (2000). Rho GTPases and their effector proteins. Biochemical Journal *348*, 241-255.

Blumenstein, L., and Ahmadian, M.R. (2004). Models of the Cooperative Mechanism for Rho Effector Recognition: IMPLICATIONS FOR RhoA-MEDIATED EFFECTOR ACTIVATION. Journal of Biological Chemistry *279*, 53419-53426.

Boettner, B., and Van Aelst, L. (2002). The role of Rho GTPases in disease development. Gene *286*, 155-174.

Boh, B.K., Smith, P.G., and Hagen, T. (2011). Neddylation-induced conformational control regulates cullin RING ligase activity in vivo. J Mol Biol *409*, 136-145.

Borda D'Agua, A.B.D. (2012). Role of RhoBTB1 in cancer cell extravasation. In In Randall Division of Cell and Molecular Biophysics (Guy's and St Thomas' School of Biomedical & Health Science) (King's College London).

Bos, J.L., Rehmann, H., and Wittinghofer, A. (2007). GEFs and GAPs: critical elements in the control of small G proteins. Cell *129*, 865-877.

Boulter, E., and Garcia-Mata, R. (2010). RhoGDI: A rheostat for the Rho switch. Small GTPases *1*, 65-68.

Boulter, E., Garcia-Mata, R., Guilluy, C., Dubash, A., Rossi, G., Brennwald, P.J., and Burridge, K. (2010). Regulation of Rho GTPase crosstalk, degradation and activity by RhoGDI1. Nat Cell Biol *12*, 477-483.

Boureux, A., Vignal, E., Faure, S., and Fort, P. (2007). Evolution of the Rho family of ras-like GTPases in eukaryotes. Mol Biol Evol *24*, 203-216.

Braga, V.M. (1999). Small GTPases and regulation of cadherin dependent cell-cell adhesion. Molecular Pathology *52*, 197-202.

Bravo-Cordero, J.J., Oser, M., Chen, X., Eddy, R., Hodgson, L., and Condeelis, J. (2011). A novel spatiotemporal RhoC activation pathway locally regulates cofilin activity at invadopodia. Curr Biol *21*, 635-644.

Breitsprecher, D., and Goode, B.L. (2013). Formins at a glance. J Cell Sci *126*, 1-7.

Brown, M., Roulson, J.A., Hart, C.A., Tawadros, T., and Clarke, N.W. (2014). Arachidonic acid induction of Rho-mediated transendothelial migration in prostate cancer. British Journal of Cancer *110*, 2099-2108.

Cailleau, R., Young, R., Olivé, M., and Reeves, W.J. (1974). Breast Tumor Cell Lines From Pleural Effusions. Journal of the National Cancer Institute *53*, 661-674.

Cain, R.J., d'Agua, B.B., and Ridley, A.J. (2011). Quantification of transendothelial migration using three-dimensional confocal microscopy. Methods Mol Biol *769*, 167-190.

Cain, R.J., Vanhaesebroeck, B., and Ridley, A.J. (2010). The PI3K p110alpha isoform regulates endothelial adherens junctions via Pyk2 and Rac1. J Cell Biol *188*, 863-876.

Campbell, I.D., and Humphries, M.J. (2011). Integrin structure, activation, and interactions. Cold Spring Harb Perspect Biol *3*.

Campellone, K.G., and Welch, M.D. (2010). A nucleator arms race: cellular control of actin assembly. Nat Rev Mol Cell Biol *11*, 237-251.

Canning, P., Cooper, C.D., Krojer, T., Murray, J.W., Pike, A.C., Chaikuad, A., Keates, T., Thangaratnarajah, C., Hojzan, V., Ayinampudi, V.*, et al.* (2013). Structural basis for Cul3 protein assembly with the BTB-Kelch family of E3 ubiquitin ligases. J Biol Chem *288*, 7803-7814.

Carman, C.V. (2009). Mechanisms for transcellular diapedesis: probing and pathfinding by `invadosome-like protrusions'. Journal of Cell Science *122*, 3025-3035.

Chae, H.D., Lee, K.E., Williams, D.A., and Gu, Y. (2008). Cross-talk between RhoH and Rac1 in regulation of actin cytoskeleton and chemotaxis of hematopoietic progenitor cells. Blood *111*, 2597-2605.

Chang, F.K., Sato, N., Kobayashi-Simorowski, N., Yoshihara, T., Meth, J.L., and Hamaguchi, M. (2006). DBC2 is essential for transporting vesicular stomatitis virus glycoprotein. J Mol Biol *364*, 302-308.

Chardin, P. (2006). Function and regulation of Rnd proteins. Nat Rev Mol Cell Biol *7*, 54-62.

Chen, B., Brinkmann, K., Chen, Z., Pak, C.W., Liao, Y., Shi, S., Henry, L., Grishin, N.V., Bogdan, S., and Rosen, M.K. (2014a). The WAVE regulatory complex links diverse receptors to the actin cytoskeleton. Cell *156*, 195-207.

Chen, Q., Chen, X., Zhang, M., Fan, Q., Luo, S., and Cao, X. (2011). miR-137 is frequently down-regulated in gastric cancer and is a negative regulator of Cdc42. Dig Dis Sci *56*, 2009-2016.

Chen, X.J., Squarr, A.J., Stephan, R., Chen, B., Higgins, T.E., Barry, D.J., Martin, M.C., Rosen, M.K., Bogdan, S., and Way, M. (2014b). Ena/VASP proteins cooperate with the WAVE complex to regulate the actin cytoskeleton. Dev Cell *30*, 569-584.

Chen, Y., Yang, Z., Meng, M., Zhao, Y., Dong, N., Yan, H., Liu, L., Ding, M., Peng, H.B., and Shao, F. (2009). Cullin mediates degradation of RhoA through evolutionarily conserved BTB adaptors to control actin cytoskeleton structure and cell movement. Mol Cell *35*, 841-855.

Chen, Z., Borek, D., Padrick, S.B., Gomez, T.S., Metlagel, Z., Ismail, A.M., Umetani, J., Billadeau, D.D., Otwinowski, Z., and Rosen, M.K. (2010). Structure and control of the actin regulatory WAVE complex. Nature *468*, 533-538.

Chen, Z., Sui, J., Zhang, F., and Zhang, C. (2015). Cullin family proteins and tumorigenesis: genetic association and molecular mechanisms. J Cancer *6*, 233-242.

Chenette, E.J., Abo, A., and Der, C.J. (2005). Critical and distinct roles of amino- and carboxyl-terminal sequences in regulation of the biological activity of the Chp atypical Rho GTPase. J Biol Chem *280*, 13784-13792.

Chenette, E.J., Mitin, N.Y., and Der, C.J. (2006). Multiple sequence elements facilitate Chp Rho GTPase subcellular location, membrane association, and transforming activity. Mol Biol Cell *17*, 3108-3121.

Cherfils, J., and Zeghouf, M. (2013). Regulation of small GTPases by GEFs, GAPs, and GDIs. Physiol Rev *93*, 269-309.

Chesarone, M.A., DuPage, A.G., and Goode, B.L. (2010). Unleashing formins to remodel the actin and microtubule cytoskeletons. Nat Rev Mol Cell Biol *11*, 62-74.

Chew, E.H., Poobalasingam, T., Hawkey, C.J., and Hagen, T. (2007). Characterization of cullin-based E3 ubiquitin ligases in intact mammalian cells-evidence for cullin dimerization. Cell Signal *19*, 1071-1080.

Chong, L.D., Traynor-Kaplan, A., Bokoch, G.M., and Schwartz, M.A. (1994). The small GTP-binding protein Rho regulates a phosphatidylinositol 4-phosphate 5-kinase in mammalian cells. Cell *79*, 507-513.

Choo, Y.S., and Zhang, Z. (2009). Detection of protein ubiquitination. J Vis Exp.

Chuang, H.-H., Liang, S.-W., Chang, Z.-F., and Lee, H.-H. (2013). Ser1333 phosphorylation indicates ROCKI activation. Journal of Biomedical Science *20*, 83-83.

Chuang, H.-H., Yang, C.-H., Tsay, Y.-G., Hsu, C.-Y., Tseng, L.-M., Chang, Z.-F., and Lee, H.-H. (2012). ROCKII Ser1366 phosphorylation reflects the activation status. Biochemical Journal *443*, 145-151.

Chuang, Y.-y., Valster, A., Coniglio, S.J., Backer, J.M., and Symons, M. (2007). The atypical Rho family GTPase Wrch-1 regulates focal adhesion formation and cell migration. Journal of Cell Science *120*, 1927-1934.

Citi, S., and Kendrick-Jones, J. (1987). Regulation of non-muscle myosin structure and function. BioEssays *7*, 155-159.

Coleman, M.L., Sahai, E.A., Yeo, M., Bosch, M., Dewar, A., and Olson, M.F. (2001). Membrane blebbing during apoptosis results from caspase-mediated activation of ROCK I. Nat Cell Biol *3*, 339-345.

Colomba, A., and Ridley, A.J. (2014). Analyzing the roles of Rho GTPases in cancer cell migration with a live cell imaging 3D-morphology-based assay. Methods Mol Biol *1120*, 327-337.

Cook, D.R., Rossman, K.L., and Der, C.J. (2014). Rho guanine nucleotide exchange factors: regulators of Rho GTPase activity in development and disease. Oncogene *33*, 4021-4035.

Coso, O.A., Chiariello, M., Yu, J.-C., Teramoto, H., Crespo, P., Xu, N., Miki, T., and Silvio Gutkind, J. (1995). The small GTP-binding proteins Rac1 and Cdc42regulate the activity of the JNK/SAPK signaling pathway. Cell *81*, 1137-1146.

Dallery-Prudhomme, E., Roumier, C., Denis, C., Preudhomme, C., Kerckaert, J.-P., and Galiegue-Zouitina, S. (1997). Genomic Structure and Assignment of

theRhoH/TTFSmall GTPase Gene (ARHH) to 4p13 byin SituHybridization. Genomics *43*, 89-94.

Dart, A.E., Box, G.M., Court, W., Gale, M.E., Brown, J.P., Pinder, S.E., Eccles, S.A., and Wells, C.M. (2015). PAK4 promotes kinase-independent stabilization of RhoU to modulate cell adhesion. J Cell Biol *211*, 863-879.

de la Vega, M., Burrows, J.F., and Johnston, J.A. (2011). Ubiquitination: Added complexity in Ras and Rho family GTPase function. Small GTPases *2*, 192-201.

de Melker, A.A., and Sonnenberg, A. (1999). Integrins: alternative splicing as a mechanism to regulate ligand binding and integrin signaling events. BioEssays *21*, 499-509.

DeGeer, J., and Lamarche-Vane, N. (2013). Rho GTPases in neurodegeneration diseases. Exp Cell Res *319*, 2384-2394.

Delestre, L., Berthon, C., Quesnel, B., Figeac, M., Kerckaert, J.P., Galiegue-Zouitina, S., and Shelley, C.S. (2011). Repression of the RHOH gene by JunD. Biochem J *437*, 75-88.

DerMardirossian, C., and Bokoch, G.M. (2005). GDIs: central regulatory molecules in Rho GTPase activation. Trends Cell Biol *15*, 356-363.

Diekmann, D., Abo, A., Johnston, C., Segal, A., and Hall, A. (1994). Interaction of Rac with p67phox and regulation of phagocytic NADPH oxidase activity. Science *265*, 531-533.

Dominguez, R. (2009). Actin filament nucleation and elongation factors-structure-function relationships. Crit Rev Biochem Mol Biol *44*, 351-366.

Dorn, T., Kuhn, U., Bungartz, G., Stiller, S., Bauer, M., Ellwart, J., Peters, T., Scharffetter-Kochanek, K., Semmrich, M., Laschinger, M*., et al.* (2006). RhoH is important for positive thymocyte selection and T-cell receptor signaling. Blood *109*, 2346-2355.

Dos Remedios, C.G., Chhabra, D., Kekic, M., Dedova, I.V., Tsubakihara, M., Berry, D.A., and Nosworthy, N.J. (2003). Actin Binding Proteins: Regulation of Cytoskeletal Microfilaments. Physiological Reviews *83*, 433-473.

Downes, C.P., Gray, A., and Lucocq, J.M. (2005). Probing phosphoinositide functions in signaling and membrane trafficking. Trends in Cell Biology *15*, 259-268.

Duda, D.M., Borg, L.A., Scott, D.C., Hunt, H.W., Hammel, M., and Schulman, B.A. (2008). Structural insights into NEDD8 activation of cullin-RING ligases: conformational control of conjugation. Cell *134*, 995-1006.

Duda, D.M., Scott, D.C., Calabrese, M.F., Zimmerman, E.S., Zheng, N., and Schulman, B.A. (2011). Structural regulation of cullin-RING ubiquitin ligase complexes. Curr Opin Struct Biol *21*, 257-264.

Eckhardt, B.L., Francis, P.A., Parker, B.S., and Anderson, R.L. (2012). Strategies for the discovery and development of therapies for metastatic breast cancer. Nat Rev Drug Discov *11*, 479-497.

Edwards, D.C., Sanders, L.C., Bokoch, G.M., and Gill, G.N. (1999). Activation of LIM-kinase by Pak1 couples Rac/Cdc42 GTPase signalling to actin cytoskeletal dynamics. Nat Cell Biol *1*, 253-259.

Ellerbroek, S.M., Wennerberg, K., and Burridge, K. (2003). Serine phosphorylation negatively regulates RhoA in vivo. J Biol Chem *278*, 19023-19031.

Elnakish, M.T., Hassanain, H.H., Janssen, P.M., Angelos, M.G., and Khan, M. (2013). Emerging role of oxidative stress in metabolic syndrome and cardiovascular diseases: important role of Rac/NADPH oxidase. J Pathol *231*, 290-300.

Etienne-Manneville, S., and Hall, A. (2001). Integrin-Mediated Activation of Cdc42 Controls Cell Polarity in Migrating Astrocytes through PKCζ. Cell *106*, 489-498.

Etienne-Manneville, S., and Hall, A. (2002). Rho GTPases in cell biology. Nature *420*, 629-635.

Faure, S., and Fort, P. (2015). Atypical RhoV and RhoU GTPases control development of the neural crest. Small GTPases *6*, 174-177.

Feng, D., Nagy, J.A., Dvorak, H.F., and Dvorak, A.M. (2002). Ultrastructural studies define soluble macromolecular, particulate, and cellular transendothelial cell pathways in venules, lymphatic vessels, and tumor-associated microvessels in man and animals. Microsc Res Tech *57*, 289-326.

Fiegen, D., Haeusler, L.C., Blumenstein, L., Herbrand, U., Dvorsky, R., Vetter, I.R., and Ahmadian, M.R. (2004). Alternative splicing of Rac1 generates Rac1b, a self-activating GTPase. J Biol Chem *279*, 4743-4749.

Firat-Karalar, E.N., and Welch, M.D. (2011). New mechanisms and functions of actin nucleation. Curr Opin Cell Biol *23*, 4-13.

Flynn, P., Mellor, H., Palmer, R., Panayotou, G., and Parker, P.J. (1998). Multiple Interactions of PRK1 with RhoA: FUNCTIONAL ASSIGNMENT OF THE HR1 REPEAT MOTIF. Journal of Biological Chemistry *273*, 2698-2705.

Foster, R., Hu, K.Q., Lu, Y., Nolan, K.M., Thissen, J., and Settleman, J. (1996). Identification of a novel human Rho protein with unusual properties: GTPase deficiency and in vivo farnesylation. Molecular and Cellular Biology *16*, 2689-2699.

Freeman, S.N., Ma, Y., and Cress, W.D. (2008). RhoBTB2 (DBC2) is a mitotic E2F1 target gene with a novel role in apoptosis. J Biol Chem *283*, 2353-2362.

Friedl, P., and Wolf, K. (2003). Tumour-cell invasion and migration: diversity and escape mechanisms. Nat Rev Cancer *3*, 362-374.

Fritsch, R., de Krijger, I., Fritsch, K., George, R., Reason, B., Kumar, M.S., Diefenbacher, M., Stamp, G., and Downward, J. (2013). RAS and RHO families of GTPases directly regulate distinct phosphoinositide 3-kinase isoforms. Cell *153*, 1050-1063.

Fritz, G., Kaina, B., and Aktories, K. (1995). The Ras-related Small GTP-binding Protein RhoB Is Immediate-early Inducible by DNA Damaging Treatments. Journal of Biological Chemistry *270*, 25172-25177.

Fueller, F., and Kubatzky, K.F. (2008). The small GTPase RhoH is an atypical regulator of haematopoietic cells. Cell Commun Signal *6*, 6.

Fujisawa, K., Fujita, A., Ishizaki, T., Saito, Y., and Narumiya, S. (1996). Identification of the Rho-binding Domain of p160ROCK, a Rho-associated Coiled-coil Containing Protein Kinase. Journal of Biological Chemistry *271*, 23022-23028.

Fujita, A., Saito, Y., Ishizaki, T., Maekawa, M., Fujisawa, K., Ushikubi, F., and Narumiya, S. (1997). Integrin-dependent translocation of p160ROCK to cytoskeletal complex in thrombin-stimulated human platelets. Biochemical Journal *328*, 769-775.

Furukawa, M., and Xiong, Y. (2005). BTB protein Keap1 targets antioxidant transcription factor Nrf2 for ubiquitination by the Cullin 3-Roc1 ligase. Mol Cell Biol *25*, 162-171.

Gadea, G., and Blangy, A. (2014). Dock-family exchange factors in cell migration and disease. Eur J Cell Biol *93*, 466-477.

Garcia-Mata, R., Boulter, E., and Burridge, K. (2011). The 'invisible hand': regulation of RHO GTPases by RHOGDIs. Nat Rev Mol Cell Biol *12*, 493-504.

Garg, R., Riento, K., Keep, N., Morris, Jonathan D.H., and Ridley, Anne J. (2008). N-terminus-mediated dimerization of ROCK-I is required for RhoE binding and actin reorganization. Biochemical Journal *411*, 407-414.

Genau, H.M., Huber, J., Baschieri, F., Akutsu, M., Dotsch, V., Farhan, H., Rogov, V., and Behrends, C. (2015). CUL3-KBTBD6/KBTBD7 ubiquitin ligase cooperates with GABARAP proteins to spatially restrict TIAM1-RAC1 signaling. Mol Cell *57*, 995-1010.

Genschik, P., Sumara, I., and Lechner, E. (2013). The emerging family of CULLIN3-RING ubiquitin ligases (CRL3s): cellular functions and disease implications. EMBO J *32*, 2307-2320.

Geyer, R., Wee, S., Anderson, S., Yates Iii, J., and Wolf, D.A. (2003). BTB/POZ Domain Proteins Are Putative Substrate Adaptors for Cullin 3 Ubiquitin Ligases. Molecular Cell *12*, 783-790.

Gioanni, J., Le François, D., Zanghellini, E., Mazeau, C., Ettore, F., Lambert, J.C., Schneider, M., and Dutrillaux, B. (1990). Establishment and characterisation of a new tumorigenic cell line with a normal karyotype derived from a human breast adenocarcinoma. British Journal of Cancer *62*, 8-13.

Goley, E.D., and Welch, M.D. (2006). The ARP2/3 complex: an actin nucleator comes of age. Nat Rev Mol Cell Biol *7*, 713-726.

Gomes, E.R., Jani, S., and Gundersen, G.G. (2005). Nuclear movement regulated by Cdc42, MRCK, myosin, and actin flow establishes MTOC polarization in migrating cells. Cell *121*, 451-463.

Gomez del Pulgar, T., Benitah, S.A., Valeron, P.F., Espina, C., and Lacal, J.C. (2005). Rho GTPase expression in tumourigenesis: evidence for a significant link. Bioessays *27*, 602-613.

Gonzalez-Mariscal, L., Contreras, R.G., Bolivar, J.J., Ponce, A., Chavez de Ramirez, B., and M., C. (1990). Role of calcium in tight junction formation between epithelial cells. The American Journal of Physiology *259*, C978-986.

Goto, H., Kosako, H., Tanabe, K., Yanagida, M., Sakurai, M., Amano, M., Kaibuchi, K., and Inagaki, M. (1998). Phosphorylation of Vimentin by Rho-associated Kinase at a Unique Amino-terminal Site That Is Specifically Phosphorylated during Cytokinesis. Journal of Biological Chemistry *273*, 11728-11736.

Grise, F., Sena, S., Bidaud-Meynard, A., Baud, J., Hiriart, J.B., Makki, K., Dugot-Senant, N., Staedel, C., Bioulac-Sage, P., Zucman-Rossi, J.*, et al.* (2012). Rnd3/RhoE Is down-regulated in hepatocellular carcinoma and controls cellular invasion. Hepatology *55*, 1766-1775.

Gu, Y., Chae, H.D., Siefring, J.E., Jasti, A.C., Hildeman, D.A., and Williams, D.A. (2006). RhoH GTPase recruits and activates Zap70 required for T cell receptor signaling and thymocyte development. Nat Immunol *7*, 1182-1190.

Gu, Y., Jasti, A.C., Jansen, M., and Siefring, J.E. (2005). RhoH, a hematopoietic-specific Rho GTPase, regulates proliferation, survival, migration, and engraftment of hematopoietic progenitor cells. Blood *105*, 1467-1475.

Guasch, R.M., Scambler, P., Jones, G.E., and Ridley, A.J. (1998). RhoE Regulates Actin Cytoskeleton Organization and Cell Migration. Molecular and Cellular Biology *18*, 4761-4771.

Guilluy, C., Garcia-Mata, R., and Burridge, K. (2011). Rho protein crosstalk: another social network? Trends Cell Biol *21*, 718-726.

Haglund, K., and Dikic, I. (2005). Ubiquitylation and cell signaling. The EMBO Journal *24*, 3353-3359.

Hall, A. (2012). Rho family GTPases. Biochem Soc Trans *40*, 1378-1382.

Hamaguchi, M., Meth, J.L., von Klitzing, C., Wei, W., Esposito, D., Rodgers, L., Walsh, T., Welcsh, P., King, M.C., and Wigler, M.H. (2002). DBC2, a candidate for a tumor suppressor gene involved in breast cancer. Proc Natl Acad Sci U S A *99*, 13647-13652.

Hanahan, D., and Weinberg, R.A. (2011). Hallmarks of cancer: the next generation. Cell *144*, 646-674.

Hansen, S.H., Zegers, M.M.P., Woodrow, M., Rodriguez-Viciana, P., Chardin, P., Mostov, K.E., and McMahon, M. (2000). Induced Expression of Rnd3 Is Associated with Transformation of Polarized Epithelial Cells by the Raf–MEK–Extracellular Signal-Regulated Kinase Pathway. Molecular and Cellular Biology *20*, 9364-9375.

Hayden, M.S., and Ghosh, S. (2012). NF-kappaB, the first quarter-century: remarkable progress and outstanding questions. Genes Dev *26*, 203-234.

Heasman, S.J., Carlin, L.M., Cox, S., Ng, T., and Ridley, A.J. (2010). Coordinated RhoA signaling at the leading edge and uropod is required for T cell transendothelial migration. J Cell Biol *190*, 553-563.

Heasman, S.J., and Ridley, A.J. (2008). Mammalian Rho GTPases: new insights into their functions from in vivo studies. Nat Rev Mol Cell Biol *9*, 690-701.

Higashida, C., Miyoshi, T., Fujita, A., Oceguera-Yanez, F., Monypenny, J., Andou, Y., Narumiya, S., and Watanabe, N. (2004). Actin Polymerization-Driven Molecular Movement of mDia1 in Living Cells. Science *303*, 2007-2010.

Hill, C.S., Wynne, J., and Treisman, R. (1995). The Rho family GTPases RhoA, Racl , and CDC42Hsregulate transcriptional activation by SRF. Cell *81*, 1159-1170.

Holliday, D.L., and Speirs, V. (2011). Choosing the right cell line for breast cancer research. Breast Cancer Research : BCR *13*, 215-215.

Hooper, S., Marshall, J.F., and Sahai, E. (2006). Tumor Cell Migration in Three Dimensions. *406*, 625-643.

Horiuchi, A., Imai, T., Wang, C., Ohira, S., Feng, Y., Nikaido, T., and Konishi, I. (2003). Up-Regulation of Small GTPases, RhoA and RhoC, Is Associated with Tumor Progression in Ovarian Carcinoma. Laboratory Investigation *83*, 861-870.

Hornbeck, P.V., Zhang, B., Murray, B., Kornhauser, J.M., Latham, V., and Skrzypek, E. (2015). PhosphoSitePlus, 2014: mutations, PTMs and recalibrations. Nucleic Acids Res *43*, D512-520.

Huang, B., Luo, W., Sun, L., Zhang, Q., Jiang, L., Chang, J., Qiu, X., and Wang, E. (2013). MiRNA-125a-3p is a negative regulator of the RhoA-actomyosin pathway in A549 cells. Int J Oncol *42*, 1734-1742.

Huang, M., and Prendergast, G.C. (2006). RhoB in cancer suppression. Histology and Histopathology *21*, 213-218.

Huotari, J., Meyer-Schaller, N., Hubner, M., Stauffer, S., Katheder, N., Horvath, P., Mancini, R., Helenius, A., and Peter, M. (2012). Cullin-3 regulates late endosome maturation. Proc Natl Acad Sci U S A *109*, 823-828.

Ihara, K., Muraguchi, S., Kato, M., Shimizu, T., Shirakawa, M., Kuroda, S., Kaibuchi, K., and Hakoshima, T. (1998). Crystal Structure of Human RhoA in a Dominantly Active Form Complexed with a GTP Analogue. Journal of Biological Chemistry *273*, 9656-9666.

Ishizaki, T., Maekawa, M., Fujisawa, K., Okawa, K., Iwamatsu, A., Fujita, A., Watanabe, N., Saito, Y., Kakizuka, A., Morii, N.*, et al.* (1996). The small GTP-binding protein Rho binds to and activates a 160 kDa Ser/Thr protein kinase homologous to myotonic dystrophy kinase. The EMBO Journal *15*, 1885-1893.

Ishizaki, T., Morishima, Y., Okamoto, M., Furuyashiki, T., Kato, T., and Narumiya, S. (2001). Coordination of microtubules and the actin cytoskeleton by the Rho effector mDia1. Nat Cell Biol *3*, 8-14.

Ishizaki, T., Naito, M., Fujisawa, K., Maekawa, M., Watanabe, N., Saito, Y., and Narumiya, S. (1997). p160ROCK, a Rho-associated coiled-coil forming protein kinase, works downstream of Rho and induces focal adhesions. FEBS Letters *404*, 118-124.

Islam, M., Lin, G., Brenner, J.C., Pan, Q., Merajver, S.D., Hou, Y., Kumar, P., and Teknos, T.N. (2009). RhoC expression and head and neck cancer metastasis. Mol Cancer Res *7*, 1771-1780.

Isogai, T., van der Kammen, R., Leyton-Puig, D., Kedziora, K.M., Jalink, K., and Innocenti, M. (2015). Initiation of lamellipodia and ruffles involves cooperation between mDia1 and the Arp2/3 complex. J Cell Sci *128*, 3796-3810.

Jacobs, M., Hayakawa, K., Swenson, L., Bellon, S., Fleming, M., Taslimi, P., and Doran, J. (2006). The Structure of Dimeric ROCK I Reveals the Mechanism for Ligand Selectivity. Journal of Biological Chemistry *281*, 260-268.

Jacobs, T., and Hall, C. (2005). Rho GAPs — Regulators of Rho GTPases and More (Dordrecht: Springer Netherlands).

Jaffe, A.B., and Hall, A. (2005). RHO GTPASES: Biochemistry and Biology. Annual Review of Cell and Developmental Biology *21*, 247-269.

Jähner, D., and Hunter, T. (1991). The ras-related gene rhoB is an immediate-early gene inducible by v-Fps, epidermal growth factor, and platelet-derived growth factor in rat fibroblasts. Molecular and Cellular Biology *11*, 3682-3690.

Jin, Z., Li, Y., Pitti, R., Lawrence, D., Pham, V.C., Lill, J.R., and Ashkenazi, A. (2009). Cullin3-based polyubiquitination and p62-dependent aggregation of caspase-8 mediate extrinsic apoptosis signaling. Cell *137*, 721-735.

Jordan, P., Brazao, R., Boavida, M.G., Gespach, C., and Chastre, E. (1999). Cloning of a novel Rac1b splice variant with increased expression in colorectal tumors. Oncogene *18*, 6835-6839.

Julian, L., and Olson, M.F. (2014). Rho-associated coiled-coil containing kinases (ROCK). Small GTPases *5*, e29846.

Kaiser, P., and Wohlschlegel, J. (2005). Identification of Ubiquitination Sites and Determination of Ubiquitin-Chain Architectures by Mass Spectrometry. In Methods in Enzymology (Academic Press), pp. 266-277.

Kakiuchi, M., Nishizawa, T., Ueda, H., Gotoh, K., Tanaka, A., Hayashi, A., Yamamoto, S., Tatsuno, K., Katoh, H., Watanabe, Y.*, et al.* (2014). Recurrent gain-of-function mutations of RHOA in diffuse-type gastric carcinoma. Nat Genet *46*, 583-587.

Kale, V.P., Hengst, J.A., Desai, D.H., Amin, S.G., and Yun, J.K. (2015). The regulatory roles of ROCK and MRCK kinases in the plasticity of cancer cell migration. Cancer Letters *361*, 185-196.

Kamai, T., Yamanishi, T., Shirataki, H., Takagi, K., Asami, H., Ito, Y., and Yoshida, K.-I. (2004). Overexpression of RhoA, Rac1, and Cdc42 GTPases Is Associated with Progression in Testicular Cancer. Clinical Cancer Research *10*, 4799-4805.

Kang, R., Wan, J., Arstikaitis, P., Takahashi, H., Huang, K., Bailey, A.O., Thompson, J.X., Roth, A.F., Drisdel, R.C., Mastro, R.*, et al.* (2008). Neural palmitoyl-proteomics reveals dynamic synaptic palmitoylation. Nature *456*, 904-909.

Karlsson, R., Pedersen, E.D., Wang, Z., and Brakebusch, C. (2009). Rho GTPase function in tumorigenesis. Biochim Biophys Acta *1796*, 91-98.

Kawano, Y., Fukata, Y., Oshiro, N., Amano, M., Nakamura, T., Ito, M., Matsumura, F., Inagaki, M., and Kaibuchi, K. (1999). Phosphorylation of Myosin-Binding Subunit (Mbs) of Myosin Phosphatase by Rho-Kinase in Vivo. The Journal of Cell Biology *147*, 1023-1038.

Kay, B.K., Williamson, M.P., and Sudol, M. (2000). The importance of being proline: the interaction of proline-rich motifs in signaling proteins with their cognate domains. The FASEB Journal *14*, 231-241.

Khanna, C., and Hunter, K. (2005). Modeling metastasis in vivo. Carcinogenesis *26*, 513-523.

Khuon, S., Liang, L., Dettman, R.W., Sporn, P.H.S., Wysolmerski, R.B., and Chew, T.-L. (2010). Myosin light chain kinase mediates transcellular intravasation of breast cancer cells through the underlying endothelial cells: a three-dimensional FRET study. Journal of Cell Science *123*, 431-440.

Kim, S.H., Kim, H.J., Kim, S., and Yim, J. (2010). Drosophila Cand1 regulates Cullin3-dependent E3 ligases by affecting the neddylation of Cullin3 and by controlling the stability of Cullin3 and adaptor protein. Dev Biol *346*, 247-257.

Kimura, K., Fukata, Y., Matsuoka, Y., Bennett, V., Matsuura, Y., Okawa, K., Iwamatsu, A., and Kaibuchi, K. (1998). Regulation of the Association of Adducin with Actin Filaments by Rho-associated Kinase (Rho-kinase) and Myosin Phosphatase. Journal of Biological Chemistry *273*, 5542-5548.

Kimura, K., Ito, M., Amano, M., Chihara, K., Fukata, Y., Nakafuku, M., Yamamori, B., Feng, J., Nakano, T., Okawa, K.*, et al.* (1996). Regulation of Myosin Phosphatase by Rho and Rho-Associated Kinase (Rho-Kinase). Science *273*, 245-248.

Komander, D. (2009). The emerging complexity of protein ubiquitination. Biochem Soc Trans *37*, 937-953.

Kong, W., Yang, H., He, L., Zhao, J.J., Coppola, D., Dalton, W.S., and Cheng, J.Q. (2008). MicroRNA-155 is regulated by the transforming growth factor beta/Smad pathway and contributes to epithelial cell plasticity by targeting RhoA. Mol Cell Biol *28*, 6773-6784.

Koochekpour, S., Willard, S.S., Shourideh, M., Ali, S., Liu, C., Azabdaftari, G., Saleem, M., and Attwood, K. (2014). Establishment and Characterization of a Highly Tumorigenic African American Prostate Cancer Cell Line, E006AA-hT. International Journal of Biological Sciences *10*, 834-845.

Kosako, H., Amano, M., Yanagida, M., Tanabe, K., Nishi, Y., Kaibuchi, K., and Inagaki, M. (1997). Phosphorylation of Glial Fibrillary Acidic Protein at the Same Sites by Cleavage Furrow Kinase and Rho-associated Kinase. Journal of Biological Chemistry *272*, 10333-10336.

Kovacic, H.N., Irani, K., and Goldschmidt-Clermont, P.J. (2001). Redox regulation of human Rac1 stability by the proteasome in human aortic endothelial cells. J Biol Chem *276*, 45856-45861.

Krause, M., Dent, E.W., Bear, J.E., Loureiro, J.J., and Gertler, F.B. (2003). Ena/VASP proteins: regulators of the actin cytoskeleton and cell migration. Annu Rev Cell Dev Biol *19*, 541-564.

Krause, M., and Gautreau, A. (2014). Steering cell migration: lamellipodium dynamics and the regulation of directional persistence. Nat Rev Mol Cell Biol *15*, 577-590.

Krebs, A., Rothkegel, M., Klar, M., and Jockusch, B.M. (2001). Characterization of functional domains of mDia1, a link between the small GTPase Rho and the actin cytoskeleton. Journal of Cell Science *114*, 3663-3672.

Kumper, S., Mardakheh, F.K., McCarthy, A., Yeo, M., Stamp, G.W., Paul, A., Worboys, J., Sadok, A., Jorgensen, C., Guichard, S*., et al.* (2016). Rho-associated kinase (ROCK) function is essential for cell cycle progression, senescence and tumorigenesis. Elife *5*.

Kusama, T., Mukai, M., Masaharu, T., Nakamura, H., and Inoue, M. (2006). Inhibition of transendothelial migration and invasion of human breast cancer cells by preventing geranylgeranylation of Rho. International Journal of Oncology *29*, 217-223.

Kwon, T., Kwon, D.Y., Chun, J., Kim, J.H., and Kang, S.S. (2000). Akt Protein Kinase Inhibits Rac1-GTP Binding through Phosphorylation at Serine 71 of Rac1. Journal of Biological Chemistry *275*, 423-428.

Ladwein, M., and Rottner, K. (2008). On the Rho'd: the regulation of membrane protrusions by Rho-GTPases. FEBS Lett *582*, 2066-2074.

Lang, P., Gesbert, F., Delespine-Carmagnat, M., Stancou, R., Pouchelet, M., and Bertoglio, J. (1996). Protein kinase A phosphorylation of RhoA mediates the morphological and functional effects of cyclic AMP in cytotoxic lymphocytes. The EMBO Journal *15*, 510-519.

Laurin, M., and Cote, J.F. (2014). Insights into the biological functions of Dock family guanine nucleotide exchange factors. Genes Dev *28*, 533-547.

Lee, H.-H., and Chang, Z.-F. (2008). Regulation of RhoA-dependent ROCKII activation by Shp2. The Journal of Cell Biology *181*, 999-1012.

Lee, H.-H., Tien, S.-C., Jou, T.-S., Chang, Y.-C., Jhong, J.-G., and Chang, Z.-F. (2010). Src-dependent phosphorylation of ROCK participates in regulation of focal adhesion dynamics. Journal of Cell Science *123*, 3368-3377.

Lee, S.H., and Dominguez, R. (2010). Regulation of Actin Cytoskeleton Dynamics in Cells. Molecules and cells *29*, 311-325.

Leitner, A., Walzthoeni, T., Kahraman, A., Herzog, F., Rinner, O., Beck, M., and Aebersold, R. (2010). Probing Native Protein Structures by Chemical Cross-linking, Mass Spectrometry, and Bioinformatics. Molecular & Cellular Proteomics : MCP *9*, 1634-1649.

Leung, T., Chen, X.Q., Manser, E., and Lim, L. (1996). The p160 RhoA-binding kinase ROK alpha is a member of a kinase family and is involved in the reorganization of the cytoskeleton. Molecular and Cellular Biology *16*, 5313-5327.

Leung, T., Manser, E., Tan, L., and Lim, L. (1995). A Novel Serine/Threonine Kinase Binding the Ras-related RhoA GTPase Which Translocates the Kinase to Peripheral Membranes. Journal of Biological Chemistry *270*, 29051-29054.

Li, K., Lu, Y., Liang, J., Luo, G., Ren, G., Wang, X., and Fan, D. (2009). RhoE enhances multidrug resistance of gastric cancer cells by suppressing Bax. Biochem Biophys Res Commun *379*, 212-216.

Li, X., Bu, X., Lu, B., Avraham, H., Flavell, R.A., and Lim, B. (2002). The Hematopoiesis-Specific GTP-Binding Protein RhoH Is GTPase Deficient and Modulates Activities of Other Rho GTPases by an Inhibitory Function. Molecular and Cellular Biology *22*, 1158-1171.

Liu, M., Bi, F., Zhou, X., and Zheng, Y. (2012). Rho GTPase regulation by miRNAs and covalent modifications. Trends Cell Biol *22*, 365-373.

Liu, M., Lang, N., Chen, X., Tang, Q., Liu, S., Huang, J., Zheng, Y., and Bi, F. (2011a). miR-185 targets RhoA and Cdc42 expression and inhibits the proliferation potential of human colorectal cells. Cancer Lett *301*, 151-160.

Liu, M., Tang, Q., Qiu, M., Lang, N., Li, M., Zheng, Y., and Bi, F. (2011b). miR-21 targets the tumor suppressor RhoB and regulates proliferation, invasion and apoptosis in colorectal cancer cells. FEBS Lett *585*, 2998-3005.

Lord, S.J., Rajotte, R.V., Korbutt, G.S., and Bleackley, R.C. (2003). Granzyme B: a natural born killer. Immunological Reviews *193*, 31-38.

Lowery, D.M., Clauser, K.R., Hjerrild, M., Lim, D., Alexander, J., Kishi, K., Ong, S.-E., Gammeltoft, S., Carr, S.A., and Yaffe, M.B. (2007). Proteomic screen defines the Polo-box domain interactome and identifies Rock2 as a Plk1 substrate. The EMBO Journal *26*, 2262-2273.

Lu, A., and Pfeffer, S.R. (2013). Golgi-associated RhoBTB3 targets cyclin E for ubiquitylation and promotes cell cycle progression. J Cell Biol *203*, 233-250.

Luxton, G.W., and Gundersen, G.G. (2011). Orientation and function of the nuclear-centrosomal axis during cell migration. Curr Opin Cell Biol *23*, 579-588.

Lyapina, S., Cope, G., Shevchenko, A., Serino, G., Tsuge, T., Zhou, C., Wolf, D.A., Wei, N., Shevchenko, A., and Deshaies, R.J. (2001). Promotion of NEDD8-CUL1 Conjugate Cleavage by COP9 Signalosome. Science *292*, 1382-1385.

Lynch, E.A., Stall, J., Schmidt, G., Chavrier, P., and D'Souza-Schorey, C. (2006). Proteasome-mediated degradation of Rac1-GTP during epithelial cell scattering. Mol Biol Cell *17*, 2236-2242.

Madaule, P., and Axel, R. (1985). A novel ras-related gene family. Cell *41*, 31-40.

Madaule, P., Eda, M., Watanabe, N., Fujisawa, K., Matsuoka, T., Bito, H., Ishizaki, T., and Narumiya, S. (1998). Role of citron kinase as a target of the small GTPase Rho in cytokinesis. Nature *394*, 491-494.

Madaule, P., Furuyashiki, T., Reid, T., Ishizaki, T., Watanabe, G., Morii, N., and Narumiya, S. (1995). A novel partner for the GTP-bound forms of rho and rac. FEBS Letters *377*, 243-248.

Madigan, J.P., Bodemann, B.O., Brady, D.C., Dewar, B.J., Keller, P.J., Leitges, M., Philips, M.R., Ridley, A.J., Der, C.J., and Cox, A.D. (2009). Regulation of Rnd3 localization and function by protein kinase C alpha-mediated phosphorylation. Biochem J *424*, 153-161.

Maekawa, M., Ishizaki, T., Boku, S., Watanabe, N., Fujita, A., Iwamatsu, A., Obinata, T., Ohashi, K., Mizuno, K., and Narumiya, S. (1999). Signaling from Rho to the Actin Cytoskeleton Through Protein Kinases ROCK and LIM-kinase. Science *285*, 895-898.

Maesaki, R., Ihara, K., Shimizu, T., Kuroda, S., Kaibuchi, K., and Hakoshima, T. (1999). The Structural Basis of Rho Effector Recognition Revealed by the Crystal Structure of Human RhoA Complexed with the Effector Domain of PKN/PRK1. Molecular Cell *4*, 793-803.

Mamdouh, Z., Mikhailov, A., and Muller, W.A. (2009). Transcellular migration of leukocytes is mediated by the endothelial lateral border recycling compartment. J Exp Med *206*, 2795-2808.

Mammoto, A., Huang, S., Moore, K., Oh, P., and Ingber, D.E. (2004). Role of RhoA, mDia, and ROCK in cell shape-dependent control of the Skp2-p27kip1 pathway and the G1/S transition. J Biol Chem *279*, 26323-26330.

Marinissen, M.J., Chiariello, M., and Gutkind, J.S. (2001). Regulation of gene expression by the small GTPase Rho through the ERK6 (p38γ) MAP kinase pathway. Genes & Development *15*, 535-553.

Marinissen, M.J., Chiariello, M., Tanos, T., Bernard, O., Narumiya, S., and Gutkind, J.S. (2004). The Small GTP-Binding Protein RhoA Regulates c-Jun by a ROCK-JNK Signaling Axis. Molecular Cell *14*, 29-41.

Matsui, T., Amano, M., Yamamoto, T., Chihara, K., Nakafuku, M., Ito, M., Nakano, T., Okawa, K., Iwamatsu, A., and Kaibuchi, K. (1996). Rho-associated kinase, a novel serine/threonine kinase, as a putative target for small GTP binding protein Rho. The EMBO Journal *15*, 2208-2216.

Matthys, A., Van Craenenbroeck, K., Lintermans, B., Haegeman, G., and Vanhoenacker, P. (2012). RhoBTB3 interacts with the 5-HT7a receptor and inhibits its proteasomal degradation. Cell Signal *24*, 1053-1063.

Mazieres, J., Antonia, T., Daste, G., Muro-Cacho, C., Berchery, D., Tillement, V., Pradines, A., Sebti, S., and Favre, G. (2004). Loss of RhoB Expression in Human Lung Cancer Progression. Clinical Cancer Research *10*, 2742-2750.

McKinnon, C.M., Lygoe, K.A., Skelton, L., Mitter, R., and Mellor, H. (2008). The atypical Rho GTPase RhoBTB2 is required for expression of the chemokine CXCL14 in normal and cancerous epithelial cells. Oncogene *27*, 6856-6865.

McMahon, M., Thomas, N., Itoh, K., Yamamoto, M., and Hayes, J.D. (2006). Dimerization of substrate adaptors can facilitate cullin-mediated ubiquitylation of proteins by a "tethering" mechanism: a two-site interaction model for the Nrf2-Keap1 complex. J Biol Chem *281*, 24756-24768.

Mego, M., Mani, S.A., and Cristofanilli, M. (2010). Molecular mechanisms of metastasis in breast cancer-clinical applications. Nat Rev Clin Oncol *7*, 693-701.

Mettouchi, A., and Lemichez, E. (2012). Ubiquitylation of active Rac1 by the E3 ubiquitin-ligase HACE1. Small GTPases *3*, 102-106.

Mierke, C.T., Frey, B., Fellner, M., Herrmann, M., and Fabry, B. (2011). Integrin α5β1 facilitates cancer cell invasion through enhanced contractile forces. Journal of Cell Science *124*, 369-383.

Miles, F.L., Pruitt, F.L., van Golen, K.L., and Cooper, C.R. (2008). Stepping out of the flow: capillary extravasation in cancer metastasis. Clin Exp Metastasis *25*, 305-324.

Millan, J., Hewlett, L., Glyn, M., Toomre, D., Clark, P., and Ridley, A.J. (2006). Lymphocyte transcellular migration occurs through recruitment of endothelial ICAM-1 to caveola- and F-actin-rich domains. Nat Cell Biol *8*, 113-123.

Millán, J., and Ridley, Anne J. (2005). Rho GTPases and leucocyte-induced endothelial remodelling. Biochemical Journal *385*, 329-337.

Minden, A., Lin, A., Claret, F.-X., Abo, A., and Karin, M. (1995). Selective activation of the JNK signaling cascadeand c-Jun transcriptional activity by the small GTPases Rac and Cdc42Hs. Cell *81*, 1147-1157.

Moon, S.Y., and Zheng, Y. (2003). Rho GTPase-activating proteins in cell regulation. Trends in Cell Biology *13*, 13-22.

Morgan-Fisher, M., Wewer, U.M., and Yoneda, A. (2013). Regulation of ROCK Activity in Cancer. Journal of Histochemistry and Cytochemistry *61*, 185-198.

Mukai, H. (2003). The Structure and Function of PKN, a Protein Kinase Having a Catalytic Domain Homologous to That of PKC. Journal of Biochemistry *133*, 17-27.

Muller, A.M., Hermanns, M.I., Skrzynski, C., Nesslinger, M., Muller, K.M., and Kirkpatrick, C.J. (2002). Expression of the endothelial markers PECAM-1, vWf, and CD34 in vivo and in vitro. Exp Mol Pathol *72*, 221-229.

Muller, P.A., Vousden, K.H., and Norman, J.C. (2011). p53 and its mutants in tumor cell migration and invasion. J Cell Biol *192*, 209-218.

Narumiya, S. (1996). The Small GTPase Rho: Cellular Functions and Signal Transduction. Journal of Biochemistry *120*, 215-228.

Narumiya, S., Tanji, M., and Ishizaki, T. (2009). Rho signaling, ROCK and mDia1, in transformation, metastasis and invasion. Cancer Metastasis Rev *28*, 65-76.

Nethe, M., Anthony, E.C., Fernandez-Borja, M., Dee, R., Geerts, D., Hensbergen, P.J., Deelder, A.M., Schmidt, G., and Hordijk, P.L. (2010). Focal-adhesion targeting links caveolin-1 to a Rac1-degradation pathway. Journal of Cell Science *123*, 1948-1958.

Nethe, M., and Hordijk, P.L. (2010). The role of ubiquitylation and degradation in RhoGTPase signalling. Journal of Cell Science *123*, 4011-4018.

Neve, R.M., Chin, K., Fridlyand, J., Yeh, J., Baehner, F.L., Fevr, T., Clark, L., Bayani, N., Coppe, J.P., Tong, F.*, et al.* (2006). A collection of breast cancer cell lines for the study of functionally distinct cancer subtypes. Cancer Cell *10*, 515-527.

Nishi, H., Hashimoto, K., and Panchenko, A.R. (2011). Phosphorylation in protein-protein binding: effect on stability and function. Structure (London, England : 1993) *19*, 1807-1815.

Nobes, C.D., and Hall, A. (1995). Rho, Rac, and Cdc42 GTPases regulate the assembly of multimolecular focal complexes associated with actin stress fibers, lamellipodia, and filopodia. Cell *81*, 53-62.

Nobes, C.D., Lauritzen, I., Mattei, M.-G., Paris, S., Hall, A., and Chardin, P. (1998). A New Member of the Rho Family, Rnd1, Promotes Disassembly of Actin Filament Structures and Loss of Cell Adhesion. The Journal of Cell Biology *141*, 187-197.

Ohta, Y., Hartwig, J.H., and Stossel, T.P. (2006). FilGAP, a Rho- and ROCK-regulated GAP for Rac binds filamin A to control actin remodelling. Nat Cell Biol *8*, 803-814.

Oinuma, I., Kawada, K., Tsukagoshi, K., and Negishi, M. (2012). Rnd1 and Rnd3 targeting to lipid raft is required for p190 RhoGAP activation. Mol Biol Cell *23*, 1593-1604.

Oude Weernink, P.A., Schmidt, M., and Jakobs, K.H. (2004). Regulation and cellular roles of phosphoinositide 5-kinases. European Journal of Pharmacology *500*, 87-99.

Pajic, M., Herrmann, D., Vennin, C., Conway, J.R., Chin, V.T., Johnsson, A.K., Welch, H.C., and Timpson, P. (2015). The dynamics of Rho GTPase signaling and implications for targeting cancer and the tumor microenvironment. Small GTPases *6*, 123-133.

Pampaloni, F., Reynaud, E.G., and Stelzer, E.H.K. (2007). The third dimension bridges the gap between cell culture and live tissue. Nat Rev Mol Cell Biol *8*, 839-845.

Pankova, K., Rosel, D., Novotny, M., and Brabek, J. (2010). The molecular mechanisms of transition between mesenchymal and amoeboid invasiveness in tumor cells. Cell Mol Life Sci *67*, 63-71.

Park, S.Y., Lee, J.H., Ha, M., Nam, J.W., and Kim, V.N. (2009). miR-29 miRNAs activate p53 by targeting p85 alpha and CDC42. Nat Struct Mol Biol *16*, 23-29.

Parri, M., and Chiarugi, P. (2010). Rac and Rho GTPases in cancer cell motility control. Cell Communication and Signaling *8*, 1-14.

Pelham, C.J., Ketsawatsomkron, P., Groh, S., Grobe, J.L., de Lange, W.J., Ibeawuchi, S.R., Keen, H.L., Weatherford, E.T., Faraci, F.M., and Sigmund, C.D. (2012). Cullin-3 regulates vascular smooth muscle function and arterial blood pressure via PPARgamma and RhoA/Rho-kinase. Cell Metab *16*, 462-472.

Perez-Torrado, R., Yamada, D., and Defossez, P.A. (2006). Born to bind: the BTB protein-protein interaction domain. Bioessays *28*, 1194-1202.

Perona, R., Montaner, S., Saniger, L., Sánchez-Pérez, I., Bravo, R., and Lacal, J.C. (1997). Activation of the nuclear factor-kappaB by Rho, CDC42, and Rac-1 proteins. Genes & Development *11*, 463-475.

Pertz, O. (2010). Spatio-temporal Rho GTPase signaling – where are we now? Journal of Cell Science *123*, 1841-1850.

Petroski, M.D., and Deshaies, R.J. (2005). Function and regulation of cullin-RING ubiquitin ligases. Nat Rev Mol Cell Biol *6*, 9-20.

Petry, A., Weitnauer, M., and Görlach, A. (2009). Receptor Activation of NADPH Oxidases. Antioxidants & Redox Signaling *13*, 467-487.

Pintard, L., Willems, A., and Peter, M. (2004). Cullin-based ubiquitin ligases: Cul3–BTB complexes join the family. The EMBO Journal *23*, 1681-1687.

Pollard, T.D., and Borisy, G.G. (2003). Cellular Motility Driven by Assembly and Disassembly of Actin Filaments. Cell *112*, 453-465.

Psaila, B., and Lyden, D. (2009). The Metastatic Niche: Adapting the Foreign Soil. Nature reviews Cancer *9*, 285-293.

Qiu, R.-G., Chen, J., Kirn, D., McCormick, F., and Symons, M. (1995a). An essential role for Rac in Ras transformation. Nature *374*, 457-459.

Qiu, R.G., Abo, A., McCormick, F., and Symons, M. (1997). Cdc42 regulates anchorage-independent growth and is necessary for Ras transformation. Molecular and Cellular Biology *17*, 3449-3458.

Qiu, R.G., Chen, J., McCormick, F., and Symons, M. (1995b). A role for Rho in Ras transformation. Proceedings of the National Academy of Sciences of the United States of America *92*, 11781-11785.

Radisky, D.C., Levy, D.D., Littlepage, L.E., Liu, H., Nelson, C.M., Fata, J.E., Leake, D., Godden, E.L., Albertson, D.G., Nieto, M.A.*, et al.* (2005). Rac1b and reactive oxygen species mediate MMP-3-induced EMT and genomic instability. Nature *436*, 123-127.

Raftopoulou, M., and Hall, A. (2004). Cell migration: Rho GTPases lead the way. Developmental Biology *265*, 23-32.

Rajakyla, E.K., and Vartiainen, M.K. (2014). Rho, nuclear actin, and actin-binding proteins in the regulation of transcription and gene expression. Small GTPases *5*, e27539.

Ramos, S., Khademi, F., Somesh, B.P., and Rivero, F. (2002). Genomic organization and expression profile of the small GTPases of the RhoBTB family in human and mouse. Gene *298*, 147-157.

Ran, F.A., Hsu, P.D., Wright, J., Agarwala, V., Scott, D.A., and Zhang, F. (2013). Genome engineering using the CRISPR-Cas9 system. Nat Protocols *8*, 2281-2308.

Ren, X.D., Bokoch, G.M., Traynor-Kaplan, A., Jenkins, G.H., Anderson, R.A., and Schwartz, M.A. (1996). Physical association of the small GTPase Rho with a 68-kDa phosphatidylinositol 4-phosphate 5-kinase in Swiss 3T3 cells. Molecular Biology of the Cell *7*, 435-442.

Reymond, N., d'Agua, B.B., and Ridley, A.J. (2013). Crossing the endothelial barrier during metastasis. Nat Rev Cancer *13*, 858-870.

Reymond, N., Im, J.H., Garg, R., Vega, F.M., Borda d'Agua, B., Riou, P., Cox, S., Valderrama, F., Muschel, R.J., and Ridley, A.J. (2012). Cdc42 promotes transendothelial migration of cancer cells through beta1 integrin. J Cell Biol *199*, 653-668.

Ridley, A.J. (1999). Stress fibres take shape. Nat Cell Biol *1*, E64-E66.

Ridley, A.J. (2001). Rho GTPases and cell migration. Journal of Cell Science *114*, 2713-2722.

Ridley, A.J. (2011). Life at the leading edge. Cell *145*, 1012-1022.

Ridley, A.J. (2013). RhoA, RhoB and RhoC have different roles in cancer cell migration. J Microsc *251*, 242-249.

Ridley, A.J. (2015). Rho GTPase signalling in cell migration. Curr Opin Cell Biol *36*, 103-112.

Ridley, A.J., and Hall, A. (1992). The small GTP-binding protein rho regulates the assembly of focal adhesions and actin stress fibers in response to growth factors. Cell *70*, 389-399.

Ridley, A.J., Paterson, H.F., Johnston, C.L., Diekmann, D., and Hall, A. (1992). The small GTP-binding protein rac regulates growth factor-induced membrane ruffling. Cell *70*, 401-410.

Ridley, A.J., Schwartz, M.A., Burridge, K., Firtel, R.A., Ginsberg, M.H., Borisy, G., Parsons, J.T., and Horwitz, A.R. (2003). Cell Migration: Integrating Signals from Front to Back. Science *302*, 1704-1709.

Riento, K., and Ridley, A.J. (2003). ROCKs: multifunctional kinases in cell behaviour. Nat Rev Mol Cell Biol *4*, 446-456.

Riento, K., Totty, N., Villalonga, P., Garg, R., Guasch, R., and Ridley, A.J. (2005). RhoE function is regulated by ROCK I-mediated phosphorylation. The EMBO Journal *24*, 1170-1180.

Riou, P., Kjaer, S., Garg, R., Purkiss, A., George, R., Cain, R.J., Bineva, G., Reymond, N., McColl, B., Thompson, A.J.*, et al.* (2013). 14-3-3 proteins interact with a hybrid prenyl-phosphorylation motif to inhibit G proteins. Cell *153*, 640-653.

Riou, P., Villalonga, P., and Ridley, A.J. (2010). Rnd proteins: multifunctional regulators of the cytoskeleton and cell cycle progression. Bioessays *32*, 986-992.

Rivero, F., Dislich, H., Glöckner, G., and Noegel, A.A. (2001). The Dictyostelium discoideum family of Rho-related proteins. Nucleic Acids Research *29*, 1068-1079.

Roberts, P.J., Mitin, N., Keller, P.J., Chenette, E.J., Madigan, J.P., Currin, R.O., Cox, A.D., Wilson, O., Kirschmeier, P., and Der, C.J. (2008). Rho Family GTPase

modification and dependence on CAAX motif-signaled posttranslational modification. J Biol Chem *283*, 25150-25163.

Rolli-Derkinderen, M., Sauzeau, V., Boyer, L., Lemichez, E., Baron, C., Henrion, D., Loirand, G., and Pacaud, P. (2005). Phosphorylation of serine 188 protects RhoA from ubiquitin/proteasome-mediated degradation in vascular smooth muscle cells. Circ Res *96*, 1152-1160.

Rossman, K.L., Der, C.J., and Sondek, J. (2005). GEF means go: turning on RHO GTPases with guanine nucleotide-exchange factors. Nat Rev Mol Cell Biol *6*, 167-180.

Ruth, M.C., Xu, Y., Maxwell, I.H., Ahn, N.G., Norris, D.A., and Shellman, Y.G. (2006). RhoC promotes human melanoma invasion in a PI3K/Akt-dependent pathway. J Invest Dermatol *126*, 862-868.

Sabeh, F., Shimizu-Hirota, R., and Weiss, S.J. (2009). Protease-dependent versus -independent cancer cell invasion programs: three-dimensional amoeboid movement revisited. J Cell Biol *185*, 11-19.

Sahai, E. (2007). Illuminating the metastatic process. Nat Rev Cancer *7*, 737-749.

Sahai, E., Garcia-Medina, R., Pouyssegur, J., and Vial, E. (2007). Smurf1 regulates tumor cell plasticity and motility through degradation of RhoA leading to localized inhibition of contractility. J Cell Biol *176*, 35-42.

Sahai, E., and Marshall, C.J. (2002). RHO-GTPases and cancer. Nat Rev Cancer *2*, 133-142.

Sahai, E., Olson, M.F., and Marshall, C.J. (2001). Cross-talk between Ras and Rho signalling pathways in transformation favours proliferation and increased motility. The EMBO Journal *20*, 755-766.

Sailem, H., Bousgouni, V., Cooper, S., and Bakal, C. (2014). Cross-talk between Rho and Rac GTPases drives deterministic exploration of cellular shape space and morphological heterogeneity. Open Biology *4*, 130132.

Sakata-Yanagimoto, M., Enami, T., Yoshida, K., Shiraishi, Y., Ishii, R., Miyake, Y., Muto, H., Tsuyama, N., Sato-Otsubo, A., Okuno, Y.*, et al.* (2014). Somatic RHOA mutation in angioimmunoblastic T cell lymphoma. Nat Genet *46*, 171-175.

Sander, E.E., ten Klooster, J.P., van Delft, S., van der Kammen, R.A., and Collard, J.G. (1999). Rac Downregulates Rho Activity: Reciprocal Balance between Both Gtpases Determines Cellular Morphology and Migratory Behavior. The Journal of Cell Biology *147*, 1009-1022.

Saras, J., Wollberg, P., and Aspenstrom, P. (2004). Wrch1 is a GTPase-deficient Cdc42-like protein with unusual binding characteristics and cellular effects. Exp Cell Res *299*, 356-369.

Sarikas, A., Hartmann, T., and Pan, Z.-Q. (2011). The cullin protein family. Genome Biology *12*, 220-220.

Sasaki, Y., Suzuki, M., and Hidaka, H. (2002). The novel and specific Rho-kinase inhibitor (S)-(+)-2-methyl-1-[(4-methyl-5-isoquinoline)sulfonyl]-homopiperazine as a probing molecule for Rho-kinase-involved pathway. Pharmacology & Therapeutics *93*, 225-232.

Schiavone, D., Dewilde, S., Vallania, F., Turkson, J., Di Cunto, F., and Poli, V. (2009). The RhoU/Wrch1 Rho GTPase gene is a common transcriptional target of both the gp130/STAT3 and Wnt-1 pathways. Biochem J *421*, 283-292.

Schmidt, A., and Hall, A. (2002). Guanine nucleotide exchange factors for Rho GTPases: turning on the switch. Genes & Development *16*, 1587-1609.

Schnelzer, A., Prechtel, D., Knaus, U., Dehne, K., Gerhard, M., Graeff, H., Harbeck, N., Schmitt, M., and Lengyel, E. (2000). Rac1 in human breast cancer: overexpression, mutation analysis, and characterization of a new isoform, Rac1b. Oncogene *19*, 3013-3020.

Schofield, A.V., and Bernard, O. (2013). Rho-associated coiled-coil kinase (ROCK) signaling and disease. Critical Reviews in Biochemistry and Molecular Biology *48*, 301-316.

Schonichen, A., and Geyer, M. (2010). Fifteen formins for an actin filament: a molecular view on the regulation of human formins. Biochim Biophys Acta *1803*, 152-163.

Schwartz, M. (2004). Rho signalling at a glance. J Cell Sci *117*, 5457-5458.

Sebbagh, M., Hamelin, J., Bertoglio, J., Solary, E., and Bréard, J. (2005). Direct cleavage of ROCK II by granzyme B induces target cell membrane blebbing in a caspase-independent manner. The Journal of Experimental Medicine *201*, 465-471.

Sebbagh, M., Renvoize, C., Hamelin, J., Riche, N., Bertoglio, J., and Breard, J. (2001). Caspase-3-mediated cleavage of ROCK I induces MLC phosphorylation and apoptotic membrane blebbing. Nat Cell Biol *3*, 346-352.

Sequeira, L., Dubyk, C.W., Riesenberger, T.A., Cooper, C.R., and van Golen, K.L. (2008). Rho GTPases in PC-3 prostate cancer cell morphology, invasion and tumor cell diapedesis. Clin Exp Metastasis *25*, 569-579.

Sharpe, R., Pearson, A., Herrera-Abreu, M.T., Johnson, D., Mackay, A., Welti, J.C., Natrajan, R., Reynolds, A.R., Reis-Filho, J.S., Ashworth, A.*, et al.* (2011). FGFR signaling promotes the growth of triple-negative and basal-like breast cancer cell lines both in vitro and in vivo. Clin Cancer Res *17*, 5275-5286.

Shaulian, E., and Karin, M. (2002). AP-1 as a regulator of cell life and death. Nat Cell Biol *4*, E131-E136.

Shi, J., Wu, X., Surma, M., Vemula, S., Zhang, L., Yang, Y., Kapur, R., and Wei, L. (2013). Distinct roles for ROCK1 and ROCK2 in the regulation of cell detachment. Cell Death & Disease *4*, e483.

Shimizu, T., Ihara, K., Maesaki, R., Amano, M., Kaibuchi, K., and Hakoshima, T. (2003). Parallel Coiled-coil Association of the RhoA-binding Domain in Rho-kinase. Journal of Biological Chemistry *278*, 46046-46051.

Shutes, A., Berzat, A.C., Cox, A.D., and Der, C.J. (2004). Atypical mechanism of regulation of the Wrch-1 Rho family small GTPase. Curr Biol *14*, 2052-2056.

Singh, A., Karnoub, A.E., Palmby, T.R., Lengyel, E., Sondek, J., and Der, C.J. (2004). Rac1b, a tumor associated, constitutively active Rac1 splice variant, promotes cellular transformation. Oncogene *23*, 9369-9380.

Siripurapu, V., Meth, J., Kobayashi, N., and Hamaguchi, M. (2005). DBC2 significantly influences cell-cycle, apoptosis, cytoskeleton and membrane-trafficking pathways. J Mol Biol *346*, 83-89.

Sit, S.-T., and Manser, E. (2011). Rho GTPases and their role in organizing the actin cytoskeleton. Journal of Cell Science *124*, 679-683.

Sivaraj, K.K., Takefuji, M., Schmidt, I., Adams, R.H., Offermanns, S., and Wettschureck, N. (2013). G13 controls angiogenesis through regulation of VEGFR-2 expression. Dev Cell *25*, 427-434.

Stanley, A., Thompson, K., Hynes, A., Brakebusch, C., and Quondamatteo, F. (2014). NADPH oxidase complex-derived reactive oxygen species, the actin cytoskeleton, and Rho GTPases in cell migration. Antioxid Redox Signal *20*, 2026-2042.

Steeg, P.S. (2006). Tumor metastasis: mechanistic insights and clinical challenges. Nat Med *12*, 895-904.

Stengel, K., and Zheng, Y. (2011). Cdc42 in oncogenic transformation, invasion, and tumorigenesis. Cell Signal *23*, 1415-1423.

Stogios, P.J., Downs, G.S., Jauhal, J.J., Nandra, S.K., and Prive, G.G. (2005). Sequence and structural analysis of BTB domain proteins. Genome Biol *6*, R82.

Suetsugu, S. (2013). Activation of nucleation promoting factors for directional actin filament elongation: allosteric regulation and multimerization on the membrane. Semin Cell Dev Biol *24*, 267-271.

Sumara, I., Quadroni, M., Frei, C., Olma, M.H., Sumara, G., Ricci, R., and Peter, M. (2007). A Cul3-based E3 ligase removes Aurora B from mitotic chromosomes, regulating mitotic progression and completion of cytokinesis in human cells. Dev Cell *12*, 887-900.

Sumi, T., Matsumoto, K., and Nakamura, T. (2001). Specific Activation of LIM kinase 2 via Phosphorylation of Threonine 505 by ROCK, a Rho-dependent Protein Kinase. Journal of Biological Chemistry *276*, 670-676.

Tan, J.L., Ravid, S., and Spudich, J.A. (1992). Control of Nonmuscle Myosins by Phosphorylation. Annual Review of Biochemistry *61*, 721-759.

Tao, W., Pennica, D., Xu, L., Kalejta, R.F., and Levine, A.J. (2001). Wrch-1, a novel member of the Rho gene family that is regulated by Wnt-1. Genes & Development *15*, 1796-1807.

Tian, M., Bai, C., Lin, Q., Lin, H., Liu, M., Ding, F., and Wang, H.R. (2011). Binding of RhoA by the C2 domain of E3 ligase Smurf1 is essential for Smurf1-regulated RhoA ubiquitination and cell protrusive activity. FEBS Lett *585*, 2199-2204.

Toksoz, D., and Merdek, K.D. (2002). The Rho small GTPase: functions in health and disease Histology and Histopathology *17*, 915-927.

Tong, J., Li, L., Ballermann, B., and Wang, Z. (2013). Phosphorylation of Rac1 T108 by extracellular signal-regulated kinase in response to epidermal growth factor: a novel mechanism to regulate Rac1 function. Mol Cell Biol *33*, 4538-4551.

Tremblay, P.L., Huot, J., and Auger, F.A. (2008). Mechanisms by which E-selectin regulates diapedesis of colon cancer cells under flow conditions. Cancer Res *68*, 5167-5176.

Truebestein, L., Elsner, D.J., Fuchs, E., and Leonard, T.A. (2015). A molecular ruler regulates cytoskeletal remodelling by the Rho kinases. Nat Commun *6*, 10029.

Tu, S., Wu, W.J., Wang, J., and Cerione, R.A. (2003). Epidermal growth factor-dependent regulation of Cdc42 is mediated by the Src tyrosine kinase. J Biol Chem *278*, 49293-49300.

Uchide, K., Sakon, M., Ariyoshi, H., Nakamori, S., Tokunaga, M., and Monden, M. (2007). Cancer cells cause vascular endothelial cell (vEC) retraction via 12(S)HETE secretion; the possible role of cancer cell derived microparticle. Ann Surg Oncol *14*, 862-868.

Ueno, K., Hirata, H., Shahryari, V., Chen, Y., Zaman, M.S., Singh, K., Tabatabai, Z.L., Hinoda, Y., and Dahiya, R. (2011). Tumour suppressor microRNA-584 directly targets

oncogene Rock-1 and decreases invasion ability in human clear cell renal cell carcinoma. British Journal of Cancer *104*, 308-315.

Valastyan, S., and Weinberg, R.A. (2011). Tumor metastasis: molecular insights and evolving paradigms. Cell *147*, 275-292.

Vega, F.M., Fruhwirth, G., Ng, T., and Ridley, A.J. (2011). RhoA and RhoC have distinct roles in migration and invasion by acting through different targets. The Journal of Cell Biology *193*, 655-665.

Vega, F.M., and Ridley, A.J. (2008). Rho GTPases in cancer cell biology. FEBS Lett *582*, 2093-2101.

Vicente-Manzanares, M., Webb, D.J., and Horwitz, A.R. (2005). Cell migration at a glance. J Cell Sci *118*, 4917-4919.

Villalonga, P., Guasch, R.M., Riento, K., and Ridley, A.J. (2004). RhoE inhibits cell cycle progression and Ras-induced transformation. Mol Cell Biol *24*, 7829-7840.

Vincent, S., and Settleman, J. (1997). The PRK2 kinase is a potential effector target of both Rho and Rac GTPases and regulates actin cytoskeletal organization. Molecular and Cellular Biology *17*, 2247-2256.

Visvikis, O., Lores, P., Boyer, L., Chardin, P., Lemichez, E., and Gacon, G. (2008). Activated Rac1, but not the tumorigenic variant Rac1b, is ubiquitinated on Lys 147 through a JNK-regulated process. FEBS J *275*, 386-396.

Visvikis, O., Maddugoda, M.P., and Lemichez, E. (2010). Direct modifications of Rho proteins: deconstructing GTPase regulation. Biol Cell *102*, 377-389.

Wang, D., Dou, K., Xiang, H., Song, Z., Zhao, Q., Chen, Y., and Li, Y. (2007). Involvement of RhoA in progression of human hepatocellular carcinoma. J Gastroenterol Hepatol *22*, 1916-1920.

Wang, H.-R., Zhang, Y., Ozdamar, B., Ogunjimi, A.A., Alexandrova, E., Thomsen, G.H., and Wrana, J.L. (2003). Regulation of Cell Polarity and Protrusion Formation by Targeting RhoA for Degradation. Science *302*, 1775-1779.

Wang, K., Yuen, S.T., Xu, J., Lee, S.P., Yan, H.H., Shi, S.T., Siu, H.C., Deng, S., Chu, K.M., Law, S*., et al.* (2014). Whole-genome sequencing and comprehensive molecular profiling identify new driver mutations in gastric cancer. Nat Genet *46*, 573-582.

Ward, Y., Yap, S.-F., Ravichandran, V., Matsumura, F., Ito, M., Spinelli, B., and Kelly, K. (2002). The GTP binding proteins Gem and Rad are negative regulators of the Rho–Rho kinase pathway. The Journal of Cell Biology *157*, 291-302.

Watanabe, G., Saito, Y., Madaule, P., Ishizaki, T., Fujisawa, K., Morii, N., Mukai, H., Ono, Y., Kakizuka, A., and Narumiya, S. (1996). Protein Kinase N (PKN) and PKN-Related Protein Rhophilin as Targets of Small GTPase Rho. Science *271*, 645-648.

Watanabe, N., Kato, T., Fujita, A., Ishizaki, T., and Narumiya, S. (1999). Cooperation between mDia1 and ROCK in Rho-induced actin reorganization. Nat Cell Biol *1*, 136-143.

Watanabe, N., Madaule, P., Reid, T., Ishizaki, T., Watanabe, G., Kakizuka, A., Saito, Y., Nakao, K., Jockusch, B.M., and Narumiya, S. (1997). p140mDia, a mammalian homolog of Drosophila diaphanous, is a target protein for Rho small GTPase and is a ligand for profilin. The EMBO Journal *16*, 3044-3056.

Weernink, P.A.O., Meletiadis, K., Hommeltenberg, S., Hinz, M., Ishihara, H., Schmidt, M., and Jakobs, K.H. (2004). Activation of Type I Phosphatidylinositol 4-Phosphate 5-Kinase Isoforms by the Rho GTPases, RhoA, Rac1, and Cdc42. Journal of Biological Chemistry *279*, 7840-7849.

Weernink, P.A.O., Schulte, P., Guo, Y., Wetzel, J., Amano, M., Kaibuchi, K., Haverland, S., Voß, M., Schmidt, M., Mayr, G.W*., et al.* (2000). Stimulation of Phosphatidylinositol-4-phosphate 5-Kinase by Rho-Kinase. Journal of Biological Chemistry *275*, 10168-10174.

Wei, J., Mialki, R.K., Dong, S., Khoo, A., Mallampalli, R.K., Zhao, Y., and Zhao, J. (2013). A new mechanism of RhoA ubiquitination and degradation: roles of SCF(FBXL19) E3 ligase and Erk2. Biochim Biophys Acta *1833*, 2757-2764.

Welsh, C.F., Roovers, K., Villanueva, J., Liu, Y., Schwartz, M.A., and Assoian, R.K. (2001). Timing of cyclin D1 expression within G1 phase is controlled by Rho. Nat Cell Biol *3*, 950-957.

Wennerberg, K., and Der, C.J. (2004). Rho-family GTPases: it's not only Rac and Rho (and I like it). Journal of Cell Science *117*, 1301-1312.

Wennerberg, K., Forget, M.-A., Ellerbroek, S.M., Arthur, W.T., Burridge, K., Settleman, J., Der, C.J., and Hansen, S.H. (2003). Rnd Proteins Function as RhoA Antagonists by Activating p190 RhoGAP. Current Biology *13*, 1106-1115.

Wertheimer, E., Gutierrez-Uzquiza, A., Rosemblit, C., Lopez-Haber, C., Sosa, M.S., and Kazanietz, M.G. (2012). Rac signaling in breast cancer: a tale of GEFs and GAPs. Cell Signal *24*, 353-362.

Wheeler, A.P., and Ridley, A.J. (2004). Why three Rho proteins? RhoA, RhoB, RhoC, and cell motility. Exp Cell Res *301*, 43-49.

Wilkins, A., Ping, Q., and Carpenter, C.L. (2004). RhoBTB2 is a substrate of the mammalian Cul3 ubiquitin ligase complex. Genes & Development *18*, 856-861.

Wimuttisuk, W., and Singer, J.D. (2007). The Cullin3 ubiquitin ligase functions as a Nedd8-bound heterodimer. Mol Biol Cell *18*, 899-909.

Wirth, A., Chen-Wacker, C., Wu, Y.W., Gorinski, N., Filippov, M.A., Pandey, G., and Ponimaskin, E. (2013). Dual lipidation of the brain-specific Cdc42 isoform regulates its functional properties. Biochem J *456*, 311-322.

Worthylake, R.A., Lemoine, S., Watson, J.M., and Burridge, K. (2001). RhoA is required for monocyte tail retraction during transendothelial migration. The Journal of Cell Biology *154*, 147-160.

Wu, J.T., Lin, H.C., Hu, Y.C., and Chien, C.T. (2005). Neddylation and deneddylation regulate Cul1 and Cul3 protein accumulation. Nat Cell Biol *7*, 1014-1020.

Xu, G., and Jaffrey, S.R. (2011). The new landscape of protein ubiquitination. Nat Biotechnol *29*, 1098-1100.

Xu, R.S., Wu, X.D., Zhang, S.Q., Li, C.F., Yang, L., Li, D.D., Zhang, B.G., Zhang, Y., Jin, J.P., and Zhang, B. (2013). The tumor suppressor gene RhoBTB1 is a novel target of miR-31 in human colon cancer. Int J Oncol *42*, 676-682.

Yamaguchi, H., Kasa, M., Amano, M., Kaibuchi, K., and Hakoshima, T. (2006). Molecular Mechanism for the Regulation of Rho-Kinase by Dimerization and Its Inhibition by Fasudil. Structure *14*, 589-600.

Yamashiro, S., Totsukawa, G., Yamakita, Y., Sasaki, Y., Madaule, P., Ishizaki, T., Narumiya, S., and Matsumura, F. (2003). Citron Kinase, a Rho-dependent Kinase, Induces Di-phosphorylation of Regulatory Light Chain of Myosin II. Molecular Biology of the Cell *14*, 1745-1756.

Yoneda, A., Multhaupt, H.A.B., and Couchman, J.R. (2005). The Rho kinases I and II regulate different aspects of myosin II activity. The Journal of Cell Biology *170*, 443-453.

Yoo, H.Y., Sung, M.K., Lee, S.H., Kim, S., Lee, H., Park, S., Kim, S.C., Lee, B., Rho, K., Lee, J.E.*, et al.* (2014). A recurrent inactivating mutation in RHOA GTPase in angioimmunoblastic T cell lymphoma. Nat Genet *46*, 371-375.

Zhang, C., Zhou, F., Li, N., Shi, S., Feng, X., Chen, Z., Hang, J., Qiu, B., Li, B., Chang, S.*, et al.* (2007). Overexpression of RhoE has a prognostic value in non-small cell lung cancer. Ann Surg Oncol *14*, 2628-2635.

Zhang, S., Tang, Q., Xu, F., Xue, Y., Zhen, Z., Deng, Y., Liu, M., Chen, J., Liu, S., Qiu, M.*, et al.* (2009). RhoA regulates G1-S progression of gastric cancer cells by modulation of multiple INK4 family tumor suppressors. Mol Cancer Res *7*, 570-580.

Zhao, Y., Sato, Y., Isaji, T., Fukuda, T., Matsumoto, A., Miyoshi, E., Gu, J., and Taniguchi, N. (2008). Branched N-glycans regulate the biological functions of integrins and cadherins. FEBS J *275*, 1939-1948.

Zhao, Y., Xiong, X., Jia, L., and Sun, Y. (2012). Targeting Cullin-RING ligases by MLN4924 induces autophagy via modulating the HIF1-REDD1-TSC1-mTORC1-DEPTOR axis. Cell Death Dis *3*, e386.

Zheng, F., Liao, Y.-J., Cai, M.-Y., Liu, Y.-H., Liu, T.-H., Chen, S.-P., Bian, X.-W., Guan, X.-Y., Lin, M.C., Zeng, Y.-X.*, et al.* (2012). The putative tumour suppressor microRNA-124 modulates hepatocellular carcinoma cell aggressiveness by repressing ROCK2 and EZH2. Gut *61*, 278-289.

Zhou, C., Licciulli, S., Avila, J.L., Cho, M., Troutman, S., Jiang, P., Kossenkov, A.V., Showe, L.C., Liu, Q., Vachani, A.*, et al.* (2013). The Rac1 splice form Rac1b promotes K-ras-induced lung tumorigenesis. Oncogene *32*, 903-909.

Zhou, J., Hayakawa, Y., Wang, T.C., and Bass, A.J. (2014). RhoA mutations identified in diffuse gastric cancer. Cancer Cell *26*, 9-11.

Zhou, J., Zhu, Y., Zhang, G., Liu, N., Sun, L., Liu, M., Qiu, M., Luo, D., Tang, Q., Liao, Z.*, et al.* (2011). A distinct role of RhoB in gastric cancer suppression. Int J Cancer *128*, 1057-1068.